THE UNIVERSITY
of EDINBURGH

Perivascular stem cells at the crossroads of tissue regeneration and pathology

Iain R Murray

B Med Sci (Hons), MBChB, MRCSEd, Dip SEM

Doctor of Philosophy

University of Edinburgh

2014

Declaration

This dissertation is the result of my own work and includes nothing which is the outcome of work done in collaboration, except where specifically indicated in the text.

The data included in this text has not been submitted for any other degree or professional qualification, nor does it exceed the word limit of 100,000 words set by the College of Medicine and Veterinary Medicine.

Iain R Murray

Abstract

Pericytes represent a population of potential mesenchymal stem cells (MSC) that reside within a perivascular niche until they are required in normal homeostasis and the response to injury. Their mesenchymal capacities for multipotent differentiation, immune modulation and release of trophic factors hold great promise for regenerative therapies. Pathological expression of these potentials has been described in disease states, while acute or chronic inflammation following injury can lead to the production of signalling molecules that ultimately drive these progenitors to a fibrotic fate. The aim of this work was to explore how fate decisions of pericytes are regulated by their niche (in the setting of osteogenesis), and in the response to acute and chronic injury (in the setting of fibrosis).

It was hypothesized that interactions between pericytes and endothelial cells (EC) within their perivascular niche are responsible for regulating mesenchymal differentiation. The osteogenic, adipogenic and chondrogenic potential of pericytes following isolation from multiple human organs was confirmed. The interactions between pericytes and EC in 2D and 3D coculture and the production of basement membrane proteins in these settings were confirmed. The osteogenic differentiation of pericytes was accelerated by EC but no influence of EC on the adipogenic and chondrogenic differentiation of pericytes was detected. Furthermore, data indicated that the influence on pericyte osteogenic potential by EC may occur through wnt signaling.

The activation of TGFβ (transforming growth factor beta) through αv integrins has been suggested as central mediator of fibrosis in multiple organs. We hypothesized that selective αv integrin deletions in PDGFRβ (platelet derived growth factor receptor beta) expressing pericytes identifies a targetable pathway regulating fibrosis in skeletal muscle. We report that PDGFRβ-Cre inactivates genes in murine skeletal muscle pericytes with high efficiency. Deletion of the αv integrin subunit in pericytes protected mice from chemical injury induced skeletal muscle fibrosis. Pharmacological blockade of αv integrins by a novel small molecule (CWHM 12) attenuated muscle fibrosis, even when administered after fibrosis was established.

Acknowledgements

I would like to extend my heartfelt thanks to my supervisors Bruno Péault, Neil Henderson and Mirko Corselli who have been a great inspiration and support. I would also like to thank John Iredale, Brian Walker and Andrew Jackson (Edinburgh Clinical Academic Training Directors) for the opportunity to do this work and for ongoing mentorship throughout. I would like to thank all members of the Péault and Henderson groups who have tolerated my poor sense of humour and offered countless hours of their time. In particular I would like to thank Reef Hardy and Mirko Corselli for their friendship and guidance during my time at UCLA, and to Zaniah Gonzalez for her contribution to the work on coculture models as a Masters student under my direction, and for her help with the validation of reporter mice and qPCR. Furthermore, special thanks should go to collaborators on this work particularly Hamish Simpson, Gustavo Miranda-Carboni, Michael Prinsen, David Griggs and Peter Ruminski. I would also like to thank Fiona Rossi, Shonna Johnston, Claire Cryer and Valeria Berno for their input and expertise with flow cytometry and imaging. Special thanks also go to Marilyn Thomson and Helen Henderson for their technical assistance in tissue culture and to Jo Ness and Lorraine Vaughan for their organisational support.

On a personal note I would like to thank my parents and family for their endless inspiration, enthusiasm and support. Finally and most importantly, thanks to my wife Katie - your support means the world to me and this thesis could not have come about with you.

This work was supported by the Wellcome Trust through the Edinburgh Clinical Academic Training (ECAT) programme.

Table of Contents

Table of Figures and Tables

Figures

Tables

List of abbreviations

2D	Two-dimensional
3D	Three-dimensional
ADAM12	A disintegrin and metalloproteinase 12
ALCAM	Activated leukocyte cell adhesion molecule
ALK	Activin-linked kinase
AP	Alkaline phosphatase
APC	Allophycocyanin
ASC	Adipose-derived stem cell
αSMA	Alpha smooth muscle actin
BD	Bone density
BCL9	B-cell CLL/lymphoma 9
BGP	β-glycerophosphate
BM	Bone marrow
BMP	Bone morphogenetic protein
BSA	Bovine serum albumin
BV	Bone volume
CBP	CREB binding protein
CD-	Cluster of differentiation
cDNA	Complementary DNA
C/EBPα	CCAAT/enhanced binding protein alpha
CFU	Colony forming unit
CMFDA	Chloromethylfluorescein diacetate
C_T	Theshold cycle
CT	Computed tomography

CTX	Cardiotoxin
DAPI	4’,6-diamidino-2-phenylindole
DLK-1	Delta-like 1
DMD	Duchenne muscular dystrophy
DMEM	Dulbecco’s modified eagle medium
DMSO	Dimethyl sulfoxide
DNA	Deoxyribonucleic acid
dNTPs	Deoxynucleoside triphosphates
EC	Endothelial cells
ECM	Extracellular matrix
EDL	Extensor digitorum longus
EDTA	Ethylenediaminetetraacetic acid
EGM2	Endothelial growth media 2
ELISA	enzyme-linked immunosorbent assay
EMEA	European Medicines Agency
EMT	Epithelial-mesenchymal transition
EndMT	Endothelial-mesenchymal transition
EPC	Endothelial progenitor cell
ER	Oestrogen receptor
ERK	extracellular signal-regulated kinase
ES	Embryonic stem
FACS	Flourescence-activated cell sorting
FAP	Fibro-adipogenic progenitor
FBS	Fetal bovine serum
FDA	Food and Drug Administration
FGF	Fibroblast growth factor

FITC	Fluorescein isothiocyanate
FOP	Fibrodysplasia ossificans
FSC	Forward scatter
FZD	Frizzled
GCSF	Granulocyte-colony stimulating-factor
GFP	Green fluorescent protein
GSK3	Glycogen synthase kinase 3
GVHD	Graft versus host disease
HAMEC	Human adipose-derived microvascular endothelial cells
HBSS	Hanks balanced salt solution
HDF	Human dermal fibroblasts
HLA-DR	Human leukocyte antigen-DR
HOP	Human osteoprogenitor cells
HPRT	Hypoxanthine-guanine phosphoribosyltransferase
HSC	Haematopoietic stem cell
HSVEC	Human saphenous vein endothelial cells
HUVEC	Human umbilical vein endothelial cells
IAM2	Intercellular adhesion molecule 2
IBMX	3-isobutyl-1-methylxanthine
IGF	Insulin-like growth factor
IgG	Immunoglobulin G
IHC	Immunohistochemistry
IL	Interleukin
IVF	In vitro fertilisation
iPSC	induced pluripotent stem cells
ISCT	International Society for Cellular Therapy

JNK	Jun kinase
LAMP	Lysosomal-associated membrane protein
LAP	Latency associated peptide
LCA	Leukocyte common antigen
LDH	Lactate dehydrogenase
LNGFR	Low affinity nerve growth factor receptor
LRP	Lipoprotein receptor-related protein
LTBP	Latent TGFβ binding protein
mAbs	Monoclonal antibodies
MACS	Magnetic-activated cell sorting
MAPC	Multipotent adult progenitor cell
MAPK	Mitogen activated protein kinase
MASC	Multipotent adult stem cell
MCAM	Melanoma cell adhesion molecule
MI	Myocardial infarction
MIAMI	Marrow isolated adult multilineage inducible cell
MMP	Matrix metalloproteinase
mRNA	messenger RNA
MS	Multiple sclerosis
MSC	Mesenchymal stem/stromal cell
mTmG	Membrane targeted TdTomato, membrane targeted GFP
Myf	Myogenic factor
MyoD	Myogenic differentiation 1
NAD	Nicotinamide adenine dinucleotide
NCAM	Neural cell adhesion molecule
NG2	Neural/glial antigen 2

NKD	Naked cuticle
OCT	Optimum cutting temperature
OD	Optical density
OSX	Osterix
PAI	Plasminogen activator inhibitor
PBS	Phosphate buffered saline
PCR	Polymerase chain reaction
PDGFRβ	Platelet-derived growth factor receptor β
PDT	Population doubling time
PE	Phycoerythrin
PECAM	Platelet/endothelial cell adhesion molecule
PFA	Paraformaldehyde
PI	Propridium iodide
PIC	PW1+/Pax7- interstitial cells
PPARG	Peroxisome proliferator activated receptor gamma
PS	Penicillin and streptomycin
PSC	Perivascular stem cell
PSR	Picrosirius red
RGD	Arginylglycylaspartic acid
RGE	arginylglycylglutamate
RIN	RNA integrity number
RNA	Ribonucleic acid
ROS	Reactive oxygen species
RPM	Revolutions per minute
RT	Room temperature
RUNX2	Runt-related transcription factor 2

SSC	Side scatter
SD	Standard deviation
SEM	Standard error of the mean
SFRP	Secreted frizzled-related protein
SHH	Sonic hedgehog
SM22	Smooth muscle specific protein 22
SPP1	Secreted phosphoprotein 1 / Osteopontin
SVF	Stromal vascular fraction
TA	Tibialis anterior
TBE	Tris/Borate/EDTA
TCF	T-cell factor
TCF4	Transcription factor 4
TGF	Transforming growth factor
TIMP	tissue inhibitor of metalloproteinase
qPCR	Quantitative PCR
VCAM	Vascular cell adhesion molecule
VE	Vascular endothelial
VEGF	Vascular endothelial growth factor
vWF	von Willebrand factor
WIF	Wnt inhibitory factor
Wnt	Wingless-related integration site
WT	Wildtype
YFP	Yellow fluorescent protein

General Introduction

Adult stem cells: position among other stem cells in terms of biologic and therapeutic potentials

Stem cell therapies offer potential treatments for a wide range of diseases that involve the failure of tissues and organs. The transplantation of bone marrow has been used for over 40 years to treat patients with a wide range of haematological malignancies but is currently the only stem cell therapy that is widely practiced. Although a great deal of stem cell therapy remains experimental, greater understanding of how stem cells behave in their native environment, and how these characteristics can be harnessed, holds great promise for future therapies.

Stem cells are undifferentiated (biological) cells that can differentiate into specialised cells and self renew to maintain the stem cell pool. There are two broad groups of therapeutic stem cells: embryonic stem (ES) cells, which are isolated from the inner mass of the 5-7 day old blastocyst, and adult stem cells which are found in various tissues. In a developing embryo, ES-like cells differentiate into cell types from each of the three embryonic germ layers: the endoderm, mesoderm and ectoderm. In adult organisms, stem cells provide a source of cells during normal tissue homeostasis and act as a repair system, replenishing tissue in response to injury[1 2].

Human embryonic and adult stem cells each have advantages and disadvantages regarding potential for cell-based regenerative therapies. The differentiation potential of ES cells is broader than adult stem cells and therefore each ES cell line has a wider repertoire of potential therapeutic targets. However, adult stem cells, with their more restricted differentiation potential are established to have lower tumorigenic potential. Unlike ES cells, the use of adult stem cells in research and therapy is not controversial,

as they are derived from adult tissue samples rather than human 5 day old embryos generated by in-vitro fertilisation (IVF) clinics designated for scientific research. Furthermore, adult stem cells can be used autologously, overcoming many of the risks of viral transmission and immune rejection associated with allogeneic transplantation.

Induced pluripotent stem cells (iPSC) are pluripotent somatic cells reprogrammed to enter an embryonic cell-like state by being forced to express factors important for maintaining "stemness". Mouse iPSC were first reported in 2006 and human iPSCs were first reported in late 2007. Mouse iPSC demonstrate important characteristics of pluripotent stem cells, including the expression of stem cell markers, the formation of tumours containing cells from all 3 germ layers, and the ability to contribute to many different tissues when injected into mouse embryos at a very early stage in development. Human iPSC also express stem cell markers and are capable of generating cell characteristics of all 3 germ layers. iPSC offer the broad differentiation potential of ES cells without the associated ethical barriers, although these cells require further characterisation with ongoing concerns regarding tumorigenicity.

Mesenchymal stem cells (MSC)

In the 1960's, the Russian scientist Friedenstein identified a population of adult cells within rodent bone marrow that were rapidly adherent to plastic, had the appearance of fibroblasts and formed clonal colonies *in vitro*. These cells were also capable of osteogenic differentiation in culture, and could generate bone when implanted in ectopic locations *in vivo* [3-5]. In addition, their demonstrated ability to generate heterotopic bone tissue in serial implants suggested their self-renewal[6]. Since Friedenstein's early descriptions, numerous laboratories have confirmed and expanded

these findings showing that cells with similar abilities to be sub-passaged and differentiated *in vitro* into a variety of mesenchymal cell types such as osteoblasts, chondrocytes, adipocytes and myoblasts could be isolated from human bone marrow [7-10]. Friedenstein had isolated from the bone marrow of rodents what would later be coined "mesenchymal stem cells" or MSC by Caplan [11].

MSC have now been isolated from multiple different human tissue types including fat [12 13] and skeletal muscle[14 15]among others (Table 1, p5)**.** Considerable work has been done to characterise and expand these cells *in vitro*, and to explore strategies to maintain these cells in their stem like state [16-21]. This work was driven by the promise of therapeutic translation using these progenitors to replace or repair damaged musculoskeletal tissues. Therefore, current knowledge of MSC is almost entirely based on characterisation and observations of behaviour in culture – the setting in which they are defined - and until recently the *in vivo* counterpart of culture expanded MSC remained a mystery.

With interest so far focused on multipotency and tissue engineering, little is currently understood regarding the ontogeny of these cells, their anatomical localisation or their natural role in tissue homeostasis, physiology or pathology. Characterisation of native MSC could allow for either pharmacological or genetic manipulations of this cellular pool *in vivo*, or facilitate the purification of populations for tissue engineering applications.

- Bone marrow[22 23 14]
- Periosteum[22 23]
- Trabecular bone[22 23]
- Articular cartilage
- Synovium and synovial fluid[24]
- Adipose tissue[14 22 23]
- Skeletal muscle[14 15]
- Tendon[25 26]
- Brain[22 23]
- Kidney[22 23]
- Umbilical cord[27]
- Periodontal ligament and dental pulp[28 29]
- Amniotic fluid[30]
- Blood [22 23]
- Skin[14 31]
- Thymus[22 23]
- Liver[22 23]
- Spleen[22 23]
- Placenta[32]

Table 1 Described sources of MSC (non-exhaustive list)

Definitions and *in vitro* behaviours of MSC

Attempts have been made to standardize the nomenclature used in MSC research. However, the variation in methods of isolation, culture and assays used to examine them has made this issue both difficult and at times misleading. The International Society for Cellular Therapy (ISCT) produced in 2006 a position statement in which it suggested the minimum criteria required to define MSC [33]. They stated that cells must:

- Be plastic adherent
- Express the cell surface antigens CD105, CD73 and CD90
- Not express the cell surface antigens CD45, CD34, CD14, CD11b, CD79α, CD19 or HLA-DR
- Differentiate into osteoblasts, adipocytes and chondroblasts *in vitro*

These criteria were established to standardize human MSC isolation but may not apply uniformly to other species. For example, murine MSC differ subtly in marker

expression and behaviour compared with human MSC [34]. Although not included within defining criteria, MSC are recognised to perform a number of roles beyond multipotency including immune modulation, haematopoiesis support, and the release of trophic factors in response to injury.

(i) Multilineage potential

The ability of MSC to differentiate into all the mesodermal cell lineages (bone, muscle cartilage, fat, tendon, ligament, marrow stroma, connective tissue) in appropriate conditions is well established [11]. This is routinely achieved *in vitro* by supplementation of cultures with lineage specific growth factor combinations. For example, dexamethasone, 3-isobutyl-1-methylxanthine (IBMX) and insulin are used to induce adipogenic differentiation while dexamethasone, β-glycerophosphate (BGP) and ascorbic acid are used to promote osteogenic differentiation.

(ii) Support of haematopoiesis

The crucial role of bone marrow stromal progenitors in supporting haematopoiesis was first described by Friedenstein *et al.,* who observed the formation of heterotopic ossicles containing bone and haematopoietic tissue, upon ectopic CFU-fibroblast derived colony transplantation in semi-syngeneic animals [4]. The haematopoietic cells were of recipient origin whereas bone-forming cells originated from the donor suggesting that transplanted colonies provided a microenvironment favorable for haematopoietic stem cell (HSC) homing and subsequent establishment of haematopoiesis. Subsequently, Dexter *et al.* established a system of murine long-term cultures to demonstrate that bone marrow stromal cells can maintain haematopoiesis for periods longer than 6 months [35]. It was confirmed that a subset of human bone marrow stromal cells expressing the STRO-1 antigen possesses haematopoiesis

supporting ability, along with the potential to differentiate into multiple mesenchymal cell lineages [36] [37]. There is accumulating evidence to suggest that bone marrow MSC also have promoting effects on HSC engraftment and repopulation. Several studies have demonstrated that co-transplantation of human HSC and MSC results in increased chimerism and/or haematopoietic recovery, in both animal models and humans [38-44].

(iii) Immune regulation

The immunomodulatory properties of bone marrow-derived MSC, including their immunosuppressive effects during allogeneic stem cell transplantation have been well documented [45-49]. The immunoactivity of the cells is mediated by direct cell-cell contact and through secreted bioactive molecules involving dendritic cells, B and T cells including T regulatory cells and T helper cells and killer cells[49] [50].

(iv) Secretion of trophic factors

Experiments using transplantation of cultured MSC into animals led to the realisation that MSC therapeutic effects could not be explained by differentiation into tissue specific cells alone [51] [52]. As such, transplanted MSC may exert beneficial effects through their vast secretome beyond immune regulation [53] [54]. Bioactive factors secreted by MSC have angiogenic and antiapoptotic properties that serve to limit the extent of tissue damage at the injured sites, re-establish blood supply and recruit local progenitors. These MSC paracrine effects have been referred to as trophic effects [55].

Nomenclature

Due to the lack of a unique MSC function and anatomic identity, these cells were termed ‘mesenchymal stem cells (MSC)’ or more or less synonymously ‘marrow stromal cells’,

'BM stromal cells' and 'mesenchymal stromal cells' [56-58]. Populations of cells that fulfill the ISCT MSC criteria yet exhibit broader differentiation capacity have also been described [59]. Investigators described such cells as 'multipotent adult progenitor cells' (MAPC) [60], 'marrow isolated multilineage inducible cells' (MIAMI) [61] or 'multipotent adult stem cells' (MASC) [62]. The relationship of these cells to MSC is currently not clear.

Are MSC true stem cells?

Stem cells are strictly defined by their ability to reconstruct *in vivo* the tissue of origin while contributing to its long term maintenance and repair. Stem cells differ from progenitor cells (or transient amplifying cells) that exhibit extended proliferative capacity and multipotent differentiation *in vitro* but have little ability to contribute to long term tissue regeneration *in vivo*[63]. There is very little evidence for long term skeletal regeneration of MSC *in vivo*. Transplantation of MSC through intravenous infusion has resulted in little or no engraftment of cells to bone or bone marrow[40 64]. However, intra-femoral injection of a subset of murine marrow stromal cells has shown limited engraftment at the site of injection 4-6 weeks post-transplantation suggesting that the quality of the cells injected may be a major determinant of engraftment[65 66].

The immunophenotype of MSC

Assuming that MSC represent a distinct cell population, it is intuitive that they would have a specific repertoire of cell surface antigens that would enable identification, isolation and purification based on phenotype. Flow cytometry is a powerful and relatively easy to handle approach for phenotyping of cells using fluorescence labelled monoclonal antibodies (mAbs) against cell surface antigens. The cell surface antigen profile of MSC has been well explored, and in recent years various combinations of cell

surface markers were published for characterising MSC (Table 2, p10 and Table 3, p11) [67] [68]. A particular challenge for the field has been the absence of any specific marker to define MSC, although a large number of different determinants have been associated, albeit not exclusively, with them (reviewed by Lindner *et al*., 2010; for human MSC [69]).

Defining MSC *in vitro* adds complexity to their study because the artificial culture conditions may introduce experimental artifacts. It has been proposed that certain natively expressed surface markers are modified following explantation, while new markers may be acquired. For example, an MSC line was isolated that uniformly expressed HLA-DR (a marker that should not be expressed on MSC by the above definition) while also expressing CD90 and CD105, adhering to plastic in culture, and being capable of differentiating into osteoblasts, adipocytes, and chondroblasts [70].

Similarly, the expression of CD105, CD73 and CD90 is not uniform and can be modulated by *in vitro* conditioning. The expression or absence of these factors does not appear to be inclusive or exclusive of multipotency and discrete subpopulations of MSC like cells have been isolated with varying levels of expression [71]. Numerous other markers have been suggested including PDGFRβ, CD271 [72] [73], and recently decorin, a marker specific to MSC in adipose tissue has been identified [74]. A nomenclature that focuses on anatomically defined, *in vivo* populations is preferential to one that is based on inherently variable and imprecise *in vitro* populations.

Marker	Also known as	MSC	Pericyte	Adventitial
CD3		[75]		
CD9	Tetraspanin-29	[75-78]		
CD10	Neural endopeptidase	[14 76]	[14]	
CD13	Alanine aminopeptidase N	[14 76]	[14]	
CD18		[79]		
CD29	Integrin beta 1	[75-78]	[80]	
CD34	Mucosialin	[14 81]		[82 83]
CD44	Receptor for hyaluronic acid	[79 84]	[14 80]	[85]
CD49A	Half of α1β1 integrin duplex	[75 76 78 79]		
CD49B	Half of α2β1 integrin duplex	[75 76 78 79]		
CD49C	Integrin α 3	[75 76 78 79]		
CD49E	Integrin α 5	[75 76 78 79]		
CD49F	Integrin α 6	[75 76 78 79]		
CD51	Integrin α V	[79]		
CD54	Intercellular adhesion molecule 1	[75 76 78 79]		
CD55		[76 78]		
CD56	Neural cell adhesion molecule (NCAM)	[79]		
CD58	LFAA 3	[75]		
CD59	Protectin	[76]		
CD61	Integrin β 3	[77]		
CD63	Lysosomal-associated membrane protein3 (LAMP-3)	[77]		
CD71	Transferrin receptor	[75-78]		
CD73	5'-nucleotidase, ecto	[33]	[86 87]	[86]
CD90	Thy-1	[14 81]	[14 81]	[14 81]
CD97	Leucocyte antigen	[77]		
CD98		[77]		
CD99	E2 antigen	[77]		
CD104	Integrin β4	[79]		
CD105	Endoglin	[33]	[80 87]	[83]
CD106	Vascular cell adhesion molecule 1 (VCAM1)	[84]		
CD120A	Tumour necrosis factor receptor	[8]		
CD124	Interleukin-4 receptor	[8]		
CD140	Platelet derived growth factor beta (PDGFRβ)	[14 81]	[14 81]	
CD146	Melanoma cell adhesion molecule (MCAM)	[14 81]	[14 81]	
CD166	Activated leukocyte cell adhesion molecule (ALCAM)	[78 79]	[88]	
CD271	Low affinity nerve growth factor receptor (LNGFR)	[89]		
CD276		[77]		
CD304		[77]		
CD324		[79]		
CD340		[89]		
CD349		[89]		
αSMA		[14 81]	[14 81]	
NG2		[81]	[81]	[81]
STRO-1			[87]	

Table 2 Markers used for positive selection of MSC
[Modified from Murray et al, Cell Mol Life Sci 2014;71(8):1353-74]

Marker	Also known as	MSC	Pericyte	Adventitial
CD11a	Integrin αL chain	[8 33]		
CD11b	Integrin α M chain	[33]		
CD14	Lipopolysacharride (LPS) receptor	[8 33 77 84]	[80 88]	
CD16		[75]		
CD19		[8 33]		
CD27		[75]		
CD28		[75]		
CD31	Platelet/Endothelial cell adhesion molecule 1 (PECAM-1)	[75 78 79 82]	[14 80-82 86-88]	[81 86 87]
CD33		[75]		
CD34	Mucosialin	[33 75 81 84]	[14 81 82 86 87]	
CD36		[75]		
CD45	Leucocyte common antigen (LCA)	[33 75 77 78 84]	[14 80 82 86-88]	[83 86]
CD50		[79]		
CD56	Neural cell adhesion molecule (NCAM)		[14 87]	
CD79a	Ig- α	[33]		
CD102	Intercellular adhesion molecule 2 (IAM2)	[79]		
CD106	Vascular cell adhesion molecule 1 (VCAM1)		[88]	
CD117	c-kit	[86]	[86]	[86]
CD133	Prominin-1	[77 84]	[14]	
CD144	VE-cadherin	[14 84]	[14]	
CD146	Melanoma cell adhesion molecule (MCAM)			[81-83 86]
Cd243		[75]		
αSMA				[81 83]

Table 3 Markers used for negative selection of MSC
[Modified from Murray *et al,* Cell Mol Life Sci 2014;71(8):1353-74]

MSC isolated from different organs exhibit unique features.

The equivalency of MSC populations from distinct anatomic origins has not been robustly demonstrated. Despite fulfilling the ISCT criteria, differences have been observed with respect to the immunophenotype, secreted cytokine profile, and results obtained by proteome analysis, depending on the source and the native or cultivated state of the MSC population characterized[90-92]. Cloned human MSC isolated from fat and bone marrow default to an adipogenic or osteogenic potential, respectively, suggesting that the tissue environment of origin imprints such character. The ability of MSC to differentiate *in vitro* into adipocytes, chondrocytes, osteoblasts, myoblasts, and of late, into haematopoiesis- or osteogenesis- supporting stromal cells has been used to stratify the multipotency of these cells as well as to search for markers indicative of lineage commitment. While surface antigens like CD105, CD73, and CD29 are conserved by most MSC[33], others such as Sca-1 (rodents), CD24 [93-95], CD140-a & -b, CD146 [96], CD271[97 98], CD338 [99] and many others [93] betray the underlying heterogeneity in these cells. Some markers like PDGFRα correlated with the adipogenic potential of these cells, both in humans and in rodents, while others like CD146 may be associated with greater multipotency, and a higher colony-forming efficiency and proliferation rate [100].

Anatomical location of MSC

With interest focused on multipotency and tissue engineering and repair, the native origin and physiological roles *in vivo* of MSC have been considerably overlooked. As such, cells that could be identified only retrospectively in long-term culture were being proposed for therapeutic purposes, without true understanding of their native origin or function. The real, *in vivo* counterpart of culture expanded MSC was unknown, and it could be argued that based on the ISCT definition, MSC represented a mere artifact of culture with no exact equivalent in the living organism. Somewhat surprisingly, the lack

of understanding of the *in vivo* origin of these cells did not constrain their clinical uses (305 clinical trials registered on clinicaltrials.gov at the time of writing). However, such a retrospective characterization *in vitro* meant that any clinical exploitation of MSC would make use of a heterogeneous population of cells exposed to the hazards of extended culture. In search of ways to fully exploit the therapeutic characteristics of MSC, researchers sought an improved understanding of the native identity and biology of these cells.

The massive stem cell recruitment, expansion, migration and differentiation that can be visualised at early embryonic stages wanes with maturity. As development proceeds stem cells become less prevalent and tissue regeneration and repair become quantitatively marginal. This makes the documentation of stem cell presence and activity in anatomic terms increasingly challenging. It is established that adult tissue specific stem cells are located in specialized "niches" in their corresponding tissues of origin [101]. For example, HSC can be found in the bone marrow [102], epidermal stem cells in mammalian hair follicles [103], and neural stem cells in the subventricular zone [104]. MSC have perhaps proved to be the most elusive of all adult stem cells.

The main cell types suggested to descend from MSC including bone, cartilage, fat and muscle are not limited to one anatomical region. Wherever MSC originate they must be capable of reaching these tissues throughout the body or be locally available. With this in mind, a number of potential explanations have been suggested [105]. Firstly, MSC may originate from a single organ, from which they migrate towards areas of need in response to systemic signals. In support of this, experiments using rats exposed to low-oxygen conditions suggest that MSC are specifically mobilized into peripheral blood as a consequence of hypoxia[106], while elevated numbers of MSC were noted in the

peripheral blood of patients immediately following traumatic hip injury. However, the origin(s) of the mobilized cells remains unclear and it has proved extremely difficult to establish MSC cultures from conventional blood either in physiological conditions or following stimulation with cytokines [22 107 108].

Conversely, the ability to derive apparently identical MSC from multiple tissues led to the hypothesis that these cells share a common *in vivo* location. A growing body of published reports has described perivascular cells which appear indistinguishable from vascular pericytes as a possible source of MSC [28 41 109 110], a situation that would explain why MSC can be isolated from all organs. Association of these mesenchymal progenitor cells with the vasculature would allow them to function as a source of new cells for physiological turnover and for the repair or regeneration of local lesions. The establishment of MSC-like cultures from blood vessels alone supports this hypothesis. More recently another subset of vascular cells, namely adventitial cells, have been identified that may behave in a similar manner to pericytes[83].

Perivascular stem cells (PSC)

Recent results have acknowledged the regenerative potential, under certain conditions, of a subset population residing in the wall of blood vessels [43 44]. Pericytes have been recognised as a distinct cellular entity that share a common immunophenotype and differentiation potential to mesenchymal stem/progenitor cells [23]. In a variety of human organs, perivascular mesenchymal progenitor cells can be identified by a combination of perivascular (CD146, NG2, PDGFRβ) and MSC (CD29, CD44, CD73, CD90, CD105, alkaline phosphatase) markers, as well as lack of haemato-endothelial cell markers (CD31, CD34, CD45, CD144, von Willebrand factor (vWF)) (Figure 1, p15).

Pericytes have been shown to differentiate into multiple mesodermal lineages *in vitro* including bone [111 112], fat [113], cartilage [110] and skeletal muscle [114 115]. Similarly to culture-expanded bone marrow-derived MSC, T-lymphocyte surveillance shut-down effects have also been reported with pericytes [116 117].

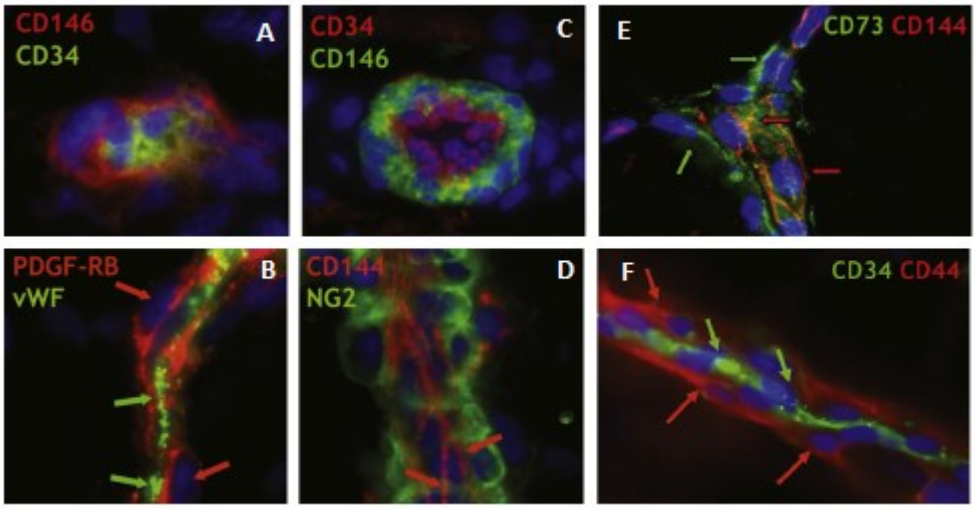

Figure 1 Immunodetection of pericytes in human organs and confirmation that pericytes natively express MSC markers.
(A) Myocardium: a capillary EC in transverse section marked by CD34 expression (green) is closely surrounded by a CD146+ pericyte (red) (x900). (B) Skeletal muscle: small vessel longitudinal section; PDGFRβ+ perivascular cells (red; red arrows) surrowund vWF+ endothelial cells (green; green arrows) (x400). (C) Skeletal muscle: small vessel transverse section; CD146+ pericytes (green) surround CD34+ endothelial cells (red) (x400). (D) Fetal pancreas: small vessel longitudinal section; NG2-positive pericytes (green; green arrows) surround CD144+ endothelial cells (red; red arrows) (x400). (E) Frozen sections of adult human muscle were co-stained with antibodies to CD144 (red) to reveal endothelial cells (red arrows) and CD73 (green). Pericytes lining the small blood vessel express CD73 ([H], x600, green arrows). (F) Frozen sections of human adipose tissue were co-stained with antibodies to CD34 (green) to reveal EC (green arrows) and CD44 to label pericytes(red, [F]). [Modified from Crisan *et al.* Cell Stem Cell 2008;3(3):301-13]

Tottey *et al.* demonstrated that perivascular cells isolated from human fetal muscle proliferate at a higher rate under hypoxic condition (6%) than normoxia (21%) and that they migrate more rapidly when exposed to degraded extracellular matrix (ECM) products [118]. This indicates some degree of activation in the presence of injury. Perivascular cells can release various cytokines, including basic-fibroblast growth factor (b-FGF), a well-known chemotactic and mitogenic agent and vascular endothelial

growth factor (VEGF), a regulator of angiogenesis, which can also participate in tumour progression [119].

There is now increasing evidence that pericytes can play a natural role as progenitor cells in development and in various injured tissues. Perivascular cells represent a ubiquitous cell population, distinct from tissue specific progenitors such as myogenic satellite cells [120]. However, it has also been demonstrated that pericytes resident in postnatal skeletal muscle differentiate into muscle fibres and generate satellite cells following chemical damage to the muscle[121], and that they can contribute directly to tooth regeneration by differentiating into odontoblasts[42].

Nonpericyte perivascular cells as MSC ancestors

Cells displaying MSC phenotypic and developmental properties have also been isolated from the *tunica adventitia* of the human pulmonary artery [122]. The *tunica adventitia* was long considered an inactive component of blood vessels mainly functioning as structural support for the *tunica media*. Only recently has it been demonstrated that the adventitia plays a crucial role in vascular remodeling and the development of vascular diseases including arteriosclerosis and restenosis[123]. Activation of adventitial cells has been described in response to physical stressors including injury [124], vein grafting [125], hypoxia [126] and hypertension [127]. In these settings adventitial cells may differentiate into myofibroblasts that migrate into the inner layers of the vascular wall, alter extracellular matrix deposition, and release paracrine factors regulating vascular remodeling [128]. In apoE$^{-/-}$ mice Hu *et al.* [125] identified and isolated Sca1+ adventitial cells able to differentiate *in vitro* and *in vivo* into smooth muscle cells. It has subsequently been demonstrated that the differentiation potential of adventitial cells is not restricted to myofibroblasts. These observations suggest indirectly that pericytes, exclusively

present around capillaries and microvessels, are not the only ancestors of MSC, as hypothesized previously [129].

Along a systematic search by flow cytometry for alternative non-pericyte cells at the origin of MSC, Corselli *et al.* identified a subset of CD34+ CD45- CD56- CD146- NG2- cells in the *tunica adventitia* of human arteries and veins [83]. These adventitial cells grew like MSC in culture and exhibited typical MSC differentiation properties. Interestingly, adventitial cells express natively the MSC markers CD44, CD73, CD90 and CD105. No potential to give rise to MSC in culture was detected outside the perivascular subsets including pericytes and adventitial cells.

Although pericytes and adventitial cells have been described for more than a century, it is only recently that the blood vessel wall was demonstrated as a reservoir of progenitors. It is now clear that perivascular cells, i.e pericytes and adventitial cells, are *in vivo* counterparts of MSC obtained in culture from various organs [110] [130]. These perivascular cells can be prospectively purified by flow cytometry using a well-defined surface marker combination, common in all human organs tested. Importantly, pericytes and adventitial cells dissociated from vessel walls contain multipotent precursors with robust regeneration properties similar to those of classic heterogeneous MSC.

A Perivascular Niche for MSC precursors

A perivascular niche for MSC-like cells throughout the body is intuitive. A rich supply of mesenchymal progenitors within all vascularised tissues facilitates a swift reparative and regenerative response to injury. A schematic diagram of proposed roles of MSC *in vivo* in normal tissue homeostasis, and in response to injury, can now be proposed

(Figure 2, p19). As a result of injury, MSC are dislodged from their attachment domains in vessels and become 'activated' MSC, which divide and contribute to a regenerative microenvironment. Bioactive factors inhibit immunosurveillance of the damaged tissue, preventing autoimmunity, while vascular in-growth is stimulated. Some of the MSC, or their progeny, may serve as progenitor cells for the regeneration of the damaged tissue, or might stimulate the mitosis of the tissue-intrinsic progenitors that replace the damaged tissue. Therefore, these cells can contribute to tissue regeneration through direct differentiation into tissue-specific mesodermal lineage cells and/or through paracrine mechanisms promoting angiogenesis, immunomodulation and survival. PSC have now been extensively characterised, and they exhibit defined identity and purity[131]. Importantly, purified PSC also exhibit defined potency with respect to *in vivo* chondrogenesis, *in vitro* and *in vivo* myogenesis, and *in vivo* BMP-2 stimulated osteogenesis[14].

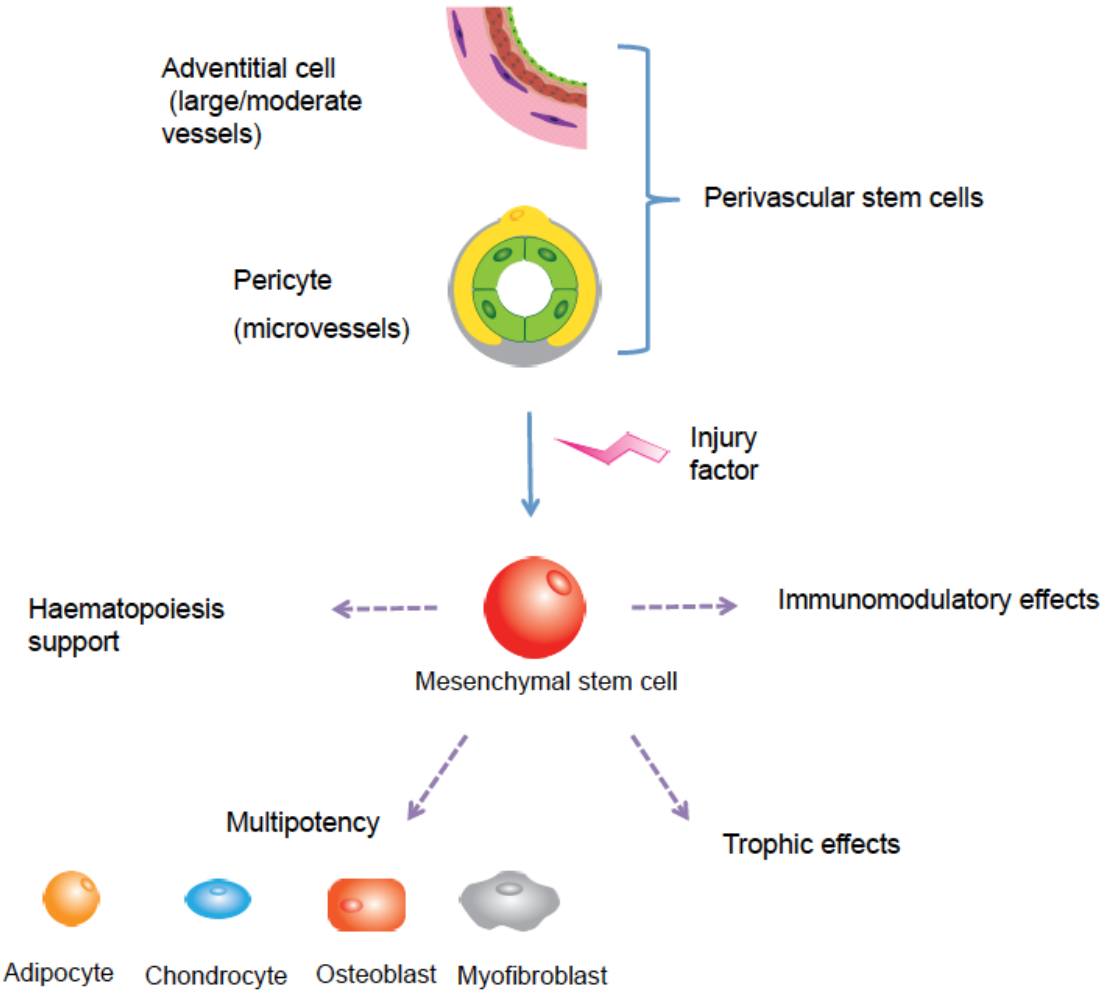

Figure 2 Following mesenchymal 'activation', pericytes can express a mesenchymal phenotype.
Diagram showing proposed roles of perivascular stem cells (PSC) in normal tissue homeostasis and in response to injury. In the latter, pericytes and adventitial cells are released from the vasculature, becoming activated mesenchymal stem cells (MSC), which proliferate, contribute to regeneration through multipotency, organise a regenerative microenvironment, and regulate local immune responses. MSC are also able to support haematopoiesis, and contribute to normal tissue turnover. [Modified from Murray *et al,* Bone Joint J. 2014 Mar;96-B(3):291-8]

PSC as regenerative units

There is accumulating data to confirm that PSC exhibit their MSC characteristics and serve as regenerative units in native tissues. Pericytes have been shown to contribute to the turnover of mesenchymal tissues in normal homeostasis and in response to

injury through differentiation, while their capacity to regulate local immune environments and secrete trophic factors in response to injury is increasingly described.

Pericytes can contribute to skeletal myoblasts and satellite cells, and odontoblasts.

Through the long term culture of human muscle, Dellavalle *et al.,* isolated a pericyte-like population of cells that showed heterogeneous expression of pericyte markers NG2, PDGFRβ and aSMA and more reliably alkaline phosphatase (AP), and were negative for myogenic markers[120]. In appropriate *in vitro* conditions, a proportion of these cells were capable of myogenic differentiation, and following expansion in culture and injection into dystrophic mice these pericytes yielded a measurable improvement in muscle function[120]. Using a tamoxifen inducible Cre recombinase under the control of AP, they were able to demonstrate that AP+ pericytes enter myogenesis and contribute to maturing myofibres during development as well as in response to injury in the early post-natal period[121]. Further lineage tracing studies indicate that pericyte contribution to myofibres varies among different muscles, ranging from <1% (tibialis anterior muscle) to 7% of the fibres (diaphragm) and is enhanced (although only modestly) by acute or chronic muscle regeneration. In addition to contributing to the myoblast pool, pericytes can also contribute directly to the satellite cell pool, during unperturbed, postnatal growth of the mouse. When pericytes are isolated and cultured from postnatal skeletal muscle in appropriate conditions, they show the ability to undergo skeletal myogenesis although some variation is seen between donors. Using an inducible NG2-Cre system, Feng *et al.,* demonstrated that pericytes contribute to regeneration of tooth following injury by differentiating into odontoblasts although other populations of cells are also involved[42].

Implanted pericytes can contribute to myogenesis

Given the observation that pericytes can differentiate readily *in vitro* into myoblasts in appropriate myogenic conditions, a number of investigators have sought to harness their potential as myogenic precursors. Indeed intramuscular injection of freshly sorted or cultured PCs derived from human adipose or skeletal muscle regenerated human myofibers efficiently in the mouse dystrophic or injured muscle[14]. It has also been shown that intramuscular implantation of dissected human placental villi results in crude outgrowth of human cells in dystrophic mice[115]. In this study cells of human origin participated in host muscle regeneration, revealed by the detection of human dystrophin-positive (hDys3t) and/or human spectrin-positive myofibers. Many of these human myofibers coexpressed human lamin A/C, indicating their sole human origin and not intermediate products of cell fusion. Surprisingly, human myofibers were located at regions distant (up to 2 cm) to the implantation site, suggesting active migration of outgrown human myogenic precursors over long distances [115].

Bioactive factors released by MSC are capable of supporting muscle regeneration through angiogenic and anti-apoptotic effects[49]. The immunomodulatory properties of these cells inhibit immunosurveillance of the injured tissues preventing autoimmunity. Clinical and animal studies of MSC indicate that the release of trophic factors is the primary contribution of pericytes in tissue regeneration, rather than differentiation and engraftment[49].

PSC as regenerative units in cell therapy

Understanding the native anatomical origins of MSC has clinical implications for both cell therapy and also manipulation of tissues resident cells *in situ*. Cell therapy is the

transplantation of human or animal cells to replace or repair damaged tissue. Historically, blood transfusions were the first type of cell therapy and are now considered routine. Bone marrow transplantation has also become a well-established protocol. Bone marrow transplantation and increasingly often peripheral blood mononuclear cells (PBMC) are used to treat blood disorders, including anemias, leukemias, lymphomas, and rare immunodeficiency diseases.

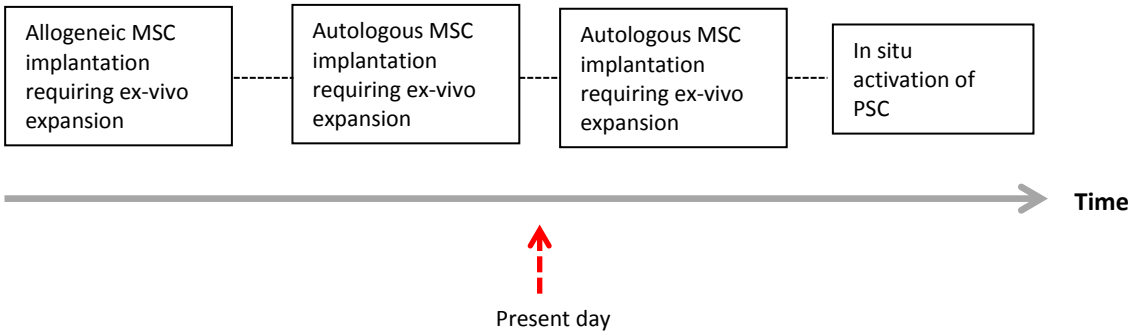

Figure 3 MSC can be used and delivered for therapeutic purposes
In each of these settings MSC may be used with the aim of engraftment, or to harness their trophic or immunomodulatory effects. [Modified from Murray *et al,* Bone Joint J. 2014 Mar;96-B(3):291-8]

The multipotency as well as the trophic and immunoregulatory effects of MSC have vast potential clinical applications, with many treatments already at the stage of clinical trials. The mechanisms by which MSC can be used and delivered for therapeutic purposes is evolving, with researchers seeking to overcome a dependence on allogeneic transplantation and the requirement for *ex-vivo* expansion (Figure 3, p22). Conventional unpurified MSC preparations have significant drawbacks including contamination from non-MSC populations and the requirement of *in vitro* culture to enrich the MSC population. Approaches to delivering cell-based therapies are increasingly being guided by regulatory frameworks. Within these frameworks, cells that require *in vitro* manipulation or culture must undergo stringent safety trials prior

to approval for clinical use while cells that can be directly implanted directly bypass much of this legislation. Many of these drawbacks can be addressed with the ability to identify and isolate pure populations of MSC precursors as perivascular cells using FACS. The practical and therapeutic consequences of understanding the identity and anatomical origin of native MSC have therefore been considerable:

(i) Perivascular stem cells can be sorted to purity

Whole bone marrow cell suspensions and the stromal vascular fraction (SVF) of adipose tissue have been used directly with the aim of harnessing the potential of the contained stem cells. However both represent highly heterogeneous cell populations, which include non-mesenchymal stem cell types, such as inflammatory cells, haematopoietic cells, endothelial cells, and non-viable cells among others [132]. Available studies using SVF show poor and unreliable tissue formation [133], or lower tissue regeneration efficacy relative to cultured MSC [134]. In fact, recent studies have suggested that the presence of endothelial cells have inhibiting effects on bone differentiation, among other lineages [135] [136]. Despite the process of enrichment through plastic adherence, it is inevitable that preparations will be contaminated by non-MSC populations, and the contribution of each contained population to repair process cannot be definitively established. However, it is likely that subsets of functionally distinct cells exist even within purified populations of PSC and MSC. Identification of MSC subsets with the most desirable characteristics for clinical applications is likely to be a major focus of future research. Finally, variability in cell composition presents clear disadvantages for regulatory body (for example the FDA (Food and Drug Administration)) approval of a future stem cell-based therapeutic for tissue engineering, potentially including reduced safety, purity, identity, potency and efficacy. With these regulatory hurdles in mind, and notwithstanding the improved potency

observed with homogeneous cell populations, the use of purified MSC, i.e pericytes and adventitial cells, collectively designated as perivascular stem cells (PSC), has clear practical advantages.

(ii) PSC do not require *in vitro* selection

The selection and preparation of MSC through adherence to culture plastic is time consuming, and introduces additional risks such as immunogenicity and infection through exposure to animal-derived culture products. Investigators have documented the influence of MSC culture on genetic instability [137], and tumorigenicity [138] [139], although these results have been challenged [140]. Multipotentiality hence therapeutic potency has been shown to diminish with serial passaging, with human BM MSC progressively losing their potential for adipogenic and chondrogenic differentiation potential as the number of cell divisions increases [141]. Regardless of the protocol for culture expansion, MSC undergo replicative senescence in culture limiting their clinical applications[142]. In addition, expression of adhesion molecules and chemokines, and the ability to respond to chemokines decline with time in culture [141].

(iii) PSC can be isolated in sufficient numbers to negate *ex-vivo* expansion

In addition to the advantages of negating the need for *in vitro* selection of MSC, the ability to isolate PSC from adipose tissue in clinically relevant numbers has significant therapeutic implications. Low stem cell numbers and high donor site morbidity limit the use of fresh autologous bone marrow [138] [143], periosteum [144] and the majority of other MSC sources. Adipose tissue represents a largely dispensible source of MSC, that are readily accessible through lipoaspiration, even in patients of healthy weight [145]. It has attracted much attention as a potentially plentiful source of MSC, particularly using uncultured cells (SVF or PSC) but also with cells following *in vitro* expansion. Relative

to the lower yield, limited donor sites, and high morbidity associated with bone marrow or periosteal harvest, adipose tissue is now a well-documented, easily accessible, abundant source of such cells. James *et al.* reported the yields from lipoaspirate isolated from 60 consecutive donors in cosmetic procedures [112]. From 100 ml of whole lipoaspirate the mean yield of total nucleated cells (SVF) was $39.4x10^6$ (range $10 x10^6$ to $70 x10^6$). On FACS sorting, pericytes most frequently represented 30% or less of total SVF (mean 19.5%) with adventitial cells representing 40% or less (mean 23.8%) of total SVF. When added in combination, the total PSC content most commonly fell between 30% and 60% of total viable SVF (mean, 43.2%; median, 41.7%). Given this prevalence of PSC, it has been estimated that less than 200 ml of lipoaspirate would be sufficient starting material for the clinical application of PSC in localized bone repair. For example, 200 ml of lipoaspirate would theoretically yield 31 million cells, which would be sufficient for healing of a 2-cm mid-diaphyseal femoral defect (cell seeding density of 1 million per 0.4 ml) [112 146]. In cases where there is a requirement for extremely large numbers of cells (for example GVHD where 1-2million cells/kg body weight may be required for infusion) or where the availability of fat for lipoaspirate is limited, some expansion in culture is inevitable.

In addition to the requirement for robust trials to demonstrate safety and efficacy of PSC for tissue regeneration, a number of practical challenges must also be overcome before widespread clinical application of this technology. The number of facilities currently set up with flow sorters to produce clinical grade cells in accordance with a formal accreditation from State or other body is currently limited. The financial costs of clinical grade sorting, taking in account the price of the antibodies (also certified for clinical purposes) is high. However, this may be offset by savings made by the lack of requirement for expansion in culture. The use of the use of an automated clinical

grade immunodepletion system has been proposed as a more affordable alternative for bulk sorting to FACS. However, the complex phenotype of PSC, and the requirement for both positive and negative selection render this impractical.

Conventionally derived MSC and purified PSC – emerging pre-clinical and clinical data

There is a rapidly expanding body of pre-clinical data evaluating the potential therapeutic benefits of exogenous MSC. The list of MSC-related applications includes a broad and diverse range of clinical targets (Table 4, p27)[49]. Almost all of these trials and preclinical models utilize conventionally derived MSC for their immunomodulatory or trophic effects rather than their ability to differentiate in different cell lineages. The limited emerging data from animal studies confirm that PSC are at least as effective as conventionally derived MSC in terms of clinical effect [131] [146]. It is expected that the added benefits of prospective isolation and the avoidance of culture will enable these treatments to become more accessible to patients from a wider range of conditions.

Potential Clinical Application of MSC (non exhaustive list)
Bone regeneration
*Skeletal defect healing[147]
Osteoporosis[148 149]
Osteogenesis imperfecta[150]
Cartilage regeneration
* Cartilage defect healing[147]
Meniscus injury[151]
*Rheumatoid arthritis[152 153]
*Osteoarthritis[154]
Muscle regeneration
*Skeletal muscle regeneration[155]
*Cardiac muscle regeneration[156]
Smooth muscle regeneration[157]
Tendon Regeneration
*****Repair of tendon defects[158]
Neural regeneration and injury prevention
Traumatic brain injury[159]
*Spinal cord injury[159]
*Multiple sclerosis[159]
*Parkinson's disease[159]
*Multiple system atrophy[159]
*Ischemic stroke[160]
Prevention of injury in acute ischemia
*Ischemic stroke[160]
*Limb ischemia[161 162]
*Acute lung injury[163]
*Myocardial infarction[164]
*Acute kidney injury[165 166]
Immunomodulation
*Diabetes, Type I[167]
*Sepsis[163]
*Multiple sclerosis[159]
*Acute lung injury[163]
*Rheumatoid arthritis[152 153]
*Hepatic cirrhosis[168-170]
Other
*Renal failure[163]
*Skin grafting[171]
*Urinary incontinence[172]

Table 4 Potential clinical applications of MSC (non exhaustive list)
*Theses applications are undergoing clinical trials [Modified from Murray *et al*, Cell Mol Life Sci 2014;71(8):1353-74]

PSC at the origins of fibrosis

Fibrosis is characterised by persistence of myofibroblasts

Fibrosis is the pathological persistent accumulation of collagenous extracellular matrix[173]. Fibrosis can impair tissue function and cause chronic disease in a large variety of vital organs and tissues, including skeletal muscle. Despite the diverse range of tissues susceptible to fibrosis, all fibrotic reactions share common cellular and molecular mechanisms. Often starting as a beneficial physiological repair response to organ injury with hemostatic, inflammatory and remodelling phases, fibrosis is characterised by the persistent activity of matrix remodelling myofibroblasts[174]. Multiple cell types have been proposed to fulfil this myofibroblast precursor role, including epithelial cells (via the process of epithelial-mesenchymal transition [EMT])[175 176], bone marrow-derived cells including fibroblasts[177 178] and tissue-resident cells[179]. EMT was initially proposed as a major source of myofibroblasts in fibrotic disease, but recent cell fate-mapping studies in multiple organs in rodent models have shown that EMT does not directly contribute to the pool of collagen-producing myofibroblasts during fibrogenesis *in vivo*[180]. Several recent studies using cutting edge murine genetic cell labelling techniques have identified pericytes as major myofibroblast progenitors in multiple organs[180 181].

Tracing pericytes in organ fibrosis

The rapid increase in sophisticated mouse genetic tools has facilitated cellular fate mapping in a diverse range of biological processes. The Cre/loxP system which is widely used for this purpose employs the gene for bacterial Cre recombinase (Cre), which is linked to a cell- or lineage-specific promoter prior to incorporation in the genome of a transgenic mouse. Fate mapping experiments commonly employ inducible

Cre strains which enable temporal and spatial control of Cre expression, as Cre expression in these mice only occurs in the presence or absence of exogenous compounds (commonly tamoxifen). Using a range of these techniques a central role for pericytes as myofibroblast precursors has been shown in the kidney[181], central nervous system[182], liver[183] and lung[180].

Origins of fibrosis in skeletal muscle

The native source of myofibroblasts in skeletal muscle has been less investigated. Pericytes (identified by expression of AP) are increased in biopsies from patients affected by different forms of muscular dystrophy, implicating a role for them in the fibrotic process[184]. The most robust study exploring myofibroblast pre-cursors in skeletal muscle was performed by Dulauroy *et al*.[185], who examined the role of ADAM12+ cells following muscle injury. Initial studies demonstrated that transient expression of ADAM12 identifies a distinct pro-inflammatory subset of stromal cells that become activated following injury. The authors then fate-mapped these cells using an inducible, tetracycline transactivator based system. This involved the generation of triple transgenic mice that expressed tetracycline transactivator under control of the ADAM12 locus, Cre under control of the tetracycline transactivator and the conditional reporter Rosa26floxSTOP-YFP locus. In these mice, yellow fluorescent protein (YFP) labelling of the progeny of ADAM12+ cells was temporally controlled by the administration of doxycycline to prevent Cre expression. This allowed the separate fate-mapping of fetal and adult ADAM12+ cells following CTX induced muscle injury. The genetic strategies employed by the authors, combined with a parabiosis experiment, allowed them to demonstrate that the majority of collagen-producing, αSMA+ myofibroblasts developing following acute dermal or muscle injury are generated from tissue-resident ADAM12+ cells. Furthermore, ablation of ADAM12+ cells in skeletal muscle (using mice that also expressed the human diphtheria toxin

receptor under control of the ADAM12 locus) markedly reduced the generation of profibrotic cells and interstitial collagen accumulation. The authors were able to demonstrate that the ADAM12+ profibrotic progenitors developing in injured skeletal muscle originate from ADAM12+ perivascular cells.

Global burden of muscle disease

The global burden of disease study of 2010 estimates that 1.7 billion people worldwide are affected by musculoskeletal disorders, making them the greatest cause of disability in terms of disability adjusted life years[186]. Muscle is affected by a broad range of conditions from congenital dystrophies characterised by wasting, fatty infiltration and fibrosis to pathological responses to injury including heterotopic ossification. As progenitors of osteoblasts, adipocytes and myofibroblasts, pericytes are emerging as central protagonists in these conditions and as a result represent key cellular targets for future therapies.

Heterotopic ossification

Myositis ossificans traumatica is characterised by heterotopic ossification (calcification) at the site of injured skeletal muscle. Up to one-third of all patients undergoing hip arthroplasty or who have had a severe long bone fracture develop heterotopic ossification that can result in pain, swelling and restricted range of motion[187]. Myositis ossificans progressiva (also known as fibrodysplasia ossificans progressiva or FOP) is an extremely rare inherited condition in which ossification in muscle and connective tissues and occur spontaneously or following injury[188]. Although the mutation for FOP is known, this is merely a proximate genetic cause – the cells that respond by forming bone in acquired and genetic forms of heterotopic ossification are not known. As pre-MSC resident in skeletal muscle with robust

osteogenic potential, pericytes have emerged as key candidates[189]. Understanding why these progenitors pathologically express their osteogenic potential in this setting may provide insights into future therapies.

Fibrosis

In skeletal muscle, fibrosis is often associated with the muscular dystrophies which are a molecularly and clinically heterogeneous group of diseases. Phenotypically these diseases are characterized by fatty infiltration of muscle tissue, muscle wasting and fibrosis which compromise function and mobility. In the most severe cases, such as Duchenne Muscular Dystrophy (DMD, caused by lack of dystrophin protein), muscle loss and fibrosis can cause premature death through respiratory failure[190]. Patients are given corticosteroids which prolong muscle strength and walking capacity in the early years, but eventually lead to disabling secondary effects[191]. There is no effective clinical treatment to combat or attenuate the underlying fibrosis[192].

Acute muscle injuries are a common problem in trauma and orthopaedic surgery. Skeletal muscle injuries constitute the majority of sports-related injuries in many epidemiological studies[193] [194] and almost all orthopaedic surgical procedures involve incision through muscle. Moderate to severe muscle injuries in athletes may result in inability to train or compete for several weeks and have a high tendency to recur[195]. Muscle injuries undergo the healing phases of degeneration, inflammation and fibrosis, with established fibrosis resulting in diminished function and susceptibility to re-injury. Fibrosis that occurs following surgery can restrict rehabilitation and functional outcomes and makes secondary or revision procedures technically challenging. Currently there are no European Medicines Agency (EMEA)- or Food and Drug Administration (FDA)-approved anti-fibrotic therapies, underscoring the urgent need for potent and novel treatments for tissue fibrosis.

Architecture of skeletal muscle

Skeletal muscle makes up about 45% of total human body weight. As part of the locomotor system the primary task of the musculature involves moving and stabilizing the skeleton. Therefore, muscles are attached to the bones by collagen-rich tendons. Innervation is carried out by the somatic nervous system so that (almost) all skeletal muscles may be controlled voluntarily. A motor neuron and its associated muscle fibres make up a motor unit. Fine muscles (e.g. outer eye muscles) have small motor units and therefore can be controlled more precisely in comparison to gross muscles (e.g. back muscles).

A layer of dense connective tissue, called the epimysium surrounds each muscle and is continuous with the tendon. Skeletal muscle is composed of numerous fascicles which are surrounded by a connective layer termed perimysium. These fascicles contain bundles of muscle fibres (myofibres) which are themselves separated by connective tissue called endomysium. Each myofibre is a multinucleate syncytium formed by fusion of immature muscle cells termed myoblasts and is around 20-100 μm thick and up to 20 cm long. The myofibers of skeletal muscle are long, cylindrical cells that possess multiple, peripheral nuclei (Figure 4, p34).

Myofibres can be type 1 or type 2 based on physiologic properties. Type 1 myofibres (slow-twitch or slow-oxidative fibres) have a slow contraction time following electrical stimulation and generate less force than type 2 myofibres. Type 1 myofibres are equipped with numerous large mitochondria and abundant lipid for oxidative stress and are used for sustained, low level activity. Type 2 myofibres (fast twitch or fast-glycolytic fibres) have a rapid contraction time and are specialised for anaerobic

metabolism. As such these fibres contain smaller, less numerous mitochondria, less lipid and have larger glycogen stores than type 1 fibres. The ratio of type 1 and type 2 myofibres varies between muscles based on function – for example over 95% of the fibres in tibialis anterior muscle are of type 2.[196] The innervation of a particular muscle fibre determines whether it is a type 1 or type 2 fibre. As such, if the type of motor neuron innervating a myofibre is changed, that myofibre acquires a new phenotype from its new innervation.

In healthy adult muscle, muscle fibres are of relatively uniform size and shape fitting together in a mosaic pattern. In normal muscle, less than 3% of myofibres should have nuclei located in the center of the myofibre (internal nuclei), with over 97% of nuclei located in the periphery of the cell. In addition to myofibres, the "muscle neighbourhood" is composed of satellite cells that reside beneath the basal lamina and constitute the major muscle stem cell population. Blood vessels, composed of endothelial cells, permeate the interstitial space of the muscle fibers, and in addition to providing a blood supply the endothelial cells promote satellite cell proliferation through secretion of growth factors and delivery of circulating inflammatory cells. Pericytes actively contribute to postnatal muscle growth and regeneration. The interstitial space is occupied by mesenchymal progenitors as well as connective tissue cells. Microvessels plunge into and penetrate muscle fascicles with larger vessels and nerves organised in neurovascular bundles between perimysium.

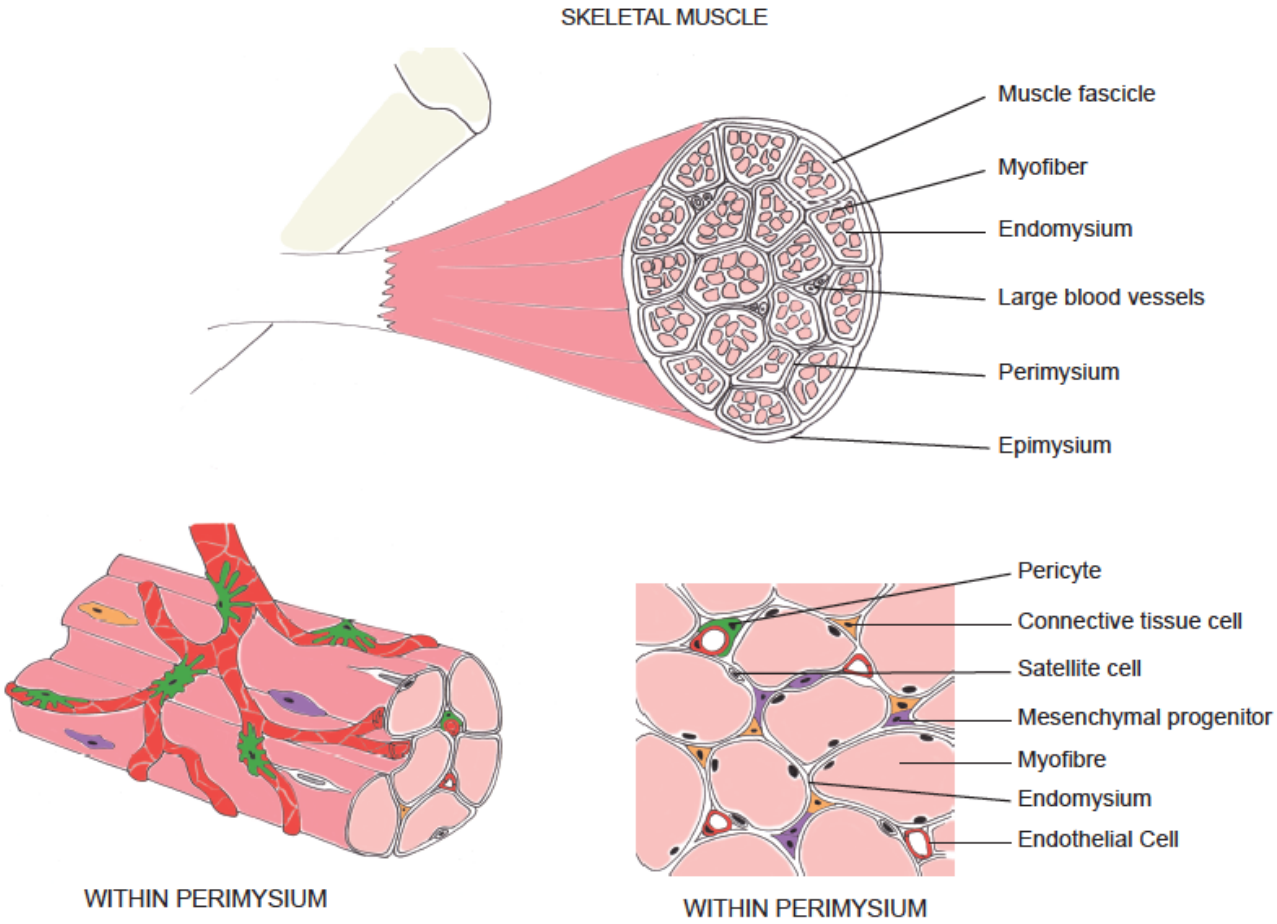

Figure 4 Skeletal muscle architecture
(illustration by Iain Murray, based on images from: Pannerec A, Morazzi G, Sassoon D. Stem Cells in the hood: the skeletal muscle niche. Trends in Molecular Medicine 2012;18(10):599-606

Progenitors in adult skeletal muscle

It is now recognised that several distinct populations of multipotent cells exist within skeletal muscle. These cells may have myogenic potential, capable of regenerating and replacing damaged myofibres, they may contribute to the regenerative response through the release of trophic factors, or they may modify the immune response. These progenitor populations may result in aberrant calcification, fatty accumulation or deposition of ECM in disease settings. Many of these populations do not have specific markers, with overlapping characteristics and phenotypes, while the nomenclature is often unhelpful or misleading. To minimise confusion these populations are briefly summarised below and in Table 5 (p38).

Progenitors with myogenic potential

Satellite Cells

The principal stem cell involved in the regeneration of myofibres is the satellite cell[197]. These cells, most reliably identified by expression of paired box transcription factor Pax7, are located between the basal lamina and sarcolemma of myofibres remaining quiescent until recruited to contribute to myofibres or self-renew[198-200]. Lineage tracing and serial transplantation studies have conclusively demonstrated that satellite cells [201] [202] generate myofibres and self-renew, replenishing the existing stem cell pool[203-206]. The absolute requirement for satellite cells in myogenic repair has been demonstrated through genetic ablation of Pax7 cells in adult mice, suggesting that satellite cells are an exclusive source of stem cells in the regeneration of skeletal myofibres [207-209].

Side population cells

Muscle resident 'side population' cells located in the interstitium with myogenic potential have been described by several groups. Subpopulations expressing CD34, Sca-1 and Pax7 have been described. They are able to differentiate into myofibres *in vitro* when exposed to myogenic factors[210], when cocultured with myoblasts[211], and when injected into regenerating muscle[212 213]. These cells were first identified by Gussoni *et al.*, by the preferential exclusion of Hoechst 33342 and the ability to give rise to dystrophin positive myofibres[212]. Other than their apparent ability to efflux Hoechst, the functional differences between these 'side population' cells and the other progenitors with myogenic potentials is not entirely clear.

PICs

A population of myogenic cells have been identified by the expression of the stress mediator PW1. These PW1+/Pax7- interstitial cells (or PICs) were first isolated by Mitchell *et al.,* by FACs sorting on the basis of cell surface antigen expression (CD45-/Ter119-/Sca1+/CD34+)[214]. These cells were capable of acquiring Pax7 and differentiating into myoblasts, particularly when in coculture with myoblasts. *In vivo* studies have confirmed their capacity to regenerate myofibres following transplantation into injured muscle, while also contributing to the satellite cell pool and self-renewing[214].

Myoendothelial cells

Skeletal muscle contains a population of cell that co-express myogenic and endothelial markers and are capable of regenerating myofibres and differentiating into myogenic, osteogenic and chondrogenic lineages under appropriate culture conditions[215].

Non-myogenic progenitors

Fibro/adipogenic progenitors (FAPs)

Skeletal muscle progenitors with bipotent fibro/adipogenic potential which do not arise from the myogenic lineage have been described by several groups[216-218]. Using FACS, Joe *et al.,* isolated murine FAPS (CD45-/CD31-/alpha7integrin-/Sca1+/CD34+) while Uezumi isolated a phenotypically and functionally equivalent population (CD45-/CD31-/C2.6-/PDGFRα+). FAPs spontaneously differentiated into adipocytes and fibroblasts in *in vitro* culture[217]. The close association of FAPs with regenerating myofibres, together with their expression of factors influencing myogenic differentiation such as IGF-1 and IL-6 suggests that these stromal cells play a supportive role in myogenic differentiation[217]. However, FAPs can also give rise to ectopic adipocytes that accumulate in degenerating muscles *in vivo*[218]. The fibrogenic potential of PDGFRα+ population has also been verified *in vivo* following transplantation of GFP labelled cells into cardiotoxin injured muscle. A contribution of this population to aberrant cartilage and bone production in models of heterotopic ossification has also been demonstrated using lineage tracing studies based on a Tie2-driven Cre-dependent GFP reporter. 90% of these cells were PDGFRα+/Sca1+. FAPS are localised to the muscle interstitium, adjacent to myofibre-associated blood vessels [217 219], although they lack expression of the pericyte makers NG2 and CD146[220].

Population	Cellular markers	In vitro	In vivo	References
Satellite Cells	Pax7, CD34, Myf5, caveolin-1 and VCAM1	Myogenic and fibrogenic	Myogenic	202 203-206 221 222 223
Side Population Cells	Hoechst-negative	Myogenic, adipogenic, fibrogenic, osteogenic and haematopoietic	Myogenic	211-213
PICs	PW1, Sca-1 and CD34	Myogenic (smooth muscle)	Myogenic	214
Myo-endothelial cells	CD56, CD34, CD144	Myogenic, osteogenic, chondrogenic	Myogenic	215
FAPS	Sca-1, CD34, PDGFRα, ADAM12	Adipogenic, fibrogenic, osteogenic and chondrogenic	Adipogenic, fibrogenic, osteogenic and chondrogenic	185 217-220 224
Pericytes	AP, PDGFRβ and NG2	Myogenic, adipogenic and osteogenic	Myogenic, Osteogenic	110 115 120 121

Table 5 Summary of differing populations of skeletal muscle progenitors.
(VCAM1, vascular cell adhesion molecule 1; ADAM12, A Disintegrin And Metalloproteinase 12; AP, Alkaline phosphatase)

The response to skeletal muscle injury

Following skeletal muscle injury a series of well-coordinated events takes place that serve to repair the damaged tissue (Figure 5, p39). These events are initiated by the release of growth factors and cytokines from injured blood vessels and infiltrating inflammatory cells. Cytokines promote the migration, proliferation and survival of various cell types at the injury site, while inflammatory cells phagocytose cell debris. The formation of new muscle fibres begins with the activation of quiescent satellite cells that reside beneath the muscle basal lamina. Satellite cells then proliferate extensively and commit to the myoblast lineage, either fusing to each other to generate new myofibres or fusing to established, injured myofibres. Pericytes make a minor

(<5%) contribution to the regenerating myofibres. Basement membranes of necrotic myofibres serve as a scaffold to guide the orientation of myofibres generated from satellite cells while also guiding the formation of neuromuscular junctions. The basement membrane of necrotic fibres is eventually phagocytosed during the final stages of muscle regeneration. In parallel, muscle repair requires the migration and activation of tissue resident fibroblasts which produce ECM components. Following minor injury and in the absence of chronic inflammation these ECM components are degraded as regeneration and growth of new myofibres proceeds. New vascular networks are also established. Finally, growth and maturation of newly formed muscle fibres occurs. Disruption at any of these stages can result in compromised muscle regeneration, typically characterized by persistent myofibre degeneration, inflammation and fibrosis. Similarly, in the setting of moderate to severe injury or chronic inflammatory events, the persistence of activated myofibroblasts inevitably results in excessive ECM accumulation and fibrosis.

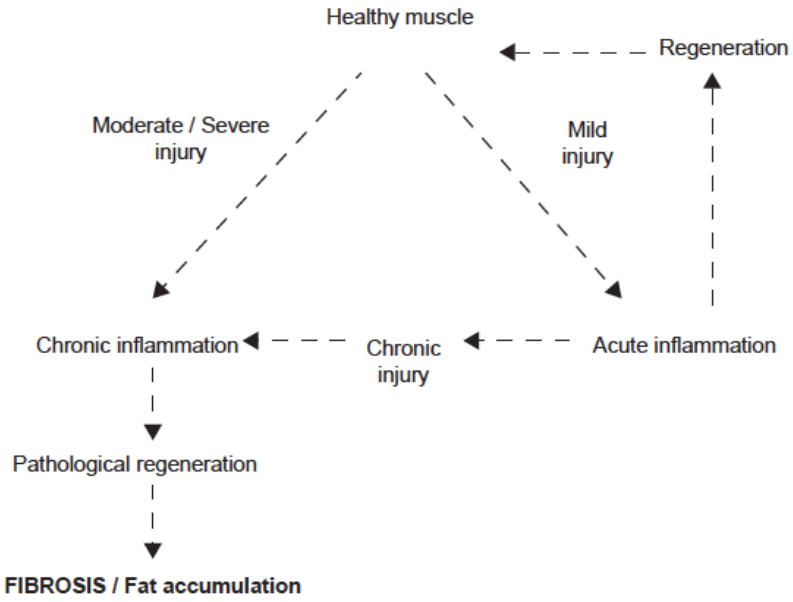

Figure 5 Stages in the response to muscle injury

SECTION 1: ENDOTHELIAL CELLS ACCELERATE THE OSTEOGENIC DIFFERENTIATION OF PERICYTES

Chapter 1.1 Introduction

Adult stem cell niches

Adult stem cells

Adult stem cells are found in almost all organs of the postnatal human body where they are a source for organ-specific cell replacement either during the normal cell turnover or under pathological conditions. They reside within niches that regulate how they participate in tissue generation, maintenance and repair [225 226]. Some adult stem cell types, such as haematopoietic stem cells (HSC) or enteric stem cells, have a high proliferation rate in normal tissue maintenance, whereas in other organs adult stem cells only divide under certain conditions, stimulated by injury, for example.

Stem cell niches consist of both anatomic and functional dimensions, integrating signals that mediate the ability of stem cells to remain within the niche, self-renew or exit and differentiate [227]. Niches are capable of modulating stem cell function in response to physiological challenges or injury. This dynamic capability is particularly important to the realisation of regenerative medicine. However, niches may also contribute to disease by imposing aberrant function on stem cells. In contrast to ES cells, the differentiation potential of adult stem cells is regarded as more restricted, usually to the cells of the tissue in which they reside. This suggests that differentiation of an adult stem cell into a specialised cell is dependent on the surrounding tissue. However, this classical paradigm of tissue-specific differentiation capacity continues to be debated, and has been challenged by observations of a different degree of plasticity in some adult tissues that has resulted in differentiation beyond tissue boundaries[228].

What makes up a stem cell niche?

The niche microenvironment serves as a convergence of signaling pathways that balances the stem cell response to the needs of the organism. Here adult stem cells can receive signals

from neighbouring heterologous cells, the surrounding ECM, neural connections or from paracrine, humoral or metabolic sources.

(i) Heterologous cell types: Numerous examples of heterologous cell types regulating stem cell behaviour within stem cell niches have been described including the regulation of HSC by osteoblasts within bone marrow [229] and the endothelium in the regulation of hippocampal neurogenesis[230]. However, it is not clear whether it is necessary for cell types other than the stem cell itself to be present for a niche to function.

(ii) Extracellular matrix: The basement membrane of the niche may participate in regulation of adult stem cells [231]. Matrix components can contribute stimulatory, or impose inhibitory, influences on the stem-cell pool[232]. Within skin, β1 integrins are known to participate in localisation of the stem-cell population through interactions with matrix glycoproteins [233]. Similarly, tenascin c alters neural stem-cell number and function in the subventricular zone of the nervous system [234].

(iii) Paracrine and humoral factors: Soluble factors are known to be key regulators of stem cell function. The influence of wnts and their antagonists, soluble notch modulators, FGFs and hedgehog (HH) on various niches have been reported [225]. The circulatory system is an obvious means of connecting stem cell reservoirs with information from distant sites.

(iv) Metabolic: Metabolic products allow stem cells to respond to varying conditions of tissue state in real time[225]. p16[1], a cyclin-dependent kinase inhibitor associated with senescence is associated with the presence of reactive oxidative species (ROS).

(v) Neural: Neural connections have been reported to influence stem cell behaviour[235]. For example, mice with altered sympathetic nervous system function lack the ability to mobilize stem cells from the bone marrow in response to granulocyte colony-stimulating factor (GCSF)[235].

[1] also known as cyclin-dependent kinase inhibitor 2A, multiple tumour suppressor 1

The balance of signals from these sources serves to control the behaviour of adult stem cells in terms of quiescence, self-renewal and differentiation [236]. This enables the provision of cells for turnover or repair while ensuring that the niche pools can be sufficiently replenished for futures times of need. A growing number of studies have highlighted the vasculature as a niche for neural, hematopoietic, and MSC[85 236-238].

Mesenchymal stem cell ancestors reside in the perivascular niche

Sources of MSC are not restricted to the bone marrow as first thought. Indeed MSC have been isolated from multiple tissues (Table 1, p5). Pericytes are presumptive MSC that reside within a perivascular niche in multiple organs. Based on knowledge of well-characterised adult stem cell niches, it is logical that niche components may be involved in their regulation (Figure 6, p45). This appears particularly plausible given the vastly different phenotypes of pericytes seen when they reside within this niche or are dissociated from vessel walls. Indeed a significant obstacle in identification of the perivascular origin of MSC was the reluctance of pericytes to express mesenchymal phenotypes in their native environment[129]. However when dissociated in culture the cells readily differentiated down mesenchymal lineages. Although feasible that pericytes acquire MSC potentials on exiting the vasculature, it is intuitive that they are natively present and environmentally down regulated. Studies using unfractionated stromal vascular fraction (SVF) have demonstrated poor and unreliable tissue formation [133] or lower regeneration efficacy relative to prospectively isolated and purified MSC [133], lending further support to a hypothesis that a cellular component of SVF may have an inhibitory effect on differentiating MSC. Osteogenic and adipogenic differentiation is not seen within the perivasculature of healthy tissues where the pericyte/EC

relationship is undisturbed. However, disturbed pericyte/EC relationships have been observed in conditions associated with pathological mineralisation and adipogenesis (e.g. heterotopic ossification and atherosclerosis)[232 239]. In addition, the extracellular matrix (ECM) proteins, also present within a perivascular niche, have been shown to modify growth and differentiation of MSC, with collagen 1, fibronectin and vitronectin treated plates enhancing mineralization in vitro[240].

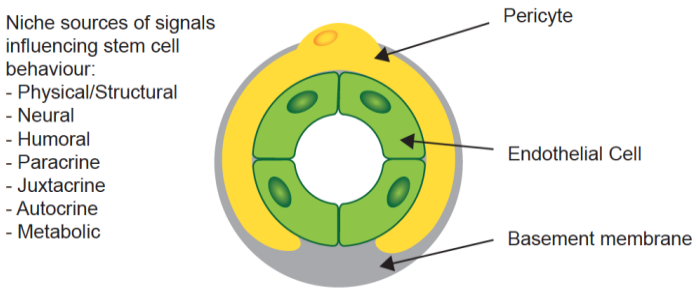

Figure 6 Components of the perivascular niche for MSC-precursors
Here, adjacent EC, extracellular matrix, paracrine, humoral, metabolic and neural factors control the balance between quiescence, self-renewal and differentiation.

Pericytes/Endothelial Interactions – what is known?

Although the concept of a perivascular niche for MSC precursors is relatively novel, interactions between pericytes and EC have been studied extensively in the context of angiogenesis. Knowledge gained in these settings is likely to be relevant to understanding the regulation of pericytes in their roles as MSC-precursors.

Genetic mouse models have demonstrated that these two vascular cell types are interdependent; primary defects in one cell type have obligated consequences for the other. There is growing evidence to suggest that EC can manipulate the migratory and angiogenic properties of pericytes while the intimate anatomical relationship between EC and pericytes suggests close interactions involving paracrine or juxtacrine signalling. Pericytes are

ubiquitously present in blood microvessels where they extend primary cytoplasmic processes along the abluminal surface of the endothelial tube. They are enveloped in a basement membrane that is continuous with the EC basement membrane to which both cells contribute [241 242]. The majority of the pericyte-EC interface is separated by basement membrane, with the two cell types contacting each other at discrete points through peg and socket type interactions, occluding contacts, gap junctions and adhesion plaques[243 244]. EC to pericyte ratios in normal tissues vary between 1:1 and 10:1 and pericyte coverage of the endothelial abluminal surface ranges between 10% and 70%[43 245]. Pericyte density and coverage appear to correlate with endothelial barrier properties (i.e. brain>lungs>muscle)[246], EC turnover (large turnover=less coverage)[244] and orthostatic blood pressure (larger coverage in lower body parts)[43] in keeping with a role of pericytes in regulating capillary barriers, endothelial proliferation and capillary diameter[246].

The formation of capillary-like structures during angiogenesis requires a series of well-orchestrated cellular events allowing EC and pericytes to migrate into the perivascular space. In vessel sprouting, angiogenic factors (e.g., VEGF) stimulate EC, which in turn start secrete proteases that degrade basement membrane and allow EC invasion. An endothelial column, guided by a migrating EC at the very tip then moves toward a VEGF gradient[243]. Studies of the corpus luteum indicate that pericytes are also capable of guiding sprouting processes by migrating ahead of EC and expressing VEGF[247-249]. Emerging endothelial tubes then secrete growth factors, partly to attract pericytes that envelop the vessel wall, and promote vessel maturation. Key pathways implicated in pericyte-EC signalling include PDGF/PDGFRβ, angiopoietins and tie receptors, sphingosine-1-phosphate signalling, TGFβ signalling, Notch and wnt[245 250-252]. It is believed that pericytes, because of their vessel-embracing position, are able to transfer angiogenic signals along the vessel length by contacting numerous EC. Pericyte recruitment and migration frequently occur in response to pathophysiological events such as wound healing, inflammation, or angiogenesis. Increase of pericyte density by

activation of PDGF-BB/ PDGFRβ signaling pathways has also been detected during wound healing and tumor vascular remodeling[246 253].

Endothelial cells influence the differentiation of MSC

Even without reference to the perivascular niche, a number of investigators have reported that EC influence the differentiation of conventionally (culture) derived MSC with divergent results (Table 6, p48).

Niche Component	Model	Stem cell surrogate	Niche surrogate	Lineage assessed	Effect on differentiation	Context	Proposed mechanism	Investigator
Endothelial Cell	3D	ASC	HUVEC	Osteogenesis	↓	paracrine	↑Wnt	Rajashekhar[135]
Endothelial Cell	3D	ASC	HUVEC	Osteogenesis	↓	juxtacrine	↑Wnt	Rajashekhar[135]
Endothelial Cell	2D	BMSC	HUVEC	Osteogenesis	↑	Paracrine	(Wnt, FGF, PDGF, BMP, TGFβ, Notch)	Saleh[254]
Endothelial Cell	2D	BMSC	HUVEC	Adipogenesis	-	Paracrine	-	Saleh[255]
Endothelial Cell	2D	BMSC	HUVEC	Osteogenesis	↑	juxtacrine	-	Xue[256]
Endothelial Cell	2D	BMSC	HDMEC	Osteogenesis	↑	juxtacrine	BMP-2	Kaigler[257]
Endothelial Cell	2D	BMSC	HDMEC	osteogenesis	-	paracrine	-	Kaigler[257]
Endothelial Cell	2D	BMSC	HDMEC	Osteogenesis	↑	juxtacrine	N-cadherin	Li[258]
Endothelial Cell	2D	BMSC	HDMEC	Osteogenesis	↑	paracrine	VEGF	Grellier[259]
Endothelial Cell	2D	BMSC	HDMEC	Osteogenesis	↓	Paracrine	Osterix/OSX	Meury[136]
Endothelial Cell	2D	BMSC	HUVEC	Osteogenesis	↑	juxtacrine	Cx43/gap junctions	Villars21[260]
Endothelial Cell	2D	BMSC	HUVEC	Osteogenesis	↑	juxtacrine	-	Villars 22[261]
Endothelial Cell	2D	HOP	HUVEC	Osteogenesis	↑	juxtacrine	-	Guillotin[262]
Endothelial Cell	2D	HOP	EPC, HSVEC	Osteogenesis	↑	juxtacrine	Cx43/gap junctions	Guillotin[262]

Table 6 The influence of EC on the multipotency of tissue specific MSC
(ASC, adipose-derived stem cells; BMSC, bone marrow MSC, HOP, human osteoprogenitor cells, HUVEC, human umbilical vein endothelial cells; HDMEC, human dermal microvascular endothelial cells; EPC, endothelial progenitor cells; HSVEC, human saphenous vein endothelial cells)

Regulators of conventional MSC differentiation: overview

The perivascular niche for MSC represents a relatively novel concept and so there have been few studies exploring the regulation of pericyte "MSC" functionality by niche components. However, there is also an extensive literature describing signaling pathways recognized to control MSC fate decisions (Figure 7, p50). These include bone morphogenetic protein (BMP), Sonic Hedgehog (SHH), Wnt, pparg, Sox9 and Runx2. Interestingly, inducers of differentiation along one lineage often inhibit differentiation along the other. For example, the transcription factor peroxisome proliferator-activated receptor gamma (pparg) is a prime inducer of adipogenesis that inhibits osteogenesis highlighting the mutual exclusivity of these lineages[263]. (BMP) signaling molecules (particularly BMP2, BMP4, BMP6 and BMP7) act as major osteogenic inducers and may influence adipocyte differentiation[264]. Downstream pathways of an intercellular sonic hedgehog (SHH) signaling molecule have been shown to inhibit adipogenesis and induce osteogenesis[265]. EC are recognized to actively signal through a number of these pathways. It is likely that signalling mechanisms responsible for the mesenchymal fate of pericytes will be multifactorial and distinct for different lineages. Pericytes have many important roles within specific tissues unrelated to their mesenchymal phenotype (e.g. control of vascular tone and the production of renin within the kidney). These factors may be affected differently by detachment from perivascular niche components.

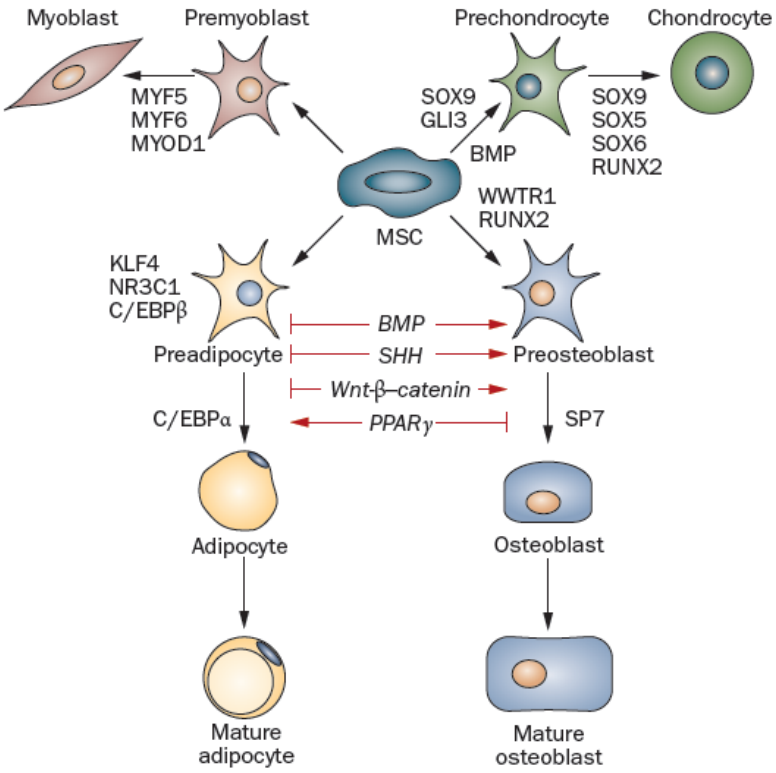

Figure 7 Regulators of MSC fate.
MSC are capable of differentiating into cells of functionally distinct lineages. A number of regulators control MSC lineage fate. (Abbreviations: BMP, bone morphogenetic protein; C/eBP, CCAAT/enhancer binding protein; GLi, GLi family zinc finger; KLF, Kruppel-like factor; MSC, mesenchymal stem cell; MYF, myogenic factor; MyoD, myogenic differentiation 1; Nr3C1, nuclear receptor subfamily 3, group C, member 1; PPARγ, peroxisome proliferator-activated receptor gamma; RUNX2, runt-related transcription factor 2; SOX, sex determining region Y-box; SHH, sonic hedgehog homolog; sP7, sp7 transcription factor (formerly known as osterix); TGF-β, transforming growth factor β; wwTr1, ww domain containing transcription regulator 1 (formerly known as TAZ)). [From Takada I, Kouzmenko AP, Kato S. Wnt and pparδ signalling in osteoblastogenesis and adipogenesis. Nat. Rev. Rheumatology 2009;5:442-447]

Section 1 hypothesis and aims

It is our central hypothesis that interactions with EC modulate the osteogenic differentiation of pericytes.

In order to address this hypothesis the following aims were established.

(i) Isolate pericytes and demonstrate their mesenchymal phenotype *in vitro*

(ii) Generate two- and three-dimensional models of the perivascular niche

(iii) Establish the influence of EC on the osteogenic, adipogenic and chondrogenic differentiation of pericytes.

(iv) Establish a potential role for wnt signalling in the EC mediated acceleration of pericyte osteogenic differentiation

Why is this of clinical importance?

Understanding the native regulation of osteogenic differentiation of pericytes in muscle and other organs is of significant clinical importance. Pathological osteogenic differentiation contributes to heterotopic ossification in over 40% of patients undergoing total hip replacement. Furthermore, down regulating pericyte multipotency has implications for conditions where pathologic pericyte potentials are contributory such as tumorigenesis, atherosclerosis and aberrant calcification. An ability to modulate this process would facilitate future therapies.

In addition, this knowledge could also be harnessed where accelerated osteogenesis is desirable and treatments are currently limited by inadequate graft material. Bone disease has a major impact on the population as a whole and especially on affected individuals and their families. Osteoporotic fractures alone account for 1.5 million fractures in the US annually leading to over 500,000 hospitalizations, with direct costs over $15 billion. There is great

need for improved methods of preventing and treating fractures. Current stem cell strategies depend on the transplantation of cells with additional morbidity of harvesting autologously. Stimulation of osteogenic differentiation by pericytes could improve bone mineral density and even accelerate normal bone healing to reduce treatment times following fracture. Systemic stimulation of pericytes to differentiate into bone could be harnessed in the treatment of osteoporosis. Local targeted stimulation of pericytes could be used to accelerate healing and prevent non-union. The principle of pericyte stimulation could be applied to other lineages including cardiomyocyte, myogenic and chondrogenic differentiation with implications for the treatment of a vast number of medical conditions.

Graphical Abstract

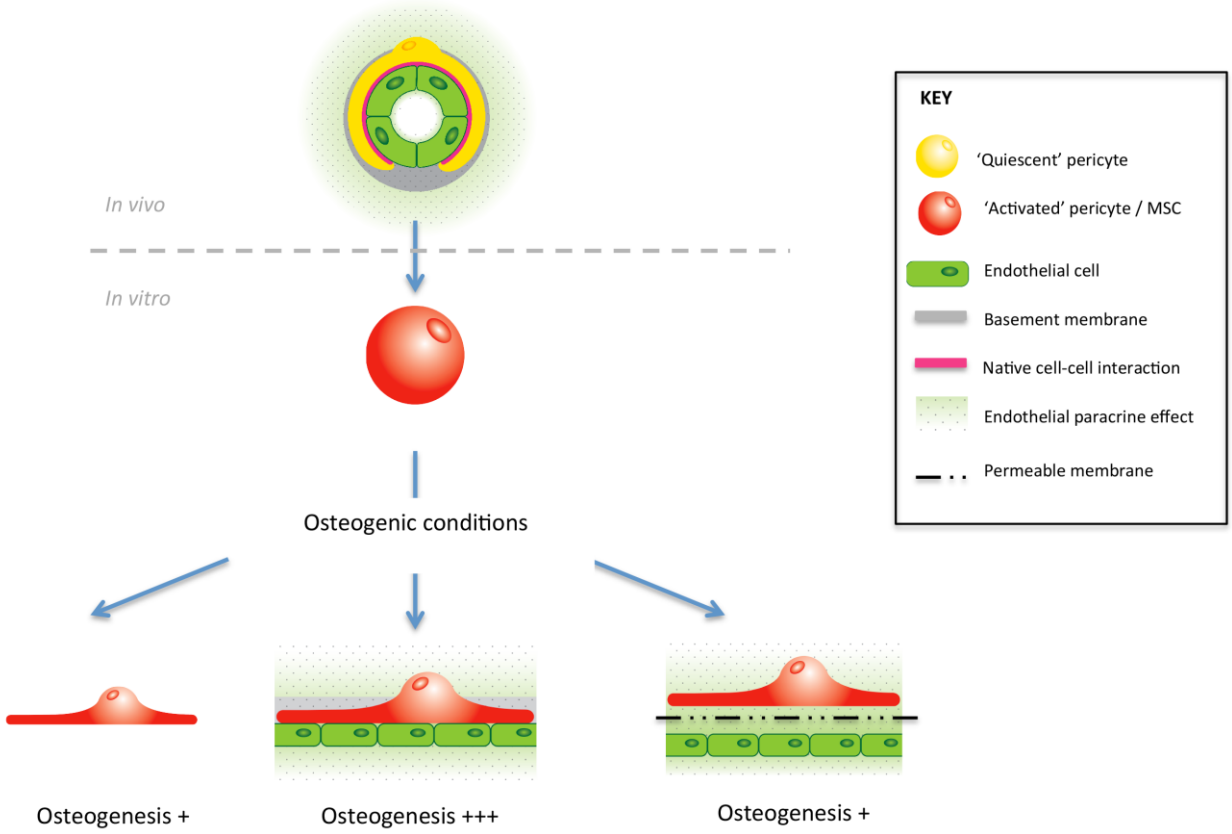

Chapter 1.2 Materials and methods

Sorting of Perivascular Cells

Procurement and storage of tissues

Human foetal tissues were obtained from elective medical pregnancy interruptions, with informed consent from the donor with full ethics committee approval (Lothian Research Ethics Committee 10/S1103/45). The age of the foetus was verified using the crown to rump length and foot length prior to dissection carried out using sterile scissors and forceps. Samples were placed in HBSS/5%FBS/1%PS for transfer to the laboratory and stored for a maximum of 48 hours prior to use.

Adult whole fat and lipoaspirate were obtained from surgery, upon which they would normally have been discarded (Lothian Research Ethics Committee 10/S1103/45). Samples were placed in DMEM/20%FBS/1%PS for transfer to the laboratory and stored for a maximum of 48 hours prior to use.

Extraction of cellular fraction from human foetal tissues

Individual tissues (skeletal muscle and placenta) were cut into small pieces (2mm3) and digested in collagenase containing medium [DMEM with 0.5mg/ml of each collagenase IA-S, II-S and IV-S (Sigma Aldrich)] for 30 min in a shaking water bath (200rpm) at 37oC. An equal volume of DMEM/10%FBS/1%PS was added to halt the digestion and the total suspension was passed through a sterilized nylon mesh to remove large clumps. The suspension was then passed through a 100µm, 70µm, and 30µm strainers consecutively and centrifuged (300 g, RT, 5 min). The supernatant was discarded and the pellet was re-suspended in 5ml red cell lysis buffer (Sigma Aldrich) and incubated at RT for 2 min. 40mls of DMEM/10%FBS/1%PS was added and the suspension centrifuged (1500 rpm, RT, 5 min). The supernatant was again discarded and the pellet was resuspended in 1ml PBS/5%mouse serum (blocking step) with a 10ul aliquot taken

for counting in a haemocytometer using Trypan blue to distinguish non-viable cells. After 10 min of blocking, 40mls of PBS/2%FCS was added and the cell solution entrifuged at 1500rpm for 5 min in preparation for staining (see below).

Extraction of cellular fraction from whole fat and lipoaspirate

Whole fat was grated to increase the surface area prior to digestion. Grated adipose tissue or lipoaspirate was transferred to a flask with digestion medium at a volume ratio of 1:1. The digestion medium was composed of DMEM, collagenase type II (1mg/ml final concentration) and 3.5% bovine serum albumin (BSA). Adipose tissue was incubated in the digestion medium for 30 min in a shaking waterbath (250rpm) at 37^{o}C. An equal volume of DMEN/10%FCS/1%PS was added and the suspension centrifuged for 10 min at 1500rpm. The supernatant was removed with the residual pellet resuspended in 50ml PBS/2%FCS. This cell solution was then passed through a 100µm, 70µm, and 30µm strainers consecutively and centrifuged (300 g, RT, 5 min). The supernatant was discarded and the pellet was re-suspended in 5ml red cell lysis buffer (Sigma Aldrich) and incubated at RT for 2 min. 40mls of DMEM/10%FBS/1%PS was added and the suspension centrifuged (1500 rpm, RT, 5 min). The supernatant was again discarded and the pellet was resuspended in 1ml PBS/5%mouse serum (blocking step) with a 10ul aliquot taken for counting in a haemocytometer using Trypan blue to distinguish non-viable cells. After 10 min of blocking, 40mls of PBS/2%FCS was added and the cell solution entrifuged at 1500rpm for 5 min in preparation for staining (see below).

Fluorescence-activated cell sorting of PSC and EC

In preparation for fluorescence activated cell sorting (FACS), cells were resuspended at a concentration of 30x10^{6}/ml and incubated with all antibodies at the appropriate

dilution (Table 7, p57). As controls, $5x10^5$ cells were incubated with isotype control antibodies in the same conditions. The cell suspensions were incubated with the antibodies on ice and in the dark for 20 min then washed with PBS/2%FBS and centrifuged (300 g, RT, 5 min). The supernatant was then discarded and the cells resuspended in 1ml PBS/2%FBS.

Antibody Specificity	**Conjugate**	**Supplier**	**dilution**	**Isotype control antibody**
CD146	Alexa flouro 647	Serotec	1:100	Alexa flouro – conjugated mouse IgG1 (1:100;serotec)
CD45	APC-Cy7	BD Biosciences	1:100	APC-Cy7 – conjugated mouse IgG1 (1:100; BD Biosciences)
CD56	PE-Cy7	BD Biosciences	1:100	PE-Cy7- conjugated mouse IgG1 (1:100; BD Biosciences)
CD34	FITC	BD Biosciences	1:100	FITC-conjugated mouse IgG1 (1:100; BD Biosciences)
CD31	PE	BD Biosciences	1:100	PE- conjugated mouse IgG1 (1:100; BD Biosciences)
CD144	PerCp Cy5	BD Biosciences	1:100	PerCp Cy5 - conjugated mouse IgG1 (1:100;BD Biosciences)

Table 7 Antibodies and corresponding isotype controls for HUMAN perivascular cell purification and analysis

Cells were sorted using a flow cytometer (FACSAria, Becton-Dickinson). The fluorescence compensation settings were optimized using anti-mouse Ig, κ/negative control beads plus (BD Biosciences) incubated with the range of FACS antibodies used. Unstained cells were used to account for the autofluorescence of samples and fluorescently matched isotypes and fluorescence-minus-one samples were used as negative controls. Prior to selection of perivascular cell populations, a side versus forward scatter plot was used to remove debris then a height versus width plot was used to eliminate doublets. DAPI [0.1-0.5μg/ml (Invitrogen)] was used to eliminate dead cells then cells positive for CD45 and CD56 were negatively gated to remove hematopoietic and myogenic cells respectively. Remaining cells that were positive for CD31, CD34 and CD144 were collected as EC. Cells negative for CD31, CD34, CD144 and positive for CD146 were collected as pericytes. Cells negative for CD31, CD144, CD146 and positive for CD34 were collected as adventitial cells. The cell surface marker

profiles used to distincguish these cell types are summarised in (Table 8, p58). All cells were collected in endothelial cell growth medium [EGM2 (Lonza)]. A portion of the selected populations were reanalysed using flow cytometry to confirm purity. In addition, reverse transcription polymerase chain reaction (RT-PCR) was used during culture to assess transcription of genes expressed by cells that should have been excluded.

Cell Surface Marker	Pericytes	Adventitial Cells	Endothelial Cells
CD45	-	-	-
CD56	-	-	-
CD31	-	-	+
CD144	-	-	+
CD34	-	+	+
CD146	+	-	+

Table 8 Cell surface marker profiles used to distinguish pericytes, adventitial cells and endothelial cells using FACS.

Cell culture

Sorted cells were seeded onto fibronectin coated tissue culture plates, at a density of $2x10^4$ cells per cm^2 and cultured in EGM2 medium in a 37°C, 5% CO_2 incubator. EGM2 medium was changed after 7 days and then three times/wk until 100% confluence was reached. After an initial passage, pericytes and adventitial cells were seeded on uncoated tissue culture plates at $2x10^4$ cells/cm^2 in high-glucose DMEM/20%FBS/1%PS, and grown until confluent in a 37°C, 5% CO_2 incubator. After an initial passage, EC were seeded on fibronectin coated tissue culture plates at $2x10^4$ cells/cm^2 in EGM2, and grown until confluent in a 37°C, 5% CO_2 incubator. On subsequent passages the cells were re-plated in larger vessels with the appropriate volume of medium (Table 9, p59). Once confluent in a T75 flask the cells were passaged at a ratio of 1:6.

Container	Surface Area (cm^2)	Volume of Medium (ml)
1 well of a 96-well culture plate	0.32	0.370
1 well of a 48-well culture plate	0.75	0.5-0.8
1 well of a 24-well culture plate	2	0.8-1
1 well of a 12-well culture plate	3.8	1.5-2.2
1 wells of a 6-well culture plate	9.6	2.5-3
$25cm^2$ culture flask	25	5
$75cm^2$ culture flask	75	10

Table 9 Media volumes used for perivascular cell culture

Surplus cells were frozen in FBS/10% DMSO (dimethyl sulfoxide) at a concentration of $5x10^5$-$1x10^6$ cells/ml in cryovials and stored at -80°C prior to transfer to liquid nitrogen for long-term storage. Cells were also resuspended in TRIzol (Invitrogen) and frozen at -80°C prior to extraction of RNA.

Two dimensional coculture of PSC and EC

Gelatin coated 12-well plates were seeded with HUVEC and cultured in EGM2 until confluent. A single well was sacrificed for counting with pericytes then seeded in isolation or in coculture at a ratio of HUVEC:pericyte 4:1. When overlying pericytes reached 80% confluence wells were transferred to differentiation conditions.

Two-dimensional Transwell co-culture

In order to determine the influence of EC on pericytes independent of direct contact, EC and pericytes were cultured together separated by a semipermeable membrane (0.2μm pores) in a Transwell (Corning) system. Gelatin coated 12-well plates were seeded with pericytes and cultured in EGM2 until confluent. A single well was sacrificed for counting. HUVEC (at a ratio of 4 HUVEC to 1 pericyte) were then seeded onto gelatin-coated Transwell inserts (Corning) and placed within wells. After 24hrs of Transwell coculture in EGM2, wells were changed to osteogenic medium (Lonza).

Three-dimensional coculture of PSC and EC

For the spheres and pellet assays we used a non-endothelial control cell type in order to maintain 3D spheroid size and conditions. We selected human dermal fibroblasts (HDF) as controls, representing a related stromal cell type, but lacking both endothelial and pericyte characteristics.

Spheres assay

Coculture spheroids of pericytes with HUVEC or HDF were generated statically. In brief, equal numbers of suspended pericytes and HUVEC as well as equal numbers of both pericytes and HDF (15,000 cells each per spheroid) were mixed, centrifuged and resuspended in co-culture medium of DMEM: EGM2 (1:1)/ 10% FBS /1%PS. Mixed cells were then seeded into non-adherent round-bottom 96-well plates (Fisher) to generate overnight pericyte/HUVEC and pericyte/HDF spheroids containing 30,000 cells /spheroid.

Pellet culture

Pellet cultures were generated and cultured in basal conditions. Approximately 250,000 pericytes were placed either alone or together with HUVEC or HDF (in 15ml polypropylene falcon tubes) and centrifuged to pellet (1500rpm for 5 min).

Tube assemble (vasculogenic) assay

Pericytes and HUVEC were fluorescently labelled using red (PKH26, Sigma Aldrich) and green (PKH67, Sigma Aldrich) membrane dyes as per manufacturers guidelines. In short, cells were trypsinized, centrifuged to pellet and the supernatant removed. Cells were then resuspended in 5μM PKH24 or PKH67 in pre-warmed serum-free basal medium for 3 min at 37°C. Labelling was terminated by addition of FBS and any unincorporated stain was removed by washing with complete culture medium twice.

Labelled EC were then suspended whether alone or with labelled pericytes in EGM2 to a total concentration of $2x10^4$ cells/ml. 50µl of cell solution was added per well of a 15 well angiogenesis µ-slide (Ibidi), precoated with a thick layer of Matrigel (BD Biosciences) as per slide manufacturer's guidelines. The assembly of vascular networks over time was captured using fluorescent and brightfield time-lapse imaging (Axio Observer, Zeiss).

Differentiation medias

Complete osteogenic and adipogenic media were purchased from Lonza. Chondrogenic medium was made within our lab from published protocols (DMEM containing 10% FBS, 1% PS, 8µl/ml proline, 10µl/ml ITS + Premix [Becton Dickinson; 6.25g/ml insulin, 6.25g/ml transferrin, 6.25ng/ml selenious acid, 1.25 mg/ml BSA, and 5.35 mg/ml linoleic acid], 10µl/ml sodium pyruvate, 1µl/ml transforming growth factor (TGF)-β3, 10µl/ml ascorbic acid and 0.1µl/ml dexamethasone).

Wnt modulators

To investigate the influence of wnt modulators on cultured cells, osteogenic medium was supplemented with ICG (ChemPacific; final concentration 10µM), C59 (Cellagen Technology; final concentration 10µM) and CHIR (Axon; final concentration 10µM).

Pericyte proliferation in coculture

To determine the influence of EC on the proliferation of pericytes, 40,000 pericytes were first seeded into 6 well plates (Corning). Pericytes were cultured alone, in direct co-culture with EC or in indirect "Transwell coculture" as described above. For EC coculture, EC were added to wells or Transwells 4 hours after the seeding of pericytes. At day 3, 6 and 9, wells were trypsinised and total viable cells counted using a haemocytometer with trypan blue used to exclude non-viable cells. Cells from individual wells were then stained with antibody to the EC marker CD144 (BD BioSciences) and analyzed using flow cytometry. The total number of pericytes per

coculture well was extrapolated from the total mixed cell count and the pericyte to EC ratio on flow cytometry.

Immunohistochemistry

Histology and preparation of tissues

Fresh human foetal tissues were frozen in Optimal Cutting Temperature (OCT) compound prior to sectioning. For freezing, tissue was immersed in OCT and lowered into a beaker of isopentane (cooled by surrounding the beaker with liquid nitrogen). 7μm sections were cut using a cryostat at -30^{o}C and mounted on Superfrost slides (Thermo Scientific) and fixed in ice-cold methanol:acetone (1:1) for 5 min. Sections were air dried and stored at -80^{o}C prior to immunohistochemistry.

Detection of perivascular cells in human tissues

Tissue sections were air dried then stained for the pericyte marker NG2. Sections were washed with PBS/Tween20 pH7.4 (2x5 min) then blocked for 1 h with 5% goat serum. After blocking, the cells were incubated with fluorochrome-coupled antibodies overnight at 4^{o}C or were blocked to prevent non-specific avidin and biotin interactions prior to overnight incubation with the primary antibody at 4^{o}C. Sections incubated with primary antibodies were washed with PBS/Tween20 pH7.4 (2x5 min) prior to incubation with the secondary antibody for one hour at RT. All sections were then washed with PBS/Tween20 pH7.4 (2x5 min) and incubated with DAPI (5μg/ml) and Alexa-Fluor coupled streptavidin [1 in 1000 dilution (Invitrogen)] for 45 min. After a final PBS/Tween20 pH7.4 wash (2x5 min) the cells were mounted in fluorescent mounting medium (Dako) and allowed to dry for 1 hr.

Presence of basement membrane proteins (collagen IV and laminin) within microvessels

Sections were stained with antibodies against the basement membrane proteins laminin and collagen IV. The optimal concentration of antibodies was determined in titration experiments. Air dried sections were fixed in ice cold methanol/acetone (1:1) for 10 min, washed with PBS/Tween20 pH7.4 (3x5 min) then blocked for one hour with 5% goat serum prior to overnight incubation with the primary antibody at 4°C. Goat serum (Sigma-Aldrich) was used as an isotype control for the polyclonal goat anti-human collagen IV (Sigma-Aldrich) antibody 1:400. Rabbit IgG (Dako) was used as an isotype control for the polyclonal rabbit anti-human laminin (Millipore) antibody.

Following overnight incubation, sections were washed with PBS/Tween20 pH7.4 (3x5 min). Donkey anti-goat Alexa Fluor 555 (Invitrogen) 1:400 was used as the secondary antibody for collagen IV staining and corresponding isotype. Goat anti-rabbit Alexa 647 (Invitrogen) 1:400 was used as the secondary antibody for laminin staining and corresponding isotype. Sections were incubated for 1 h at RT in the dark. Sections were then washed with PBS/Tween20 pH7.4 (3x5 min), stained with DAPI (5µg/ml). Following a final wash of PBS/Tween20 pH7.4 (3x5 min), sections were mounted with fluorescence medium (Dako).

Considerations for immunohistochemistry in spheres and pellet coculture

For freezing, spheroids or pellets were removed from wells and immersed in OCT prior to freezing as above. 7µm sections were cut using a cryostat at -30°C and mounted on Superfrost slides (ThermoScientific) and fixed in ice-cold methanol:acetone (1:1) for 5 min. Sections were air dried and stored at -80°C prior to immunohistochemistry as above.

Considerations for immunohistochemistry in tube assembly (vasculogenic) coculture

Vascular networks using unlabelled cells were allowed to develop for 4 h following seeding before being fixed with 2%PFA for 15 min. Immunohistochemistry for collagen IV and laminin was performed as described above. However, as Matrigel readily becomes a liquid when cooled, primary incubations were performed at RT for 1 h instead of at 4^{o}C overnight.

Fluorescence imaging

Sections were examined using a fluorescence microscope (Nikon Eclipse E800) and images were captured using a Zeiss camera. Fluorescent and brightfield images of vascular networks were captured using Axio Observer inverted microscope with a Zeiss camera. Max projection images were generated using Image J.

Histological stains

Alizarin Red Osteogenesis Assay

Alizarin red staining for mineralisation was performed using the Osteogenesis Assay Kit (Millipore). In brief, medium was first aspirated and wells washed twice with 2ml PBS. Cells were fixed with 10% PFA at room temperature for 15 min and then washed 3 times with distilled water. Wells were then covered with Alizarin Red stain solution for 20 min at room temperature. Excess dye was then removed and wells washed 4 times with distilled water. Wells were covered with distilled water for visual inspection and image acquisition. Brightfield microscopy was performed using Observer Microscope (Zeiss) with images captured on a Zeiss Colour camera.

Quantitative analysis of Alizarin Red staining was performed by determining OD_{405} values of a set of known Alizarin Red concentrations and comparing these values to

those obtained from unknown samples. In short, 400µl 10% acetic acid was added to each well and incubated at room temperature for 30 min. The loosely attached monolayer was then scraped together with the acetic acid into a 1.5ml microcentrifuge tube and vortexed for 30 s. The sample was then heated to 85^{o}C for 10 min, cooled and centrifuged at 20,000 g for 15 min. 400 µl of the supernatant was transferred to a new 1.5ml microcentrifuge tube and neutralized with 150µl 10% ammonium hydroxide. 150µl of this sample was then added to an opaque walled, transparent bottom 96-well plate and read at OD_{405}. The sample readings were compared with Alizarin Red standards at a high and low range to determine Alizarin Red concentration.

Oil Red O

Oil red O can be used to detect lipid droplets produced by adipocytes, due to high solubility in lipids. Cells were fixed with 4% PFA and washed three times with distilled water, then once with 60% isopropyl alcohol. Stock solution (Oil Red O 0.5% (w/v) in isopropyl alcohol) was diluted 3:2 in distilled water, allowed to stand for 10 min then filtered through a 0.22um filter. This 'working' solution of Oil Red O was added to cells and allowed to incubate for 15 min at room temperature. The cells were then rinsed briefly with 60% isopropyl alcohol, then washed three times with water prior to imaging.

von Kossa

von Kossa staining was carried out to assess mineralisation in the form of phosphate crystals. The principle of this stain is the silver ions react with phosphate and precipitate as a metallic silver under bright light, resulting in black staining. Briefly, cells were fixed in 4% PFA, washed three times with distilled water, then incubated with 5% (w/v) silver nitrate solution before being exposed to a 60 watt light bulb for 10-15 min. This allowed staining of any mineralized matrix produced, but not of the substrates that also contain calcium phosphate. Following exposure, cells were washed

in distilled water and incubated in 5% (w/v) sodium thiosulphate solution for 5 min to remove any unreacted silver nitrate. Cells were washed three times in distilled water and the cells counterstained with DAPI.

Safranin O

Safranin O is a dye that binds to glycosaminoglycans, which make up a large proportion of extracellular matrix found in cartilage[266]. Cells were fixed with 4% PFA for 10mins and washed three times with distilled water and once with 1% acetic acid for 10 s. Safranin O 0.1% (w/v) solution was added to cells and allowed to incubate for 5 min at room temperature. Then the cells were washed three times with water and counterstained with DAPI.

Staining for Cell Viability

Chloromethylfluorescein diacetate (CMFDA) and propridium iodide (PI)

To establish the survival of cells within spheroids, a live/dead assay was performed. Green CMFDA (5-chloromethylfluorescein diacetate) Cell Tracker (MolecularProbes, Invitrogen) was used to visualize live cells, and propidium iodide (PI), a nucleic acid stain, was used to identify non-viable cells. Fluorescence was observed on Z-stack analysis of confocal microscopy images. Max projection images were generated using Velocity 3D Image Analysis software.

Assessment of cell viability within pellets by lactate dehydrogenase (LDH) activity

Viable cells were identified in cryostat sections (8μm) by means of their LDH activity as previously described[267 268]. Tetrazolium salt methods are well-established precipitation reactions that allow observation of the activity of dehydrogenases. Here, enzyme-catalyzed oxidation of lactate, which is a substrate for LDH, releases protons that are picked up by the co-enzyme NAD. The reduced co-enzyme reduces 1-methoxy-

methylsulfate which is an electron carrier that transfers the electrons to the tetrazolium salt to generate formazan, a dark, purple, water insoluble precipitate[269]. Briefly, the reaction was performed using 1.75mg/ml nicotinamide-adenine dinucleotide, 60mm lactic acid, 3mg/ml nitroblue tetrazolium and 50% polypep in 0.05M glycine (all Sigma Aldrich) buffer (pH 8.0). Sections were incubated for 3 h at 37°C in a humidified chamber, subsequently rinsed in warm water, fixed in 4% PFA and mounted.

Molecular biology

RNA extraction

Cells were lysed by repeated pipetting in TRIzol [1ml per 5-10x10^6 cells (Invitrogen)] after which the homogenate was incubated for 5 min at RT. Chloroform (0.2ml per 1ml of TRIzol) was added to the homogenate and the solution was shaken vigorously for 15 s then incubated at RT for 3 min. Samples were centrifuged (12000 g, 4°C, 15 min) and the colourless, upper aqueous phase containing RNA was transferred to a fresh tube and the RNA was precipitated by mixing with isopropyl alcohol (0.5ml per 1ml TRIzol). Samples were incubated at RT for 15 min then centrifuged (12000 g, 4°C, 10 min). The supernatant was discarded and the pellets were washed in 75% ethanol (1ml per 1ml TRIzol) then the samples were centrifuged (7500 g, 4°C, 5 mins). Finally, the pellets were air-dried then dissolved in 20µl of RNAse free water an incubated for 10 min at 55°C. A spectrophotometer (NanoDrop ND-1000, Thermo Scientific) at a spectrum of 230-280nm was used to determine RNA concentration and protein contamination. The RNA was stored at -80°C prior to further analysis.

cDNA synthesis

RNA was denatured (5min, 65°C) in a reaction mixture containing 1µg RNA, 25ng of random primers (Promega) and dNTPs at a final concentration of 0.5mM (Bioline). The

samples were then cooled on ice for 1 min after which 4µl 5xFirst strand buffer and 1µl 0.1mM DTT were added. After 2 min, 1µl SuperScript reverse transcriptase was added [all reagents provided with SuperScript III reverse transcriptase system kit (Invitrogen)]. Samples were incubated at 25°C for 10 min then at 42°C for 50 min and finally 70°C for 15 min. The cDNA was stored at -20°C prior to further analysis.

Polymerase chain reaction

The reaction mixture was composed of 4µl MyTaq reaction buffer, dNTPs at a final concentration of 0.5mM and 0.2µl Taq polymerase (all Bioline) in addition to 13.6µl RNAse free water, 1µl cDNAsample, 0.5µl of forward primer and 0.5µl of reverse primer (10µM, Integrated DNA Technologies Inc). Reactions were carried out in a Venti 96 Well thermo cycler (Applied Biosystems) using the cycle conditions listed in Table 10, p68. Sequences of validated target and reference genes are listed in the Table 11, p68.

Number of cycles	**Duration**	**Temperature (°C)**
1	10 min	94
35	10 s	94
	30 s	58
	50 s	72
1	7 min	72

Table 10 Thermal cycler program details for PCR

Primer		**Sequence**
CD45	F	CATGTACTGCTCCTGATAAGA
	R	GCCTACACTTGACATGCATAC
CD56	F	GATTTTGCCTATCCCAGTGCC
	R	CATACTTCTTCACCCACTGCT
CD31	F	GAAGTACGGATCTATGACTCAG
	R	GTGAGTCACTTGAATGGTGCA
CD144	F	TGGAGACTCCTTCAAGCTTCA
	R	GCTTCCACCACGATCTCATAC
CD34	F	CATCACTGGCTATTTCCTGAT
	R	AGCCGAATGTGTAAAGGACAG
CD146	F	AAGGCAACCTCAGCCATGTCG
	R	CTCGACTCCACAGTCTGGGAC
Beta-actin	F	CCTCGCCTTTGCGCATCC
	R	GGAATCCTTCTGACCCATGC

Table 11 Primer sequences used to perform mRNA analysis

Agarose gel electrophoresis

The PCR products were electrophoresed on 1.7% agarose [SeaKem LE agarose (Lonza)] gels made with 0.5xTBE buffer (45mM Trisbase, 45mM boric acid, 0.625M EDTA) and Gel Red (5µl/100ml). For sample loading, 2µl PCR product was mixed with 8µl RNAse free water and 2µl loading buffer. The PCR product was electrophoresed at 120V for 80 min after which the PCR product bands were visualized by exposure to ultraviolet light using a UVI pro system (UVItec).

Quantitative real-time PCR

The reaction mixture was composed of 4µl 2x Master Mix (Roche), 1.92µl of 2µM primers R + L (Applied Biosystems), 0.08µl UPL probes (Roche) and 2µl cDNA (1/10 dilution). Reactions were carried out in a LightCycler 480 real time PCR system (Roche) using the cycle conditions listed in Table 12 (p69). Sequences of validated target and reference genes are listed in Table 13 (p69).

Program	**Number of cycles**	**Duration (s)**	**Temperature (°C)**
Pre-incubation	1	10	95
Amplification	45	10	95
		30	60
Cooling	1	30	72

Table 12 Thermal cycler programme details for qPCR.

Primer		**Sequence**
HPRT	F	TGACCTTGATTTATTTTGCATACC
	R	CGAGCAAGACGTTCAGCCT
beta-actin	F	CCAACCGCGAGAAGATGA
	R	CCAGAGGCTGACAGGGATAG
Alkaline phosphatase (AP)	F	TCACTCTCCGAGATGGTGGT
	R	GTGCCCGTGGTCAATTCT
Osteopontin (SPP1)	F	CGCAGACCTGACATCCAGTA
	R	GGCTGTCCCAATCAGAAGG
Collagen 1 (Col 1)	F	GGGATTCCCTGGACCTAAAG
	R	GGAACACCTCGCTCTCCA

Table 13 Primer sequences for qPCR

Chapter 1.3 - Isolation of Perivascular MSC and EC

Pericytes expressing all known markers of mesenchymal stem cells (MSC) can be sorted to homogeneity using fluorescence activated cell sorting (FACS).[14 270] Pericytes sorted in this way maintain expression of pericyte and MSC markers in long term culture, while also maintaining capacity to differentiate into bone, cartilage and fat. [14 146]

EC can also be purified from tissues on the basis of cell surface marker expression using FACS[271] and magnetic activated cell sorting (MACS)[272]. However, primary EC isolated in this way are known to be extremely sensitive to alterations in culture and regularly lose their endothelial phenotype or are overgrown rapidly by more robust cells[273]. With HUVEC, however, the initial isolate is almost exclusively composed of EC and so the potential for overgrowth by other populations is more limited.

The aim of this descriptive chapter is to optimise protocols for the isolation and culture of pericytes and EC so that they may be used within *in vitro* coculture models. To increase physiological relevance I set out to use primary EC and pericytes sorted from the same tissue and donor for the coculture experiments. I initially chose adult fat as this has been[146 274], and continues to be[275], a major focus of our laboratory. As adult fat is widely used in clinical trials as a source of MSC (www.clinicaltrials.gov) I felt that any breakthroughs in understanding would be most amenable to clinical translation by focussing on this tissue. I chose skeletal muscle as it offered an alternative tissue in which pathological expression of MSC potentials (eg heterotopic ossification) has been described[276].

Unfortunately, there is currently no single cell surface marker that can be used for the specific isolation of pericytes[144]. Therefore, current protocols utilise a series of antibodies allowing for both positive and negative selection of cell populations[277 278] Published protocols for the FACS isolation of pericytes include one positive marker for

pericytes (CD146), together with a number of negative selection markers including CD34 (to exclude EC and adventitial cells), CD45 (to exclude haematopoietic cells) and CD56 (to exclude myogenic cells)[277]. As adipose tissue is not thought to contain CD56 positive myogenic cells, isolation protocols for adipose tissue tend not to include a negative selection for CD56[277].

Pericytes are damaged by the digestion/sorting process

From my early experiences of sorting adipose tissue using published protocols from our laboratory[277], it became clear that pericytes are damaged by the isolation process. I found that yields were low when compared to the prevalence of pericytes that I expected from examining tissue sections. Furthermore, cultures of sorted cells regularly did not become established, and if they did, it followed a significant lag period of up to 20 days. Furthermore, the yield and integrity of RNA that could be extracted from a given number of sorted pericyte events was extremely poor when compared to other similar populations such as adventitial cells. This indicated to me that pericytes were particularly susceptible to the isolation process irrespective of whether the cells are isolated from adipose tissue (shown in Figure 8, p73) or skeletal muscle. It was therefore important to optimize the isolation process not only to increase yield but also to minimize the trauma to which cells are exposed, as this may affect their behavior and influence downstream experiments.

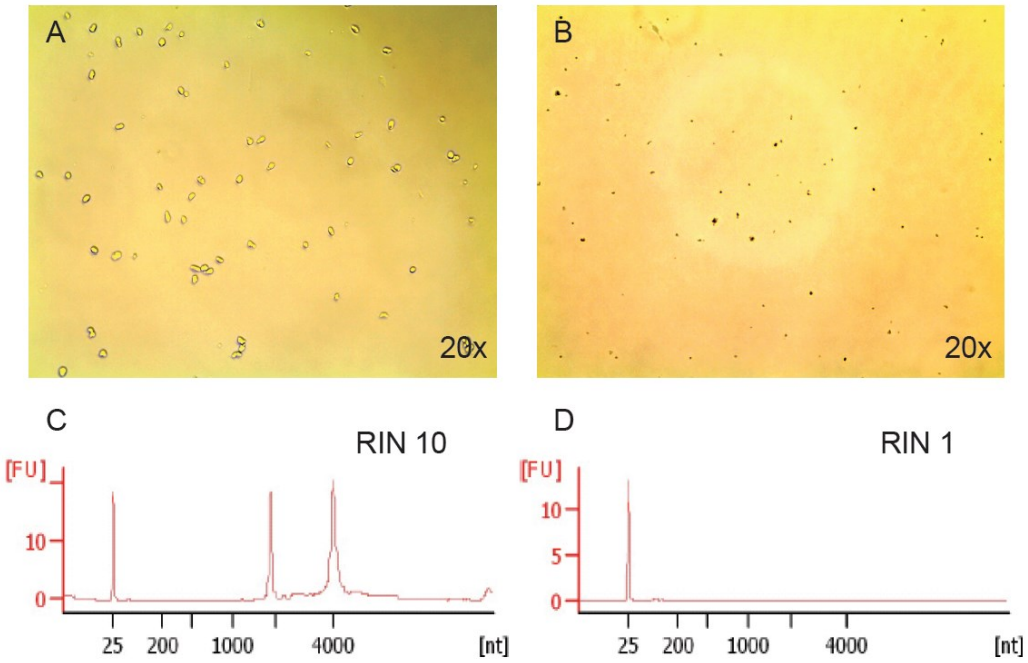

Figure 8 Adipose derived pericytes are damaged in the isolation process
While adventitial cells appear as healthy round cells on light microscopy immediately following sorting (A), pericyte preparations appeared to contain considerable debris and unhealthy cells (B). Despite high RNA integrity of adventitial cell RNA (C), RNA extractions with an equivalent number of pericytess yielded almost no intact RNA (D) as indicated by the RNA integrity number (RIN) where 10 represents high integrity and 1 indicates completely degraded RNA.

Optimisation of isolation protocols to improve yield and viability of pericytes from adipose tissue

The sorting of pericytes from adipose tissue is central to the UCLA Peault group and so with the help of my post-doctoral colleague, Dr Reef Hardy, I have refined existing protocols for the sorting of pericytes from foetal placenta and skeletal muscle and adult fat using fluorescence-activated cell sorting (FACS). This process is similar irrespective of the tissue of origin and for the purpose of optimization we split this into 4 key phases:

1. Tissue retrieval and storage
2. Processing and digestion
3. Sorting
4. Recovery and culture

With refinements to all 4 phases of the process we were able to improve the yield and recovery in culture, but were not able to overcome the challenge of poor RNA integrity immediately following sorting. The isolation strategy developed in this way is shown in Figure 9, p75.

Special considerations at each phase

1. Tissue retrieval and storage

In Edinburgh, human foetal tissue samples were from scheduled pregnancy interruptions and lipoaspirates were from planned cosmetic procedures. During my time at UCLA I only had access to lipoaspirate samples from scheduled cosmetic procedures. In both Edinburgh and UCLA we had minimal warning that samples had become available and no control over the time delay between procedure and delivery of sample to laboratory. To minimise the time period that tissues were at RT, samples were always dissected, washed in PBS and stored at 4^{o}C in appropriate media immediately on arrival.

2. Processing and digestion

We explored the influence of altering the length of enzymatic digestion and changing the brand of collagenase on the yield and viability of pericytes from adipose tissue.

Changing the time of digestion reduces pericyte degradation but RNA integrity and viability are still poor

Lipoaspirate from the same sample was exposed to enzymatic digestion for 60, 40, 20 or 10 min. Each sample was stained with Annexin V to determine the ratio of apoptotic to non-apoptotic cells. We found that the yield of pericytes was greatest at 30 min. The number of debris and apoptotic events increased markedly with increasing time beyond 30 min digestion. This was repeated with a total of 3 different donors.

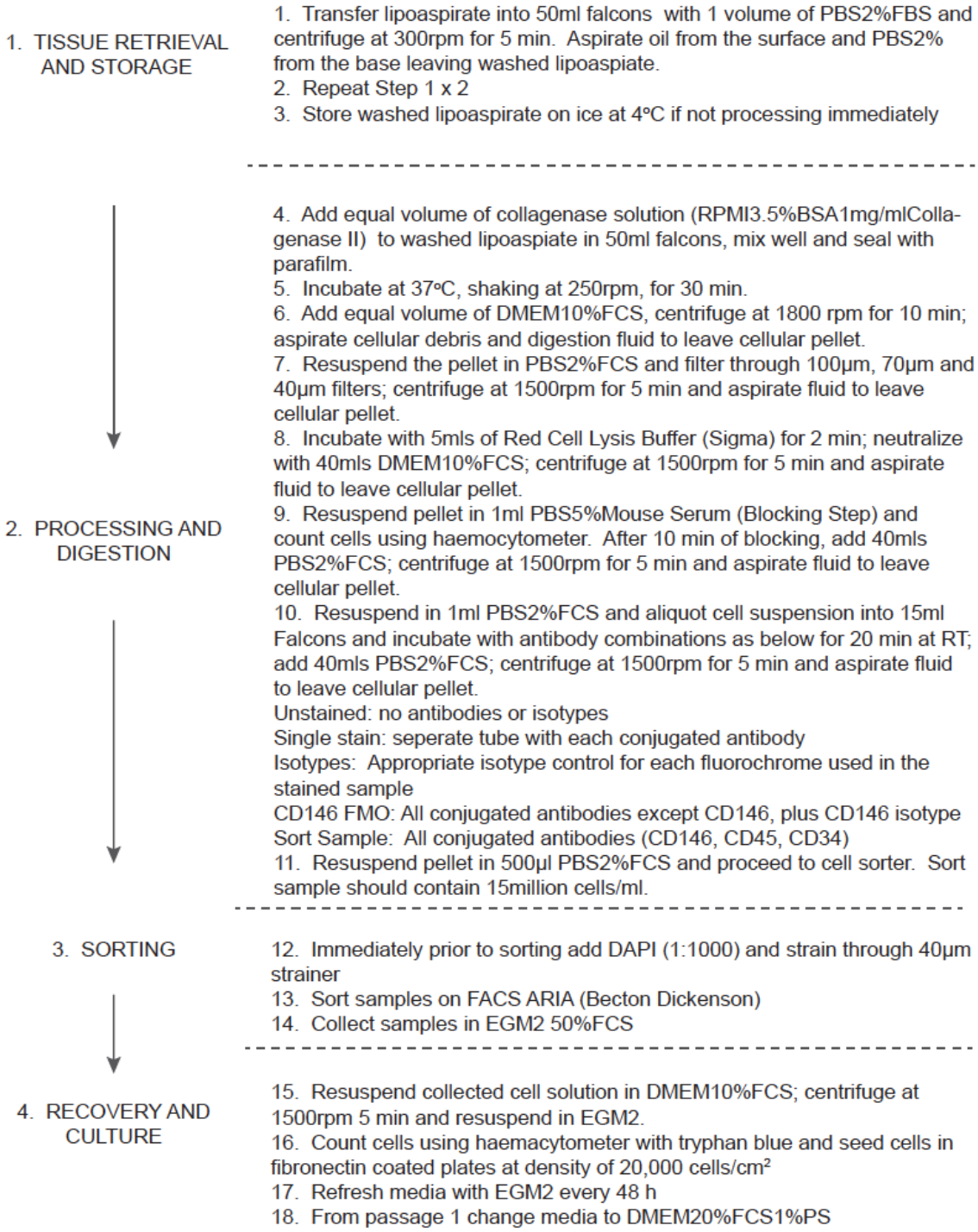

Figure 9 Protocol for the sorting of pericytes from lipoaspirate

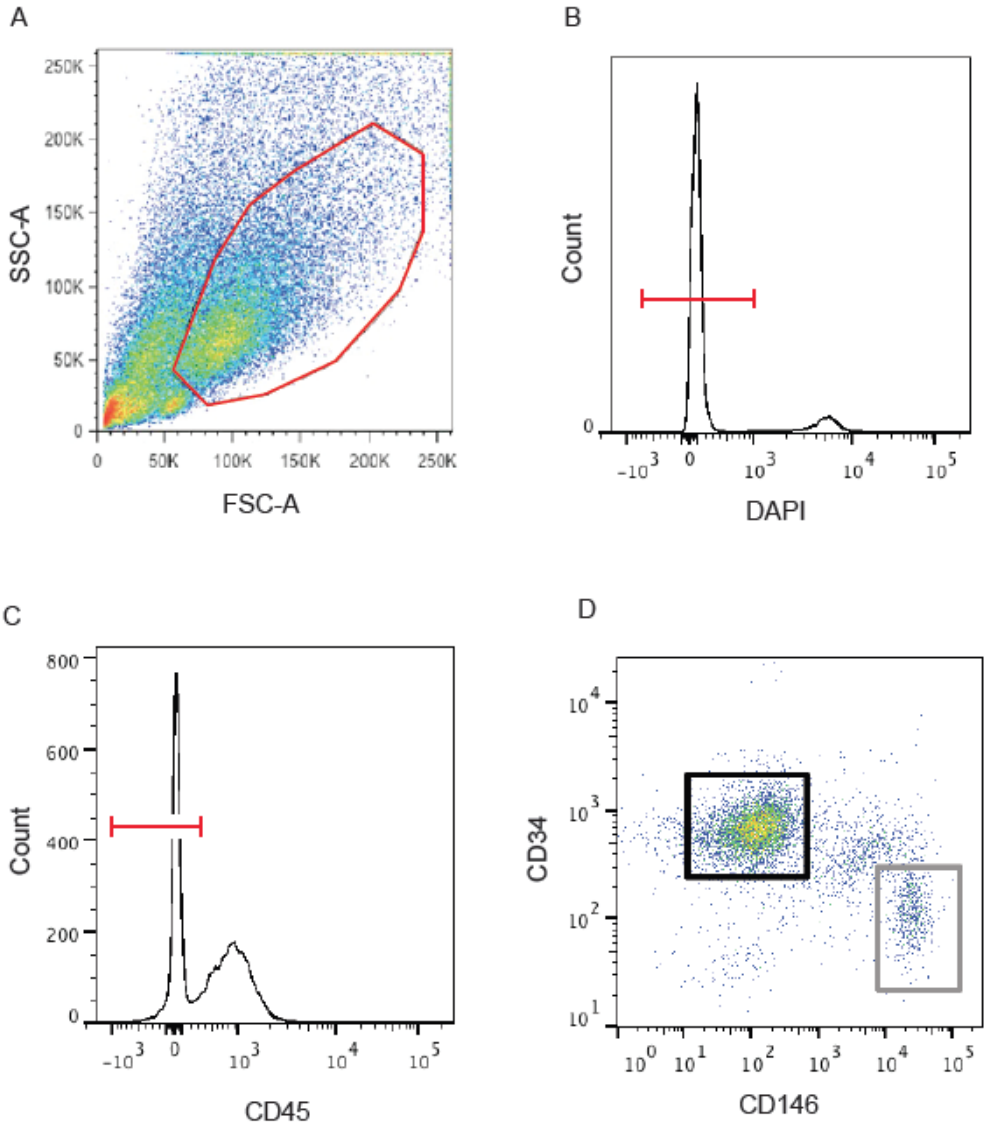

Figure 10 Gating strategy for the sorting of pericytes from human adipose tissue. Following double scatter cell selection (A), exclusion of doublets (not shown), non viable cells (B) and CD45+ cells (C). CD146+ and CD34- pericytes are sorted in the gate represented in grey (D). CD34+CD146- adventitial cells are shown in the black gate (D). The purity of pericyte populations sorted on cell surface marker expression (CD45-, CD31-, CD34-, CD146+) was confirmed immediately following sorting by running the suspension of purified cells back through the flow cytometer (not shown). (SSC-A, side scatter – area; FSC-A, forward scatter-area).

Changing brand of collagenase

We tested three brands of commercially available collagenase, all marketed for the isolation of MSC from fat. For all brands the recommended concentration and manufacturers guidelines were used with a digestion time of 30 min. Each sample was

stained with Annexin V to determine the ratio of apoptotic to non-apoptotic cells. The collagenases tested were:

Sigma (0.5 mg/mL)

Serva (0.2 mg/mL)

Liberase (0.08 mg/mL)

We found that the yield of pericytes from both the Sigma and Serva preparations was higher than for the Liberase preparation.

3. Sorting

The FACS Aria (Becton Dickinson) is a high through-put, multi laser, multi parameter cell sorter. Up to 11 fluorescent parameters can be used to sort up to four populations simultaneously at rates of up to 40,000 cells/second.

Sorting pressure and nozzle diameter

The nozzle diameter and the system pressure used within the cell sorter are important to consider, and depend on the size and characteristics of the cells being sorted. The nozzle size should be approximately 5 times that of the cells being sorted. For example, sorts targeting lymphocytes are generally performed with a 70μm nozzle, with the 100μm nozzle reserved for larger cells. Increased pressures and a smaller nozzle diameter exposes cells to harsher conditions during sorting. This was reflected in our observation that cells sorted using the 100μm nozzle appeared to recover more rapidly than those sorted with smaller nozzles.

Appropriate gating to exclude apoptotic cells and debris

By analyzing my own FACS data and the historical samples from our lab it became clear that the majority of cells detected from the machine as CD146+CD34-CD45- cells may instead represent debris or apoptotic cells. I was able to ascertain this by back-gating

analysis of pericytes showing where they fall when plotted for SSC and FSC (Figure 11, p79). It is interesting to note that much of the cellular debris had the exact phenotypic profile as pericytes indicating that they could represent remnants of pericytes. As such, unless a very strict initial SSC and FSC gating strategy was used, the percentage of viable cells can easily be overestimated. This would in part explain the poor RNA quality and outgrowth of pericytes we observed. By culturing CD146+CD45-CD34- "pericyte events" from different regions of the SSC-FSC back gate we were able to show that most apoptotic cells lie towards the SSC axis while most debris events lie clost to the origin of both the SSC and FSC axes. However, a number of apoptotic cells also lay in characteristic scatter locations for healthy pericytes, confirming that the identification of healthy pericytes can not be based solely on their SSC-FSC profile.

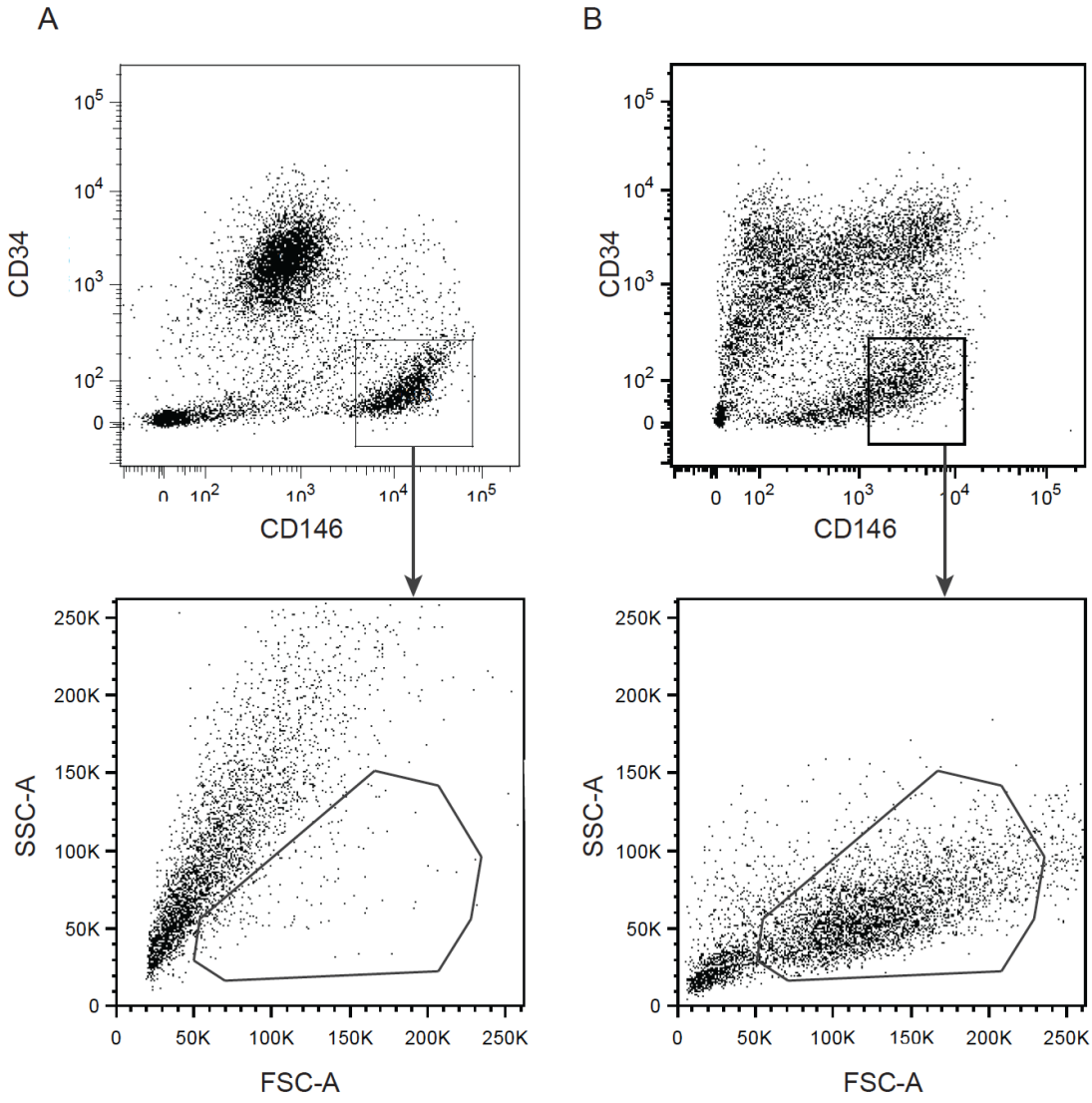

Figure 11 The importance of appropriate scatter gating to enrich for healthy pericytes
In the first example preparation (A), back gating of adipose derived pericytes to a SSC-A FSC-A scatter plot reveals that the majority of events lie within areas typically associated with apoptotic cells and debris. Despite the CD34 CD146 plot appearing similar within this next sample (B), back gating to a scatter plot reveals that the majority of events lie within the area typically associated with viable pericytes. Note that a large number of debris events remain in this second preparation.

4. Recovery and culture

Coating of culture plates

The hydrophobic surface of polystyrene plastic is routinely treated using either corona discharge under atmospheric conditions or gas-plasma under vacuum so that the surface becomes hydrophilic and negatively charged once medium is added[279]. Good

cell attachment is especially important during recovery of cells from freezing or after sorting, as poor attachment can lead to apoptosis and necrosis resulting in slower recovery and lost research time. As such published protocols for the sorting of MSC from fat include additional pre-coating of already coated culture plastic with gelatin[146 277]. We compared a number of different biological (gelatin, collagen and fibronectin) and non-biological coating (MSC mosaic surface coating, BD) products. We found that the use of all these products improved emergence of colonies and successful outgrowth of cells following sorting – we elected to use fibronectin as this was the substrate also favoured by EC.

Seeding density

A number of studies using conventional culture derived MSC have found that the plating density is not critical for maintaining a well defined multipotent MSC population[280], while others found that seeding density influences gene expression patterns[281]. We found that the outgrowth of cultures of freshly sorted pericytes rarely occurs unless a seeding density of at least 20,000cells/cm^2 is used. If the total cell count at sorting includes debris and apoptotic cells then the actual number of viable cells seeded per cm^2 will be considerably less than 20,00/cm^2. As such we include in our protocol a further cell count using a haemocytometer and trypan blue to confirm the true count of viable pericytes to enable accurate seeding at 20,000cells/cm^2.

Analysis of Péault group adipose sorts (2011-2014)

There is growing enthusiasm for the use of non-cultured MSC and it is therefore of clinical interest to establish the yield of perivascular stem cells from lipoaspirate. Together with Dr Hardy we set out to establish the yield and frequency of PSC in human lipoaspirate (from all samples including my own) to establish patient and processing

factors that influenced this yield. In n=129 donors, 100ml of lipoaspirate yielded a mean of 37.8 x10^6 SVF cells (stromal vascular fraction, or total cells). The mean percentage cell viability among SVF was 82%. The prevalence of CD45+ haematopoietic cells was 31.6% of total viable SVF. Pericytes averaged 8% of total viable SVF (median=6%). Adventitial cells represented 31.6% on average of total viable SVF (median=33%). The mean total PSC content was 39.5% (median=41%). No significant change in yield, viability, or identity was observed with patient age. However, as samples were sourced from cosmetic lipoaspirate the young demographic analysed (ages ranged from 24 to 64) may not have been sufficiently broad to detect potential changes within an older population. No significant difference was apparent for either cell viability or the percentage of pericytes across gender although the percentage of adventitial cells and PSC was significantly increased in males. Menopausal status had no statistically significant effects on any cell parameters including yield, viability, or identity. The percentage of haematopoietic cells and PSC was observed to decrease slightly but significantly with increasing BMI. Although cell viability and SVF yield exhibited a 20% reduction with respect to cold storage time; the decrease in PSC yield was more subtle (only 3%), as a result of being partially offset by an ~20% and ~17.5% rise in the percentage of adventitial cells and pericytes, respectively. Interestingly, the percentage of hematopoietic cells decreased the most (up to 30%) as a function of the duration of cold storage.

Pericyte isolation protocols for human skeletal muscle

I adapted published pericyte isolation protocols considering protocols for the isolation of other cell types in skeletal muscle[205 282]. I was also able to apply what I had learned from my experience with adipose tissue. Using this protocol (Figure 12, p82) I was able to consistently isolate and purify skeletal muscle pericytes from foetal tissues that grew

well in culture. In my preparations the mean viability was 97.23% (SD 0.85%), with pericytes contributing 14.04% of all viable cells (SD 3.05%), and adventitial cells accounting for 17.36% (SD 2.16%) (n=3).

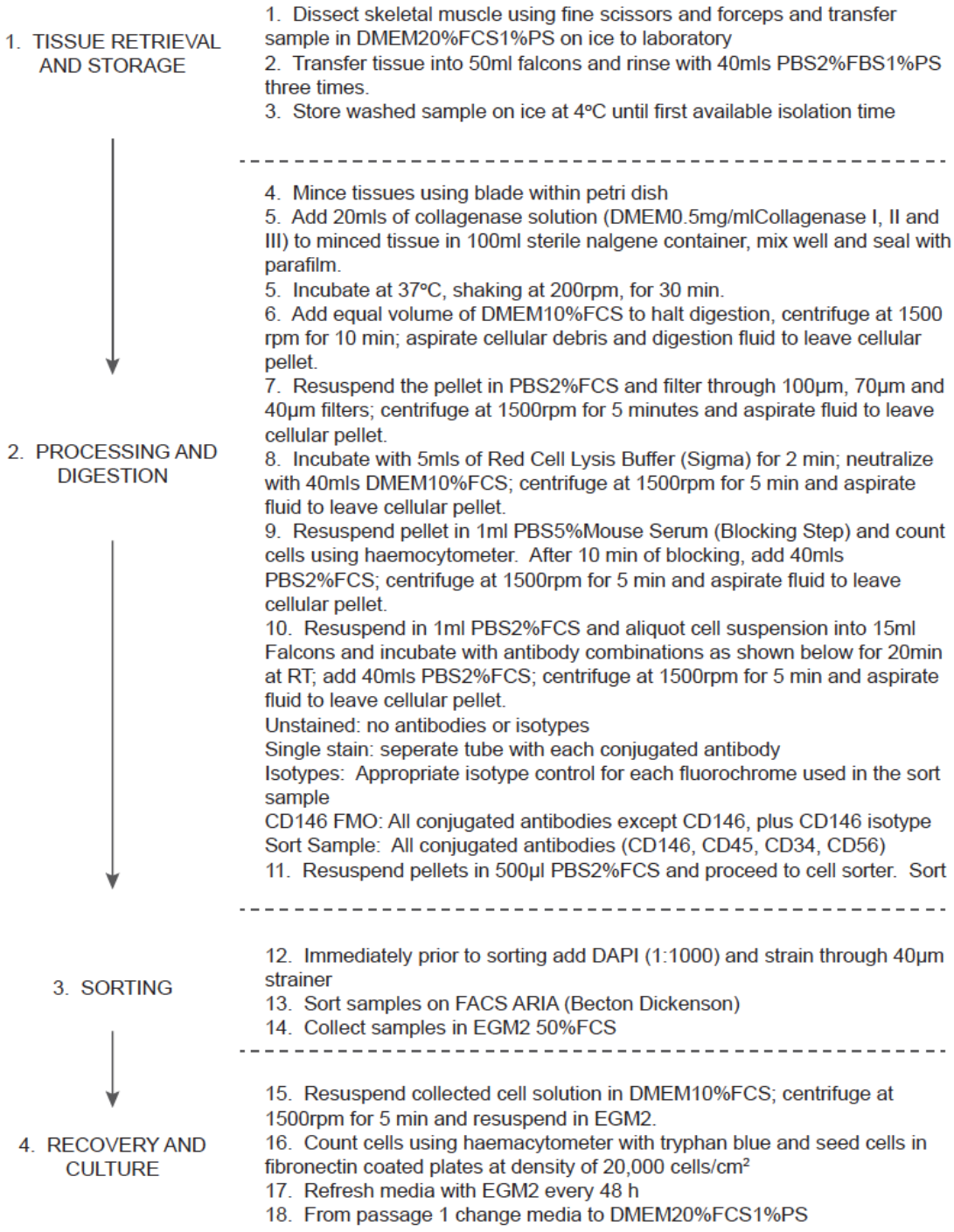

Figure 12 Protocol for the sorting of pericytes from human fetal skeletal muscle

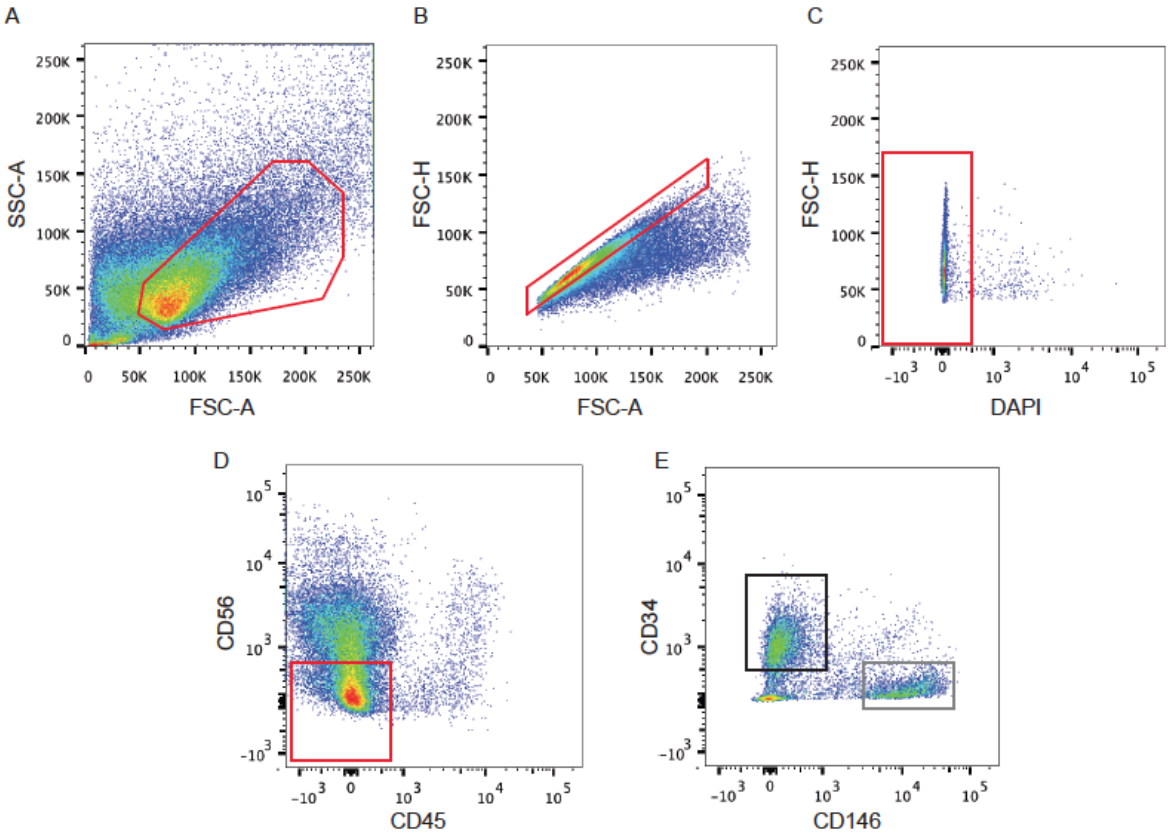

Figure 13 Gating strategy for the sorting of pericytes from human skeletal muscle
Following double scatter cell selection (A), exclusion of doublets (B), non viable cells (C) and CD45+ cells (D), CD146+ and CD34- pericytes are sorted in the gate represented in grey (E). CD34+CD146- adventitial cells are shown in the black gate (E). The purity of pericyte populations sorted on cell surface marker expression (CD45-, CD56-, CD31-, CD34-, CD146+) was confirmed immediately following sorting using FACS reanalysis (not shown).

Pericytes maintain their sorted immunophenotype in long-term culture

Once sorted to homogeneity pericytes have been described to "maintain their phenotype" in long term culture[14 283]. I found that these cells indeed maintained their sorted phenotype (ie CD146+, CD34-, CD56-, CD45-) as assessed by FACS analysis and RT-PCR (Figure 14, p84).

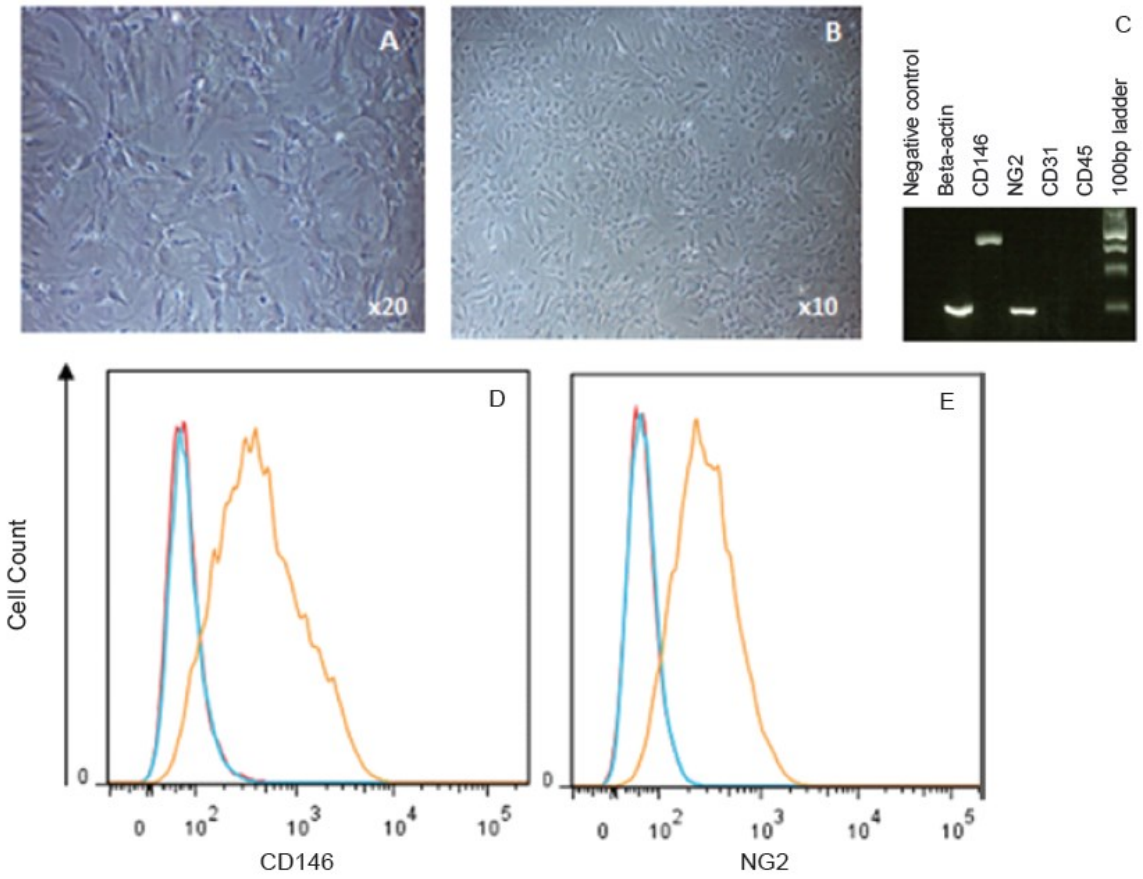

Figure 14 Confirming pericyte purity in long-term culture
Pericytes sorted from human adipose tissue adhere and proliferate in culture (A,B). The purity of sorted cells was confirmed using RT-PCR (C) and FACS analysis (D,E). (yellow, antibody stain; blue, isotype; red, unstained).

Cultured pericytes demonstrate tri-lineage differentiation potential

PEricytes sorted from adipose tissue and muscle also maintained their osteogenic and adipogenic potentials over serial passaging. My experiences support reports in the literature that several factors influence pericyte differentiation. These include confluence when differentiation factors are introduced, passage of pericytes, and history of previous over confluence in culture.

Osteogenic differentiation

In the presence of osteogenic differentiation factors pericyte cultures were capable of osteogenic differentiation as assessed by Alizarin Red and von Kossa staining for calcium deposits. Differentiation should be started with cells at 80% confluence; cells at lower confluence demonstrated limited capacity for differentiation while more confluent cells rapidly lifted from culture wells.

Adipogenic differentiation

When adipogenic differentiation is initiated with cells at high density (90-100% confluence) cultured pericytes are capable of differentiating into adipocytes as assessed by Oil Red O staining for lipid droplets.

Chondrogenic differentiation

Despite forming characteristic pellets when cultured in 15ml tubes in chondrogenic media, Safranin O and Alcian blue staining of pellet sections for evidence of chondrogenic differentiation into cartilage has so far been inconclusive (Figure 15, p86).

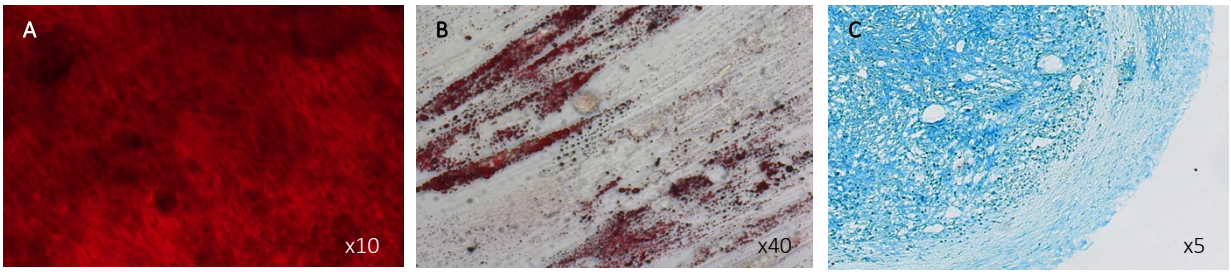

Figure 15 Multi-lineage potential of pericytes
Pericytes cultured in osteogenic medium for 14 days stained positively for mineralization by Alizarin Red staining (A). At 21 days of culture in adipogenic conditions, widespread lipid droplet formation was detected with Oil Red O (B). Weak Alcian Blue staining of pericyte pellets cultured in chondrogenic conditions was suggestive of the presence of proteoglycans at 21 days (C).

Isolation of primary EC

To increase physiological relevance I set out to use primary EC sorted from the same tissue and donor. I have established a protocol for sorting and culture of EC although I have been unable to establish sustainable cultures of these cells.

EC from human adipose tissue, muscle and placenta (CD45-, CD56-, CD34+, CD31+) exhibited characteristic cobblestone appearance with contact inhibition until passage 5. Purity was assessed by FACS analysis and RT-PCR (Figure 16, p87). When seeded onto Matrigel they formed vascular network structures (Figure 17, p87). However, beyond passage 5, these cells lost their characteristic phenotype. As these would not maintain their phenotype for the duration of differentiation experiments HUVEC were used as an alternative.

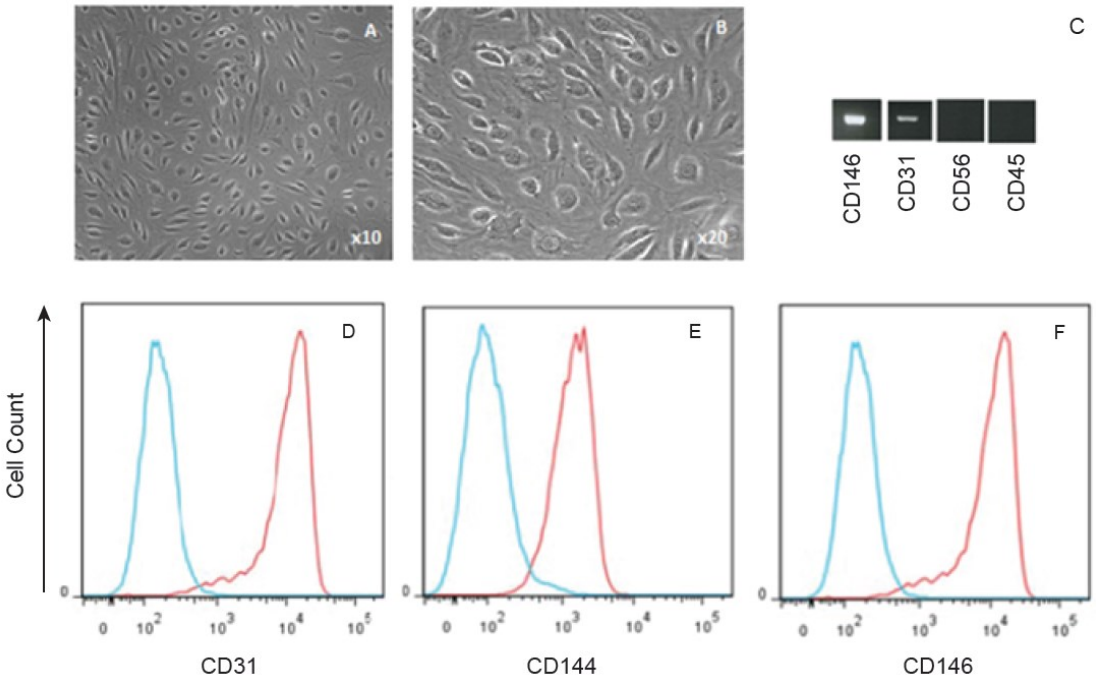

Figure 16 Confirming phenotype and purity of sorted EC
EC sorted from skeletal muscle (CD31+, CD34+) using FACS exhibit characteristic 'cobblestone' phenotype in culture at passage 3 when viewed at x10 (A) and x20(B) magnification. RT-PCR confirmed the purity of cells at passage 3 (C). When analysed at passage 3 using FACS they represented a homogenous population staining positively for directly conjugated antibodies to CD31 (D), CD144 (E) and CD 146 (F). (red, antibody stain; blue, isotype).

Figure 17 EC form vascular network like structures on Matrigel
(A, seeding; B, 4 h; C, 8 h).

Chapter 1.4 Modelling the perivascular niche

The perivascular niche consists of pericytes, EC and their enveloping basement membrane. The initial aim of this chapter is to establish models of pericyte-endothelium interactions to use as a basis for investigating the influence of EC on the differentiation potential of pericytes. The assays for osteogenic, adipogenic differentiation last a minimum of 7-14 days while chrondrogenic differentiation resquires up to 4 weeks. Stability in long-term culture is therefore a prerequisite. It was also important to show that the final constituent of the perivascular niche: the basement membrane, was produced in these settings. In this chapter I explore two and three dimensional models of the perivascular niche.

Two-dimensional model of the perivascular niche

Pericytes were seeded at varying ratios onto confluent HUVEC (Figure 18, 90). HUVEC formed a monolayer with proliferation limited by contact inhibition, while overlying pericytes formed a homogenous multilayer when cultured in EGM2 for up to three weeks. HUVEC and pericytes were able to survive as distinct populations in this culture setting (Figure 19, p91).

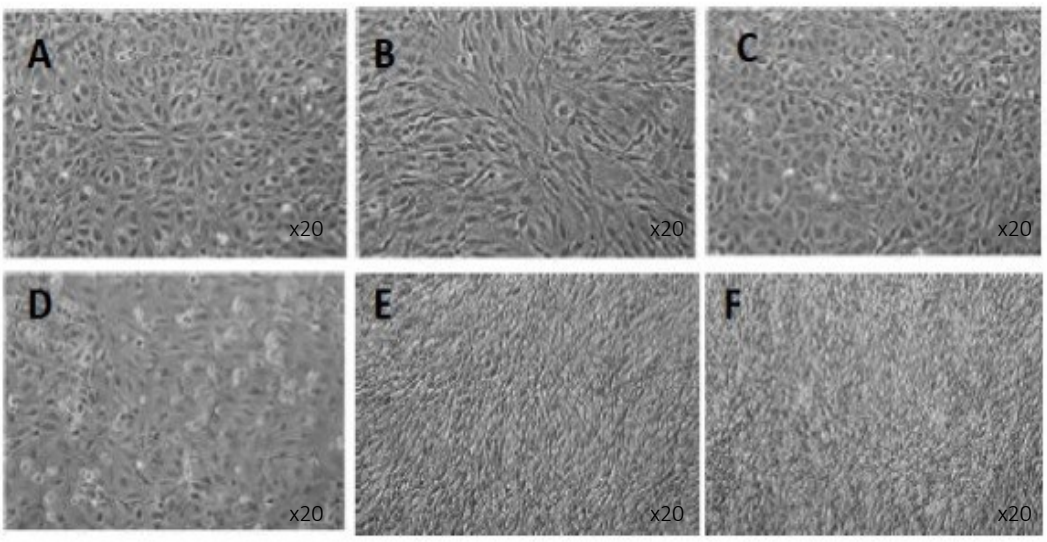

Figure 18 Light microscopy of 2D coculture
HUVEC were grown to a confluent monolayer (A). Pericytes were seeded in monoculture (B) and at varying ratios in coculture (C, shown 4:1 HUVEC:pericyte). At day 9, HUVEC remained in a monolayer (D), while pericytes proliferated without contact inhibition to form multiple layers (E), which overgrew HUVEC in coculture (F).

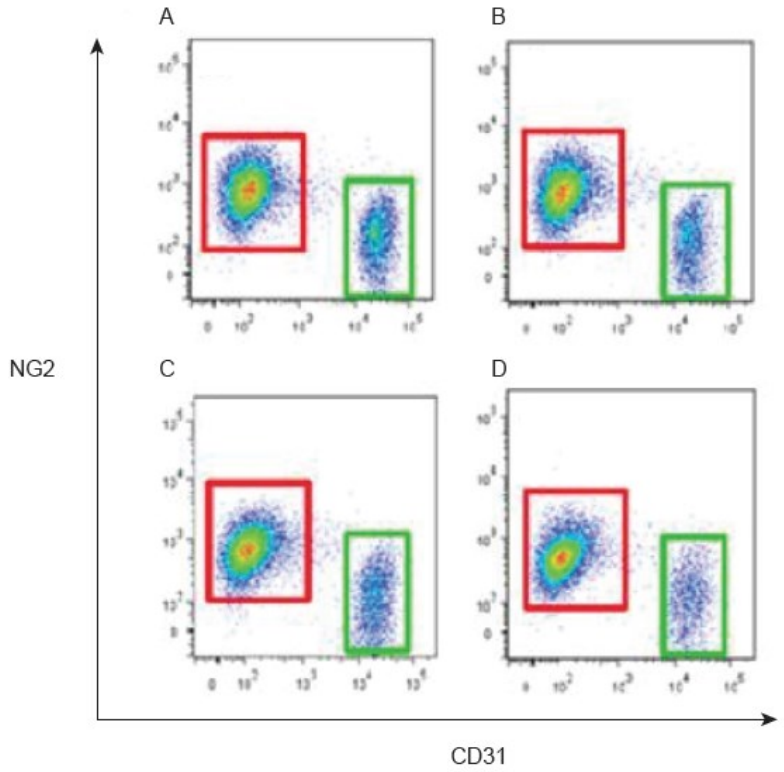

Figure 19 Flow cytometry analysis of cocultured cells
Two distinct populations of pericytes (red boxes) and HUVEC (green boxes) survived 2D coculture at 9 days. Irrespective of whether cells were seeded at a ratio of 1:1 (HUVEC: pericyte)(A), 2:1(B), 4:1(C) or 8:1(D), pericytes were more numerous on analysis.

Despite discrepancies in growth kinetics it was important to ensure that all pericytes were in contact with EC for the duration of culture. Pericyte growth was more restrained by culturing the cells in basal medium (DMEM10%FCS1%PS) rather than EGM2. In these conditions pericytes were more likely to be exposed to underlying HUVEC initially although HUVEC coverage decreased when culture extended beyond ten days in basal medium: at two weeks HUVEC coverage had diminished to 50%. To maintain EC presence within cocultures, cultures were supplemented with additional EC every two days.

Three-dimensional spheres assay

To improve physiological relevance by removing the influence of adherence to culture plastic, three dimensional perivascular niche models were developed. To generate self-assembly spheres, pericytes in isolation and in coculture with HUVEC at a 1:1 cell ratio were propagated for 7 days in non-adherent U-shaped bottom 96 well plates. Cocultures of pericytes and fibroblasts served as controls. Under optimal growth conditions, spheroids were formed overnight. Pericytes in isolation formed distinct spheroids with cells expressing pericyte markers diffusely spread throughout the spheroid at 3 days (Figure 20, p93). At day 7, cells within the core did not express the pericyte marker NG2 that may reflect a change in phenotype or loss of viability. Despite both cell types being introduced simultaneously as a single cell suspension, HUVEC and pericytes were shown to self-assemble and form organized structures with HUVEC assuming a predominantly peripheral distribution initially and with time forming increasingly substantial networks throughout the 3D structure (Figure 21, p93). The spheroids did not progressively increase in size over time – in contrast they appeared to become more compact.

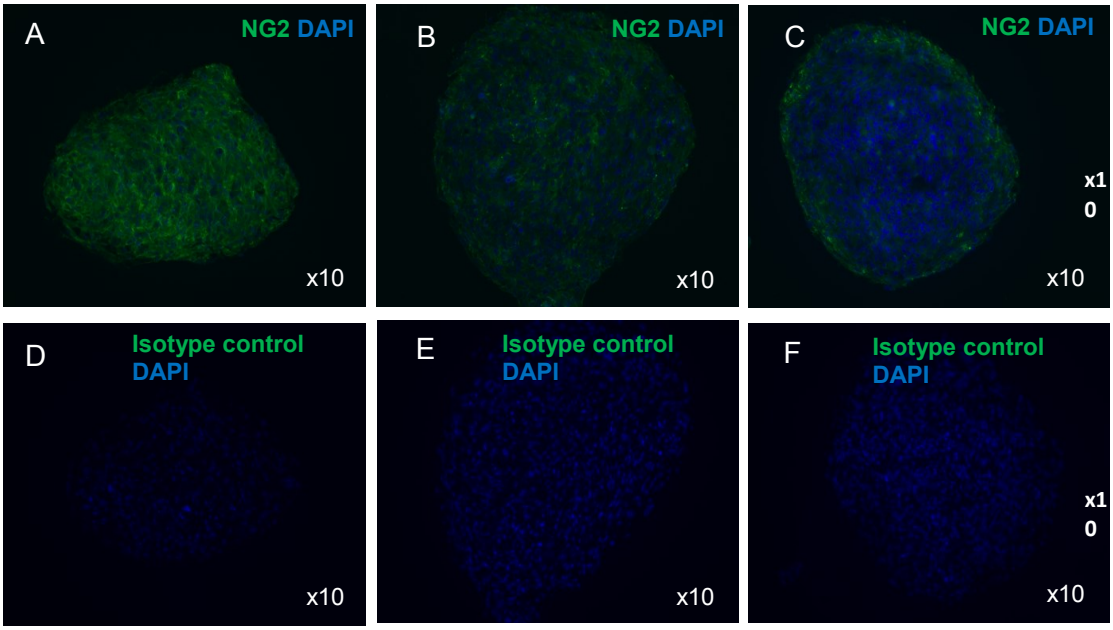

Figure 20 Immunohistochemistry of pericyte spheroids.
Fluorescent images of NG2 labelling of pericytes within spheroids at day 1 (A,D), 3 (B, E) and 7 (C, F). Over time, NG2 expression diminished within the core of spheres in keeping with increased numbers of dead cells (see Figure 1.12 below)

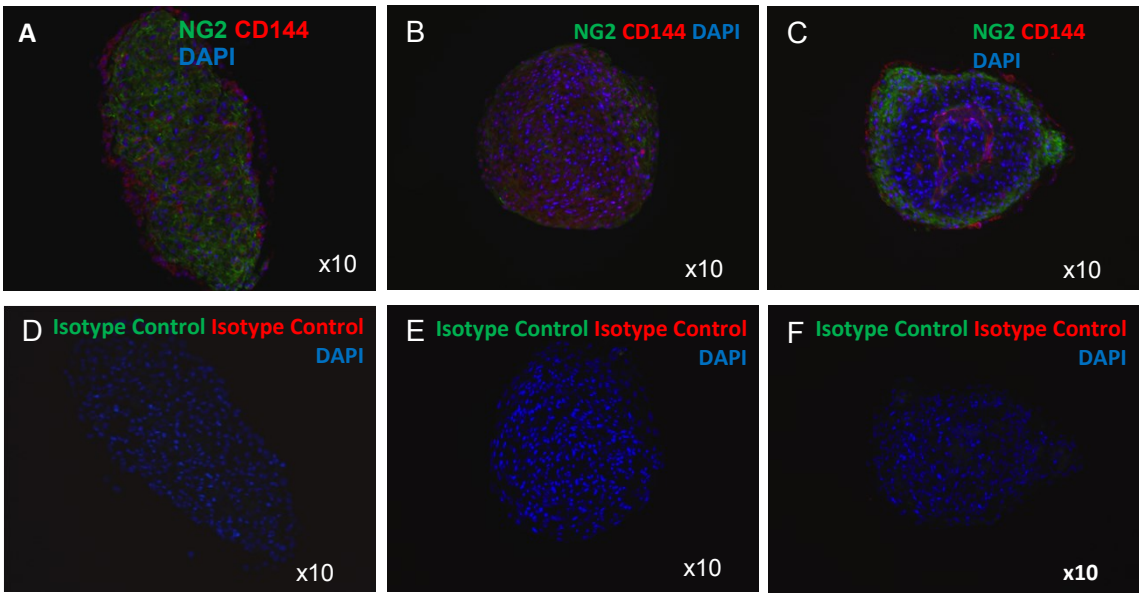

Figure 21 Immunohistochemistry of pericyte-HUVEC spheroids.
Pericyte-HUVEC spheroids at day 1 (A,D), 3 (B,E) and 7 (C,F). CD144 positive HUVEC were observed predominantly around the periphery of coculture spheroids at day 1. By day 7, HUVEC associated to form complex networks within the structure.

Viability in 3D spheres

It was necessary to establish whether cells remained viable in this setting as cells, particularly within the centre of the spheroids, may have reduced access to nutrients and oxygen. A fluorescence viability assay using CMFDA and PI was performed and visualized under confocal microscopy at day 1, 3 and 7 following sphere assembly. At day 1 the majority of cells were viable (green), with the number of dead cells increasing over time, particularly within the core of cocultured spheres (Figure 22, p94).

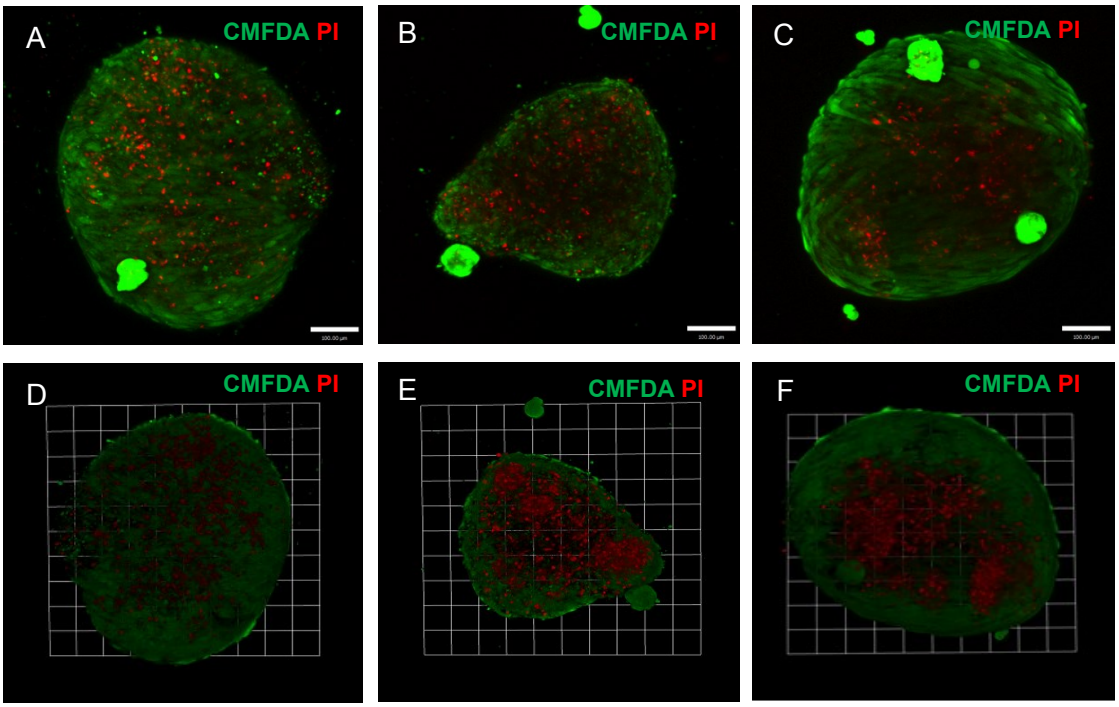

Figure 22 Viability assay of cells within 3D spheres using confocal microscopy
CMFDA labelling indicates viability (green) with PI labelling indicating non-viable cells (red). Confocal images taken of intact spheres containing pericytes (A), pericytes and HUVEC in equal numbers (B) and pericytes and fibroblasts in equal numbers (C). Cross sections indicating cell viability within the core of spheres containing pericytes (D), pericytes and HUVEC in equal numbers (E) and pericytes and fibroblasts in equal numbers (F).

Three dimensional Pellet Culture

Pellet cultures are the most widely used setting for performing chondrogenic differentiation. The culture of MSC in non-adherent pellets containing approximately $2x10^5$ cells in chondrogenic conditions is an effective method of inducing chondrogenic differentiation. We sought to establish whether this model could be modified to enable coculture with EC (Figure 23, p95).

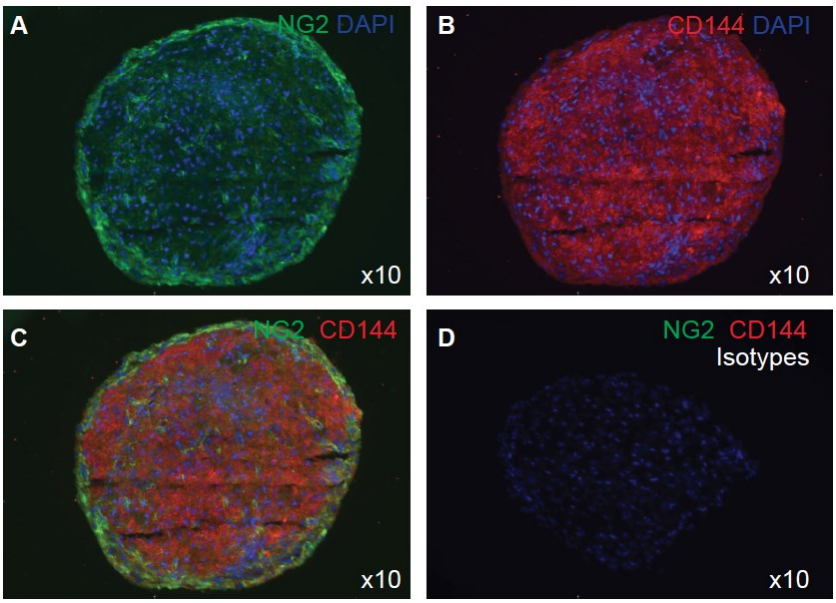

Figure 23 NG2 and CD144 immunohistochemistry of pericyte-HUVEC pellets
Antibody staining at day 21 (A-C) together with appropriate isotype control (D). CD144 positive HUVEC were observed throughout the coculture pellet with the highest concentration of pericytes found at the pellet surface.

Viable cells were identified in cryostat sections (8μm) by means of their LDH activity (dark blue) (Figure 24, p96). The highest concentration of viable cells was seen at the surface of the pellets with relatively fewer viable cells present within the core.

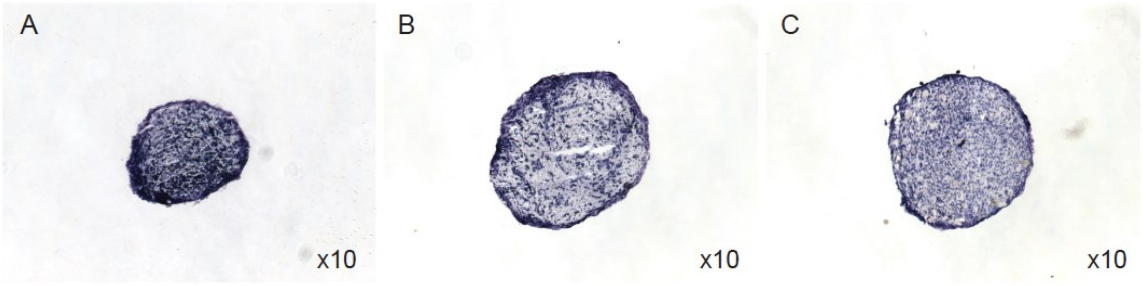

Figure 24 Cell viability within pellet cultures
LDH staining of pellet cultures of pericytes (A), pericytes plus HUVEC (B) and pericytes plus fibroblasts (C)

Three dimensional tube assembly (vasculogenic) assay

Fluorescently labelled pericytes and HUVEC were seeded at varying ratios onto Matrigel and visualized over time in an incubation chamber. HUVEC in monoculture began forming networks immediately, reaching maximal complexity at 4 hours before collapsing within 8 hours. Pericytes in monoculture associated into clumps and did not form networks. In coculture, pericytes and HUVEC both contributed to vascular networks that expanded over time reaching maximal organization at 4 hours before collapsing at eight hours (Figure 25, p97).

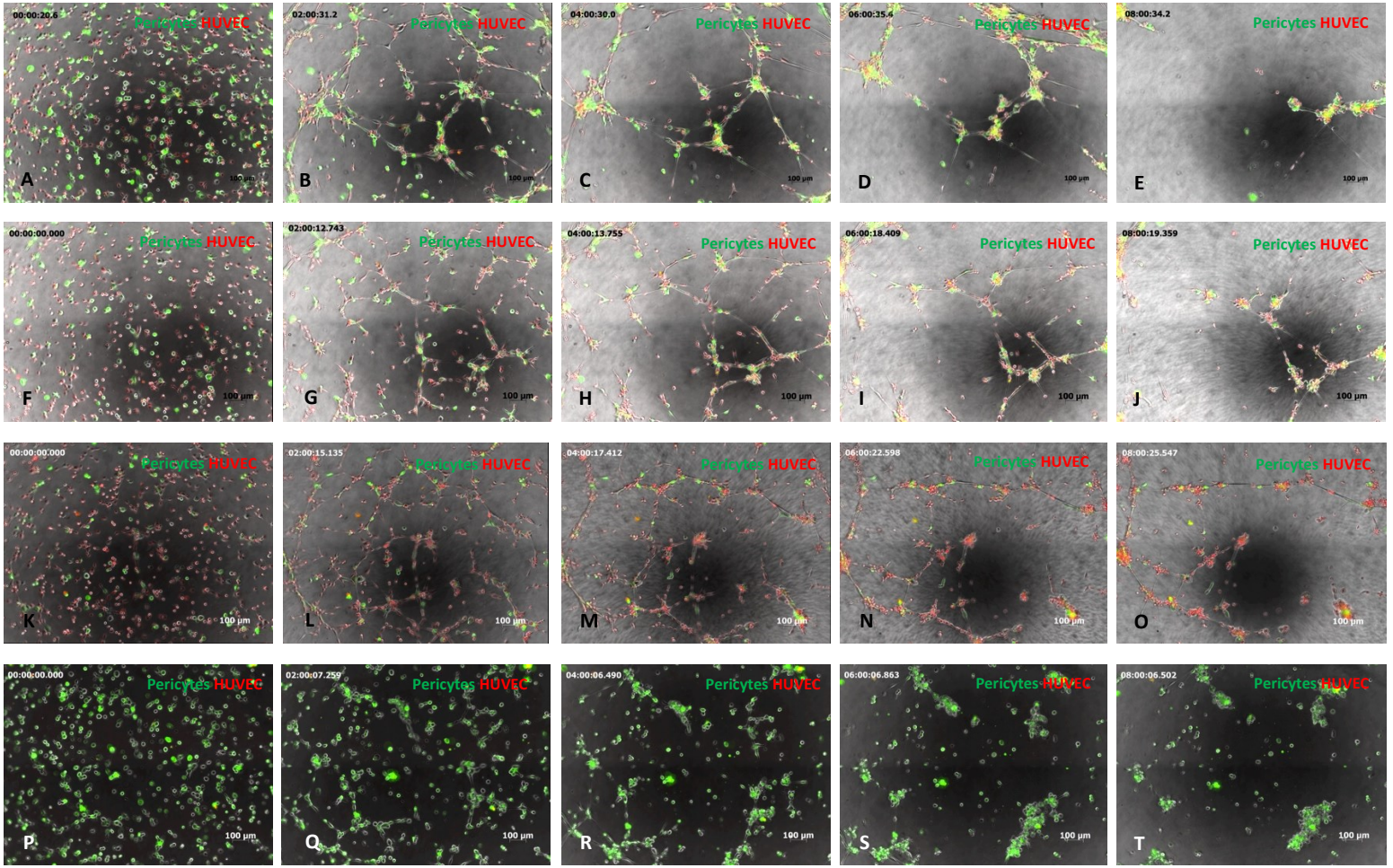

Figure 25 Pericytes contribute to 3D networks when cocultured with HUVEC on Matrigel
Single cell suspensions of pericytes (green) and HUVEC (red) were seeded onto a thick layer of Matrigel and visualized using fluorescence and brightfield microscopy. Immediately after seeding at a ratio of pericyte:HUVEC of 1:1 cells immediately began forming vascular networks (A) which had developed in complexity at 2hrs (B) and 4hrs (B) and subsequently collapsed at 6hrs (C) and 8hrs (D). A similar pattern was seen in wells seeded at pericyte:HUVEC ratios of 1:2 (images F-J) and 1:4 (images K-O). In monoculture, pericytes formed clumps that did not form distinct networks (images P-T)

Production of basement membrane proteins by pericytes and endothelial cells in coculture

Serial titrations of antibodies to the human basement membrane proteins collagen IV and laminin on human fetal placental sections revealed an optimum antibody concentration of 1:100 for both antibodies. At these concentrations the expected distribution[284] of basement proteins was optimally observed in histological tissue sections with no background staining with isotype controls (Figure 26, p98).

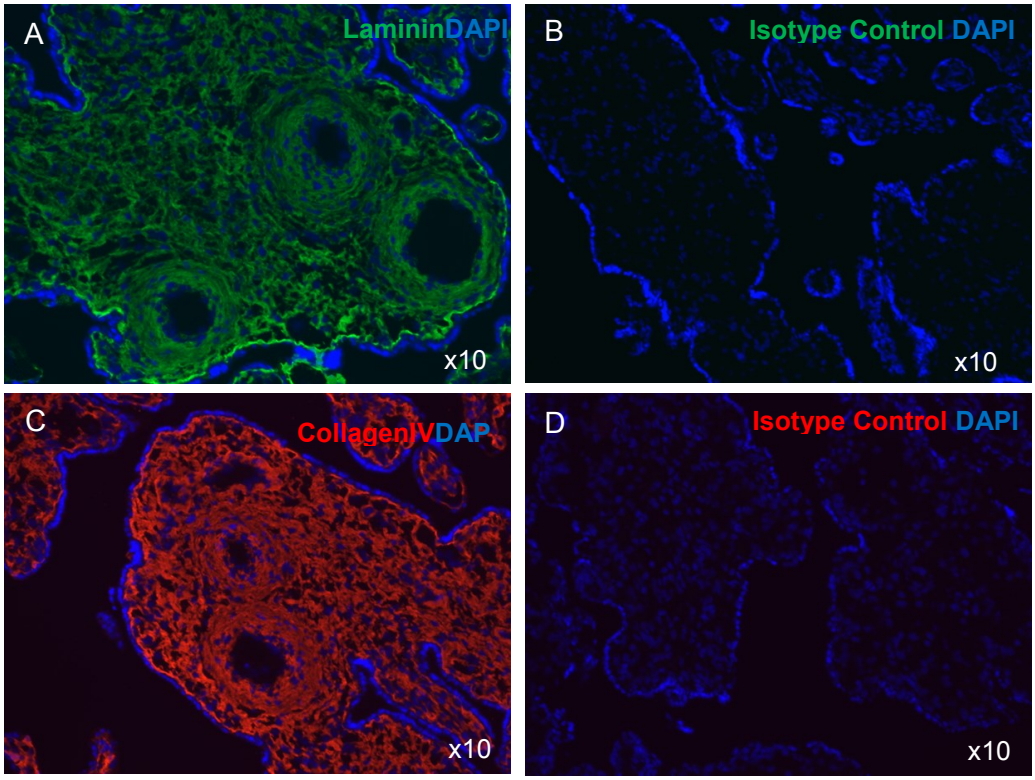

Figure 26 Distribution of collagen IV and laminin within fetal placental villous.
Laminin (A) and type IV collagen (C) are expressed in all placental basal membranes and villous stroma. The trophoblastic basement membranes and endothelial basal membranes are sharply demarcated and display high intensity. Laminin and collagen IV are also localised, but to a lesser degree, in the villous stroma, but is not evident in the epithelial layer. There was no positive staining within the isotype controls of both laminin (B) and collagen IV (D).

We used immunohistochemistry to determine the presence of laminin and in our *in vitro* models. For the 3D vasculogenic assay, a pericyte:HUVEC ratio of 1:2 was used due to the stability and organisation of networks at this ratio. Due to cross-reactivity of human antibodies to mouse derived proteins in Matrigel we were unable to assess for laminin production in 3D networks (Figure 26, p98).

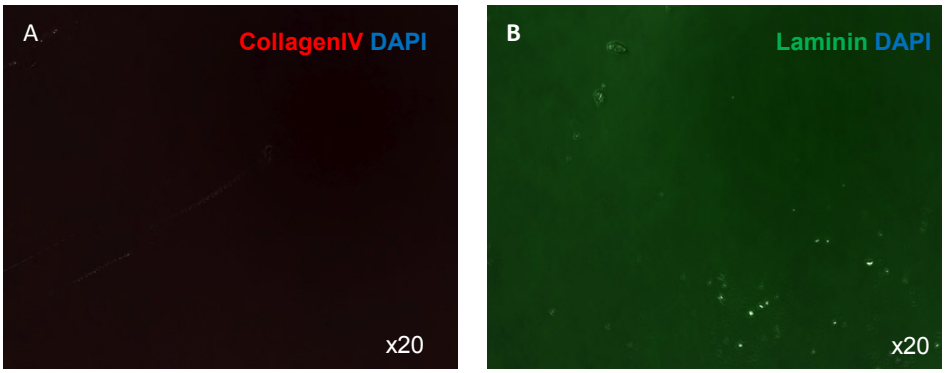

Figure 27 Staining of collagen IV and laminin on unseeded Matrigel
The anti-collagenIV monoclonal antibody did not label any proteins within Matrigel (A). However the anti-laminin antibody bound to mouse derived proteins within Matrigel (B).

Both collagen IV and laminin were produced in 2D and 3D monoculture of pericytes and EC with deposition being proportional to the time in culture. Although not formally quantified, the production of basement membrane in coculture appeared greater that would be expected for the sum of individual productions in monoculture (Figure 28, p100 and Figure 29, p101).

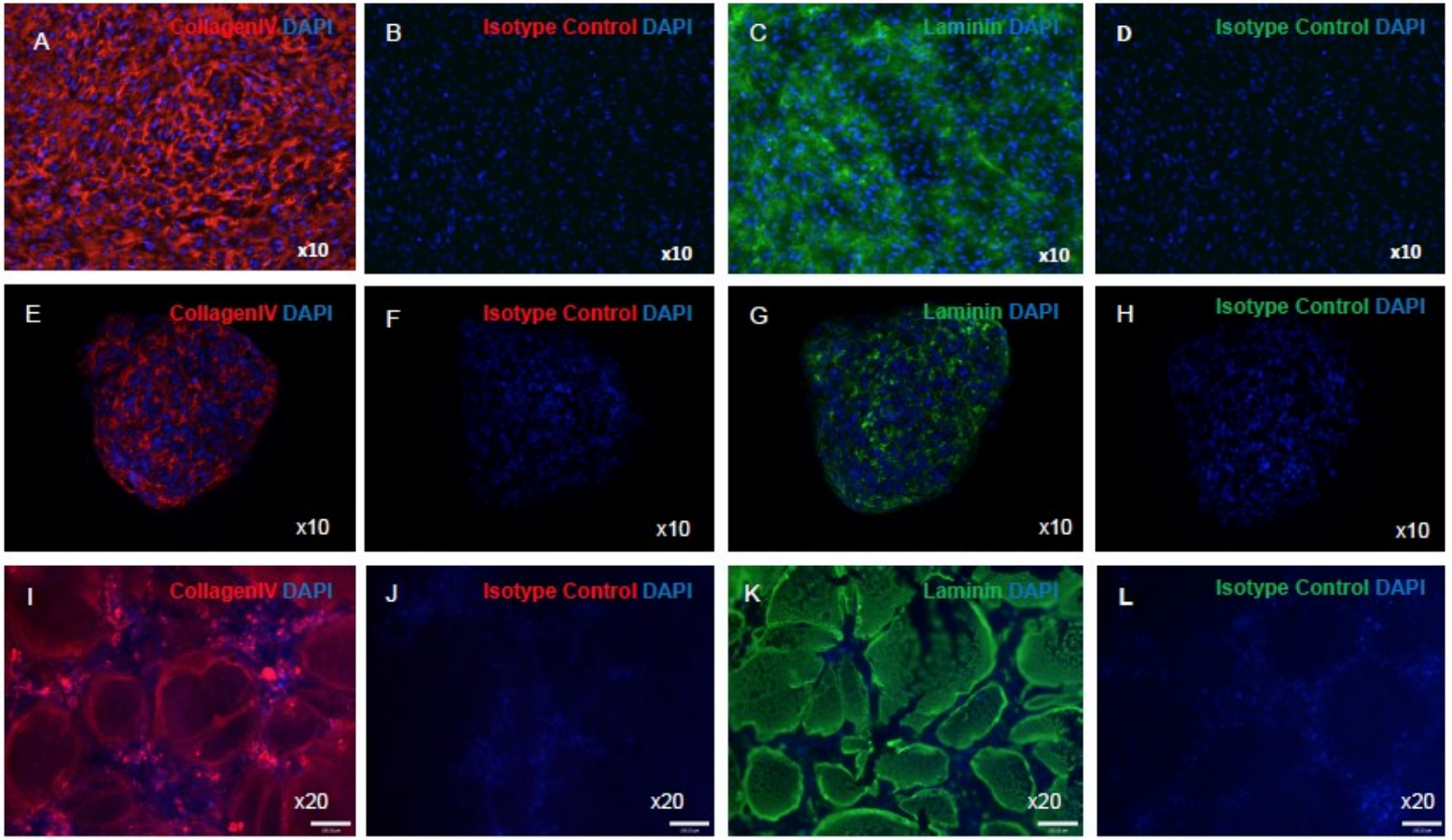

Figure 28 BM production in pericyte-EC coculture.

The production of BM proteins at day 5 of 2D coculture (A-D), 3D spheroid coculture (E-H) and in 3D tube assembly (vasculogenic) coculture of pericytes and HUVEC (I-L). At day 5 collagen IV and laminin were distributed throughout 2D cocultures and spheroid cocultures. Note that there was significant binding of anti-laminin antibody to mouse derived proteins present in in Matrigel (K).

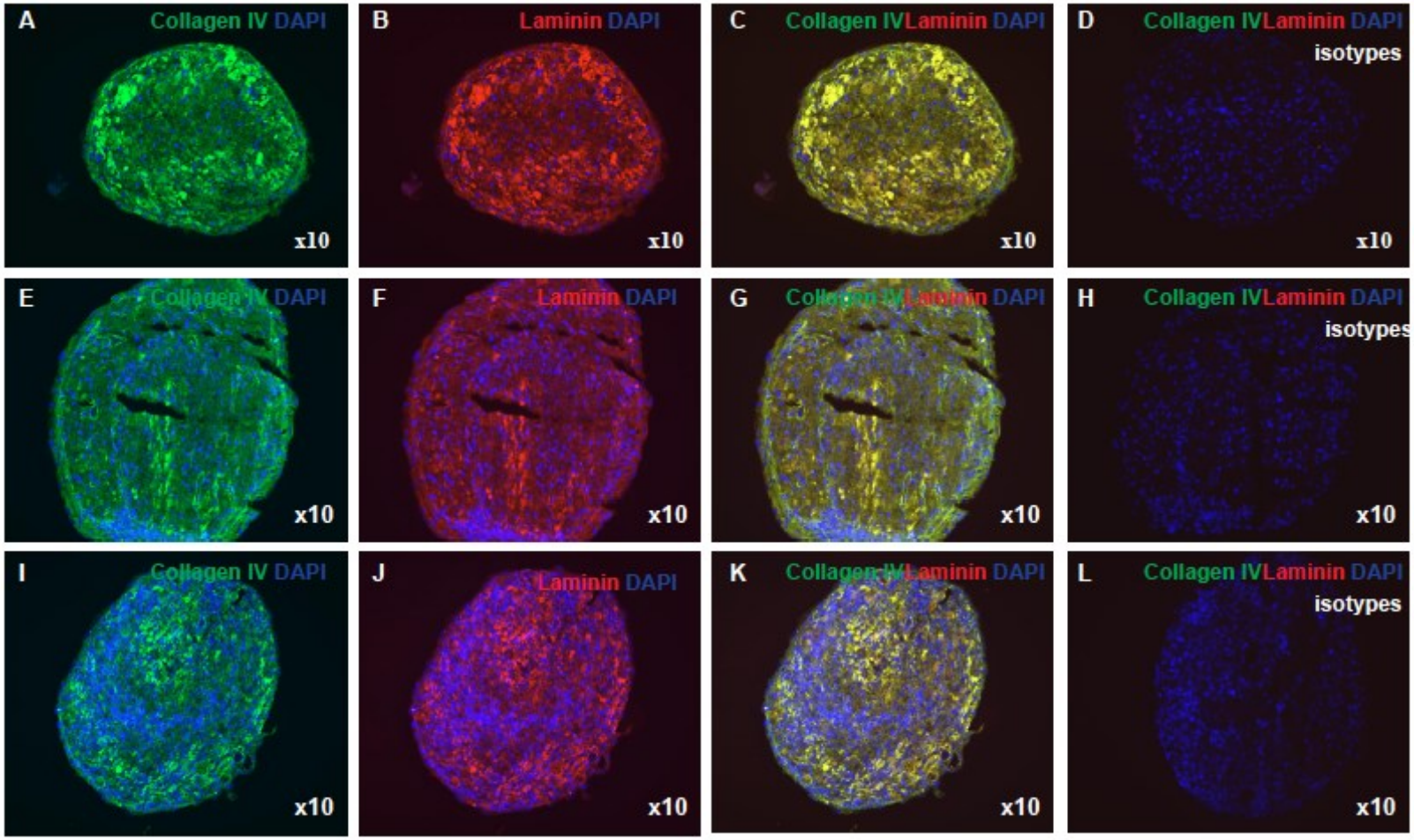

Figure 29 BM production in pellet coculture.

Basement membrane production at day 21 in pellets containing pericytes alone (A-D), pericytes and HUVEC (E-H) and pericytes and fibroblasts.

Chapter 1.5 The influence of endothelial cells on the osteogenic, adipogenic and chondrogenic differentiation of pericytes

Adult stem cell niche components provide signals that control the balance between quiescence, self-renewal, and differentiation[236]. A significant obstacle in identification of the perivascular origin of MSC was the reluctance of pericytes to express mesenchymal phenotypes – except for cell surface markers - in their native environment[129]. Although feasible that pericytes acquire MSC potentials on exiting the vasculature, it is intuitive that they are natively present and environmentally downregulated. Regulation of EC behavior by pericytes (and vice versa) has been extensively documented in the context of angiogenesis[241 285]. However, to our knowledge, no studies have evaluated the influence of perivascular niche components on the differentiation potential of pericytes. The influence of EC on the multipotency of tissue specific MSC has been explored with divergent findings (Table Chapter 1). However, the unique relationship between pericytes and EC within the context of a stem cell niche remains poorly understood.

The initial aim of this chapter was to examine whether coculture with EC influences the osteogenic differentiation of pericytes. Secondly, the influence of EC on the adipogenic and chondrogenic differentiation of pericytes will be explored.

Endothelial cells accelerate the osteogenic differentiation of pericytes *in vitro*

To establish the influence of coculture with EC on the osteogenic differentiation of pericytes in two dimensions, pericytes were seeded onto a confluent monolayer of HUVEC in EGM2 as described above. When pericytes reached 80% confluence, cells were exposed to either basal medium or basal medium supplemented with osteogenic factors. There was no evidence of differentiation by day 21 in cells cultured in basal media (Figure 30, p104)

confirming that pericytes do not spontaneously differentiate down the osteogenic lineage either in monoculture or in the presence of EC.

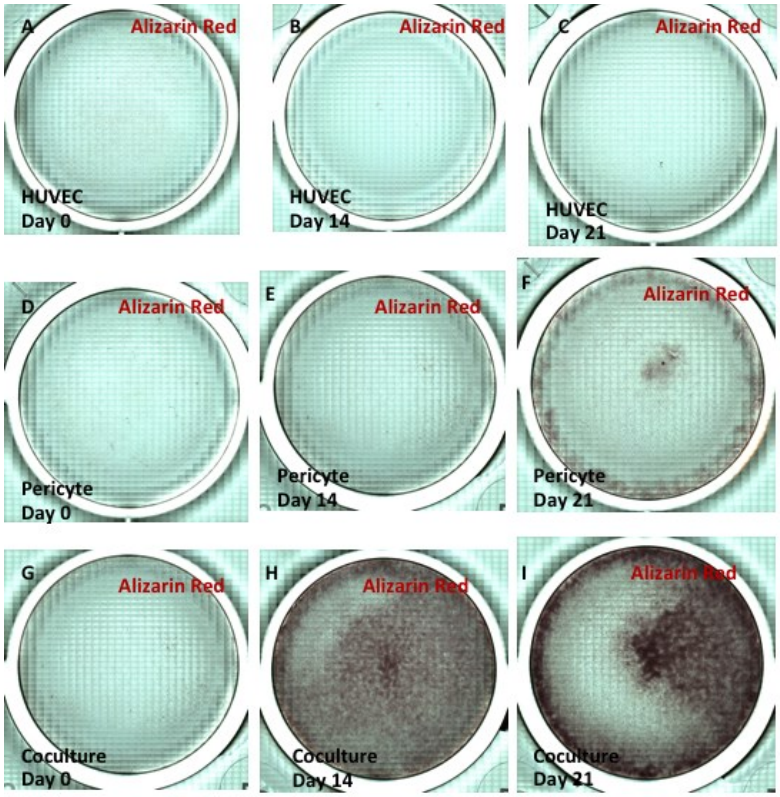

Figure 30 Pericyte-EC coculture in basal conditions
There was no evidence of osteogenic differentiation as detected by Alizarin red for mineralization when HUVEC (A-C), pericytes (D-F) or cocultures of these cells G-H) were cultured in basal medium.

In osteogenic conditions, there was no differentiation seen in wells containing EC alone (Figure 31, p105). Although considerable variation was seen between pericyte preparations, mineralization was evident in pericyte monoculture wells from week 2. Coculture wells demonstrated accelerated osteogenic differentiation with complete coverage of differentiated pericytes by week 2. To explore the influence of direct contact, the experiment was repeated with cells separated by a semi-permeable membrane (Transwell or indirect system). Pericyte differentiation remained increased in wells

containing EC Transwells indicating that EC mediated acceleration of pericyte differentiation is not dependent on direct contact (Figure 31, p105). This effect was seen using either HUVEC or HAMEC with either adipose or skeletal muscle derived pericytes (n=3 of each).

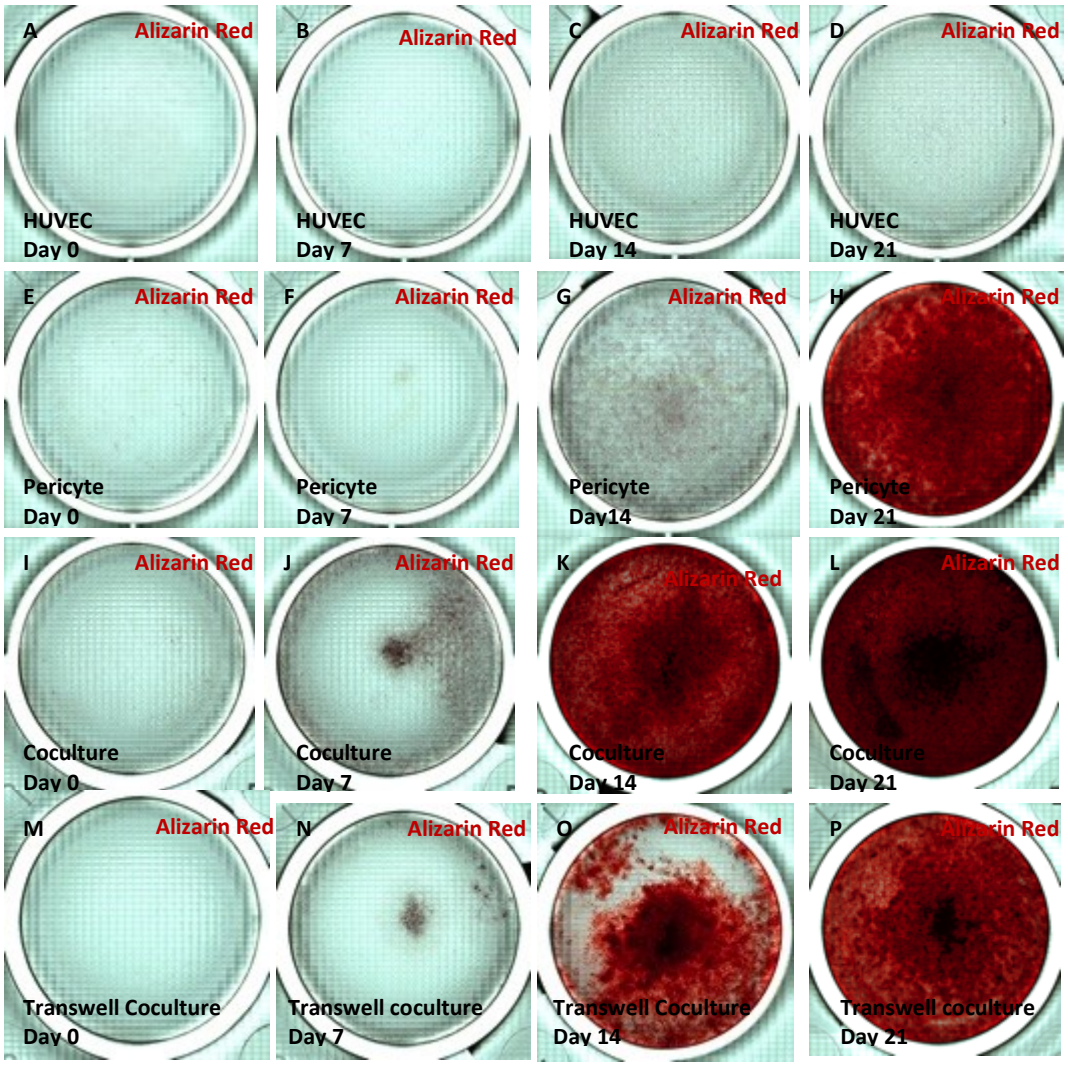

Figure 31 Pericyte-EC coculture in osteogenic conditions
HUVEC, adipose derived pericytes and cocultures of these cells were cultured in osteogenic conditions for 21 days. There was no evidence of mineralization within wells containing HUVEC alone (A-D). The osteogenic differentiation potential of pericytes (E-H) was enhanced in the presence of HUVEC (I-L). This effect was maintained when pericytes and HUVEC were physically separated, being able to communicate only by soluble factors (M-P).

The degree of osteogenic differentiation was quantified through spectrophotometric analysis of eluted Alizarin Red stain (Figure 32, p107). There was a significant increase in osteogenic differentiation at d 7 and 14 in cocultures with HUVEC and human adipose microvascular EC (HAMEC) ($p<0.05$, $n=3$). Although there was a trend to increased differentiation in indirect coculture wells, this did not reach statistical significance.

Quantitative RT-PCR was used to compare the expression of osteogenic genes in pericyte monocultures and in indirect Transwell coculture with EC. The relative expression of the osteogenic genes alkaline phosphatase (AP) and osteopontin (OPN/SPP1/bone sialoprotein/BSP) was increased at d 14 when pericytes were cocultured with HUVEC Transwells (Figure 33, p108). However, we were unable to detect differences in collagen 1 (COL1) between pericyte monoculture and indirect coculture wells at any timepoint.

In this set of experiments I used Transwell cocultures to establish whether the accelerating effect on pericytes osteogenic differentiation by EC was contact dependent. This method permits molecular "crosstalk" and is generally considered the gold standard. However, applicability is limited in 3D and the system is extremely expensive. An alternative method is the use of conditioned media. The soluble factors present in culture supernatant can be delivered directly, as supernatant concentrate or as fresh frozen. While this permits ease of use in 3D there is no "crosstalk" between cells, and factors may be affected by the transfer/freezing process.

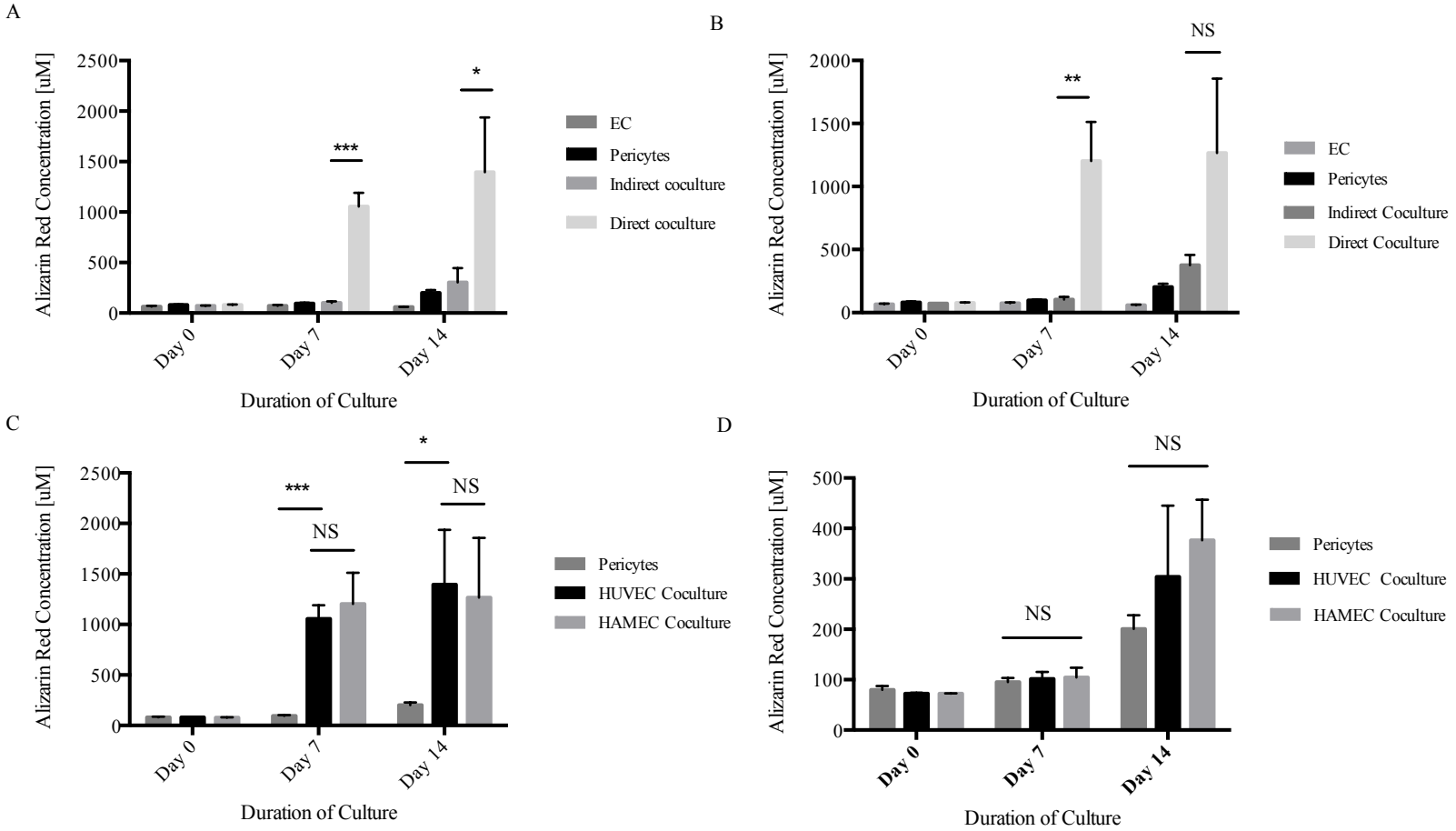

Figure 32 Quantification of osteogenic differentiation of muscle derived pericytes was performed through spectrophotometric analysis of eluted Alizarin red

HUVEC cocultures (A), HAMEC cocultures (B), comparison between HUVEC and HAMEC in indirect coculture (C) and comparison between HUVEC and HAMEC in direct coculture (D). Results shown as ± SEM; n = 3; *p<0.05.

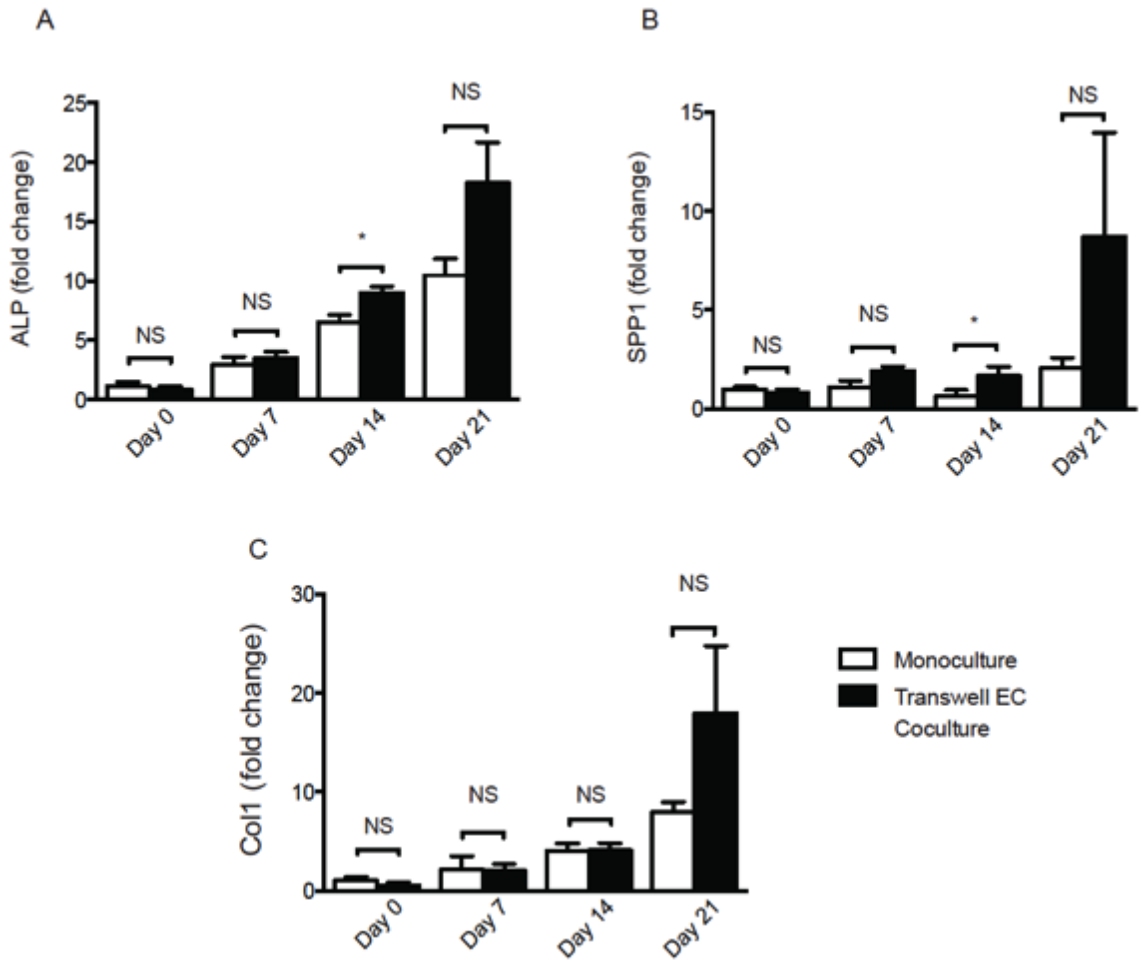

Figure 33 Expression of osteogenic genes by muscle pericytes in Transwell coculture with EC
Time course expression of the osteogenic genes AP (A), SPP1 (B) and Col1 (C) by pericytes in monoculture and pericytes in transwell coculture with EC. For each gene, values are given as the expression levels relative to pericyte monocultures at day 0 (Results shown as ± SEM;n = 3; endogenous control HBRT; *p<0.05)

Coculture with endothelial cells does not increase the proliferation rate of pericytes

EC have been shown to influence the rate of proliferation of human retinal pericytes[286] and pericytes from other sources[285]. We explored the possibility that an increase in proliferation of pericytes in coculture with EC might explain, in part, their accelerated osteogenic differentiation. Pericytes were seeded in equal numbers in monoculture, direct coculture with EC, and indirect (Transwell) coculture with EC. Wells were harvested at day 3, 6 and 9 and the number of pericytes ascertained using a combination of cell counting and FACS to confirm the proportion of pericytes. We found that the growth curves of pericytes in these three settings were very similar and the population doubling times (PDTs) were not significantly different. Pericytes exhibited a PDT of 22.06hrs (SD 1.137), 23.55hrs (SD 7.430) and 22.84hrs (SD 1.721) in monoculture, coculture and indirect coculture respectively (figure 1.5.5).

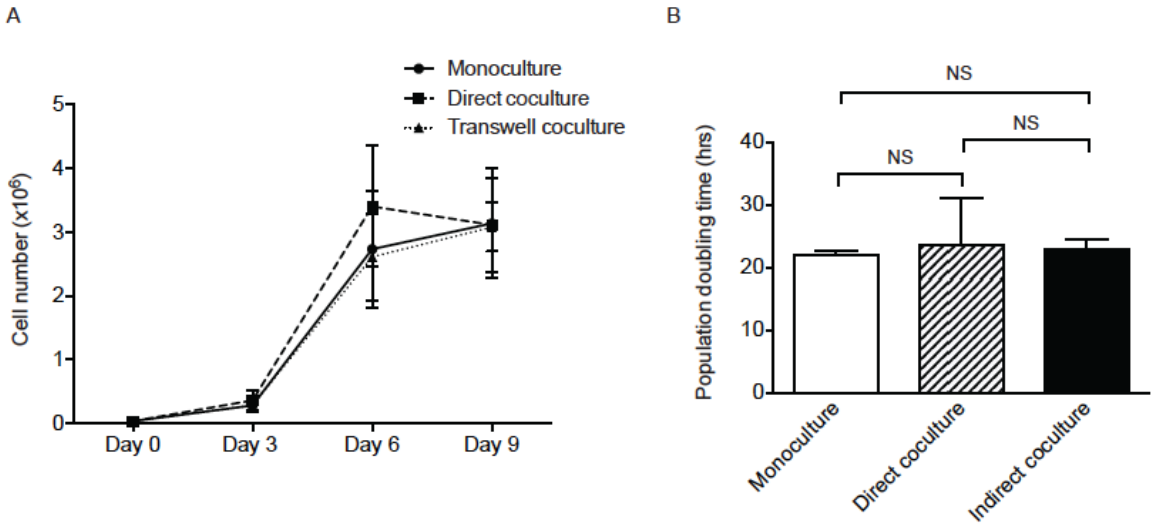

Figure 34 Proliferation of pericytes in coculture with EC.
Growth curves of pericytes in monoculture, direct coculture and indirect coculture with EC (A). There was no significant difference in population doubling times of pericytes in monoculture, direct coculture or indirect coculture with EC. (Results shown as ±SEM; n=3; NS p>0.05).

The influence of endothelial cells on the osteogenic differentiation of pericytes *in vivo*

In vivo osteogenesis experiments using MSC are most frequently accomplished using the ectopic bone formation assay[14 287]. In this assay, human MSC are seeded onto gelfoam or mixed with hydroxyapatite and implanted into intramuscular or subcutaneous pockets in immunocompromised[288 289] or immunocapable[290] rodents. Assessment for bone is done using serial radiographs and by micro CT.

To investigate whether EC would also accelerate the osteogenic differentiation of pericytes in an *in vivo* setting, gelfoam sponges were inserted into the gluteofemoral muscles of C57BL6 mice loaded with HUVEC alone, pericytes alone, pericytes and HUVEC or only PBS as a control. BMP2 was loaded onto the gelfoam sponges to stimulate osteogenesis. Serial radiographs were taken at weekly intervals for six weeks post implantation at which point mice were culled and the legs harvested for micro CT analysis of ectopic bone.

With n = 4 animals per experimental group there were no statistically significant differences in ectopic bone volume (BV) and bone density (BD) between any of the groups ($p<0.05$) (Figure 35, p112). This *in vivo* study was limited by the huge variability seen within experimental groups and the low sample size used.

The muscle pocket model of ectopic bone growth has a number of limitations which may have affected the results. The cytokine used to induce osteogenesis in this setting – BMP – is potent and can mask subtle differences in differentiation between groups. This is

highlighted by the degree of osteogenesis seen in animals who did not receive cells. Furthermore this model can have considerable variability between animals as subtle alterations in implant placement (for example in an avascular plane compared to a vascular body of muscle) can influence osteogenic differentiation. Despite practicing gelfoam placement on cadaver animals in advance it is likely that my relative inexperience with the surgical model may have contributed to the variability.

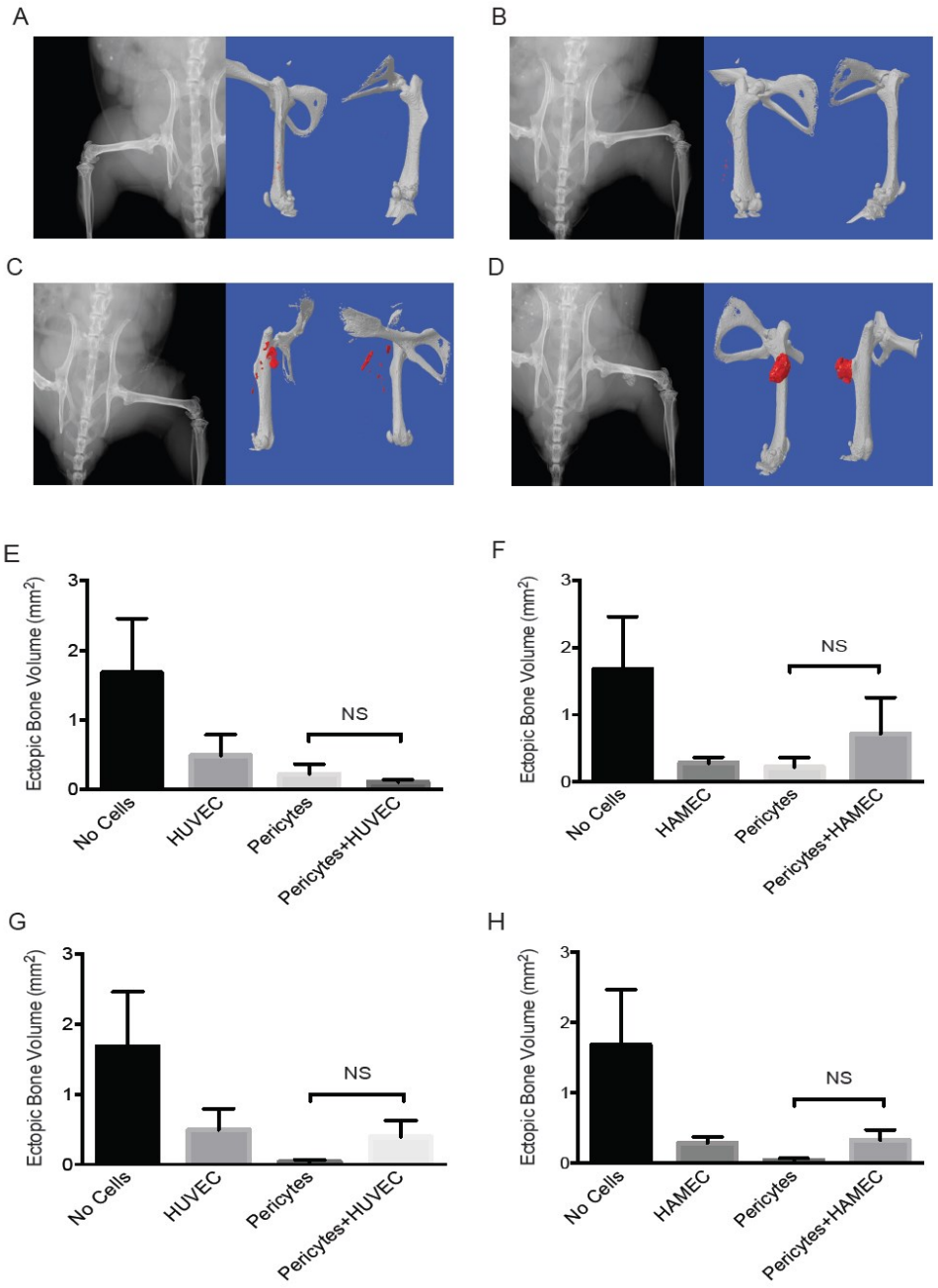

Figure 35 In vivo ectopic bone formation assay
Huge variation in ectopic bone formation was seen both within and between treatment groups with four representative patterns of bone growth observed: (A) no ectopic bone growth, (B) low ectopic bone growth, (C) high ectopic bone growth (D) high ectopic bone growth fused to the femur. No significant differences in ectopic bone volume were seen using skeletal muscle derived pericytes with HUVEC (E) and HAMEC (F), or using adipose derived pericytes with HUVEC (G) and HAMEC (H). (Results shown as ± SEM; n=3; NS p>0.05)

Influence of coculture with endothelial cells on the adipogenic differentiation of pericytes

We set out to determine whether the effects on pericyte differentiation potential in two dimensional coculture were lineage specific. Pericytes were seeded onto a confluent monolayer of HUVEC in EGM2 medium as described above. When pericytes reached 80% confluence, cells were exposed to either basal medium or basal media supplemented with adipogenic factors. There was no evidence of differentiation by day 21 as detected by Oil Red O staining of lipid droplets in basal medium. In adipogenic conditions, lipid droplets were visible in pericyte cultures from day 7 increasing to day 21 (Figure 36, p114). There were no lipid droplets in HUVEC monocultures. Subjectively, there was less evidence of pericyte adipogenic differentiation in coculture with HUVEC – a difference most marked at Day 7 and Day 14 (n=3).

The area fraction of wells staining positively for Oil Red O was determined using image analysis software. Dye taken up by lipid droplets was eluted and measured using a spectrophotometer (Figure 37, p115). Despite subjective differences in the number of lipid droplets within wells, neither of these methods were sufficiently sensitive to detect differences.

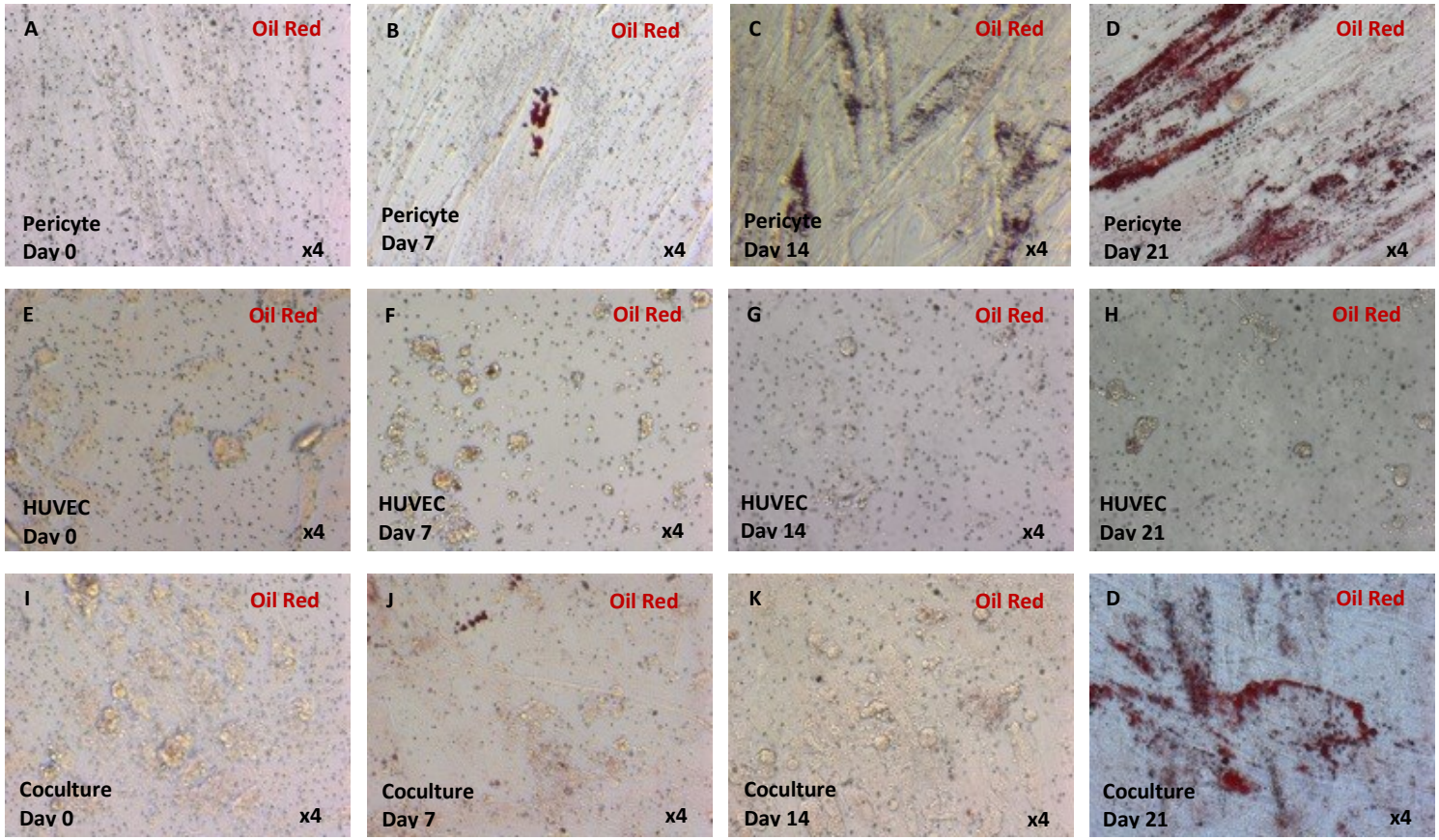

Figure 36 Pericyte adipogenic differentiation in coculture with HUVEC
In adipogenic conditions, lipid droplets were visible in pericyte cultures from day 7 increasing up to day 21 (A-D). There was no lipid droplet formation in HUVEC monocultures (E-H). Subjectively, there was less evidence of pericyte adipogenic differentiation in coculture with HUVEC – a difference most marked at Day 7 and Day 14

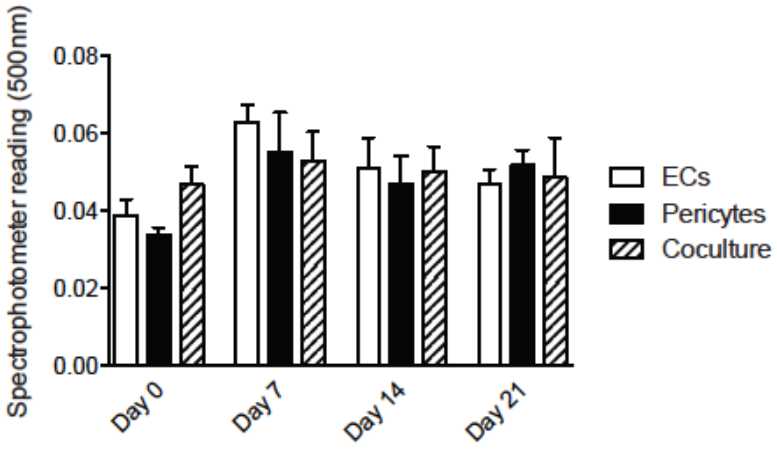

Figure 37 Quantification of pericyte adipogenic differentiation in coculture with HUVEC Cultures were stained with Oil Red O to identify lipid droplets. The dye taken up by lipid droplets was eluted and the concentration of dye eluted was used to quantify differentiation. Despite subjective differences in the levels of differentiation (for example from Day 0 to Day 21 pericytes) this dye elution method was not able to detect any statistically significant differences between wells. Furthermore there was considerable background dye quantified in this method as shown by the readings at Day 0 before adipogenesis was initiated and by the ongoing high readings in the EC only wells.

Influence of coculture with endothelial cells on the chondrogenic differentiation of pericytes

The influence of EC on conventional MSC or pericyte chondrogenic differentiation has not previously been reported. However, many of the early transcriptional changes are common to both osteogenesis and chondrogenesis. We were therefore intrigued to see if EC also had an effect on chondrogenic differentiation. Pericytes alone and cocultured with HUVEC or fibroblasts (cellular control) were centrifuged to form pellets. Over the subsequent 48hrs pellets develop into spherical micromasses that are agitated daily to prevent them from adhering to the tubes (figure 1.5.9).

Pellets composed of pericytes alone and pellets with pericytes and EC cultured in chondrogenic medium for 21 days formed compact spherical structures. The pellets

containing EC alone did not form stable pellets with cells dispersing with even slight agitation. Irrespective of the cell content, debris were present in all wells at day 21 that were distinct from the pellet itself. On histological analysis, pellets showed a highly compact central core that became increasingly compact with time in chondrogenic medium and stained positively for Alcian blue and safranin O (Figure 38, p117). This core was surrounded by a peripheral ring of flat, elongated cells suspended in extracellular matrix. Pellets cultured in basal conditions for 21 days formed a spherical structure that was less compact and stable on sectioning than pellets exposed to chondrogenic medium. Furthermore, there appeared to be a less pronounced peripheral ring of elongated cells. In these control samples, there was evidence of proteoglycans as determined by Alcian blue and safranin O staining although the level of staining was not clearly different to cells exposed to chondrogenic medium.

Our findings support the chondrogenic capacity of pericytes under appropriate environmental cues without conclusive findings of a possible regulatory effect by EC. Due to the prolonged time required to culture freshly sorted cells and the expense involved in the assay, experiments were performed with a single EC type (HUVEC) and pericytes from adipose tissue (n = 3). The staining evident in our experimental samples was considerably weaker than that from the positive control tissues (foetal cartilage) (Figure 39, p118). It is possible that the collagen matrix formed in our chondrogenic pellets represents a very early stage in cartilage development where the proteoglycan content is still relatively low. Additional proteoglycan stains such as toluidine blue could be used, or antibodies against chondrogenic proteins such as collagen type II, type X, and type IX and aggrecan could be used[41 291] A straight forward method that could have been performed to assess formation of matrix in pellets would have been to measure pellet cellularity and weight and proteoglycan content[41]. It is known that oxygen tension regulates chondrocyte differentiation and promotes cartilage matrix

formation[292 293]. This may go some way to explain the zones of variable ECM production seen within pellets.

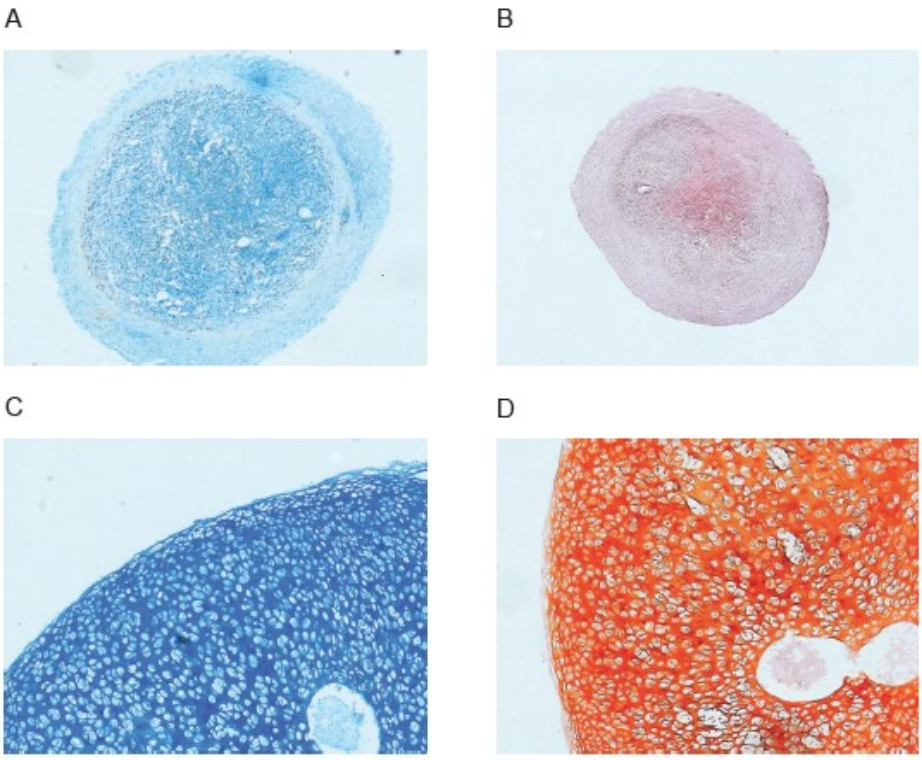

Figure 38 Chondrogenic pellet structure
(A) This histological section of a pericyte pellet exposed to chondrogenic medium for 21 days illustrates typical appearances with a central core with marked proteoglycan deposition (blue) and a peripheral ring with flatter, more elongated cells. (B) histological section of pericyte pellet exposed to chondrogenic medium for 21 days stained with safranin O. Foetal cartilage (positive control) stained with Alcian blue (C) and safranin O (D).

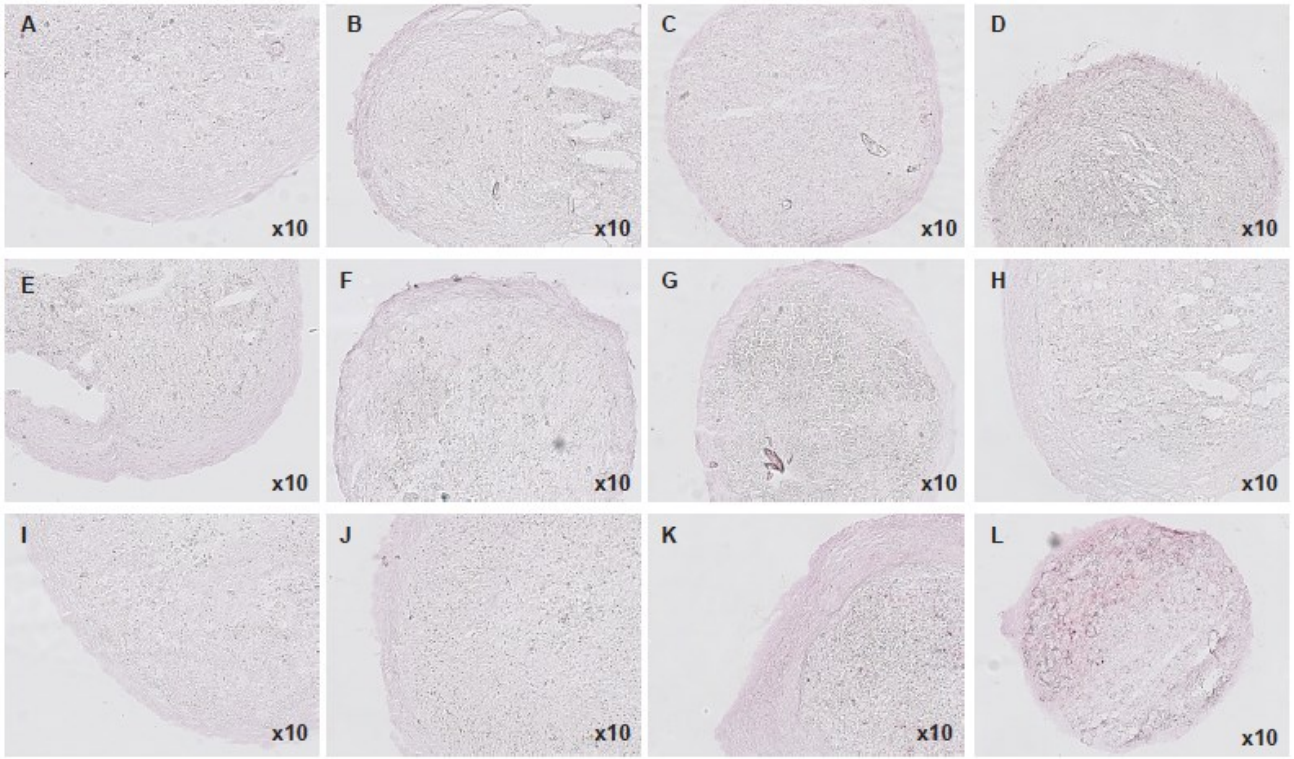

Figure 39 Safranin O analysis for proteoglycans within chondrogenic pellets.
Pericyte monocultures at day 7 (A), day 14 (B) and day 21 (C) in chondrogenic medium and at day 21 in basal medium (D). Pericyte-HUVEC cocultures at day 7 (E), day 14 (F) and day 21 (F) in chondrogenic medium and at day 21 in basal medium (G). Pericyte-fibroblast cocultures at day 7 (H), day 14 (I) and day 21 (J) in chondrogenic medium and at day 21 in basal medium (K).

Chapter 1.6 A potential role for wnt signalling in endothelial cell regulation of pericyte osteogenic differentiation

Introduction

There is an extensive literature describing signalling pathways recognised to control MSC fate decisions[263 294]. These include bone mophogenetic protein (BMP), sonic hedgehog (SHH), wnt, pparg, sox9 and runx2[263 294]. EC are recognised to actively signal through a number of these pathways[295].

Wnt proteins are cysteine rich secreted glycol-lipoproteins that regulate a vast array of biological processes including development, cell proliferation and motility, and cell fate determination[296-298]. Wnts bind to serpentine receptors of the frizzled (FZD) family on the plasma membrane to initiate several distinct cascades classified as either canonical or non-canonical, depending on whether β-catenin is involved (Figure 40, p121) [299]. So far, 19 wnt ligands have been identified in mammals[300]. Classically, wnt1, 2, 3, 3a, 8 and 8b are regarded as the canonical wnts, and wnt4, 5a, 5b, 6, 7a and 11 as the non-canonical wnts[301 302]. In the absence of a canonical wnt signal, cytosolic β-catenin is rapidly phosphorylated, ubiquitinated, and degraded. wnt-FZD binding in the presence of LRP5 or LRP6 results in inactivation of the β–catenin phosphorylation complex, so that β-catenin accumulates in the cytosol. β–catenin then translocates to the nucleus, binds transcription factors of the Tcell factor (TCF) family and promotes transcription of target genes[303]. Non-canonical wnt signaling and the molecules involved have been less well characterized, although their interactions are known to be diverse.

Wnt signalling is closely controlled by several groups of negative regulators that interfere either with receptor-ligand binding or with intracellular signalling. Secreted FZ-related peptides (sFRPs) and wnt inhibitory factor (WIF-1) compete with FZD for wnt ligand binding while dickkopf (Dkk) and Sclerostin target and antagonize LRPs (transmembrane proteins with which FZ proteins usually interact) to block wnt

signalling[304-306]. Certain cytoplasmic proteins interfere with wnt signalling to block the β–catenin dependent pathway. APC, axin1 and axin2, scaffold proteins of the β–catenin destruction complex, are required for the degradation of β–catenin. CKIα and GSK3β phosphorylate β–catenin, leading to its degradation. NKD (Naked Cuticle) 1 and -2 interact directly with Dv1 enabling Dv1 to favour the wnt/PCP pathway by stimulating JNK activity, while simultaneously preventing Dvl from activating the canonical Wnt pathway. Similarly, NLK activates the non-canonical pathway and simultaneously inhibits the canonical pathway by antagonizing TCF/LEF1[298].

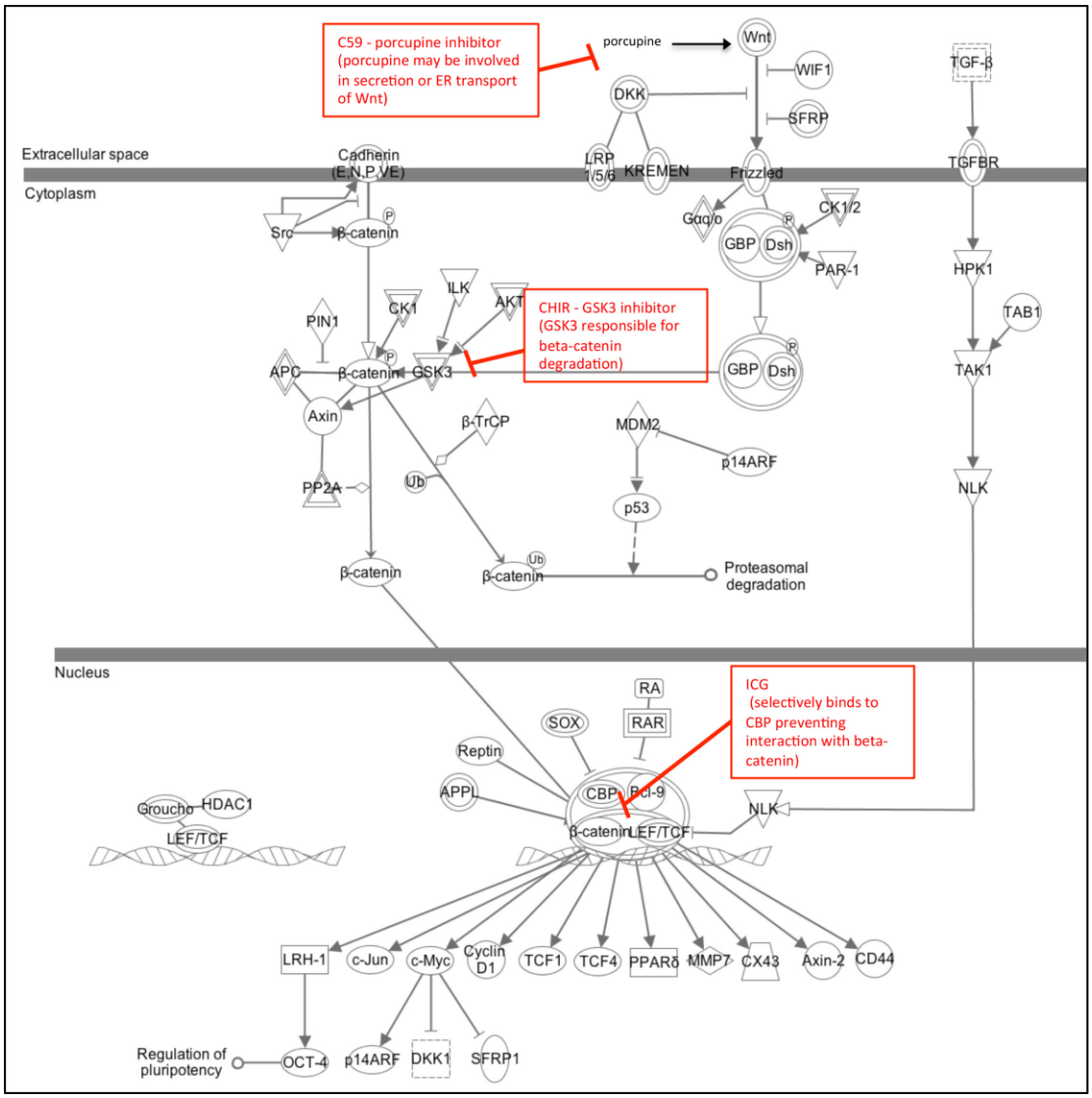

Figure 40 The mode of action of the wnt modulators C59, CHIR and ICG is highlighted in red.

MSC express a number of wnt ligands, including wnt2, wnt4, wnt5a, wnt11 and wnt16 and several wnt receptors, including FZD 2, 3, 4, 5 and 6 as well as various co-receptors and wnt inhibitors[307]. Once secreted, wnt proteins become attached to extracellular matrix or the cell surface to function in an autocrine or paracrine manner[308]. Wnt signalling plays a vital role in the regulation of self-renewal and in adipogenic, chondrogenic, and osteogenic differentiation in MSC[309-311], although the mechanisms by which this pathway exerts its effects are still not fully understood.

The lineage specification and the early differentiation potentials of MSC are controlled by both canonical and non-canonical wnt pathways[307 312], although again with divergent findings. The first study linking wnt signalling to adipogenesis demonstrated that expression of wnt10b decreases during adipogenesis *in vitro* and that ectopic secretion of wnt10b inhibits adipogenesis by suppressing adipogenic transcription factors including pparg and CCAAT/enhancer binding protein-alpha (C/EBPα)[313]. Since then wnt6, wnt10a and wnt10b have been shown to inhibit adipogenesis and stimulate osteoblastogenesis through a β–catenin-dependent pathway[314]. However, it has also been suggested that canonical signalling suppresses osteogenic differentiation[298]. In the presence of wnt3a, MSC undergoing osteogenesis exhibit reduced matrix mineralization and alkaline phosphatase activity and an increased expression of bone related markers[312].

Although numerous studies have described the role of wnt signalling on MSC isolated by traditional means, few studies have addressed these processes in native MSC, namely pericytes. Pericytes express several wnt receptors, including LDL receptor–related proteins 5 and 6, and Frizzled 1 to 4 and 7, 8, and 10, [315]. Wnt/β-catenin signalling inhibits adipogenic differentiation while enhancing chondrogenic differentiation when stimulated by lithium [315]. In these investigations, lithium enhanced chondrogenesis in

pericyte pellet cultures in the presence of transforming growth factor-β3, as demonstrated by increased sox-9 expression and glycosaminoglycan accumulation into the matrix. In contrast, transduction of pericytes with a recombinant adenovirus encoding dominant-negative T-cell factor-4 (RAd/dnTCF), which blocks wnt/β-catenin signalling, inhibited chondrogenesis, leading to reduced sox-9 and type II collagen expression and less glycosaminoglycan accumulation. Adipogenic differentiation of pericytes in both pellet and monolayer cultures was reduced, as demonstrated by decreased staining with Oil Red O and reduced pparg expression. This effect was negated by transduction of pericytes with RAd/dnTCF.

EC display endogenous activation of the canonical wnt signalling pathway and express multiple ligands, receptors, and secreted modulators of wnt signalling. A systematic RT-PCR analysis of expressed wnt signalling components has been performed on HUVEC. Of the nineteen human wnts identified to date, only wnt 2b, 3, 4, 5a, 5b, 6, 7a, 11, 14 and 15 were expressed by fresh or cultured HUVEC[295]. However these cells also secrete the wnt regulators Dkk1, Dkk2, Dkk3, SFRP1, SFRP3 and SFRP5[295].

The aim of this short chapter was to explore a potential role for wnt signalling in the EC influence on pericyte osteogenic differentiation. We evaluated the subcellular localisation of β-catenin to explore whether EC derived factors influenced canonical wnt activation of pericytes.

Wnt modulators may influence the osteogenic differentiation of pericytes in coculture with endothelial cells

HUVEC, pericytes and cocultures of these cells were cultured in osteogenic conditions supplemented with wnt modulators for 14 days (Figure 41, p125). CHIR promotes wnt signalling through the inhibition of GSK3 which acts to degrade β–catenin. ICG selectively binds to CBP preventing its interaction with β–catenin and therefore inhibiting transcription through both the canonical and non canonical pathways. At 14 days, monocultures and cocultures supplemented with the wnt agonist CHIR demonstrated increased differentiation when compared with controls (DMSO). Conversely, monocultures and cocultures supplemented with the wnt inhibitor ICG had less osteogenic differentiation at 14 days than controls.

The abolition of osteogenic differentiation in the presence of ICG, a specific inhibitor of wnt signalling, confirms that wnt signalling is necessary for the osteogenic differentiation of pericytes. In addition the enhanced osteogenic activity of pericytes in cultures supplemented with CHIR is in keeping with previous studies on MSC. Overall these findings indicate that increased wnt signalling enhances osteogenesis while inhibition of this pathway is associated with reduced osteogenic activity. However, this experiment does not provides direct evidence that the EC influence of pericyte osteogenic differentiation is mediated through wnt pathways – the pro-osteogenic effects of wnt and EC may be simply be distinct and additive.

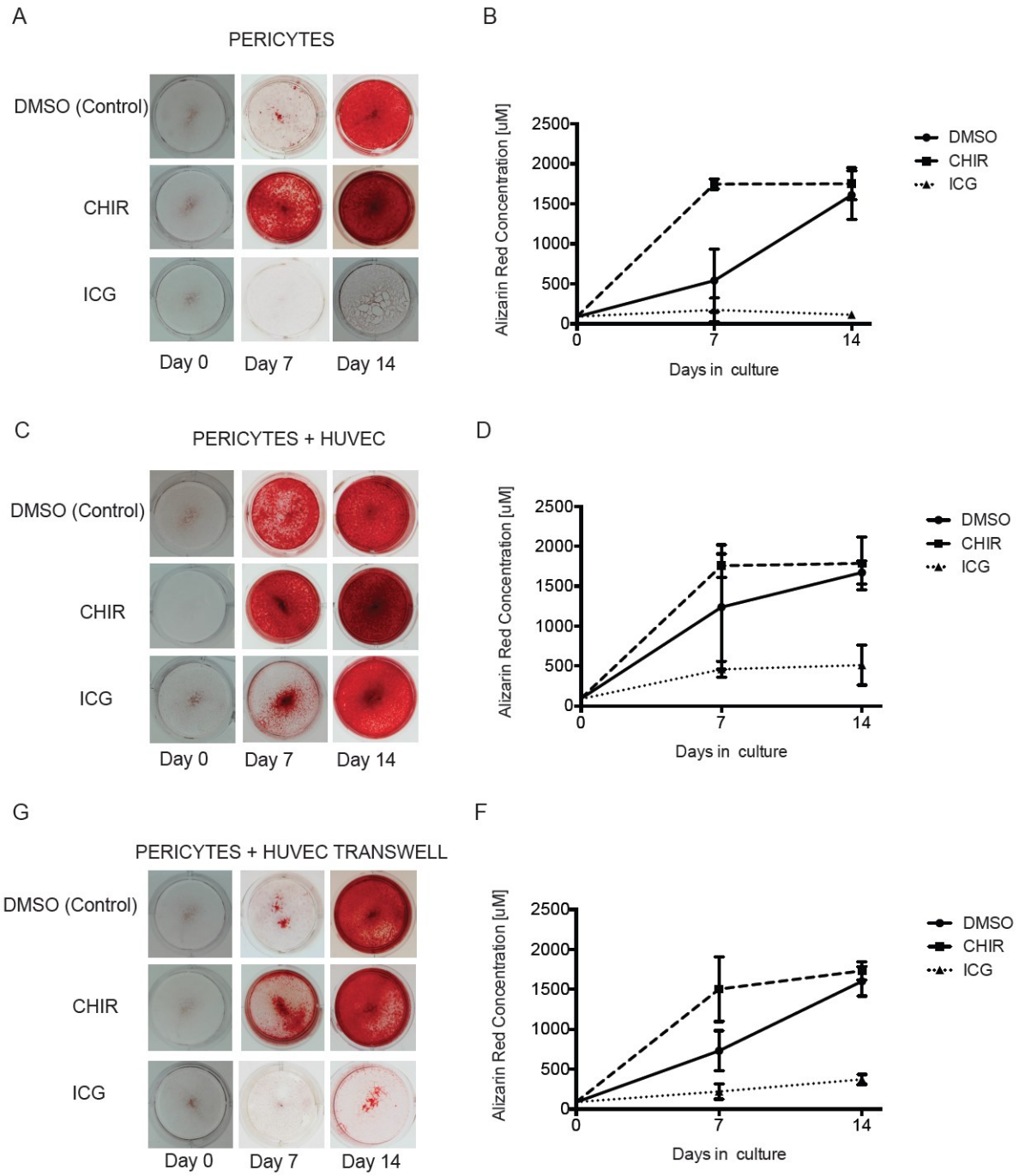

Figure 41 Coculture of pericytes and EC in the presence of the Wnt modulators
The osteogenic differentiation of pericytes in monoculture is accelerated in the presence of the wnt agonist CHIR and abolished in the presence of the wnt inhibitor ICG (A, B). In direct coculture, the osteogenic differentiation of pericytes in CHIR is similar to that of DMSO controls while the presence of ICG tempers osteogenesis (C,D). In indirect coculture with HUVEC pericyte differentiation is increased in the presence of CHIR and reduced in the presence of ICG (G,F). (Results shown are mean ± SD; n=3)

Nuclear translocation of beta β-catenin was not seen in pericytes exposed to EC Transwells or EC supernatant

β-catenin is the central component of the wnt canonical pathway, and is regarded as a hallmark of wnt pathway activation. In the absence of a wnt signal, free cytoplasmic β-catenin is phosphorylated by serine/thionine kinases, casein kinase1alpha (CK1alpha) and GSK3β in a large APC/axin scaffolding complex that targets β-catenin for degradation. In the presence of wnt, the destruction complex is disrupted and dissociation of GSK3β prevents phosphorylation of β-catenin. The increased stability of β-catenin following wnt activation leads to its translocation in the nucleus and induces transcriptional activation[316]. BCL9 is involved in signal transduction through the wnt pathway by promoting β-catenin's transcriptional activity.

We evaluated whether EC influenced the nuclear translocation of β-catenin by exposing pericytes to a number of different culture conditions including EC Transwells and EC supernatant. The addition of CHIR was used as a positive control as this is known to activate canonical wnt signaling. Cultures fixed at 6hrs and 48hrs and fluorescently stained for β-catenin and BCL9. Using Image J image analysis software, we were unable to detect any change in subcellular location of fluorescence with β-catenin or BCL 9 or in the number of cells expressing BCL9 in the nucleus following exposure to CHIR. Furthermore, we were unable to detect any changes in fluorescent staining between pericytes exposed to EC supernatant/Transwells over controls with either β-catenin (Figure 42, p127) or BCL9 (Figure 43, p127).

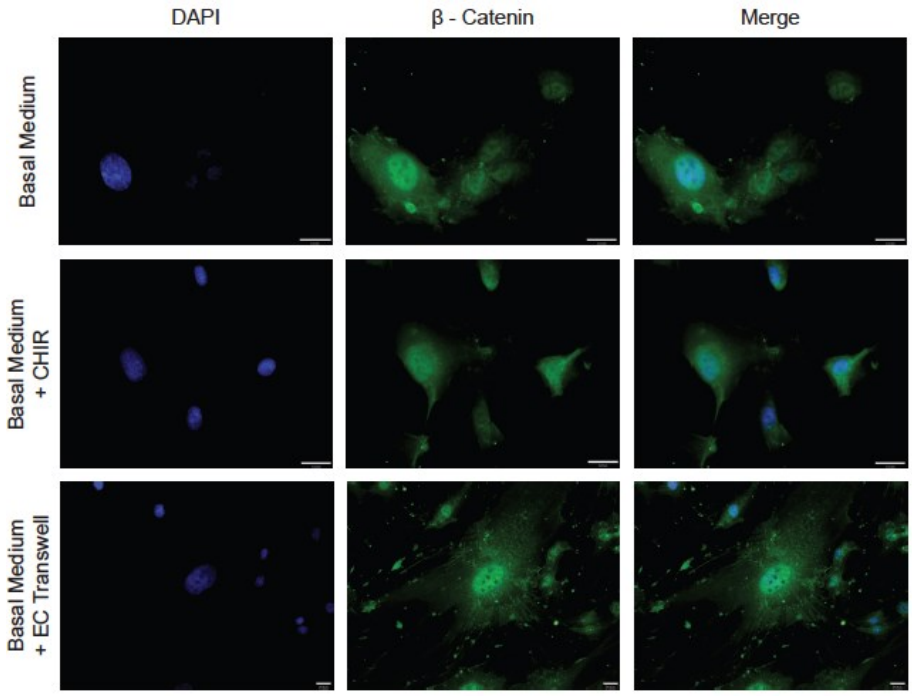

Figure 42 β-catenin and staining in pericytes exposed to wnt activators and EC Transwell. Diffuse cytostolic fluorescence was seen following anti-β-catenin staining despite exposure to the wnt agonist CHIR or exposure to EC Transwell.

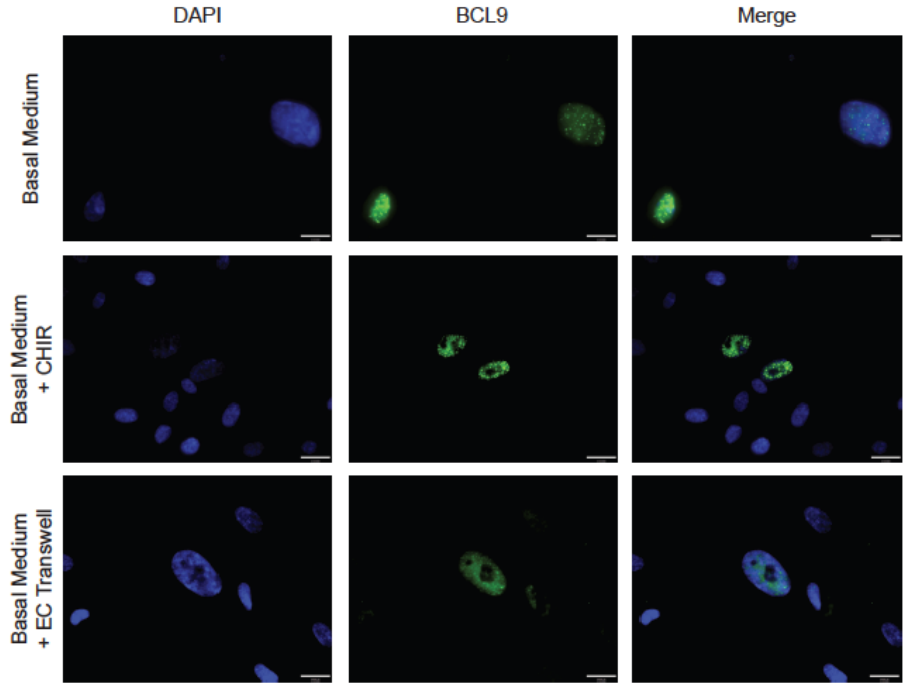

Figure 43 BCL9 and staining in pericytes exposed to wnt activators and EC Transwell. Nuclear fluorescence was seen in a number of cells cultured in basal conditions following anti-BCL9 staining. However the number of cells expressing BCL9 in their nucleus and the intensity of this staining did not quantifiably increase following treatment with the wnt agonist CHIR or in Transwell coculture with EC.

Chapter 1.7 Discussion

The ability for mesenchymal stem cells (MSC) to differentiate into osteocytes, chondrocytes and myocytes holds great promise for tissue engineering. Emerging data demonstrate that MSC derive from perivascular locations *in vivo* where their ancestors reside as pericytes and adventitial cells within an adult stem cells niche consisting of endothelial cells (EC) and the enveloping basement membrane. However, the factors that regulate mesenchymal activation and osteogenic differentiation of these cells *in vivo* are unknown. The intimate contact between pericytes and EC suggests the existence of heterotypic cell-cell "crosstalk" that regulates pericytes in their local microenvironment. Knowledge of mechanisms mediating mesenchymal activation and osteogenic differentiation of pericytes may facilitate therapeutic exploitation of MSC *in vivo* where accelerated bone regeneration is desirable or in conditions characterized by pathological osteogenic differentiation. We hypothesized that EC influence the osteogenic potential of pericytes. We studied this hypothesis using *in vitro* cell culture models of the perivascular niche making use of histological, immunohistochemical, flow cytometric and molecular biology techniques.

Pericytes were sorted to homogeneity (CD146+/34-/45-/56-) from human adult adipose tissue and fetal muscle using FACS. Sorted pericytes maintained a characteristic spindle shaped morphology and maintained their sorted phenotype (CD146+/34-/45-/56-) in long-term culture (up to passage 10). Additionally, sorted pericytes exhibited trilineage differentiation *in vitro* when cultured under appropriate conditions. Pericytes and EC integrated, and contributed basement membrane proteins (collagen IV and laminin) in 2D cocultures. Pericytes and EC formed vascular networks in 3D coculture. In the absence of osteogenic factors (basal conditions), there was no osteogenic differentiation at day 21 in EC monocultures, pericytes monocultures, and cocultures of the two cells. In osteogenic conditions, there was no evidence of mineralization within wells containing EC alone, while there was complete differentiation of the pericyte

monoculture well. The osteogenic differentiation of pericytes was accelerated in coculture with EC. A significant pro-osteogenic effect was maintained when pericytes and EC were physically separated, being able to communicate only by soluble factors, as determined by qPCR for AP and SPP1 at day 14 (the increase in qPCR for Col1 and Alizarin Red staining for mineralisation did not reach statistical significance). Both HUVEC and HAMEC accelerated osteogenesis, with no significant difference between their effects. EC, pericytes and cocultures of these cells cultured in osteogenic conditions supplemented with the wnt modulators for 14 days. At 14 days, pericyte monocultures and cocultures with EC supplemented with the wnt agonist CHIR demonstrated increased differentiation when compared to cultures without CHIR. Conversely, cocultures supplemented with the wnt inhibitor ICG had reduced osteogenic differentiation at 14 days. This data suggests that in osteogenic conditions, EC accelerate the osteogenic differentiation of MSC pre-cursors, and that this effect may be mediated through wnt signalling. However, the potential role for wnt signialling in this setting requires further investigation.

Pericytes and EC can be sorted from multiple human tissues although endothelial cells rapidly lose characteristic phenotype in culture.

In order to explore the influence of EC on pericytes, I first purified homogenous populations of pericytes and EC using FACS. FACS sorting is an attractive method of cell isolation as it can perform rapid selection of cells based on multiple fluorochromes. The capacity for this platform to select cells based on positive and negative expression of surface markers means that multiple populations can be sorted simultaneously on a standard FACS. In this thesis I initially focused on the sorting of pericytes and EC from

adult fat and human fetal skeletal muscle. Our twin laboratories at the University of Edinburgh and at the University of California, Los Angeles (UCLA) are involved in a large early translational project funded by the Californian Institute for Regenerative Medicine (CIRM) that aims to establish an autologous adipose derived perivascular stem cell based therapy for bone regeneration. My involvement in the project in Edinburgh and during an 8 month attachment at UCLA was primarily in the optimization of FACs sorting protocols from fat. However, the techniques and principles of sorting from fat are extremely transferrable and provided an excellent platform for the sorting of perivascular cells from human and mouse skeletal muscle used in this thesis.

I found that pericytes can be reliably sorted to homogeneity using FACS from both fat and skeletal muscle. By optimizing published protocols I was able to culture pure populations of pericytes revealing some particular pitfalls associated with gating of pericytes. Although I have been able to isolate populations of CD31+CD34+CD146+ EC that retain characteristic appearance and phenotype for the initial passages – these populations universally change phenotype or are over grown by more robust contaminating populations by passage 5.

Notwithstanding the problems I have had with maintenance of an EC phenotype in culture, there are several limitations of using primary EC isolated from skeletal muscle and adipose tissue using FACS. Firstly, EC sorted from these tissues are not well characterised and show significant heterogeneity in behaviour between individuals and preparations[271]. They are slow to proliferate and their characteristics change with each passage in culture[317]. It is likely that with each passage a subpopulation of cells is selected, based on their ability for *ex vivo* culture, until they eventually die out.[318] It is also possible that these cells "age" rapidly in culture becoming rapidly senescent through accelerated telomere shorting as demonstrated with MSCs[142]. As such there is a

strong case for using well characterised EC sources to improve consistency and to ensure that the set up is sensitive enough to pick up subtle experimental phenotypes. In addition, current EC sorting methods cannot distinguish between micro and macrovascular EC and sorted populations would likely contain a mixture of both. Macro- and microendothelial cell matrix differs significantly[319] and it was important to establish whether the macro- or microvascular source of EC influences cell-cell interactions with pericytes. I therefore used well characterised commercially available EC preparations in this thesis: Human Umbilical Vein Endothelial Cells or HUVEC (macrovascular EC) (Lonza) and Human Adipose Derived Microvascular Endothelial Cells (HAMEC) (ScienCell). I found that HUVEC and HAMEC were indistinguishable in terms of appearance in culture, cell surface marker expression and in their influence on pericyte proliferation and differentiation.

Strengths and weaknesses of perivascular niche models

The 2D and 3D models of the perivascular niche generated in this thesis have a number of strengths and limitations (Table 14, p134). There are a number of prerequisites for perivascular models used in the setting of osteogenic differentiation of pericytes in coculture with EC. Firstly, all three components of the perivascular niche must be present: pericytes, EC and their enveloping extracellular matrix or basement membrane. As the process of osteogenic differentiation can take from 2-3 weeks, the model must be stable for the duration of this period. Although the *in vitro* tube assembly assay more closely recapitulates the local cellular and structural environment seen in microvessels, the networks collapse within 24 h and retrieval of the cells from Matrigel can be challenging in this setting. While the 3D *in vitro* spheroid model arguably provides more physiological relevance than 2D coculture, particularly as the influence of stiff culture plastic matrix is removed, the natural structural relationship of vessels is not recreated

and further variables such as the influence of limited access to nutrients of cells in the core are thought to influence cell behaviour[135]. Furthermore, Transwell coculture and the histological processing of tissue are technically challenging. It was therefore decided to proceed using a simple 2D *in vitro* model, where the contact between the two cell types can be easily defined.

2D *in vitro* model	
Strengths	**Challenges**
- Simple - Contact between cell types can be easily defined - IHC can be performed in culture plates - Cells easily dissociated for isolation of populations - Amenable to long term culture (>3wks)	- Contact with culture plastic may modify pericyte/EC behaviour - Natural structural relationship not recreated - Differentiation dependent on confluence - Confluence of pericytes when starting influences capacity to differentiate
3D *in vitro* spheroid model	
Strengths	**Challenges**
- 3D culture more closely recapitulates local cellular environment - Allows physiological self-assembly phenomena - Amenable to sectioning - Amenable to long term culture (>3 wks)	- Natural structural relationship not recreated - Difficulty transferring to a Transwell system - Subsequent isolation of cell populations challenging - Freezing, sectioning and staining of small spheres technically challenging - Contact between cell types not easily defined
3D *in vitro* tube assembly (vasculogenic) assay	
Strengths	**Challenges**
- 3D culture more closely recapitulates local cellular and structural environment - Self organization allows physiological self-assembly phenomena	- Networks collapse within 24 h - Retrieval of cells challenging - Difficulty visualizing at >20x as large optical distance required to accommodate Matrigel layer - Unable to freeze due to thermosensitivity of Matrigel

Table 14 Strengths and weaknesses of 2D and 3D perivascular niche models

In addition to the challenges specific to the structure of each model, establishing conditions in which pericytes are capable of osteogenic differentiation and EC survive proved to be a considerable challenge. Pericytes are routinely cultured in DMEM (20%FBS,1%PS) while EC are conventionally grown in EGM2[14 215]. Survival of EC drops dramatically in DMEM (20%FBS,1%PS), and further still in the presence of differentiation factors. Conversely, pericytes cultured in EGM2 proliferate rapidly becoming a multilayer overgrowing underlying EC. Titrations of media combinations were performed to optimize coculture conditions. Increasing the EGM2 proportion improved EC viability yet resulted in rapid overgrowth of pericytes. Furthermore, diluting differentiation media with EGM2 diminished the differentiation of pericytes.

We therefore elected to use conventional commercial differentiation medium (Lonza) supplemented with fresh EC every second day to ensure a constant presence of viable EC in culture. Optimisation of differentiation conditions in this way was performed in the settings of osteogenesis, adipogenesis and chondrogenesis.

Quantifying differentiation

Functional stains to detect products of osteogenic, adipogenic and chondrogenic lineages are widely published and were therefore used in this thesis[14 216 320]. In particular, Alizarin Red staining for mineralisation provides a clear visual representation of the extent of osteogenic differentiation that can also be quantified using image analysis software. Elution and spectrophotometric measurement of these dyes provides a useful means of quantifying differentiation[320].

The differences in osteogenic differentiation seen with Alizarin Red staining and elution and von Kossa staining were not reflected by significant rises in osteogenic transcripts detected by RT qPCR. However, there was a clear trend indicating increased AP, SPP1 and Col1 in transwell EC coculture over pericyte monoculture. OPN, AP and COL1 were selected because of their early expression[321 322]. Overall, the genetic profile obtained points towards an accelerated osteogenic commitment of pericytes in the presence of EC.

We used relative quantification to determine fold differences in target gene expression normalized to an internal reference (housekeeping) gene. HPRT (hypoxanthine-guanine phosphoribosyltransferase) was selected as a reference gene as our group has found it to be stably expressed across skeletal muscle. The use of multiple stable reference genes is generally accepted as the method of choice for RT-qPCR data normalisation and

this could have improved the reliability of our data[323 324]. The presence of EC-derived reference gene within coculture wells means that accurate comparison of pericyte differentiation between monocultures and cocultures could not be made. However, differentiation in pericyte monocultures and pericytes in Transwell culture with EC could be made as EC populations were separated throughout and excluded for the analysis. We considered a number of strategies that would enable us to accurately compare monocultures and cocultures using qPCR. One potential method would be to use pericytes transfected with fluorescent proteins. The transfected pericytes could then be purified from EC using FACS or MACS immediately prior to RNA extraction. However, many cells are lost through the sorting process and the experiment would need to be performed with a prohibitively large number of cells. Furthermore the differentiated cells are encased in mineralised matrix limiting their amenability to trypsinization and resuspension as single cells prior to sorting.

EC mediated up regulation of pericyte osteogenesis supported by previous studies

The acceleration of pericyte osteogenic differentiation by EC is in keeping with previous studies using MSC (Table 6, p48), but is the first report of this effect in MSC precursors[254-256 325]. Overall, two main mechanistical dialogues have been reported: a paracrine effect through VEGF, BMP-2, IGF production and a juxtacrine mechanism by gap junctional activity [259 326]. Our data indicate that EC mediated up regulation of pericyte osteogenic potential is independent of direct contact. We demonstrate that the presence of EC (separated by Transwell) appears to increases the osteogenic differentiation of pericytes although this did not reach significance in a number of outcome measures. Experiments culturing pericytes using EC supernatant could be performed to investigate if this process requires “crosstalk” between cells or whether

the presence of EC produced cytokines is sufficient to produce this effect. The nature of this effect could be further characterised by exposing the pericytes to EC Transwells for defined periods during the differentiation process to establish whether EC "prime" pericytes for differentiation or whether they exert an effect throughout the process.

Endothelial-Mesenchymal transition is not responsible for increased osteogenesis in coculture wells

The importance of EC plasticity in the development and progression of disease is increasingly recognized[327]. Although pericytes and resident stem cells within muscle have been shown to contribute to forms of heterotopic ossification[328] [329], vascular endothelial cells have recently emerged as a candidate for the cellular origin of heterotopic cartilage and bone in the rare condition Fibrodysplasia ossificans progressive (FOP)[330]. Up to 50% of the cartilage and bone cells found in FOP heterotopic lesions appear to be of endothelial origin based on Tie2-Cre lineage tracing and expression of various endothelial markers (Tie2, Tie1, vWF, VE-cadherin)[328].

Endothelial-mesenchymal transition (EndMT) is characterized by loss of cell-cell adhesion and a strong change in cell polarity, generating elongated spindle-shaped cells. Expression of endothelial markers such as CD31, VE-cadherin, Tie1 and vWF is reduced whereas mesenchymal markers such as FSP-1, αSMA and N-cadherin increase. The newly formed cells are highly invasive and motile and give rise to various tissue types in embryonic development and disease.

We considered the possibility that the increase in osteogenic differentiation in our cocultures resulted from EndMT resulting in a secondary source of osteogenic cells. However, a number of observations make this unlikely in this setting. EC maintained

their characteristic cobblestone appearance in culture irrespective of the medium used (EGM2, basal and osteogenic) while maintaining their CD31+CD34+ phenotype. Furthermore, there was no evidence of osteogenic differentiation as assessed by Alizarin Red and von Kossa staining in EC wells. Finally, the increase in pericyte differentiation seen in the Transwell setting, where EC are physically separated suggests that EndMT is not responsible for the observed increase.

In vivo coculture (muscle pocket) unable to confirm *in vitro* findings

I used a common method of *in vivo* osteogenesis to investigate whether this phenomenon occurred in an *in vivo* setting. However, there was considerable variability within biological replicates and we were unable to draw any meaningful conclusions. The muscle pocket model of ectopic bone growth has a number of limitations which may have affected the results. The cytokine used to induce osteogenesis in this setting – BMP – is potent and can mask subtle differences in differentiation between groups. Furthermore this model can have considerable variability between animals as subtle alterations in implant placement (for example in an avascular plane compared to a vascular body of muscle) can influence osteogenic differentiation. Despite practising gelfoam placement on cadaver animals in advance it is likely that my relative inexperience with the surgical model may have contributed to the variability. If given the opportunity to repeat this experiment I would increase considerably the number of biological replicates used and minimise the concentration of BMP.

The effects of EC are lineage specific

Our results indicate that EC accelerate the osteogenic differentiation of pericytes but we were unable to demonstrate objectively an influence on adipogenic differentiation[135]. A growing body of results suggests that osteogenic and adipogenic lineages are mutually exclusive[331-333,334]. In addition to implications on bone tissue engineering, this observation is relevant to bone homeostasis, where a decline in osteoblasts and a parallel increase in adipocytes is thought to underlie osteoporosis [335]. Chemotherapy is known to induce a shift in the bone marrow MSC population towards a more adipogenic genotype with higher capacity to differentiate into adipocytes[336]. Despite this, various pathways, activated by external stimuli that induce differentiation seem to play dual roles. For example, BMP signaling - one of the main inducers of osteogenic differentiation in MSC - may also be involved in adipogenic differentiation[264].

Complex niche interactions and absent environmental cues prevent differentiation in healthy tissues

Although EC may produce factors *in vitro* that accelerate the osteogenic potential of pericytes, florid osteogenic differentiation throughout perivascular locations is not observed *in vivo* in healthy tissues. This may be due to a lack of environmental cues directing lineage fate and native pericyte-EC interactions that maintain quiescence. Our findings confirm that pericytes do not spontaneously differentiate in basal media, requiring lineage specific factors to direct differentiation. The osteogenic factors used to induce differentiation artificially *in vitro* are likely to have *in vivo* equivalents present only in certain conditions (e.g. injury or growth). It is intuitive, and in keeping with literature describing the behaviour of other adult stem cells[230] [234] that pericyte

differentiation potential natively exists and is environmentally repressed. Here, interactions that require intimate cell-cell contact may maintain stem cell quiescence until this interaction is disrupted by appropriate signals.

An emerging paradigm?

In light of our findings and findings reported by others we propose a paradigm of multilevel control of pericyte behaviour by EC. We propose that pericytes are maintained in a 'quiescent state' through native cell-cell interactions with EC. In response to injury factors, pericytes are 'activated' with respect to MSC potentials, becoming sensitive to environmental cues that initiate osteogenic differentiation and secondary factors produced by EC that accelerate osteogenesis (Figure 23). The native pericyte-EC interaction that maintains dormancy and the soluble factors that subsequently accelerate osteogenic factors represent key mechanistic targets.

Mechanism 1: Native pericyte-EC interaction maintaining quiescence

Pericyte 'quiescence' within their native perivascular niche is observed in healthy tissues where natural pericyte/EC relationships are undisturbed. Similar niche quiescence is observed within other adult stem cell niches[229] [230]. Pathological osteogenesis/adipogenesis is observed in pathological conditions where the microvascular structure is disturbed indicating that pericytes may have been 'activated' with respect to MSC potentials. Furthermore, pericytes have been shown to be capable of all MSC potentials *in vitro* following sorting (separation from EC)[110].

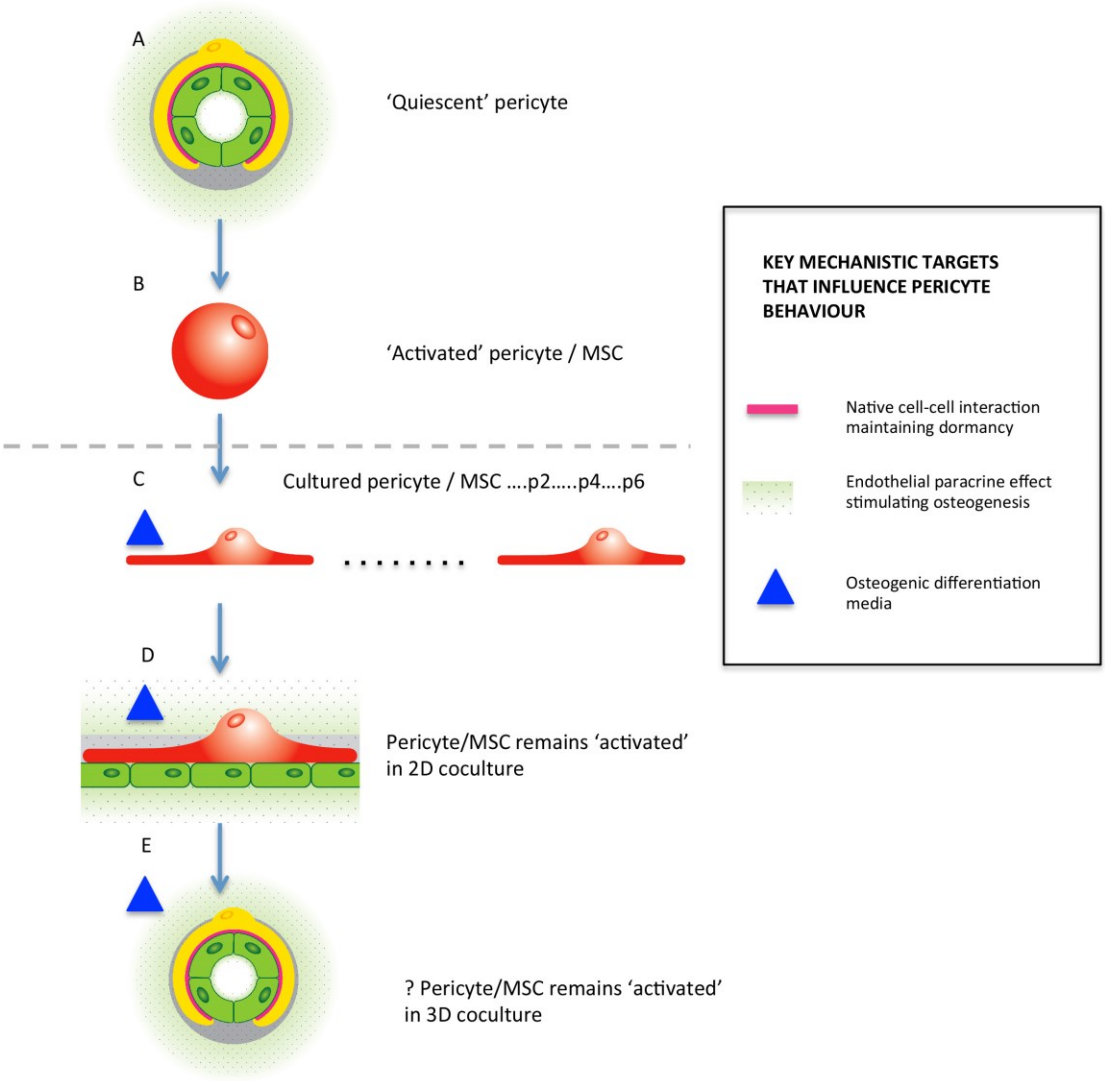

Figure 44 Proposed paradigm outlining the influence of EC on the mesenchymal 'activation' and osteogenic differentiation of pericytes.
Quiescent pericytes reside within their perivascular niche where complex interactions with EC maintain them in a dormant state (A) despite the presence of EC produced soluble factors accelerating osteogenesis. In response to injury factors pericytes are dislodged from the EC binding domains to become activated with respect to MSC characteristics (B). 'Activated' pericytes are sensitive to environmental cues directing lineage differentiation and in the case of osteogenesis to soluble factors accelerating osteogenesis (C). The behavior of pericytes is likely to be modified by long-term culture (D). The native cell-cell interaction maintaining dormancy is not recreated in 2D in vitro coculture where the unopposed EC paracrine effect stimulates accelerated osteogenic differentiation. It is not yet clear whether this native cell-cell interaction maintaining dormancy can be recreated in 3D models of the perivascular niche (E).

Mechanism 2: Endothelial paracrine effect stimulating osteogenesis

Following 'activation' pericytes become sensitive to local lineage specific factors that may be up regulated as part of the injury response – including soluble factors produced by EC. Although a dual effect of EC on pericyte differentiation appears contradictory – it

may be harnessed to maximize the response to injury. While it is important to maintain pericyte quiescence when their mesenchymal phenotypes are not desired, it is equally important to ensure their effects are maximized when their 'activation' is beneficial.

While we have observed EC mediated upregulation of pericyte osteogenic differentiation through soluble factors we have so far been unable to recreate the native cell-cell interactions responsible for maintaining dormancy. It is most likely that 2D culture limits the relevant interactions necessary for downregulation. Alternatively, the initial pericyte detachment from EC may result in irreversible activation, resulting in a downstream subset of pericytes that have so far not been identified as distinct from in situ pericytes. Finally it is feasible that EC have no inhibitory effect on pericytes – the lack of pericyte differentiation observed in healthy tissues occurs as relevant cues for differentiation are not present.

A potential role for wnt signalling

I have performed preliminary experiments to explore a possible role for wnt signalling in the EC acceleration of pericyte osteogenic differentiation. This was based on literature describing production of wnt ligands by EC[295] and the known pro-osteogenic and anti-adipogenic effects of wnt activation[294 337 338]. In the presence of the wnt inhibitor ICG, pericytes in monoculture were not able to differentiate down the osteogenic lineage confirming that wnt signalling is critical to this process. The addition of EC to ICG supplemented wells appeared to overcome this inhibition to some degree. ICG selectively binds to CBP preventing interaction with β-catenin in the nucleus and it may be that the increase in wnt ligand load associated with EC coculture was sufficient to overcome this inhibition. The addition of the wnt agonist CHIR mirrored the pro-osteogenic effect seen with the addition of EC to pericyte monocultures while the

addition of CHIR to coculture wells increased further osteogenic differentiation. It is not clear whether this reflects distinct mechanisms accelerating the osteogenic differentiation of pericytes or whether EC exert their effect through the wnt pathway. More detailed mechanistic studies are required.

Nuclear translocation of β-catenin is a defining feature of canonical wnt signalling. In order to demonstrate activation of wnt pathways in pericyte coculture with EC we set out to show that the concentration of nuclear β-catenin was higher in pericyte coculture with EC. Even in the presence of the wnt agonist CHIR (positive control) we were unable to detect an increase in nuclear β-catenin. This may indicate a technical problem with the experimental set up or that our antibodies were not sensitive enough to evaluate subtle changes in expression. It would be preferable to conduct this experiment in direct cocultures as pro-osteogenic effects are known to be dramatic, although this would have precluded accurate microscopic evaluation. Finally, lack of nuclear translocation of β-catenin in our studies may indicate that EC do not activate wnt through the canonical pathway or that the degree of activation seen with indirect coculture is not sufficiently dramatic to detect using this system.

There are a number of experiments that I could have performed to further characterise the role of wnts in the EC mediated acceleration of pericyte osteogenesis. Despite published reports of the wnt secretome of EC it will be important to confirm that EC secrete wnt ligands. This could be established by performing an ELISA to confirm the presence of wnt ligands in EC supernatant. Furthermore, any difference in wnt gene expression in the presence (using Transwell system) and absence of pericytes might indicate a loop of positive feedback.

A further experiment can be envisioned to confirm that EC modify pericyte differentiation through wnt signalling. EC could be pre-treated with C59 (a wnt modulator that prevents the secretion of all wnt ligands through inhibition of porcupine (figure 1.6.1)) prior to coculture with pericytes. Inhibition of the pro-osteogenic effect by the pre-treated pericytes would confirm that EC exerted their effect through wnt signalling. C59 is the only wnt modulator studied here that influences the production of wnt ligands (CHIR and ICG act downstream of receptor binding). Therefore, addition of CHIR and ICG to EC prior to coculture - without exposing the pericytes to these modulators - would be unlikely to influence pericyte differentiation.

SECTION 2: αV INTEGRIN DEPLETION IN PDGFRβ+ PERIVASCULAR CELLS REGULATES SKELETAL MUSCLE FIBROSIS

Chapter 2.1 Introduction

TGFβ1 has a central role in the development of fibrosis

Fibrotic disease represents one of the largest groups of disorders for which there is no effective therapy and thus fibrosis treatment represents a major unmet medical need. It is well established that myofibroblasts are the main cellular effectors of fibrosis[339]. These phenotypically modulated fibroblasts acquire expression of contractile proteins such as αSMA, and when activated, produce large amounts of extracellular matrix proteins. TGFβ is considered to be the master control cytokine in the activation of the fibrotic response[174]. TGFβ induction and activation is consistently observed in experimental models of tissue fibrosis[340], while TGFβ overexpression induces marked fibrotic changes[179]. Also of consequence is the ability of TGFβ to decrease the production of enzymes that degrade the ECM, such as collagenase, while increasing production of proteins that inhibit ECM-degrading enzymes such as TIMPs and plasminogen activator inhibitor (PAI)-1.

The TGFβ superfamily includes the bone morphogenetic proteins and the TGFβ subfamily which are involved in distinct signalling pathways. The TGFβs are some of the most pleiotropic peptides known, whose functions include critically regulating tissue homeostasis and repair, immune and inflammatory responses, ECM deposition, cell differentiation and growth[341]. The three structurally similar isoforms – TGFβ1, TGFβ2 and TGFβ3 are encoded by three different genes. Although the isoforms signal through the same surface receptors and have similar cellular targets, each isoform is expressed in a distinct tissue specific manner. TGFβ1 is almost ubiquitously found in mammalian tissues, while TGFβ2 and 3 are expressed in a more limited manner. While similar effects with each isoform are observed in vitro, genetic mouse studies have demonstrated distinct roles for each isoform in development[342]. All three isoforms are

expressed in fibrotic tissues, although the development of tissue fibrosis in multiple human organs has primarily been attributed to TGFβ1[341].

TGFβ activation

TGFβ is stored in the ECM as a latent complex consisting of a C-terminal TGFβ and an N-terminal latency associated peptide (LAP), which is bound to the latent TGFβ binding protein (LTBP) by disulphide bonds. The attachment of TGFβ to the binding proteins shields its active epitopes, preventing interactions with the TGFβ receptors. In most tissues, significant amounts of latent TGFβ are "stored" in the matrix. As such, activation of TGFβ signalling is primarily regulated by conversion of latent TGFβ to active TGFβ. One of the best characterised mechanisms of TGFβ activation requires binding of αv integrins to an RGD sequence in the prodomain and exertion of force on this domain, which is held in the ECM by latent TGFβ binding proteins. Although TGFβ synthesis and expression of its receptors are widespread, activation is localised to the sites where TGFβ is released from latency. Mice with integrin binding RGD motif mutated to RGE recapitulate all major phenotypes of TGFβ1-null mice, including multi-organ inflammation and defects in vasculogenesis, thus demonstrating the essential role of integrins in TGFβ activation. Integrin binding alone is not sufficient for TGFβ activation – contractile force exerted by integrins across the latent TGFβ binding protein (LTBP)-prodomain complex is hypothesised to change the conformation of the pro-domain and to free TGFβ for receptor binding (Figure 45, p149).

When active TGFβ is liberated it binds to a heterodimeric receptor complex consisting of one TGFβ type 1 receptor molecule, termed activin-linked kinase (ALK) 5, and one TGFβ type II receptor. In the canonical TGFβ pathway, ligand binding leads ALK5 to phosphorylate SMAD2 and SMAD3, which in turn bind to SMAD4 to form a complex that

is translocated to the nucleus, activating transcription. TGFβ has also been shown to signal via additional pathways, including p38 mitogen-activated protein kinase (MAPK), the Ras/MAPK kinase (MEK)/extracellular signal-regulated kinase (ERK) pathway, the c-abl pathway and Jun kinase (JNK). These signaling pathways modify gene expression in a promoter-selective fashion. It is therefore likely that additional signaling pathways are abnormally activated in myofibroblasts in a manner independent of the canonical TGFβ pathway.

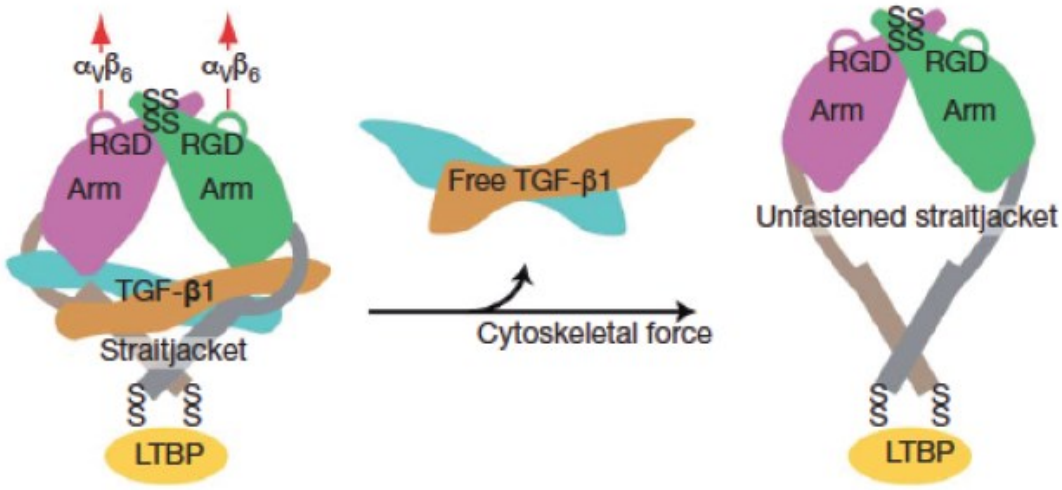

Figure 45 Schematic of the structure and activation mechanism of proTGFβ1
ss, disulphide bonds [From Shi M, Zhu J, Wang R et al. Latent TGFβ structure and activation. Nature 2011;474:343-348]

Although αv integrins are one of the only mechanisms of TGFβ activation demonstrated *in vivo*[343], a number of other methods have been reported *in vitro* including physical processes such as acidification, extreme temperature changes, and oxidation. In addition, TGFβ can also be activated by a number of proteases, including plasmin, tryptase, thrombin, elastase, matrix metalloproteinase (MMP)-2, and MMP-9, and by interactions with thrombospondin[344].

αv Integrins

Integrins are allosteric[2] receptors that signal across the plasma membrane in both directions. They are the major metazoan receptor for cell adhesion to extracellular matrix proteins and are essential for cell-cell adhesion. They make transmembrane connections to the cytoskeleton and activate many intracellular signalling pathways (Figure 46, p151). Integrins are αβ heterodimers; each subunit crosses the membrane once, with most of each polypeptide in the extracellular space and two short cytoplasmic domains. Integrins also serve as transmembrane mechanical links from those extracellular contacts to the cytoskeleton inside cells.

Integrin alpha v (αv) is known to associate with the β chains 1, 3, 5, 6 and 8. The expression of αv on myofibroblasts is thought to be critical to fibrosis[339]. Myofibroblasts express several αv containing integrins and as contractile cells, are capable of exerting force on tethered ligands. The crystal structure of the small latent complex of TGFβ has recently been solved and confirms that mechanical force generated by actomyosin cytoskeleton and transmitted by integrins is a common mechanism for activating TGFβ[345]. *In vitro* studies have shown that αv integrins can use alternative αv containing integrins to activate TGFβ[346]. Furthermore, several integrins that share the αv subunit including $\alpha v\beta_1$, $\alpha v\beta_3$, $\alpha v\beta_5$, $\alpha v\beta_6$ and , $\alpha v\beta_8$ can recognise the same RGD peptide motif and activate TGFβ in some instances[343 347-350].

[2] Allosteric regulation is the binding of an enzyme or other protein by binding to an effector molecule at the proteins allosteric site – that is, a site other than the protein's active site.

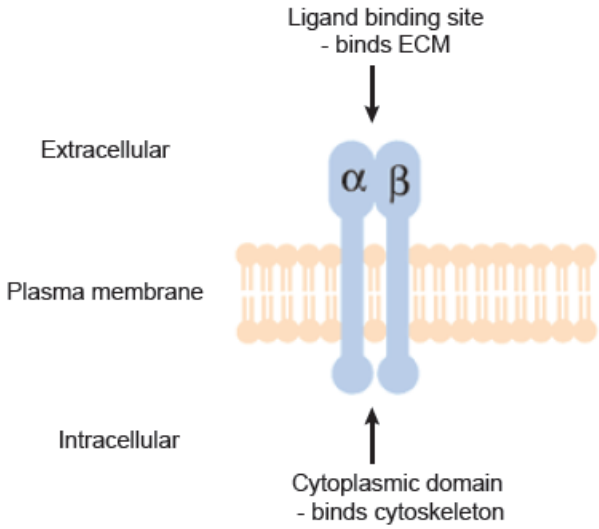

Figure 46 Integrins are transmembrane heterodimers.
The extracellular ligand binding site binds extracellular matrix while the cytoplasmic domain attaches to the cytoskeleton.

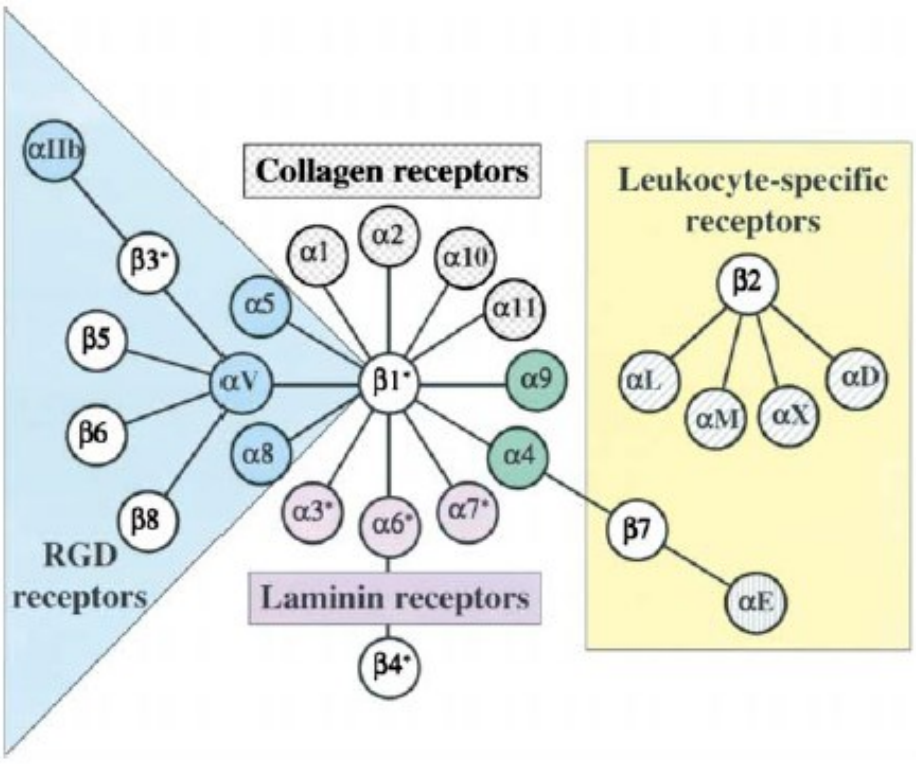

Figure 47 The integrin receptor family
Integrins are αβ heterodimers; each subunit crosses the membrane once, with most of each polypeptide (>1600 amino acids in total) in the extracellular space and two short cytoplasmic domains (20-50 amino acids). The figure depicts the mammalian subunits and their αβ associations. 8 β subunits can associate with 18 α subunits to form 24 distinct integrins. These can be considered in several subfamilies based on evolutionary relationships, ligand specificity and, in the case of β2 and β7 integrins, restricted expression on white blood cells.[Figure from Hynes RO. Integrins: Bidirectional, Allosteric Signaling machines. Cell 2002;110:673-687]

Henderson *et al.,* were the first to show that the specific targeting of the αv subunit in fibrogenic myofibroblasts effectively reduces developing and established fibrosis in liver, kidney and lungs[351]. They used this system to delete the integrin αv subunit because of the suggested role of multiple αv integrins as central mediators of fibrosis in multiple organs. In this section we set out to establish whether the activation of pericytes to myofibroblasts through αv integrins was conserved in skeletal muscle, and whether the targeting of αv integrins represented a potential therapeutic target in the prevention and treatment of skeletal muscle fibrosis.

Hypothesis and aims

Hypothesis

1. αv integrin expression on PDGFRβ+ perivascular cells regulates skeletal muscle fibrosis.

In order to address this hypothesis the following aims were established:

(i) Demonstrate that PDGFRβ-Cre effectively targets recombination in quiescent and activated skeletal muscle pericytes.

(ii) Show that selective αv integrin depletion in skeletal muscle PDGFRβ+ perivascular cells regulates skeletal muscle fibrosis.

(iii) Show that blockade of αv integrins by a novel small molecule (CWHM12) attenuates skeletal muscle fibrosis.

Graphical Abstract

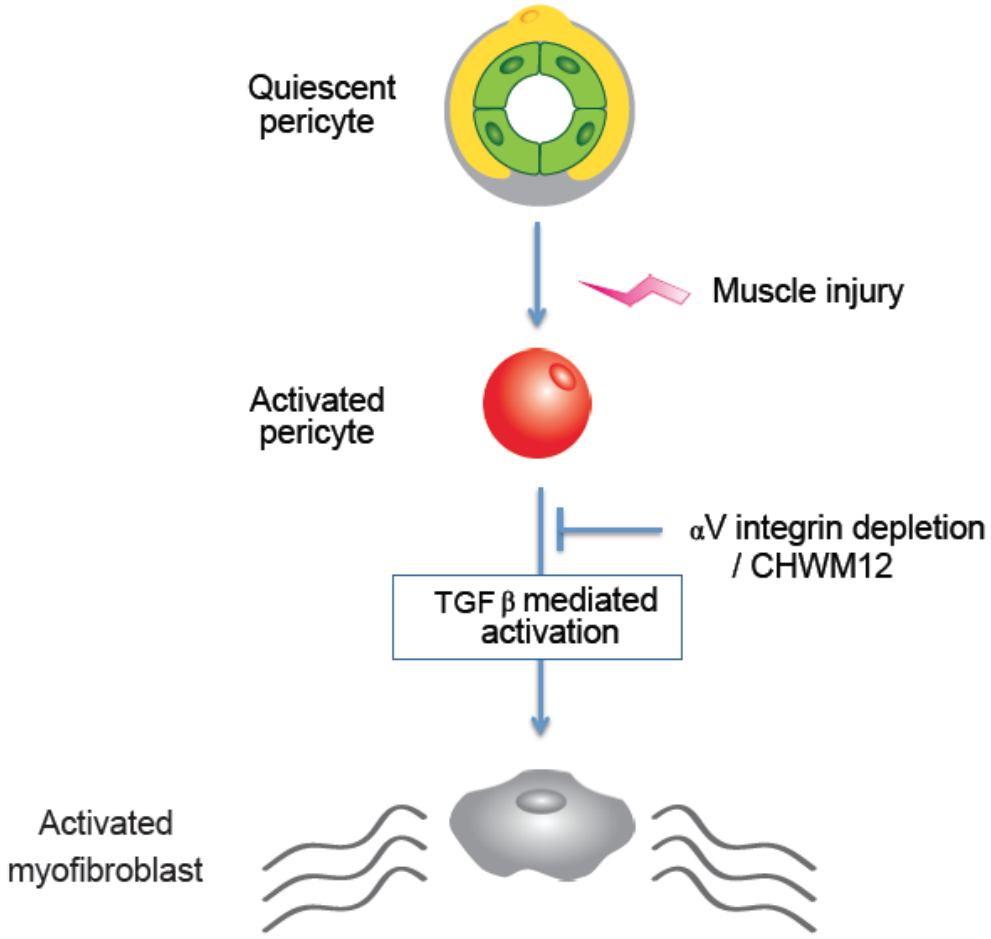

Chapter 2.1 Materials and methods

Mice

mTmG (TdTomato-EGFP)[352] mice were obtained from the Jackson Laboratory and crossed with *Pdgfrb*-Cre[353] mice. *Itgav*$^{flox/flox}$[354] mice and *Itgb8*$^{flox/flox}$[355] mice were obtained from Neil Henderson and all were maintained on C57BL/6 background. Mice used for all experiments were 8–12 weeks old and were housed under specific pathogen–free conditions in the Animal Barrier Facility of the University of Edinburgh. All experiments were approved by the Institutional Animal Care and Use Committee of the University of Edinburgh and the Home Office.

Genotyping

In preparation for PCR, ear clips were lysed overnight at 55°C in 200µl Direct PCR lysis Reagent (Peqlab) with 4µl Proteinase K (Sigma Aldrich). Samples were subsequently centrifuged at 1000rpm for 10 minutes. 40µl of supernatant was heated for a further 45 minutes at 85°C to inactivate the Proteinase K. The PCR reaction mixture was composed of 5µl 5xQ solution, 2.5µl 10xBuffer, 0.5µl dNTP(10mM), 0.8µl forward and reverse primers, 0.2µl Qiagen Taq and 14.5µl RNAse-free water (all Qiagen). Reactions were carried out in a Venti 96 Well thermo cycler (Applied Biosystems) using the cycle conditions listed in (Table 15, p156). Sequences of validated target and reference genes are listed in (Table 16, p157). Genotyping gels demonstrating αv$^{flox/flox}$ and β8$^{flox/flox}$ are shown in (Figure 48, p157) and (Figure 48, p157) respectively

Number of cycles	Duration	Temperature (°C)
1	5 min	94
30	30 sec	94
	45 sec	57
	2 min	72
1	10 min	72
1	To end	12

Table 15 Thermal cycler program details for genotyping PCR

Primer		Sequence	Amplicon size
Cre	F	TGC CAC GAC CAA GTG ACA GCA	375bp
	R	AGA GAC GGA AAT CCA TCG CTC	
αV	F	CAC AAA TCA AGG ATG ACC AAA	fl/fl = 600bp
	R	TTC AGG ACG GCA CAA AGA CCG	WT = 350bp
β8	F	GAGATGCAAGAGTGTTTACC	fl/fl = 350bp
	R	CACTTTAGTATGCTAATGATGG	WT = 300bp
mTmG	F (WT)	CTCTGCTGCCTCCTGGCTTCT	Mut = 250bp
	R (WT)	CGAGGCGGATCACAAGCAATA	WT = 330bp
	R (Mut)	TCAATGGGCGGGGGTCGTT	

Table 16 Primer sequences used to perform genotyping PCR

Figure 48 Genotyping gel demonstrating $\alpha v^{flox/flox}$ expression

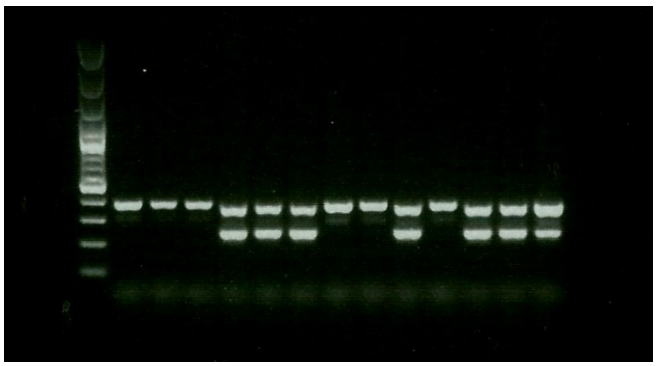

Figure 49: Genotyping gel demonstrating $\beta 8^{flox/flox}$ and $\beta 8^{flox/WT}$ expression

Muscle Fibrosis model

We injected 50µl of 20µM cardiotoxin (CTX) Naja Mossambica Mossambica (Sigma Aldrich) directly into the midbelly of the tibialis anterior (TA) muscles of 8-10 week old sex-matched mice. 50µl of PBS was used in control animals. TA muscles were harvested at multiple time points following CTX injection.

Muscle Regeneration Model

Muscle damage was induced by injection of 50 ml of 20μM cardiotoxin Naja Mossambica Mossambica (Sigma Aldrich) directly into the midbelly of TA muscle. To assess muscle damage, mice were given an intraperitoneal injection of Evans blue dye (25 mg/kg) at day 7, 24 h prior to sacrifice[216].

Primary cell isolation and fluorescence activated cell sorting (FACS)

Mouse skeletal muscle was excised, minced with scissors and digested in collagenase/dispase solution [DMEM/20%FBS/1%PS/0.5mg/ml of collagenase II-S and dispase (Sigma)] for 30 minutes at 37°C with shaking (200rpm). An equal volume of DMEN/20%FBS/1%PS was added to halt the digestion and the total suspension was passed through a sterilized nylon mesh to remove large clumps. The suspension was then passed through a 100μm followed by a 70μm strainer and centrifuged (300 x g, RT, 5mins). The supernatant was discarded and the pellet was re-suspended in 10ml red cell lysis buffer (Sigma Aldrich) and incubated at RT for 2 minutes. An equal volume of DMEN/20%FBS/1%PS was added and the suspension centrifuged (300 x g, RT, 5mins). The supernatant was again discarded and the pellet was resuspended in 1ml PBS/2%FBS. The cell suspension was then passed through a 40μm strainer. Cells were counted using a haemocytometer using tryphan blue to distinguish non-viable cells.

(i) Isolation of eGFP cells from mTmG reporter

Following live/dead staining with dapi (Invitrogen), live single eGFP positive cells from mTmG;PDGFRβ-Cre mice were sorted using a FACSAria (BD Biosciences). Fluorescence compensation settings were optimized using anti-mouse Ig, κ/negative control beads plus (BD Biosciences) incubated with the range of FACS antibodies used. Unstained cells were used to account for the autofluorescence of samples and fluorescently matched isotypes were used as negative controls.

(ii) Isolation of pericytes from non-reporter tissue

When sorting non-reporter tissues an anti-PDGFRβ antibody was used to identify PDGFRβ+ perivascular cells. A number of markers used in the identification of pericytes (CD146) and exclusion of non-pericyte cells (CD31, CD144, CD45, CD56, CD34) were used to confirm the purity of sorted cells. In brief, cells were resuspended at a concentration of $30x10^6$/ml and incubated with all antibodies at the appropriate dilution (Table 17, p160). As controls, $5x10^5$ cells were incubated with isotype control antibodies in the same conditions. The cell suspensions were incubated with the antibodies on ice and in the dark for 20 minutes then washed with PBS/2%FBS and centrifuged (300 x g, RT, 5mins). The supernatant was then discarded and the cells resuspended in 1ml PBS/2%FBS. Cells were sorted using a FACSAria (BD Biosciences). Fluorescence compensation settings were optimized using anti-mouse Ig, κ/negative control beads plus (BD Biosciences) incubated with the range of FACS antibodies used. Unstained cells were used to account for the autofluorescence of samples and fluorescently matched isotypes were used as negative controls. Prior to selection of PDGFRβ+ perivascular cell populations, a side versus forward scatter plot was used to remove debris then a height versus width plot was used to eliminate doublets. DAPI [0.1-0.5μg/ml (Invitrogen)] was used to eliminate dead cells.

Sorted cells were seeded onto tissue culture plates, at a density of $2x10^4$ cells per cm^2 and cultured in EGM2 medium in a 37°C, 5% CO_2 incubator. After 24hrs, EGM2 medium was changed to DMEN/10%FBS/1%PS which was then refreshed three times/wk until 100% confluence was reached. After an initial passage, perivascular cells were seeded on tissue culture plates at $2x10^4$ cells/cm^2 in high-glucose DMEN/10%FBS/1%PS, and grown until confluent in a 37°C, 5% CO_2 incubator.

FACS analysis of cultured cells

In preparation for flow cytometric analysis, cells were resuspended at a concentration of $30x10^6$/ml and incubated with all antibodies at the appropriate dilution (Table 17, p160). As controls, $5x10^5$ cells were incubated with isotype control antibodies in the same conditions. The cell suspensions were incubated with the antibodies on ice and in the dark for 20 minutes then washed with PBS/2%FBS and centrifuged (300 x g, RT, 5mins). The supernatant was then discarded and the cells resuspended in 1ml PBS/2%FBS. Cells were analysed using a flow cytometer (Fortessa, Becton-Dickenson). The fluorescence compensation settings were optimized using anti-mouse Ig, κ/negative control beads plus (BD Biosciences) incubated with the range of FACs antibodies used. Unstained cells were used to account for the autofluorescence of samples and fluorescently matched isotypes and fluorescence-minus-one samples were used as negative controls.

Antibody Specificity	**Fluorochrome**	**Supplier**	**Dilution**	**Isotype Control antibody**
PDGFRβ	PE	Biolegend	1/50	PE Rat IgG2b κ
PDGFRβ	APC	eBioscience	1/50	APC Rat IgG2b κ
PDGFRα	APC	BD Bioscience	1/50	APC Rat IgG2b κ
PDGFRα	PE	eBioscience	1/50	PE Rat IgG2b κ
CD146	PE	Biolegend	1/100	PE Rat IgG2b κ
CD146	Alexa Fluor 488	BD Bioscience	1/100	Alexa Fluor 488 Rat IgG2b κ
CD56	APC	Abcam	1/100	
CD56	PECy7	BD Bioscience	1/100	PE-Cy7 Rat IgG2b κ
CD146	PerCPCy5.5	BD Bioscience	1/100	PerCPCy5.5 Rat IgG2b κ
CD31	APC	eBioscience	1/50	APC Rat IgG2b κ
CD90.2	PerCPCy5.5	Molecular probes	1/100	PerCPCy5.5 Rat IgG2b κ
CD34	Alexa Fluor 700	BD Bioscience	1/100	Alexa Fluor 700 Rat IgG2b κ
CD34	FITC	BD Bioscience	1/100	FITC Rat IgG2b κ
CD45	PerCPCy5.5	BD Bioscience	1/100	PerCPCy5.5 Rat IgG2b κ
CD45	PE-Cy7	BD Bioscience	1/100	PE-Cy7 Rat IgG2b κ

Table 17 Antibodies and corresponding isotype controls for MOUSE perivascular cell purification and analysis

Immunohistochemistry and Immunofluorescence

For immunofluorescence staining, skeletal muscle tissue was fixed in 4% paraformaldehyde overnight at 4°C, immersed in graded sucrose solutions, embedded in OCT (Tissue Tek) and stored at -80°C. Tissue sections were air dried and then stained for pericyte and non-pericyte markers (Table 18, p162). Sections were washed with PBS/Tween20 pH7.4 (2x5mins), incubated with Avidin (Thermo Scientific) for 15 minutes, washed with PBS/Tween20 pH7.4 (2x5mins), then incubated with Biotin (Thermo Scientific) for 15 min. Sections were washed with PBS/Tween20 pH7.4 (3x5mins) before being blocked for one hour with Protein Block (Dako). After blocking, the cells were incubated with primary antibodies overnight at 4°C. Sections incubated with primary antibodies were washed with PBS/Tween20 pH7.4 (3x5mins) prior to incubation with the Biotinilated antibody (1/1500) for 1 h at RT. All sections were then washed with PBS/Tween20 pH7.4 (3x5mins) and incubated with Alexa-Flour coupled streptavidin (1/1000) (Invitrogen) for 45 min. After a final PBS/Tween20 pH7.4 wash (3x5mins) the cells were mounted in DAPI fluorescent mounting media (Vector) and allowed to dry for 1 h. Digital morphometric measurements of GFP expression and PDGFRβ immunostaining were performed using Image J. Ten random fields from each section were analyzed at a final magnification of 63X.

Antibody Specificity	Fluorochrome	Supplier	Dilution
PDGFRβ	Alexa Fluor 647	Abcam	1/50
PDGFRα	Alexa Fluor 647	Abcam	1/50
αSMA	Alexa Fluor 647	Sigma Aldrich	1/1000
CD146	Alexa Fluor 647	Abcam	1/100
NCAM/CD56	Alexa Fluor 647	Abcam	1/100
CD31	Alexa Fluor 647	Abcam	1/100
CD90.2	Alexa Fluor 647	Abcam	1/50
CD34	Alexa Fluor 647	Abcam	1/100
Pax7	Alexa Fluor 647	Developmental Studies Hybridoma Bank	1/3

Table 18 Antibodies and isotype controls used for immunohistochemistry of skeletal muscle sections.

IHC on Cultured Cells

Cells cultured of glass microscope cover slides (Labteck Chamber Slides) were washed with PBS/Tween20 pH7.4 (3x5mins) prior to fixation with 4% PFA for 10 min. Slides were then washed with PBS/Tween20 pH7.4 (3x5mins) and IHC performed as described for frozen sections.

Histological stains and analysis

5μM sections were stained with picrosirius red or antibody and results quantified using Nikon Elements software. Ten random fields from each section were analyzed at a final magnification of 40X.

Molecular physiology

RNA extraction

Isolation of RNA from sorted and cultured cells was performed using the RNeasy Micro Kit (Qiagen) and standard protocols. 350μl of Buffer RLT (containing 10μl of B-ME per 1ml of buffer) was added to cell pellets (not more than $5x10^5$ cells). 350μl of 70% ethanol was added to the homogenate and transferred to an RNeasy MinElute spin column placed in a 2ml collection tube and centrifuged at 12,000xg for 15 s. The flow through was discarded before 350μl Buffer RW1 was added to the RNeasy MinElute spin column and centrifuged for 15 s at 8000 x g (10,000 rpm) to wash the spin column. The

flow-through was discarded. The membrane was then incubated with10 µl DNase I stock solution in 70 µl Buffer RDD for 15 min at RT. 350 µl Buffer RW1 was added to the RNeasy MinElute spin column and centrifuged for 15 s at 8000 x g. Samples were washed with RPE buffer and then 80% ethanol by spinning for 2 min at <8000g. RNA was dried by spinning for 2 min at 13,000g. RNA was eluted in 14µl RNase free water. RNA concentration was determined using a Nanodrop from Thermofisher.

cDNA synthesis

RNA was denatured (5 min, 65^{o}C) in a reaction mixture containing 1µg RNA, 25ng of random primers (Promega) and dNTPs at a final concentration of 0.5mM (Bioline). The samples were then cooled on ice for 1min after which 4µl 5xFirst strand buffer and 1µl 0.1mM DTT then, after 2 min, 1µl SuperScript reverse transcriptase [all provided with SuperScript III reverse transcriptase system kit (Invitrogen)]. Samples were incubated at 25^{o}C for 10 min then at 42^{o}C for 50 min and finally 70^{o}C for 15 min. The cDNA was stored at -20^{o}C prior to further analysis.

Polymerase chain reaction

The reaction mixture was composed of 4µl MyTaq reaction buffer, dNTPs at a final concentration of 0.5mM and 0.2µl Taq polymerase (all Bioline) in addition to 13.6µl RNAse free water, 1µl cDNAsample, 0.5µl of forward primer and 0.5µl of reverse primer (10µM, Integrated DNA Technologies Inc). Reactions were carried out in a Venti 96 Well thermo cycler (Applied Biosystems) using the cycle conditions listed in (Table 19, p164).

Number of cycles	Duration	Temperature (°C)
1	10 min	94
35	10 sec	94
	30 sec	58
	50 sec	72
1	7 min	72

Table 19 Run protocol for PCR

Agarose gel electrophoresis

The PCR products were electrophoresed on 1.7% agarose [SeaKem LE agarose (Lonza)] gels made with 0.5xTBE buffer (45mM Trisbase, 45mM boric acid, 0.625M EDTA) and Gel Red (5µl/100ml). For sample loading, 2µl PCR product was mixed with 8µl RNAse free water and 2µl loading buffer. The PCR product was electrophoresed at 120V for 80 minutes after which the PCR product bands were visualized by exposure to ultraviolet light using a UVI pro system (UVItec).

Quantitative real-time PCR (qPCR)

qRT-PCR Total RNA was isolated using an RNeasy Micro kit as described above (Qiagen). cDNA was analyzed by SYBR-Green real-time PCR with Lightcycler thermocycler (Roche) and normalized to **β**-actin expression (cycle conditions are listed in Table 20, p165). Primers used were as follows: **β-actin** forward: TGTTACCAACTGGGACGACA, **β-actin** reverse: GGGGTGTTGAAGGTCTCAAA; **18S** forward: TAGAGGGACAAGTGGCGTTC, **18S** reverse: CGCTGAGCCAGTCAGTGT; **Itgav** forward: CCGTGGACTTCTTCGAGCC, **Itgav** reverse: CTGTTGAATCAAACTCAATGGGC; **PDGFRβ** forward: TCCAGGAGTGATACCAGCTTT, **PDGFRβ** reverse: CAGGAGCCATAACACGGACA; **GFAP** forward: CGGAGACGCATCACCTCTG, **GFAP** reverse: TCTCGGAGGCATAGGAGCG; **α-SMA** forward: GTCCCAGACATCAGGGAGTAA, **α-SMA** reverse: TCGGATACTTCAGCGTCAGGA; **Col1A1** forward: GCTCCTCTTAGGGGCCACT, **Col1A1** reverse: CCACGTCTCACCATTGGGG; **Col 3A1** forward: AACCTGGTTTCTTCTCACCCTTC, **Col 3A1** reverse: ACTCATAGGACTGACCAAGGTGG; **TGFβ1** forward: CTCCCGTGGCTTCTAGTGC, **TGFβ1** reverse: GCCTTAGTTTGGACAGGATCTG; **MMP-2** forward:

CAAGTTCCCCGGCGATGTC, **MMP-2** reverse: TTCTGGTCAAGGTCACCTGTC; **MMP-3** forward: ACATGGAGACTTTGTCCCTTTTG , **MMP-3** reverse: TTGGCTGAGTGGTAGAGTCCC; **MMP-9 forward**: CTGGACAGCCAGACACTAAAG, **MMP-9** reverse: CTCGCGGCAAGTCTTCAGAG; **MMP 13** forward: CTTCTTCTTGTTGAGCTGGACTC, **MMP 13** reverse: CTGTGGAGGTCACTGTAGACT; **TIMP-1** forward: TGCAACTCGGACCTGGTCATA, **TIMP-1** reverse: CGCTGGTATAAGGTGGTCTCG; **PPARγ** forward: GGAAGACCACTCGCATTCCTT, **PPARγ** reverse: GTAATCAGCAACCATTGGGTCA; **Itgb1** forward: CTACTTCTGCACGATGTGATGAT, **Itgb1** reverse: TTGGCTGGCAACCCTTCTTT; **Itgb3** forward: CCACACGAGGCGTGAACTC, **Itgb3** reverse: CTTCAGGTTACATCGGGGTGA; **Itgb5** forward: GAAGTGCCACCTCGTGTGAA, **Itgb5** reverse: GGACCGTGGATTGCCAAAGT; **Itgb8** forward: CTGAAGAAATACCCCGTGGA, **Itgb8** reverse: ATGGGGAGGCATACAGTCT. Melt curve analysis was performed to ensure the specificity of the amplified product.

Program	**Number of cycles**	**Duration (sec)**	**Temperature (°C)**
Pre-incubation	1	10	95
Amplification	35	10	95
		30	60
Cooling	1	30	72

Table 20 Thermal cycler programme details for qPCR

Myofibroblast activation in αv depleted PDGFRβ+ cells *in vitro*

Control and *Itgav*$^{flox/flox}$ PDGFRβ-Cre PDGFRβ expressing cells were isolated, seeded at 20,000 cells/cm^2 and cultured for 5 days on tissue culture plastic. Cells were then harvested and processed for qPCR analysis.

In vitro CWHM 12 and CWHM 96 studies

PDGFRβ expressing cells were isolated from WT mice, seeded at 20,000 cells/cm^2 and cultured for 5 days on tissue culture plastic in the presence of 10μM CWHM 12 and 10μM CWHM 96 (control). Cells were then harvested and processed for qPCR analysis.

In vivo CWHM 12 and CWHM 96 studies

For all studies CWHM 12 and CWHM 96 were solubilized in 50% DMSO (in sterile water) and dosed to 100mg/kg/day. Drug or vehicle (50% DMSO) were delivered by implantable ALZET osmotic minipumps (Durect, Cupertino, CA). For cardiotoxin induced fibrosis, pumps were inserted subcutaneously either before the cardiotoxin injection or one week following the injection. Muscles were harvested after 21 days.

Chapter 2.3 Transgenic mice and mouse models of muscle injury

Mouse models in musculoskeletal research

The accessibility of genetic manipulation has made the mouse the most commonly used laboratory animal and their use is now often favoured over rats for musculoskeletal research. The sequencing and analysis of the mouse genome has allowed many genes to be targeted and studied using this technology. [356] [357] In this thesis I combine mouse transgenic technology with conventional models of injury to dissect molecular mechanisms driving the response to muscle injury and the development of fibrosis.

Modifying genes in mice provides a unique approach to unravel gene function at a cellular and molecular level, as well as elucidating the role of genes in normal physiology and the development of pathology. Numerous disease models have been established that provide insight into that pathogenesis of disease while facilitating the development of therapies. Central to these advances has been the ability to modulate gene expression, by increasing, decreasing or eliminating expression completely. Cells can be genetically labeled with fluorescent proteins, or proteins that facilitate targeted lineage depletion. These alterations can be made cell type-specific and even inducible or reversible. The most widely used system is the Cre-LoxP system, but the use of alternative systems is becoming more widespread.

Numerous injury models have been proposed to examine skeletal muscle regenerative mechanisms, including physical, chemical and biological injury. In choosing the most appropriate animal model for research a number of key factors need to be taken into consideration.[358] These include: 1 – appropriateness of the model as an analogue of the disease being studied, 2- transferability of the information from the model to the clinical scenario, 3 – genetic uniformity where applicable, 4 – background knowledge of biological properties, 5 – cost and availability, 6 – generalisability of the results, 7 – ease

and adaptability to experimental manipulation, 8 – ecological considerations, 9 – ethical and societal implications.

In this thesis I utilize a PDGFRβ-Cre driver to target perivascular MSC precursors. I use fluorescent reporters of Cre activity to define the extent of recombination and gene knockdown to investigate genes central to the development of skeletal muscle fibrosis. The aim of this chapter is to outline the transgenic systems utilized in the project and the breeding strategies used to generate them. I will also describe mouse models used to investigate muscle regeneration and fibrosis, outlining their strengths and limitations. Lastly, I will describe the cardiotoxin (CTX) regeneration and fibrosis models used in this thesis.

Transgenic Mice

Cre Recombination

Cre-Lox technology is based on the ability of the P1 bacteriophage recombinase (Cre) to direct site-specific DNA recombination between pairs of LoxP sites[359]. Such recombination in a Cre-Lox mouse can permanently activate or inactivate a gene of interest. Cre-Lox experiments typically require two transgenic animals: a Cre strain and a LoxP strain (Figure 50, p171). The Cre strain contains a Cre recombinase transgene under the control of a tissue specific promotor, whereas a LoxP strain contains two LoxP sites that flank a genomic segment of interest, the "floxed" locus. Cre recombinase can initiate deletions, inversions, and translocations of a floxed locus depending on the location and orientation of the LoxP sites in a Cre-Lox mouse[360]. The floxed loci can be designed to allow permanent inactivation or activation of the gene of interest. The cell-type specificity of Cre depends on the availability of tissue-specific or cell-specific promotors. Tissue-specific Cre expression can be combined with time specific activity.

Cre strains have been widely used in skeletal muscle for lineage tracing and permanent gene activation or deletion[121 216].

To control the timing of Cre activity, fusion proteins have been generated between Cre and the ligand-binding domain of steroid hormone receptors. A fusion between Cre and a mutated ligand-binding domain of the oestrogen receptor (CreER^{T2}) is the most commonly used variant. ER^{T2} binds powerfully to 4-hydroxy tamoxifen (4OH-T), the active metabolite of the synthetic steroid tamoxifen but weakly to endogenous oestrogens. The CreER^{T2} has been widely used in musculoskeletal research, although the extent of recombination and the most effective dosing strategy must be determined empirically for each CreER^{T2} mouse strain. These so-called "inducible systems" are essential for lineage tracing studies but their use in gene knockdown is limited by their efficiency of recombination, which is generally lower than with constitutive Cres. I use a constitutive Cre system in this thesis as high recombination efficiency is essential for my key application – gene knockdown.

Off-target effects of the Cre recombinase have been reported in several tissues including muscle[361]. These off-target effects may be due to endogenous cryptic LoxP that cause cytotoxic chromosomal rearrangements when activated. However, not every Cre strain has off-target effects, and this variation is likely to result from differences in levels of Cre protein expression. The off-target phenotypes resulting from Cre toxicity can make the interpretation of some experiments particularly challenging[361]. The use of inducible Cre systems limit the amount of time Cre spends in the nucleus and may decrease Cre toxicity.

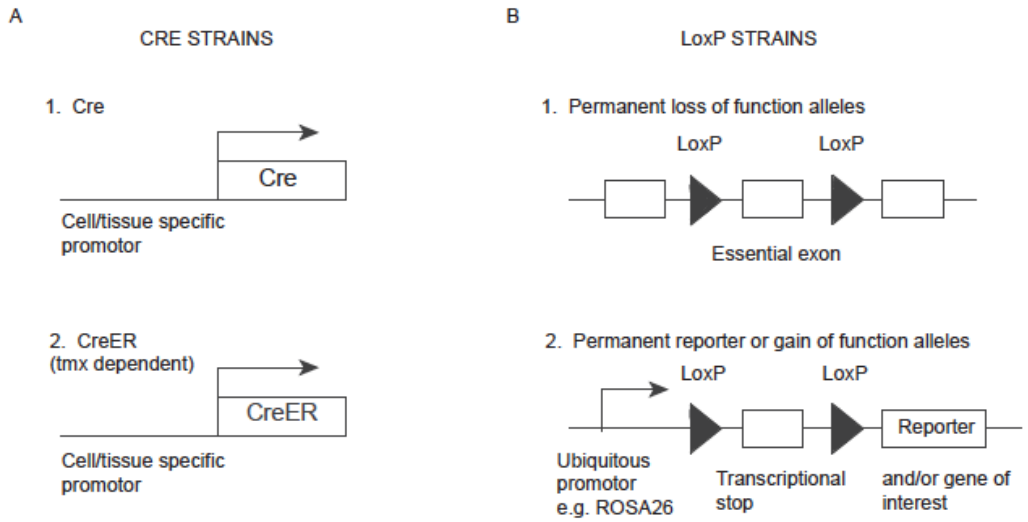

Figure 50 Schematic of the Cre-Lox system
(A) Cre, or CreER, is expressed from a cell or tissue-specific promoter. (1) Cre is active in every cell in which it is expressed. Levels of activity depend on expression levels. (2) CreER is not active and is excluded from the nucleus until tamoxifen is administered. This allows for temporal control and reduces nonspecific effects of Cre. (B) Cre catalyzes recombination between its recognition (LoxP) sites, resulting in permanent genetic rearrangement, which is inherited by daughter cells. The most common arrangement of LoxP sites are (1) flanking a critical exon of an endogenous gene to mediate loss of function or (2) flanking a transcriptional STOP to mediate reporter gene expression and/or overexpression. In this case, a ubiquitous promoter is usually used to drive the gene of interest, but the transcript is disrupted by the LoxP-flanked transcriptional STOP. After Cre-mediated deletion of the stop, the gene of interest is permanently expressed. [Modified from Rawlins et al., The a"MAZE"ing world of lung specific mouse transgenics. Am J Respir Cell Mol Biol 2012;46(3):269-82]

Reporters of Cre activity

Reporters of Cre activity are important for defining the spatial and temporal extent of Cre-mediated recombination. This is generally achieved using a Cre reporter transgene in which a fluorescent marker (e.g. GFP, TdTomato) is expressed following Cre-mediated recombination. The descendants of stem and progenitor cells can be traced by crossing a Cre mouse with a reporter mouse strain permanently expressing a reporter gene after activity. Genes are generally inserted into loci that are expressed robustly in most cell types and that are targeted with high efficiency e.g. ROSA26.

It can be helpful to label both recombined and non-recombined cells. Double fluorescent marker systems allow for visualization of recombined and nonrecombined cells

allowing the delineation of structure without additional staining. Furthermore, double reporting can be beneficial in FACS sorting where the ability to both positively and negatively select for populations can improve purity. In this thesis I use the mTmG double reporter system (Figure 51, p172), which is known for producing reliably bright fluorescence.

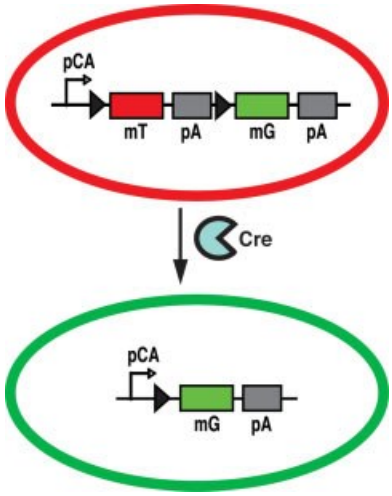

Figure 51 Schematic diagram of the mTmG construct before and after Cre-mediated recombination.
mTmG consists of a chicken β-actin core promoter with a CMV enhancer (pCA) driving a LoxP-flanked coding sequence of membrane-targeted tandem dimer Tomato (mT) resulting in tdTomato expression with membrane localisation. After Cre-mediated intra-chromosomal recombination, the mT sequence is excised allowing the pCA promoter to drive expression of membrane-targeted enhanced green fluorescent protein (mG).

Gene knockout vs knockdown

It is important to be aware of the distinction between gene "knockout" and "knockdown". With knockout mice, a gene is eliminated or a functional domain of the protein is deleted. This can be achieved through random mutation using chemical or gene trap mutagenesis, or through gene targeting[362]. Homologous recombination allows researchers to completely remove one or more exons from a gene, resulting in the production of truncated protein or no protein at all. The phenotype of knockout mice can be very complex because all tissues may be affected and embryonic lethality is

common. In this thesis I explore the role of αv integrins in muscle fibrosis. However, because of the ubiquitous expression of αv and its key role in a wide range of cellular processes, traditional knockout systems result in embryonic lethality. A conditional gene modification using Cre-Lox technology allows the gene of interest to be knocked out in a targetable subset of cells or at a particular time circumventing lethality. Furthermore the capacity for population specificity increases mechanistic insight afforded by knockdown systems. I will therefore make use of knockdown technology for this thesis.

Mouse Lines and Breeding Strategies

I use trio breeding (e.g. one male and two females) in all of my breeding strategies. Continuous trio breeding groups can result in a higher breeding efficiency by permitting breeding at the first post-partum estrus and facilitating pup survival through cross fostering. It is convention to breed the Cre strain through the male, as this has been proposed to reduce Cre toxicity. However this practice has no scientific basis.

PDGFRβ-Cre

PDGFRβ-Cre mice (Tg(PDGFRβCre)#Rha), which express Cre recombinase under control of a fragment of the gene encoding PDGFRβ, were previously developed to specifically target pericytes[353]. These mice were developed by Ralph Adams at the London Research Institute, by microinjecting a transgene containing a genomic PDGFRβ promotor fragment to a Cre recombinase and a polyA sequence into 129/B6 zygotes. Founder lines were then maintained on a mixed 129;B6 background. It has been shown that under the control of the PDGFRβ promotor, Cre inactivates LoxP flanked genes in mouse pericytes with high efficiency in the liver, lung and kidney[351 363]. We were

therefore optimistic that a high recombination efficiency would be seen in skeletal muscle.

PDGFRβCre; mTmG

In order to visualise recombined and non-recombined cells under the control of the PDGFRβ promotor I used the mTmG reporter mouse. To generate this strain I crossed a PDGFRβ heterozygous mouse (WT background) with an mTmG homozygous mouse purchased from Jackson Laboratory (Figure 52, p174). This strategy yields 50% Cre positive mTmG heterozygous and 50% cre negative mTmG heterozygous mice. The Cre positive mice were used for visualisation of PDGFRβ+ cells and cell sorting, while Cre negative mice were used as controls in calculating background fluorescence and compensation in FACS. Genotyping was performed using conventional PCR and gel electrophoresis.

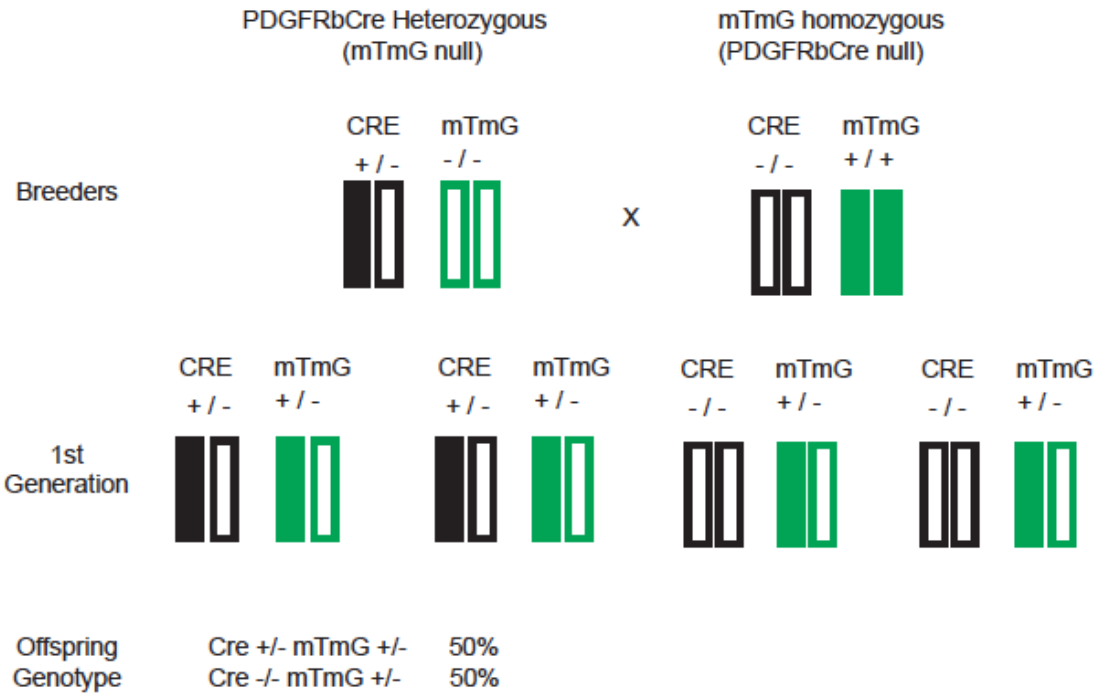

Figure 52 Breeding strategy for mTmG;PDGFRβCre

PDGFRβCre; αv $^{flox/flox}$

Using Itgαv $^{flox/flox}$ mice[354], αv integrins were deleted under the control of the promotor for PDGFRβ. Itgav$^{flox/flox}$;PDGFRβCre strains were generated by crossing PDGFRβ Cre positive αv$^{flox/flox}$ with Itgαv $^{flox/flox}$ (Figure 53, p175). This strategy resulted in 50% Cre positive αv homozygous experimental animals and 50% Cre negative littermates that could be used as experimental controls.

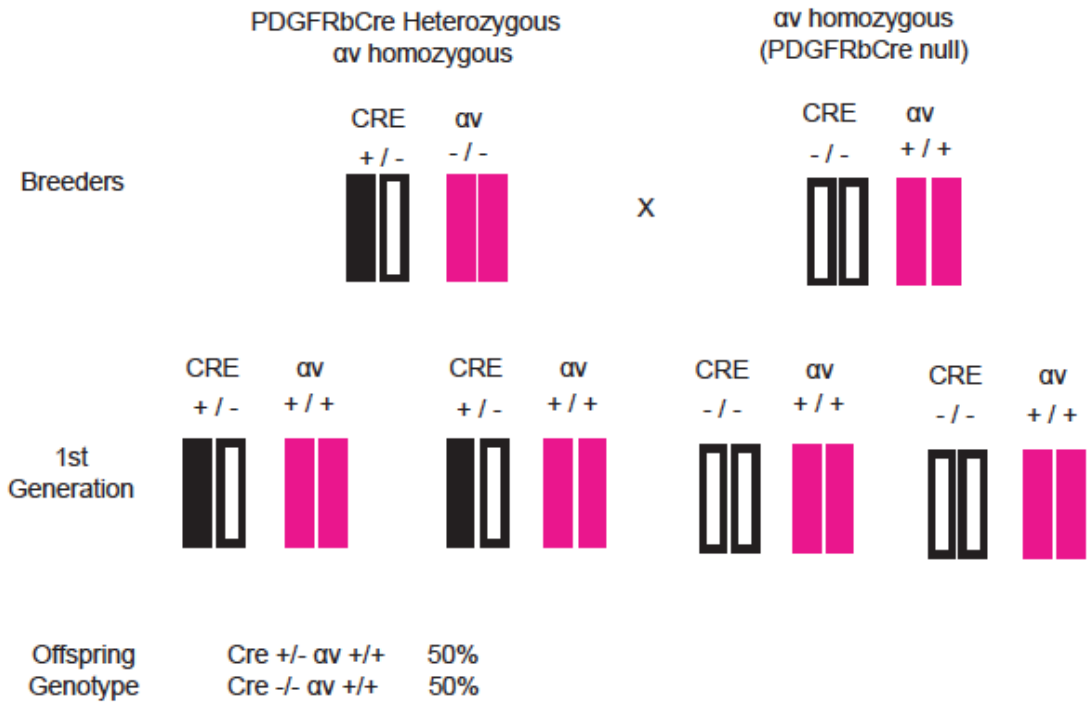

Figure 53 Breeding strategy for αv;PDGFRβCre

To visualize recombination in Itgαv$^{flox/flox}$;PDGFRβ-Cre mice we developed a breeding strategy to introduce the mTmG allele into PDGFRβ expressing cells (Figure 54, p176). This strategy requires three breeding steps to ultimately result in 50% Cre positive and 50% Cre negative offspring all with homozygous αv$^{flox/flox}$ and all containing at least one mTmG allele.

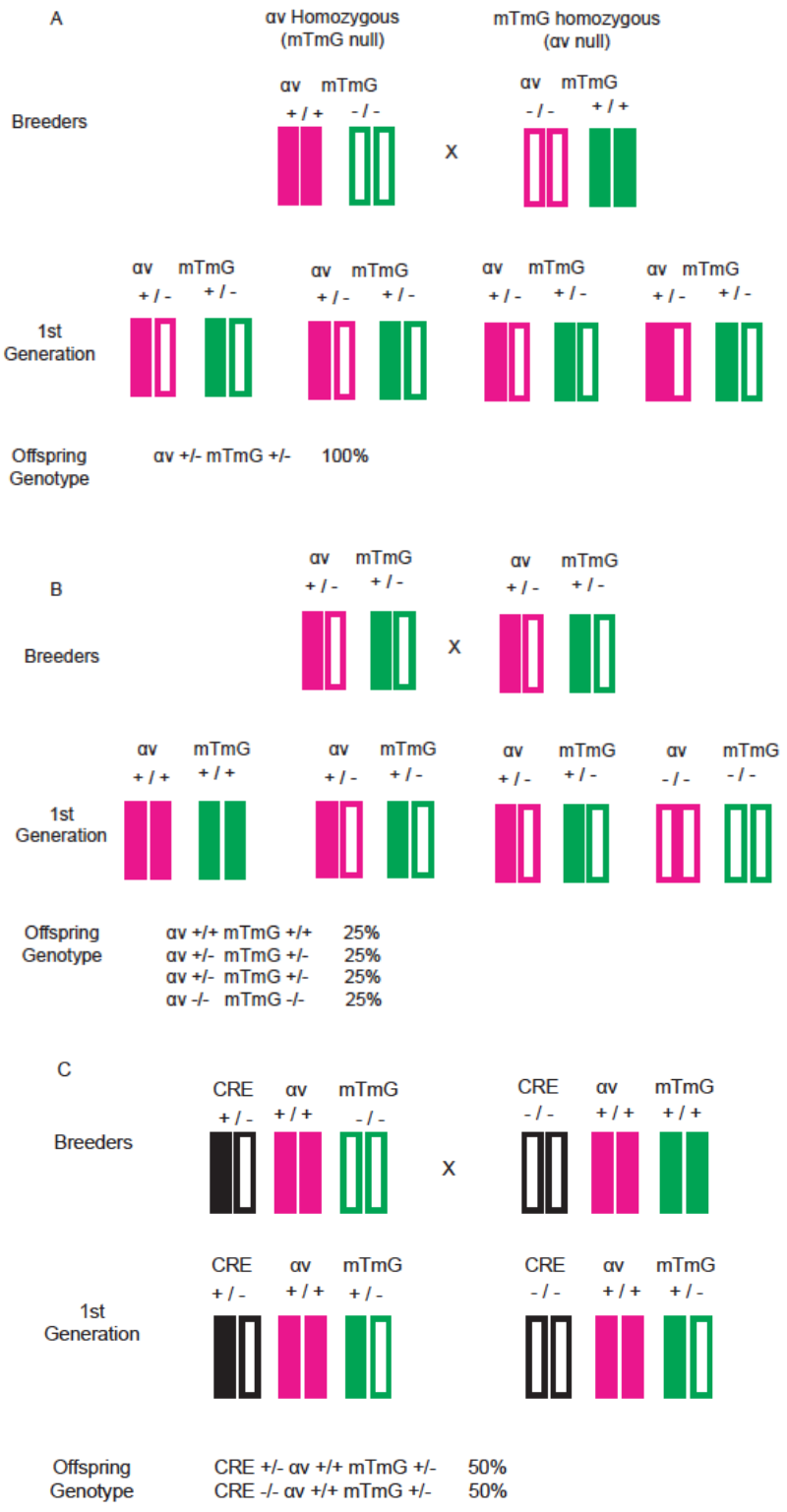

Figure 54 Breeding strategy for αv;mTmG;PDGFRβ-Cre
Three phases of breeding (A-C) are required to generate the desired phenotype ($αv^{flox/flox}$;$mTmG^{het}$;PDGFRβ-Cre positive).

PDGFRβ-Cre;β8 $^{flox/flox}$

Itgβ8$^{flox/flox}$;PDGFRβ-Cre mice were generated in a similar way (Figure 55, p177).

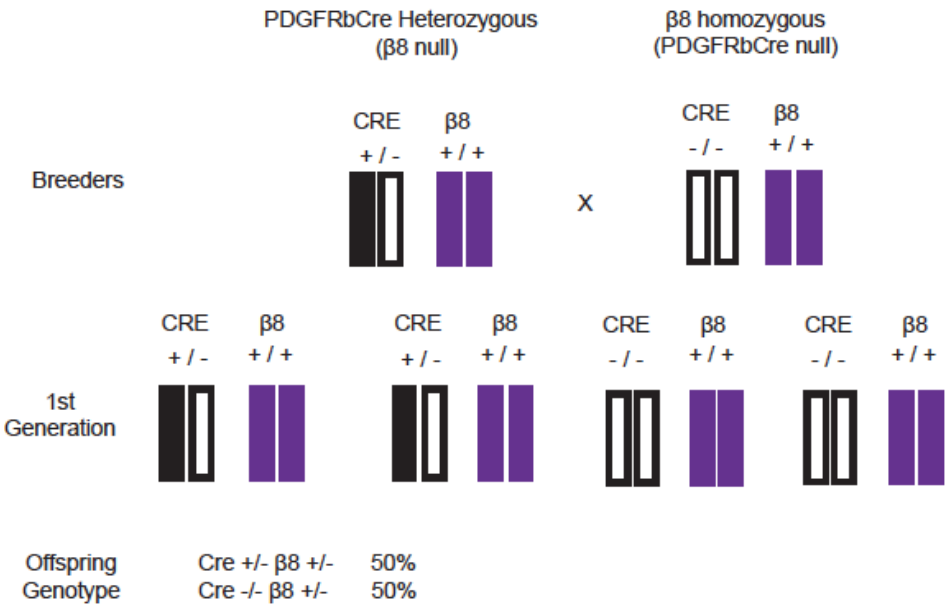

Figure 55 Breeding strategy for β8;PDGFRβ-Cre

Mouse models of skeletal muscle regeneration and fibrosis

Numerous injury models have been proposed to examine skeletal muscle regenerative mechanisms, including physical, chemical and biological. A number of models have been used to specifically examine skeletal muscle fibrosis (Table 21, p178), the most dramatic of which are the muscular dystrophies. However, skeletal muscle fibrosis can occur where the treatment of the muscle is extremely simple. This includes the mechanisms of skeletal muscle injury used in the assessment of muscle regeneration such as the intramuscular injection of cardiotoxin (CTX).

	Model	Animal (muscle)	Sample References
Mechanical	Laceration	Mouse (gastrocnemius)	364 365
	Puncture	Mouse (TA)	366
	Chronic Stretch	Rabbit (EDL)	367
	Immobilization	Mouse (soleus), Rat (TA, soleus, gastrocnemius)	368
	Hind limb suspension	Rat (soleus)	369
	Tenotomy	Mouse (supraspinatus), Rat (supraspinatus), dog (infraspinatus), sheep (infraspinatus),	370-373
Chemical or Toxin	Cardiotoxin	Mouse (TA)	185 364
	Glycerol		216
	Botulinum toxin	Rat (TA)	374
	hrTGFβ1	Mouse (TA)	364
	BaCl2	Mouse (TA, gastrocnemius)	375
Genetic	Desmin KO	Mouse	364
	Mdx	Mouse (diaphragm, biceps femoris)	376
Ageing		Rat (EDL, soleus)	377

Table 21 Models of *in vivo* skeletal muscle fibrosis

Physical injury

Generating skeletal muscle injury using cold, crushing, surgical wounding, mincing and free grafts have all been used to study regeneration and fibrosis.

Cold

Localized exposure to a low temperature (e.g. by using liquid nitrogen) of a well-defined area of skeletal muscle has been used experimentally to induce a limited area of necrosis. In this model, regeneration of the necrotic muscle (with no viable cells remaining) is entirely dependent on precursor cells from the surrounding viable skeletal muscle tissue.

Crush

Crush injury of skeletal muscle tissue causes necrosis resulting in a focal reduction of the satellite cells, invasion of macrophages and phagocytosis of the necrotic tissue.

Surgical wounding

Surgical wounding (i.e. transection) of muscle tissue produces a clean lesion, which in humans is usually followed by scarring at the site of injury. On either side of the incision, the transected myofibers often undergo abortive attempts at regeneration, and the regenerated ends commonly become embedded in connective tissue.

Minced tissue model

Using the minced muscle model of muscle regeneration, a skeletal muscle piece is chopped into small fragments destroying all the myofibres and neurovascular connections. The tissue is then transplanted subcutaneously or intramuscularly. This minced muscle can regenerate up to 30% of its original mass, but the process is often accompanied by excessive fibrosis. Minced muscle grafts eliminate the problem of inhomogeneous distribution when studying the participation of stem cells in the regeneration process.

Free transplantation

Free transplantation consists of removing a skeletal muscle completely from its bed and replacing it orthotopically. In the standard graft, the tendons are surgically restored, but revascularization and re-innervation are allowed to occur spontaneously. The center of the tissue becomes ischemic and over a few days regeneration occurs along a centripetal gradient.

Chemical injury

Numerous chemical compounds have been described that cause severe skeletal muscle damage following intramuscular administration. Most widely used are the snake toxins (cardiotoxin or CTX, and netoxin) although other chemicals such as barium chloride (BaCl2), bupivacaine, aldehydes, chloroquine (specific to type I myofibers), glycerol (promotes the replacement of myofibers by adipocytes), vincristine and hypertonic

solutions as well as solutions of varied temperature (hot or cold) and pH (acid or alkaline) have also been employed.

Cardiotoxin

Intramuscular CTX injection induces local myofibre necrosis, which is rapidly followed by recruitment of inflammatory cells, clearance of cellular debris, and regeneration of injured muscle.[218] The lesions caused by CTX are extremely reproducible and the process closely mimics the response to injury also seen following crush and freeze injury. Intra-peritoneal Evans Blue dye injection is a simple, safe and sensitive method for detection of increased myofibre permeability and ongoing inflammation.[378] It has been used to evaluate the overall efficacy of the regenerative response, as the dye accumulates in damaged muscle fibres.[216] The cardiotoxin model is an attractive model to delineate factors that influence the capacity for muscle regeneration. In particular, the reproducibility of this model facilitates the detection of subtle phenotypes in transgenic mice.

Glycerol

Muscle injury can also be induced by injection with glycerol, which has been reported to induce destabilisation of the cytoplasmic membranes followed by cell death, eventually resulting in fatty degeneration of the injected muscle. This model has been used to evaluate the efficacy of gene therapy for muscle disorders[379].

Biological injury

Examples of biological injury include forced exercise, denervation, de-vascularization and ischemia-reperfusion. Forced or eccentric physical exercise induces focal damage of the myofibres. Devascularization-denervation represents a mild form of skeletal muscle injury that can be used to study myofibre type specification. Ischaemia-reperfusion injury (e.g. by temporary clamping) results in transient ischaemia. Reperfusion is

rapidly followed by infiltration of inflammatory cells in the damaged area and skeletal muscle regeneration.

Genetic models of skeletal muscle fibrosis

Genetic models of the muscular dystrophies which have cyclic degeneration and regeneration produce the most dramatic fibrosis. In different types of dystrophy, ECM area fraction increases as much as ten-fold, and the associated muscle increases in stiffness. These models are highly complex, since cellular infiltration, muscle atrophy, fibre size variability, and regenerating fibres accompany fibrosis and fill the tissue area. Since this type of fibrosis is extreme and clinically relevant, studies of muscle fibrosis and of the potential therapeutic interventions for its prevention are often performed using dystrophic models.

Measures of muscle fibrosis

As a general rule fibrosis is characterised by abnormal accumulation of ECM. However, time and severity are important contributors to fibrosis. For example muscle fibrosis can be seen in nearly all models of muscle injury, but this is often transient and thought to stabilize the contractile apparatus while normal adaptive or regenerative responses proceed. In contrast, long-term accumulation of ECM interferes with function and does not resolve under normal physiological conditions.

Typically, skeletal muscle assays quantify the cross-sectional area fraction of ECM by excluding muscle fibres using image-processing tools reporting the amount of ECM as 'area fraction'. A limitation of this approach is that if muscle fibres atrophy and ECM remains the same, ECM will occupy a greater fraction of the muscle cross section. This approach also gives no information about isoforms and cross-linking, which can also affect function. For normal muscle the ECM area fraction is typically around 5%, but this value can increase dramatically in diseased or injured states. In addition to the

increased fractional area of ECM in fibrotic muscles, because the pathological response often includes fibre degeneration and regeneration, muscle fibrosis is also accompanied by a large increase in muscle fibre size variation.

Skeletal muscle fibrosis can also be expressed in terms of the total amount of collagen present in the tissue, as measured by the content of hydroxyproline, a major component of collagen derived from hydroxylation of the amino acid proline by prolyl oxidase. While this assay has been used for decades, expression of collagen mass relative to a known muscle protein is only rarely reported. In the majority of studies of skeletal muscle, collagen contents (typically expressed as micrograms of collagen per wet or dry muscle mass) of experimental and control groups are compared. While this content provides some insight into a tissue's response to treatment, in the few cases where collagen content has been quantified along with skeletal muscle mechanical stiffness, the two values only show weak correlation. Thus the method used to quantify fibrosis in skeletal muscle will depend on whether one uses a morphological assay such as area fraction, a biochemical assay such as collagen content, or a functional assay such as stiffness. It is not possible to quantitively interchange results of assays although they usually change in the same direction.

Optimisation of the CTX model of muscle injury and fibrosis

In this thesis I use a CTX model to study both regeneration and fibrosis within skeletal muscle. The CTX model is extremely simple and highly reproducible[216 380] and is emerging as the method of choice for producing injury in high impact publications investigating regeneration and fibrosis in skeletal muscle[121 185 216].

For the CTX fibrosis model, I have adjusted a protocol published in Nature Medicine in 2012 by Dulauroy *et al*., (Figure 56, p183). In my model mice are anaesthetised using inhaled isoflurane, given subcutaneous bupivacaine as analgesia before an intramuscular injection of 50ul of 20nM CTX (Naja mossambica mossambica, Sigma) into the right tibialis anterior muscle. 50ul of PBS is injected into the contralateral limb as an internal control. The mice are then recovered, checked hourly for the first 4 hrs and then daily until day 21. The mice are then culled by cervical dislocation and the tibialis anterior muscles harvested and analysed.

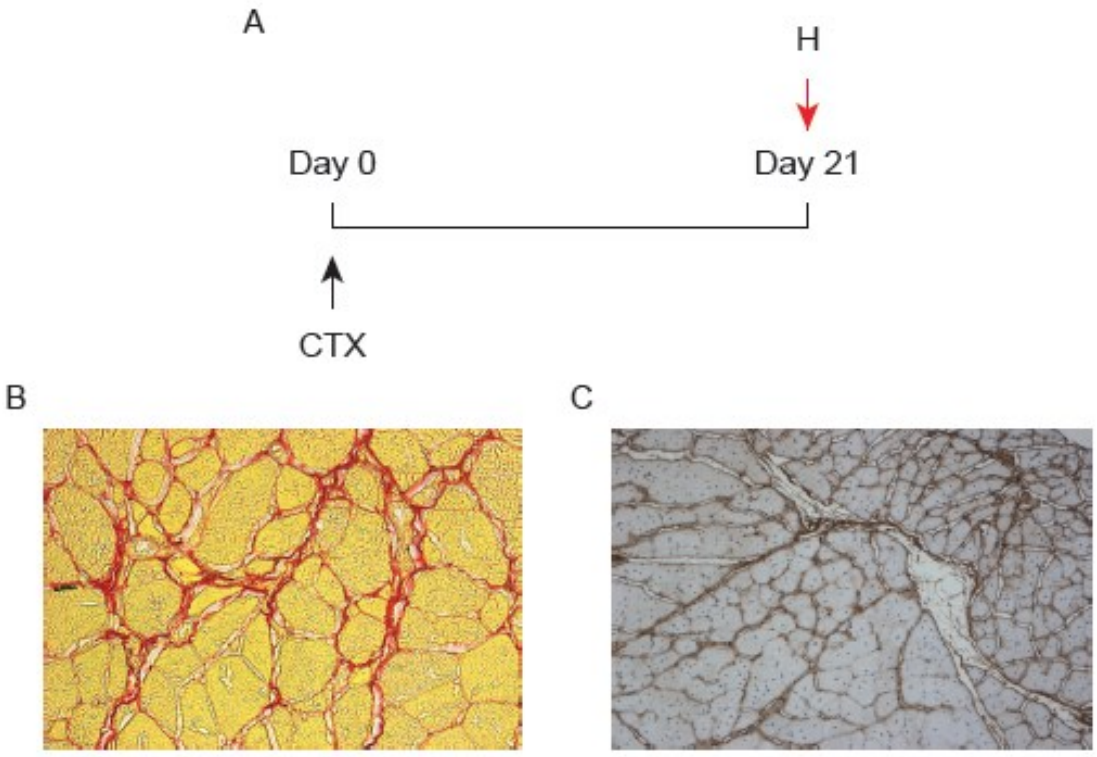

Figure 56 CTX fibrosis model
Tibialis anterior muscles are harvested 21 days following IM (TA) injection of CTX (A). Extracellular collagen can be visualised using Picrosirius Red in which collagens stain bright red and background tissues stain pale yellow (B, magnification 40x). Anti-collagen 1 antibody can also be used to detect ECM (C, magnification 20x).

Models using intramuscular cardiotoxin injections have also been used to investigate muscle regeneration[216]. In this model mice are subjected to a 50µl IM injection of 20nM CTX into the mid-portion of tibialis anterior muscle. Animals receive an IM injection of 50µl PBS on the contralateral side as a vehicle control. To evaluate the overall efficacy

of the regenerative response, mice are given an intraperitoneal injection of Evans blue dye, which accumulates in damaged muscle fibres. I performed a series of titration experiments to determine the optimum dose of Evans blue at day 8 that would allow best determination of differences in regenerative efficacy (Figure 57, p184).

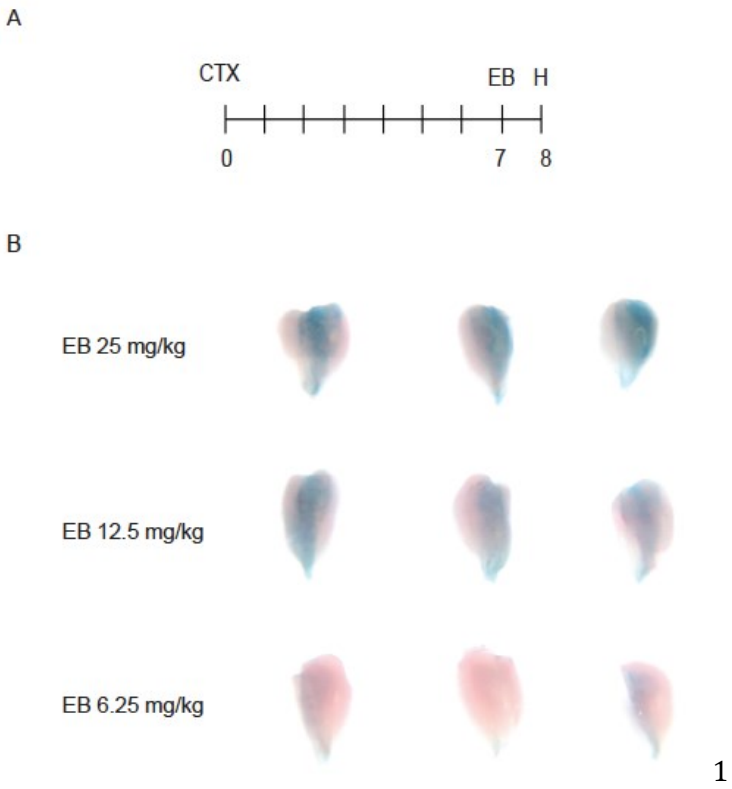

1

Figure 57 CTX skeletal muscle regeneration model
(A) CTX induces local muscle necrosis, which is rapidly followed by recruitment of inflammatory cells, clearance of cellular debris, and regeneration. To evaluate overall efficiency of the regenerative response Evans Blue can be administered intraperitoneally, accumulating in damaged muscle fibres. WT mice exhibit a robust regenerative response, resulting in the restoration of intact, regenerating fibres as evidenced by minimal Evans Blue staining at 8 days. The dose of Evans Blue was titrated establishing that 6.25mg/kg was the optimum dose to produce minimal Evans blue staining at day 8 following injury (B).

Chapter 2.4 PDGFRβ+ perivascular cells contribute to skeletal muscle fibrosis

Introduction

The origin of myofibroblasts contributing to skeletal muscle fibrosis following injury is not clear, although a number of putative progenitor populations have been implicated including so-called fibro-adipogenic progenitors (FAPs)[381] and pericytes[382].

PDGFRβ is known to label mesenchymal cells within the perivasculature that are important in fibrosis affecting the liver[351], lung[351] and kidney[181]. We therefore used a PDGFRβ-Cre system to target pro-fibrotic cells in skeletal muscle. These mice, which express Cre recombinase under the control of a fragment of the gene PDGFRβ, were previously developed to specifically target pericytes in experiments investigating angiogenesis[353].

The first aim of this chapter is to describe validations performed to show that PDGFRβ-Cre effectively targets PDGFRβ+ perivascular cells. Using PDGFRβ-Cre I then show that PDGFRβ+ perivascular cells contribute to the myofibroblast pool both following injury *in vivo* and *in vitro.* In order to visualise recombined and non-recombined cells we used double-fluorescent reporter mice that express membrane-targeted tdTomato before Cre-mediated excision and membrane-targeted GFP after excision[352]. The double reporting enabled us to assess tissue morphology – particularly important in fibrosis – and also to determine contamination after isolating the cells.

PDGFRβ-Cre efficiently targets PDGFRβ+ perivascular cells

In uninjured skeletal muscle, pericytes are found in a perivascular location in close contact with underlying endothelial cells - morphologically resembling pericytes in other organs[14]. Adventitial cells expressing CD34+CD31-CD146-CD45- reside in the outer layer (tunica adventitia) of arteries and veins. Both pericytes and adventitial cells

fulfill the defining criteria for MSC[383], and are considered to represent *in vivo* sources of mesenchymal progenitors[49 129]. Together, these two populations have been termed "perivascular stem cells"[384 385]. Using mTmG reporter mice, we found that PDGFRβ-Cre induced highly efficient recombination in cells in perivascular locations. We performed immunohistochemistry using antibodies targeting PDGFRβ and assessed for co-localisation using confocal microscopy to confirm appropriate targeting of PDGFRβ+ populations by PDGFRβ-Cre (Figure 58, p188). Furthermore, flow cytometric analysis of eGFP expressing cells confirmed co-expression of PDGFRβ (Figure 59, p189).

To evaluate the specificity of recombination in perivascular MSC we co-stained uninjured muscles from mTmG;PDGFRβ-Cre mice for α-SMA and CD146 (both well characterized markers of skeletal muscle pericytes[14]), and CD34 (well characterized marker of adventitial cells[83 384]). Virtually all of the reporting cells expressed one set of these markers (Figure 60, p191). αSMA was seen only in larger blood vessel walls in uninjured skeletal muscle (Figure 60, p191). To further assess specificity of PDGFRβ-Cre recombination, we stained uninjured control and fibrotic skeletal muscle from mTmG;PDGFRβ-Cre mice with antibodies to CD31 (endothelial cells), CD56 (myogenic cells), Pax7 (satellite cells), myosin fast and slow (myofibres). Very few of the reporting cells expressed any of these markers (Figure 60, p191). Flow cytometric analysis of GFP+ cells reflected findings on immunohistochemistry and confocal microscopy (Figure 61, p192) while also demonstrating that a subset of PDGFRβ+ Cells express PDGFRα (Figure 62, p193) – a marker previously described to identify pro-fibrogenic progenitors in muscle[219].

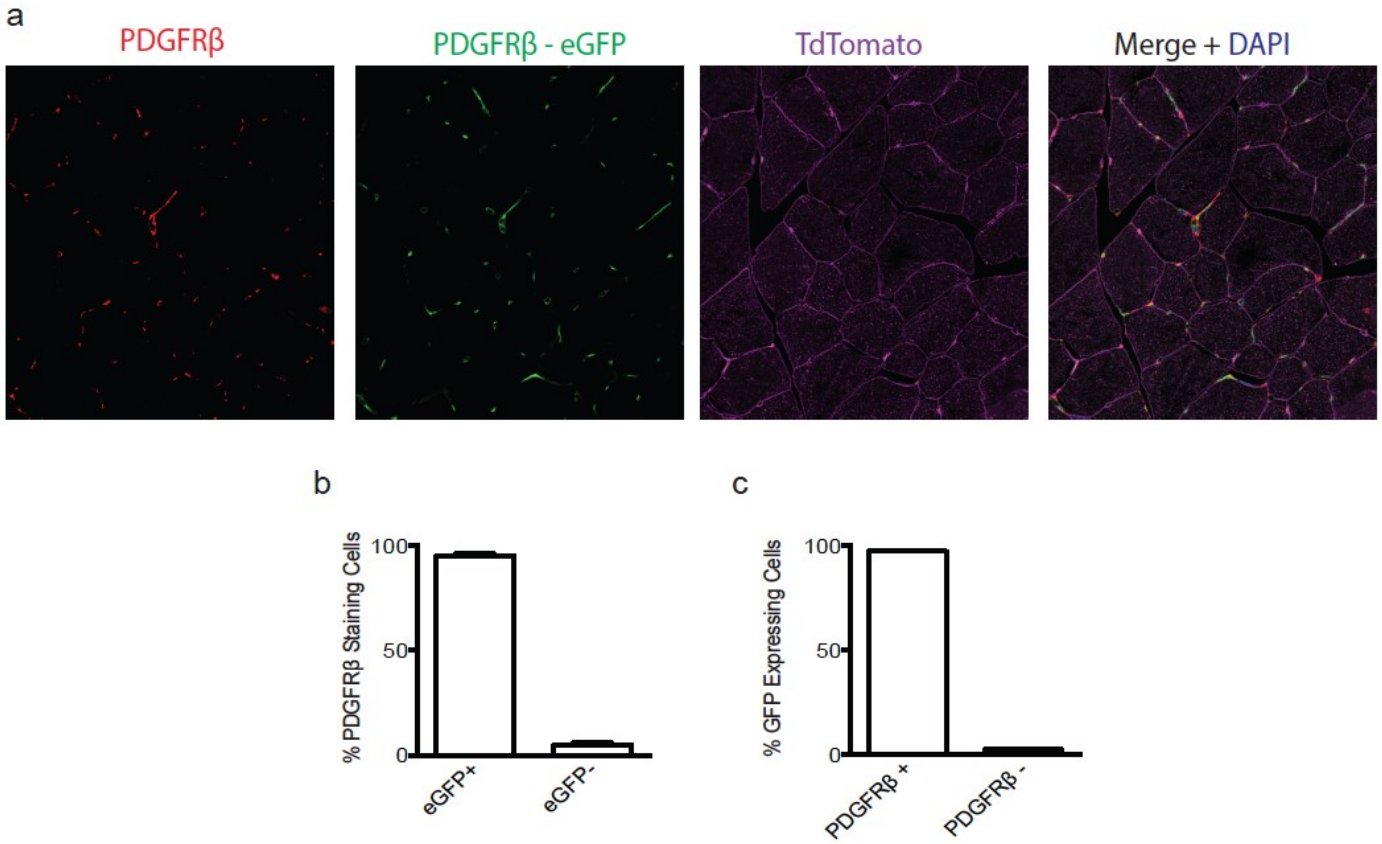

Figure 58 Immunofluorescence micrographs of skeletal muscle from mTmG;PDGFRβ-Cre mice co-staining with anti-PDGFRβ antibody
(a) Virtually all cells (97.49% SEM 0.46, n = 8) staining for PDGFRβ antibody expressed eGFP (b) and virtually all (95.28% SEM 1.08, n = 8) reporting cells stained positively for PDGFRβ antibody (c).

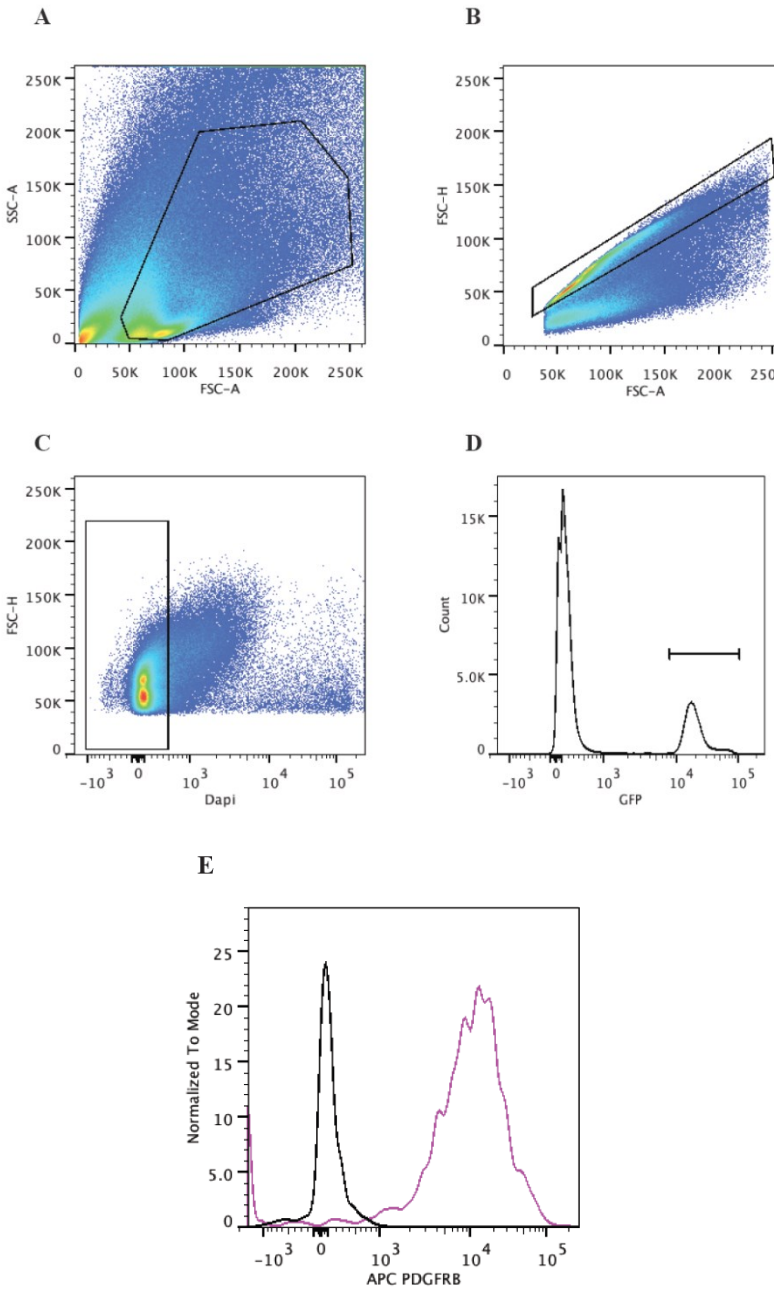

Figure 59 FACS sorting of eGFP reporting pericytes from mTmG:PDGFRβ-Cre mouse skeletal muscle.
(A) Cells were identified on the basis of size and granularity prior to selection for singlets (B), viable cells (C) and the expression of eGFP (D). (E) Co-staining with anti-PDGFRβ antibody at the time of sorting confirmed co-expression of eGFP reporting cells (pink line represents stained sample, black line indicates isotype control).

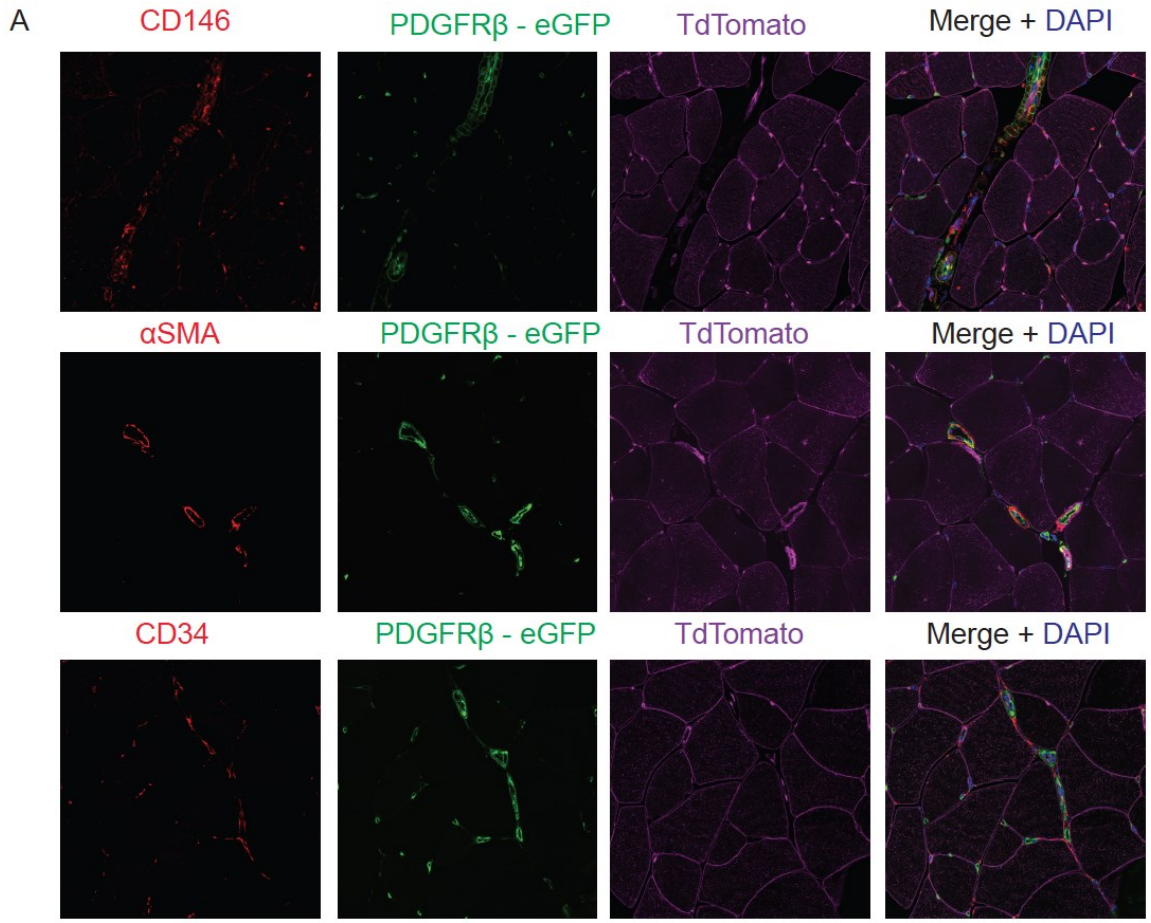
A
CD146
PDGFRβ - eGFP
TdTomato
Merge + DAPI
αSMA
PDGFRβ - eGFP
TdTomato
Merge + DAPI
CD34
PDGFRβ - eGFP
TdTomato
Merge + DAPI

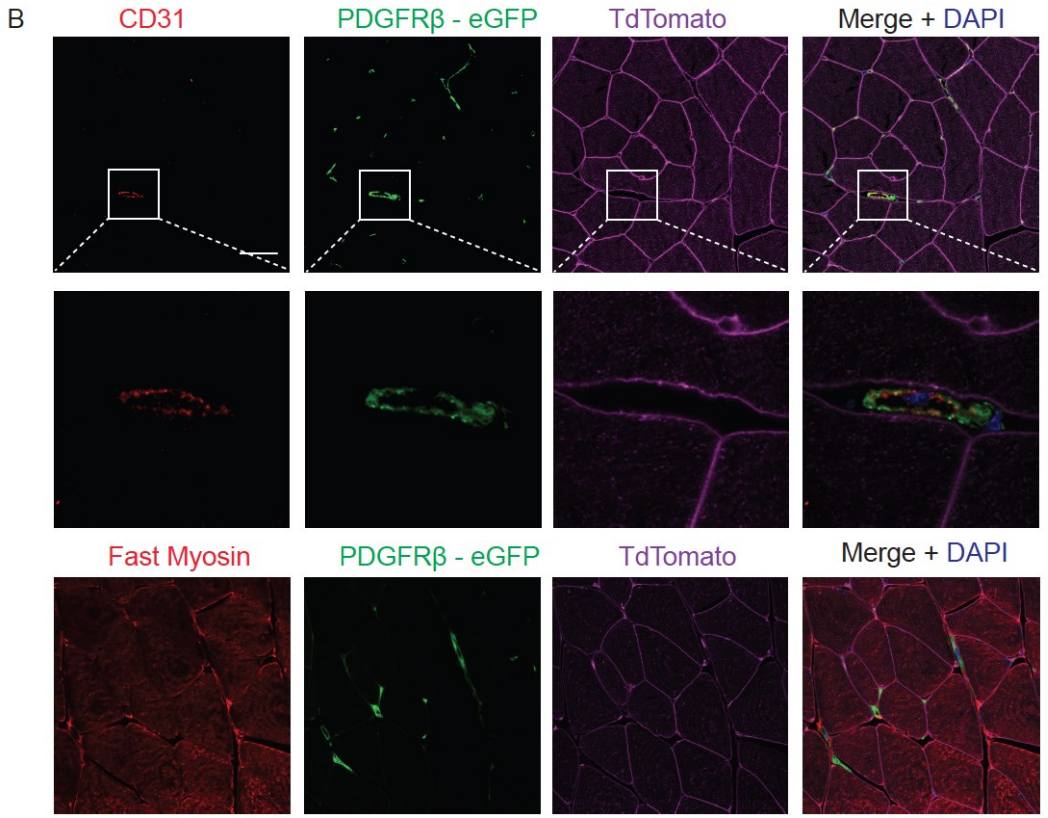

Figure 60 PDGFRβ-Cre mediates specific recombination in perivascular cells.
Immunofluorescence micrographs of skeletal muscle sections from mTmG;PDGFRβ-Cre reporter mice (n = 4) stained for pericyteS (CD146, αSMA), adventitial cells(CD34) (A), endothelial cells (CD34, CD31, CD146) and myogenic cells (myosin fast and slow) with endogenous eGFP reporting in green (B).

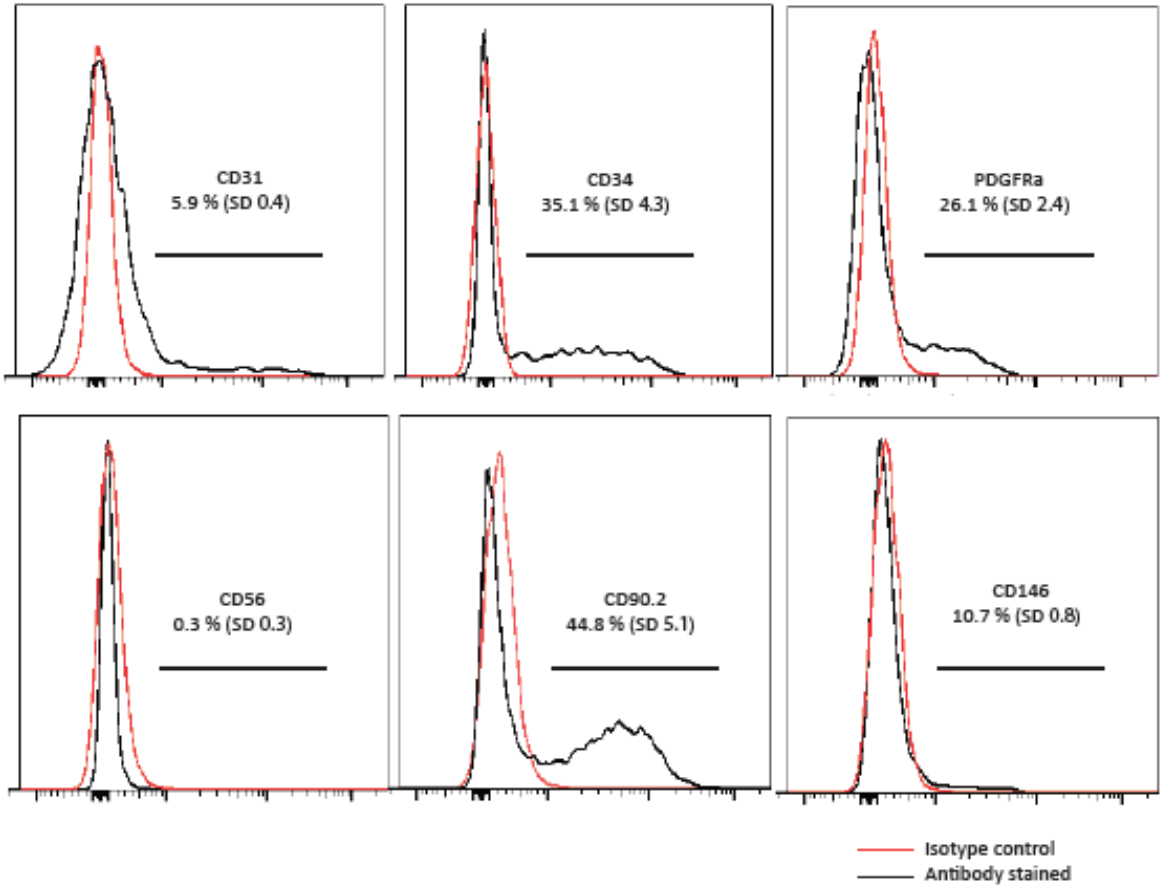

Figure 61 Flow cytometric analysis of purified eGFP+ cells from mTmG:PDGFRβ-Cre mice.
Cells were stained the indicated antibodies. The mean percentage co-localisation is indicated within each box plot (n = 3)

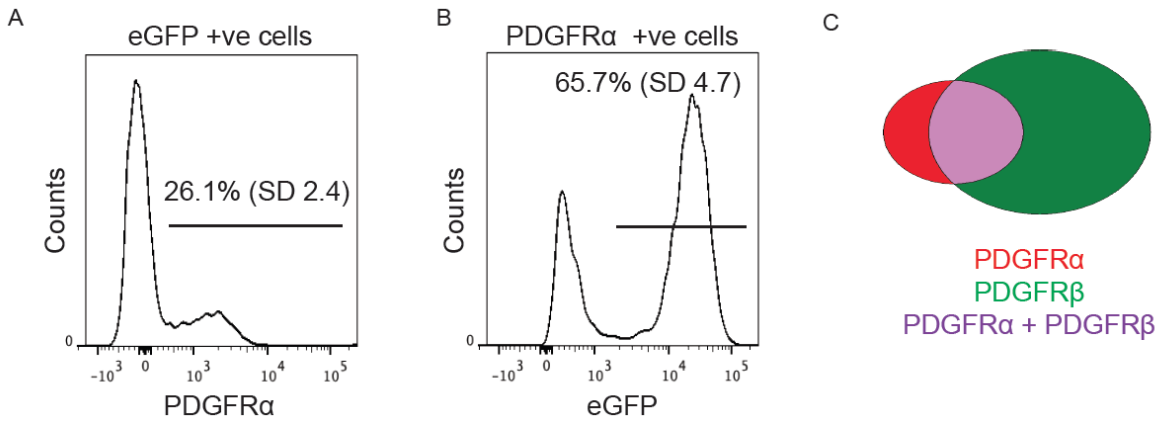

Figure 62 A subset of PDGFRβ perivascular cells express PDGFRα
(a) FACs analysis of PDGFRα expression levels in eGFP cells from mTmG;PDGFRβ-Cre reporter mice at the time of sorting. (b) FACs analysis of eGFP expression levels in PDGFRα cells from mTmG;PDGFRβ-Cre reporter mice at the time of sorting. (c) Proportional venn diagram showing the expression of PDGFRα cells on eGFP cells sorted from mTmG;PDGFRβ-Cre reporter mice.

eGFP labels a small proportion of myofibres in injured skeletal muscle of mTmG;PDGFRβ-Cre mice

Dellavalle *et al.,* reported that pericytes resident in postnatal skeletal muscle differentiate into muscle fibres and generate satellite cells. We set out to quantify the proportion of myofibres reporting eGFP in uninjured muscle. Expression of eGFP indicates that a cell currently expresses GFP, or has expressed PDGFRβ at any point in its ontogeny. Ten confocal miscroscopy aribitrary fields were taken from n = 8 mice to establish the percentage of myofibres expressing eGFP in uninjured tibialis anterior muscles for mTmG;PDGFRβ-Cre mice. While the majority of fields contained no eGFP+ myofibres, a number of fields contained clusters of eGFP+ reporting cells. The mean percentages of eGFP myofibres was 2.1% (Figure 63, p194). No eGFP+ myofibres stained positively for the PDGFRβ antibody.

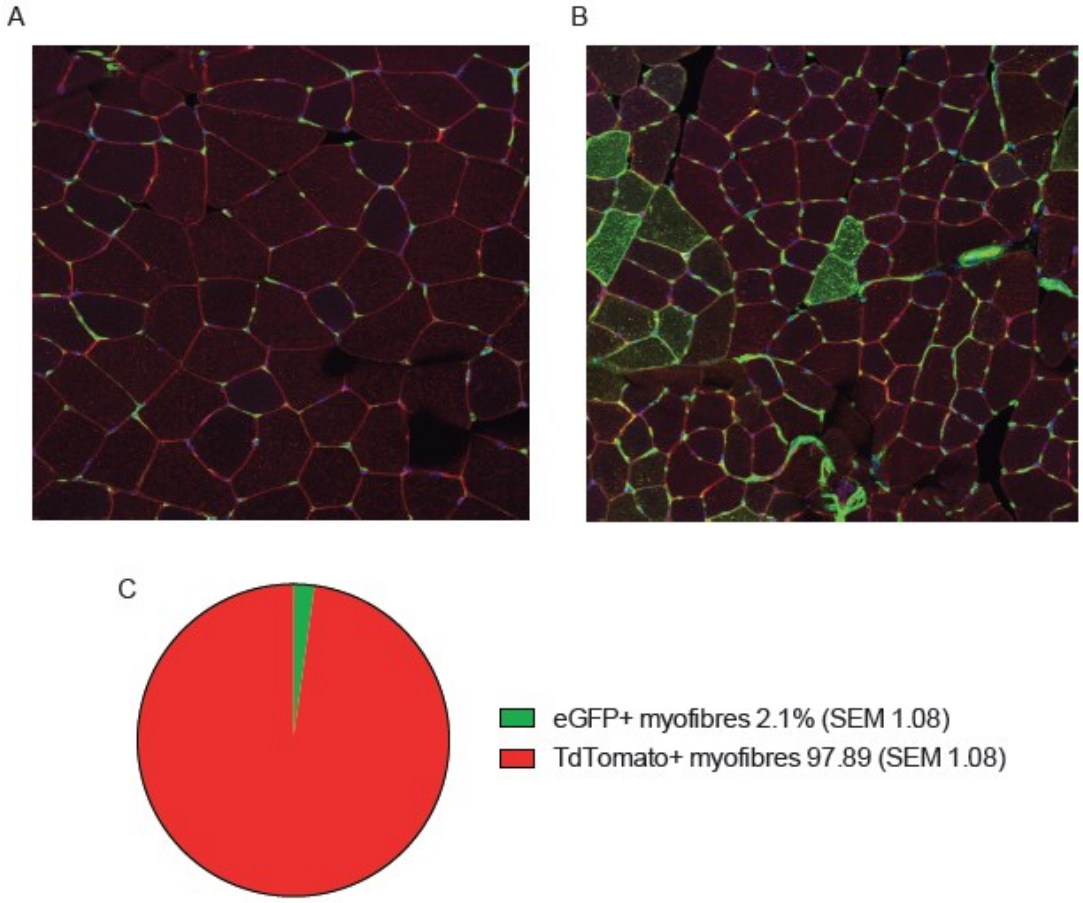

Figure 63 Expression of eGFP by myofibres.
Ten confocal miscroscopy aribitrary fields were taken from n = 8 mice to establish the percentage of myofibres expressing eGFP in uninjured tibialis anterior muscles for mTmG;PDGFRb-Cre mice. While the majority of fields contained no eGFP+ myofibres (A), a number of fields contained clusters of eGFP+ reporting cells (B). The mean percentages of eGFP myofibres and TdTomato myofibres are shown (C).

PDGFRβ+ perivascular cells proliferate in response to skeletal muscle injury and contribute to fibrosis *in vivo*

To evaluate the contribution of PDGFRβ+ perivascular cells to the myofibroblast pool following injury we observed the distribution of eGFP cells in the skeletal muscles of mTmG;PDGFRβ-Cre mice in a time course following injury (CTX injection) and control procedure (PBS injection) (Figure 64, p195).

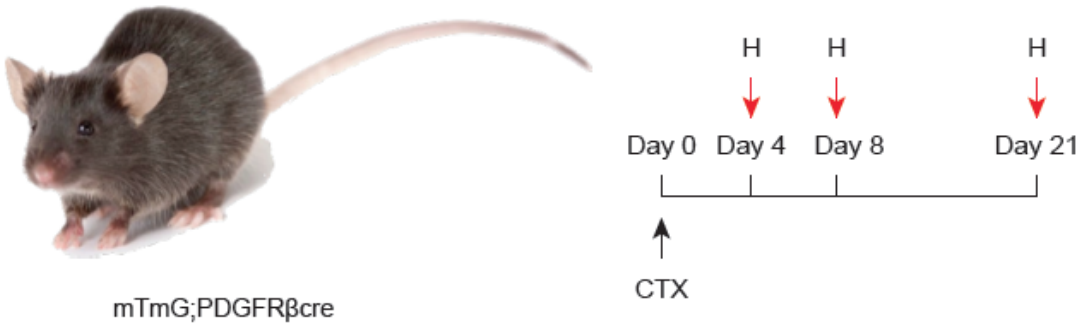

Figure 64 Skeletal muscle injury timecourse in mTmG;PDGFRβ-Cre mice
Tibialis anterior muscles are harvested and observed under confocal microscopy at day 4, 8 and day 21 following CTX injection.

We found that PDGFRβ-Cre induced highly efficient recombination in a distribution appropriate for PSC in control muscles. In response to injury, the field coverage of eGFP + cells increased markedly with eGFP cells settling in a distribution characteristic of myofibroblasts at day 21. The level of field coverage by eGFP+ cells appeared to plateau at day 21 with no difference in field coverage seen in CTX injured muscles between day 21 and day 60 (Figure 65, p196).

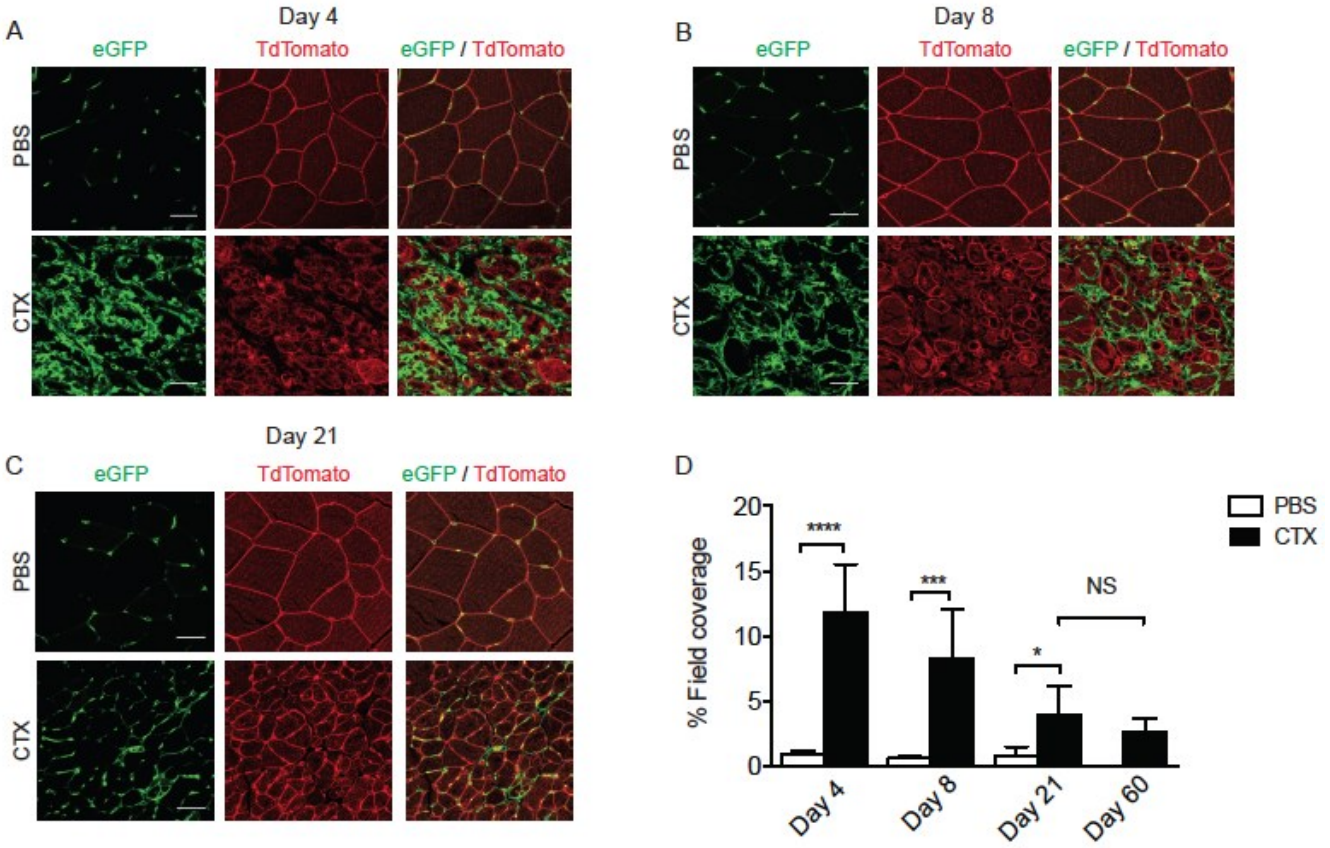

Figure 65 PDGFRβ+ perivascular cells proliferate and adopt the appearance of myofibroblasts following skeletal muscle injury**.**
(A) Immunofluorescence micrographs of skeletal muscle sections harvested from mTmG;PDGFRβ-Cre reporter mice 4 days following control (PBS) or IM CTX injection. Scale bars, 30 μm. (B) Immunofluoresence micrographs of skeletal muscle sections harvested from mTmG;PDGFRβ-Cre reporter mice 8 days following control (PBS) or CTX IM injection. Scale bars, 30 μm. (C) Immunofluorescence micrographs of skeletal muscle sections harvested from mTmG;PDGFRβ-Cre reporter mice 21 days following control (PBS) or CTX IM injection. Scale bars, 30 μm. (D) Field coverage of PDGFRβ+ perivascular cells at day 4, 8 and 21 following control (PBS) or CTX IM injection and at day 60 following CTX IM injection.

To further characterise PDGFRβ expressing cells in these settings we purified eGFP positive cells by cell sorting from uninjured control and fibrotic muscles of mTmG; PDGFRβ-Cre mice. Quantitative PCR (qPCR) of mRNA obtained from live eGFP positive cells showed marked induction of genes associated with the transition of quiescent PSC to the activated myofibroblast phenotype with injury including PDGFRβ, αSMA, TGFβ1, TIMP1, MMP2, MMP9, MMP13, Col1A1 and Col3A1 (Figure 66, p197).

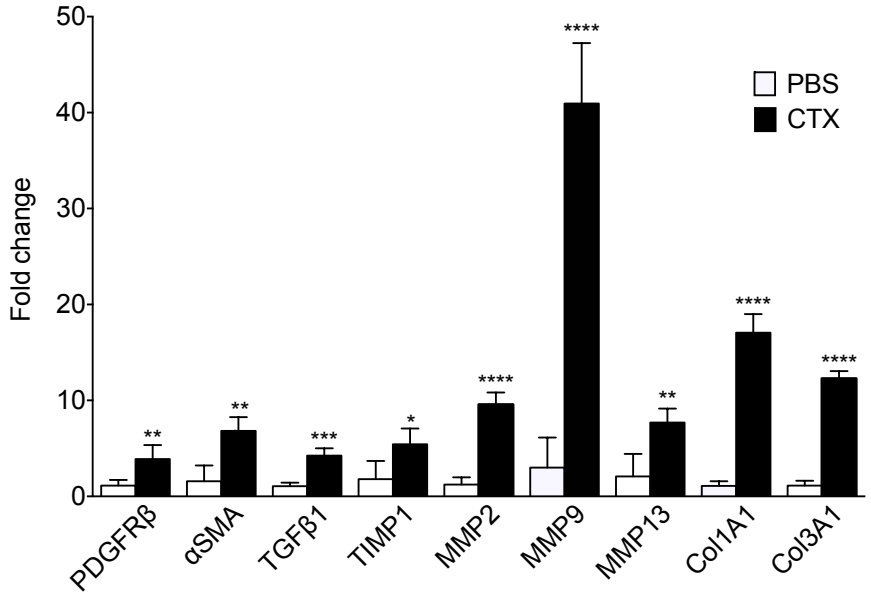

Figure 66 Gene expression profile of freshly sorted eGFP positive cells from skeletal muscle at day 10 following control (PBS) or CTX IM injection.
(Data are expressed as mean ± SEM. *p<0.05, **p<0.01, ***p<0.001, ****p<0.0001 (Student's t-test)).

PDGFRβ+ perivascular cells transition to a myofibroblast phenotype *in vitro*

To establish whether PDGFRβ+ perivascular cells were capable of adopting a myofibroblast like phenotype *in vitro,* eGFP positive cells isolated by FACS from uninjured mTmG;PDGFRβ-Cre mouse muscles were cultured for up to 14 days to induce myofibroblast activation. All of the cells in these sorted cultures expressed the myofibroblast marker αSMA (Figure 67, p199). qPCR of mRNA obtained from the cultured cells demonstrated a rise in the characteristic myofibroblast markers PDGFRβ, α-SMA, Col1A1 and TIMP1 (Figure 68, p200). The rise was also marked, but less dramatic when cells were cultured in EGM2 medium (Figure 69, p201)

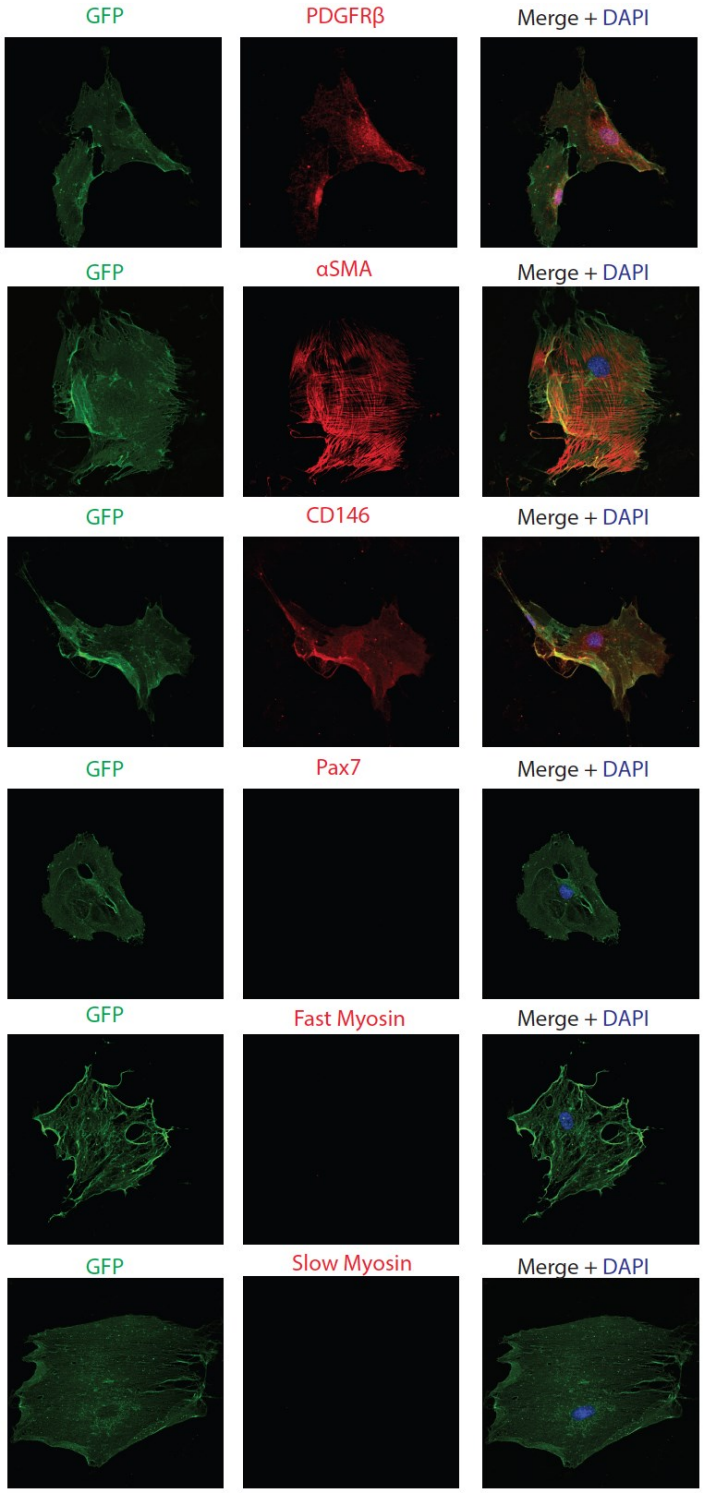

Figure 67 PDGFRβ+ perivascular cells become activated myofibroblasts *in vitro* Immunofluorescence staining of eGFP positive cells sorted from uninjured skeletal muscle of mTmG;PDGFRβ-Cre reporter mice and plated in tissue culture plastic for 7 days. Left panel shows eGFP (green), middle panel shows αSMA (red), right panel shows merged images. Scale bars, 50μm.

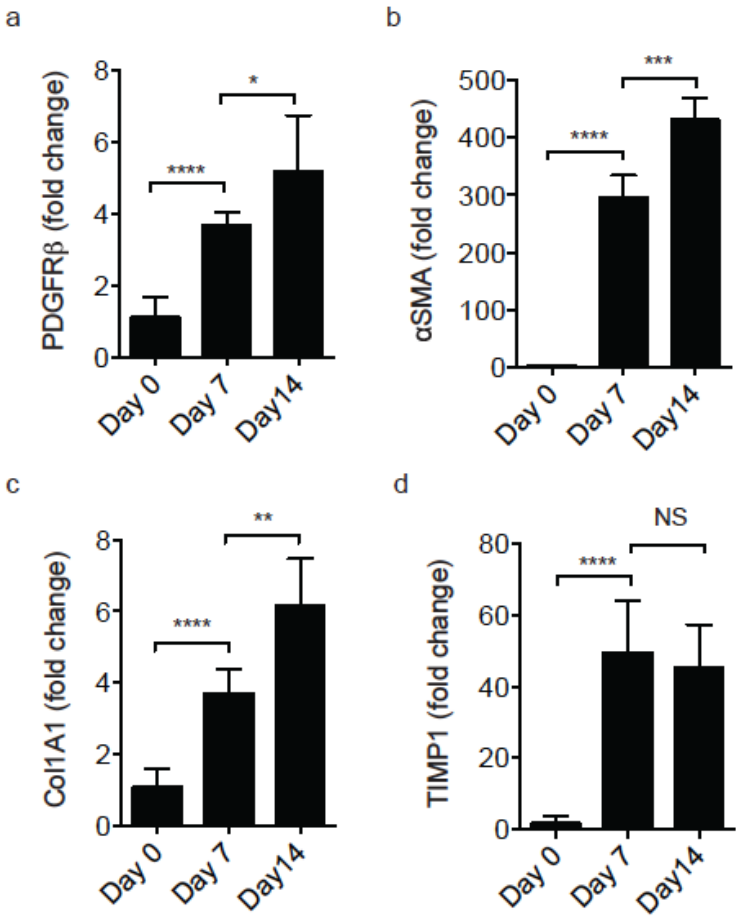

Figure 68 PDGFRβ+ perivascular cells transition to a myofibroblast phenotype in culture (DMEM10%FCS1%PS medium)
qPCR analysis of PDGFRβ, αSMA, Col1A1 and TIMP1 in freshly sorted eGFP+ cells from mTmG;PDGFRβ-Cre reporter mice and from eGFP+ cells cultured for 7 and 14 days. Data are mean ± SEM. *P < 0.05, **P < 0.01, ***p<0.001, ****p<0.0001 (Student's *t*-test).

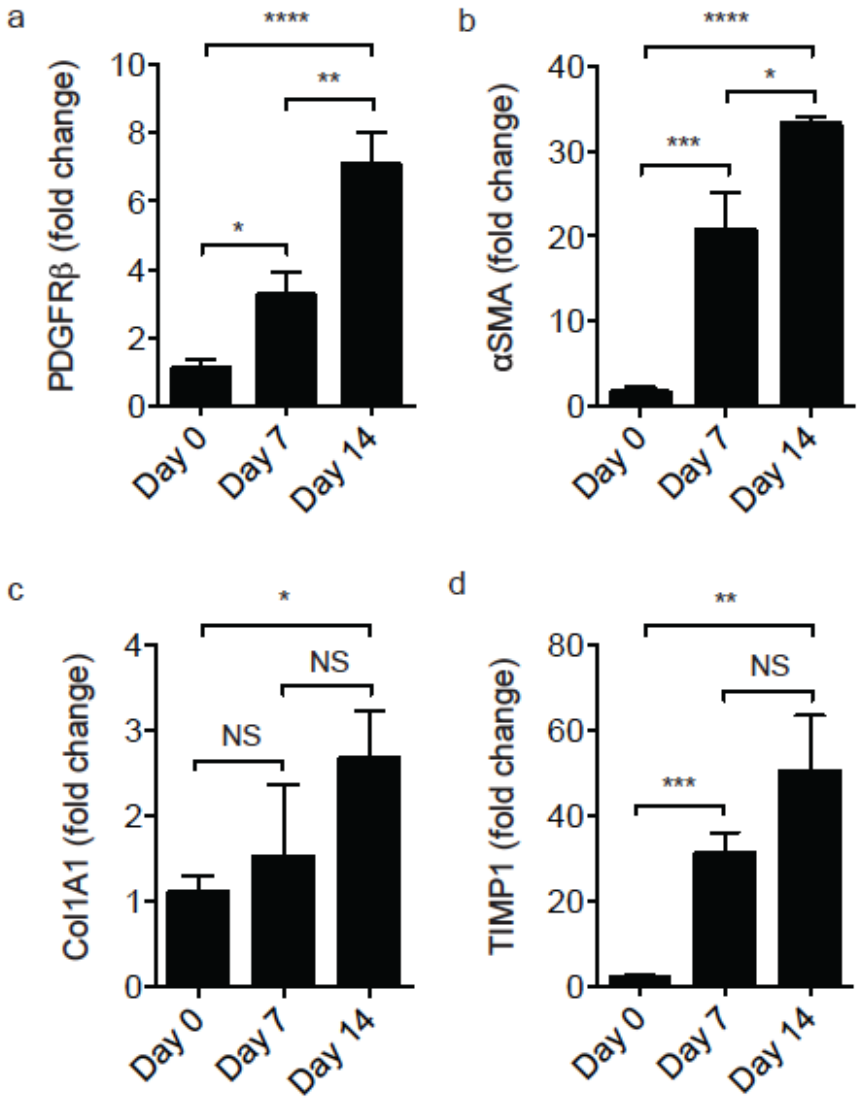

Figure 69 PDGFRb+ perivascular cells transition to a myofibroblast phenotype in culture (EGM2 culture medium)
qPCR analysis of PDGFRβ, αSMA, Col1A1 and TIMP1 in freshly sorted eGFP+ cells from mTmG;PDGFRβ-Cre reporter mice and from eGFP+ cells cultured for 7 and 14 days. Data are mean ± SEM. NS = not significant, *P < 0.05, **P < 0.01, ***P < 0.001, ****P < 0.0001 (Student's *t*-test).

Chapter 2.5 Selective αv integrin depletion in PDGFRβ+ perivascular cells regulates skeletal muscle fibrosis

Secreted transforming growth factor–β (TGFβ) is arguably the major pro-fibrogenic cytokine and a central mediator of fibrosis in multiple organs. The binding of active TGFβ1 to high affinity TGFβ1 receptors in the plasma membrane of myofibroblast precursors induces TGFβ1 signaling, which generates contractile (remodeling) cell features by promoting αSMA neoexpression and secretory cell functions such as collagen production. Although antagonists of TGFβ1 and the TGFβ1 receptor inhibit myofibroblast activation in cell culture and suppress induced fibrosis in skin, lung, kidney and liver in animal models, these strategies bear the risk of adverse effects on immunity and carcinogenesis via effects on inflammatory cells and epithelium that are also regulated by TGFβ1[173 174 386].

TGFβ is secreted as a latent complex that is present at high concentrations and directly cross-linked to the extracellular matrix. Much of the regulation of TGFβ function in tissues is based on extracellular activation of this latent complex[387 388]. Two of the three mammalian TGFβ isoforms (TGFβ1 and TGFβ3) can be activated by members of the integrin family that interact with a linear arginine-aspartic acid (RGD) motif present in an N-terminal fragment of the TGFβ gene product called the latency-associated peptide.

Myofibroblasts express several αv containing integrins and are contractile cells capable of exerting force on tethered ligands. The recently solved crystal structure of the small latent complex of TGFβ demonstrates that mechanical force generated by the contractile actomyosin cytoskeleton and transmitted by integrins is a common mechanism for activating latent TGFβ[345]. *In vitro* studies of myofibroblasts have shown that they can use alternative αv-containing integrins that share the αv subunit,

including αvβ1, αvβ3, αvβ5, αvβ6 and αvβ8, can recognize the same RGD peptide motif and at least in some circumstances can activate latent TGFβ[343 345-348].

Several investigators have shown that TGFβ activation by αvβ6 integrin has an important role in models of fibrosis in the lungs, biliary tract and kidney[343 389 390]. Henderson *et al*., showed that activation of latent TGFβ1 from the extracellular matrix by αv integrins is a key event in liver pericyte to myofibroblast differentiation and that inhibition or deletion of the αv subunit blocks liberation of active TGFβ1, myofibroblast differentiation and development of fibrosis[351].

We therefore focused on the integrin αv subunit because of the role of multiple αv integrins in activating latent TGFβ and its demonstrated regulation of the transition of pericytes to myofibroblasts in multiple solid organs. The aim of this chapter was to establish whether this key role of αv integrins on PDGFRβ+ perivascular cells was conserved within skeletal muscle.

Selective αv integrin depletion in PDGFRβ+ perivascular cells regulates skeletal muscle fibrosis

To investigate whether loss of αv integrins on PDGFRβ+ perivascular cells influences the development of skeletal muscle fibrosis we used Itgavflox/flox;PDGFRβ-Cre mice, (which are null for αv in PDGFRβ expressing cells) in our CTX model of muscle injury. Itgavf$^{lox/flox}$;PDGFRβ-Cre mice were significantly protected from CTX induced fibrosis, as determined by picrosirius red (PSR) staining for collagen (Figure 70, p205). This was not due to changes in the degree of initial injury caused by CTX, as determined by Evans

blue accumulation in damaged muscle fibres 8 days following CTX injection (Figure 71, p206).

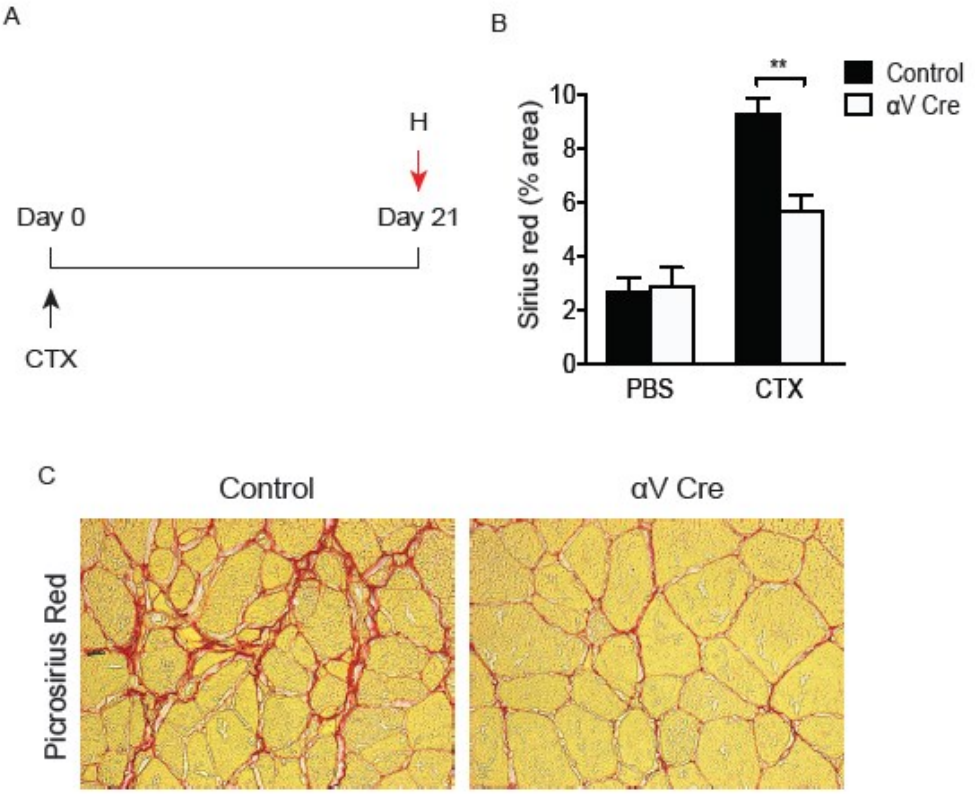

Figure 70 Deletion of αv integrins on PDGFRβ+ perivascular cells protects mice from CTX-induced skeletal muscle fibrosis
Itgavflox/flox;PDGFRβ-Cre and control mice received IM CTX injection to tibialis anterior muscle and PBS to the contralateral side. At day 21 muscles were harvested for analysis (A). Digital image analysis quantification of picrosirius red staining (collagen deposition) of muscle tissue after PBS or CTX treatment of control and itgav$^{flox/flox}$;PDGFRβ-Cre mice (n=5 mice in each group). Data are mean ± SEM. **P < 0.01 (Student's t test) (B). Representative images of picrosirius red stained sections from control and αv Cre mice 21 days following CTX injection (images are x40).

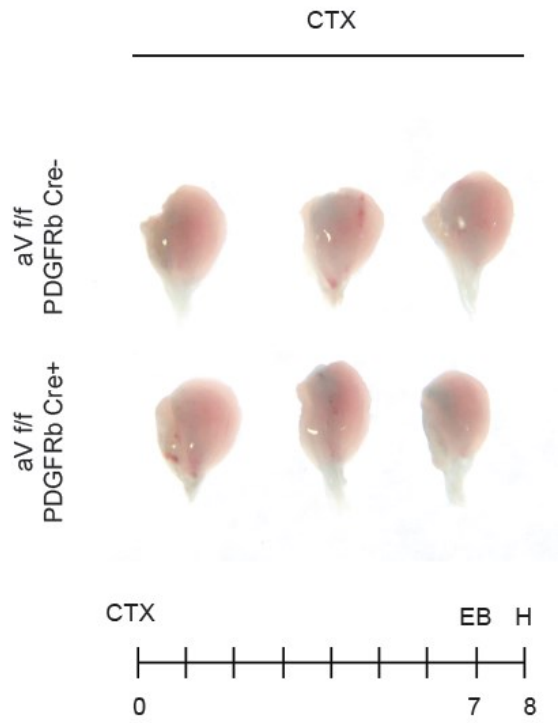

Figure 71 The overall efficacy of the regenerative response to injury in control and Itgav;PDGFRβ-Cre mice.
We gave mice an intraperitoneal injection of Evans blue dye 7 days following CTX injection. On harvesting muscles 24 hrs later (8 d following CTX injection) there was no difference in Evans blue accumulation, indicating equivalent levels of ongoing muscle damage, in αv null and control mice.

To investigate whether loss of αv integrins affected activation-induced induction of extracellular matrix protein gene expression, FACS sorted control and αv-null (Itgav$^{flox/flox}$;PDGFRβ-Cre) PDGFRβ+ perivascular cells were activated in culture for 5 d. Col1A1 expression was significantly reduced in itgavflox/flox;PDGFRβ-Cre PDGFRβ+ perivascular cells (Figure 72, p207).

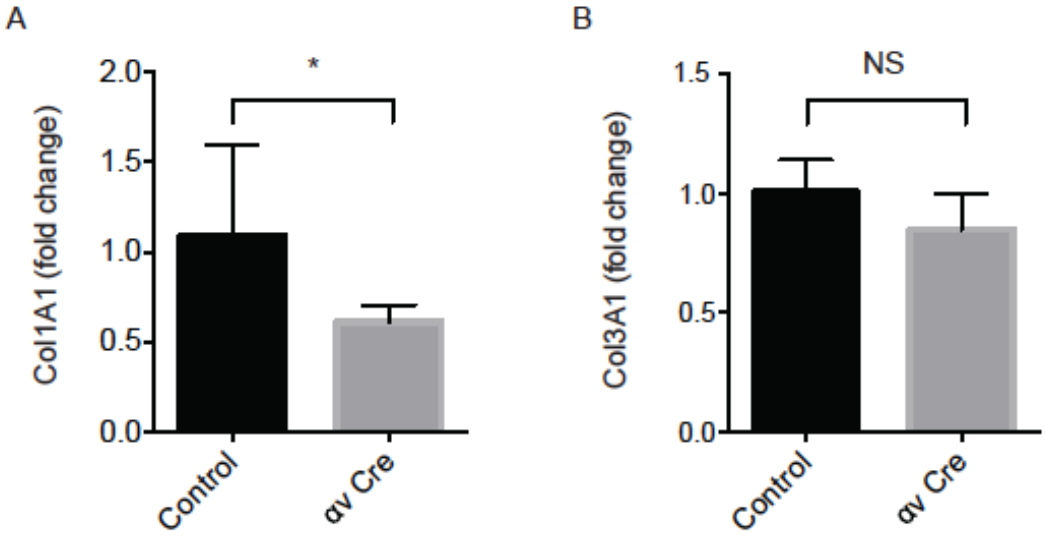

Figure 72 αv integrin depletion on PDGFRβ+ perivascular cells inhibits profibrotic gene expression
(A) qPCR of Col1A1 in control and itgav$^{flox/flox}$;PDGFRβ-Cre (αv Cre) PDGFRβ+ perivascular cells culture activated for 5 days. (B) qPCR of Col3A1 in control and itgav$^{flox/flox}$;PDGFRβ-Cre (αv Cre) PDGFRβ+ perivascular cells culture activated for 5 days.

Furthermore, treatment with an αv-blocking small molecule (CWHM12) (Figure 73, p208) inhibited expression of profibrotic genes (Figure 74, p208). CWHM12 is a synthetic small molecule RGD peptidomimetic antagonist that consists of a cyclic guanidino-substituted phenyl group as the arginine mimetic, and a phenyl substituted beta amino acid as the aspartic acid mimetic, both linked via glycine. CWHM96 is a control R-enantiomer of CWHM12 that differs only in the orientation of its carboxyl (CO_2H) group (Figure 73, p208). CWHM96 and CWHM12 were kindly provided by Michael Prinsen, David Griggs and Peter Ruminski from St Louis University, Missouri, USA.

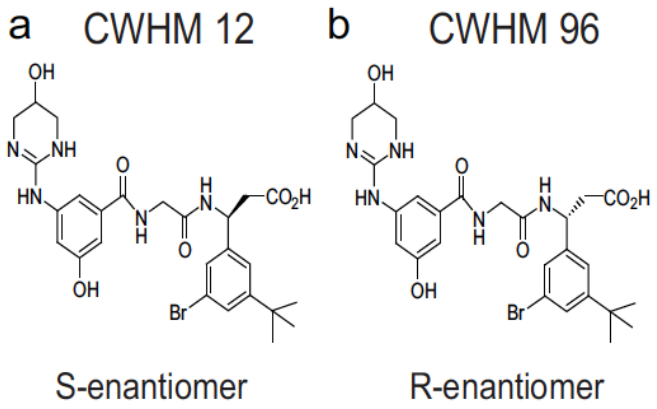

Figure 73 The chemical structure of CWHM12 and CWHM96

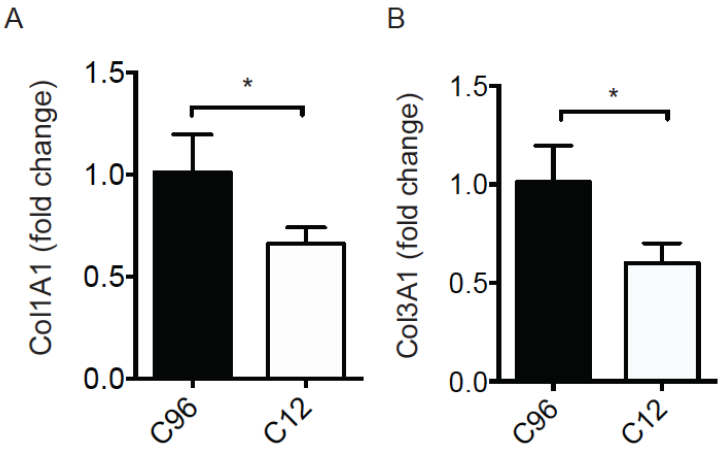

Figure 74 Myofibroblast activation *in vitro* is attenuated by inhibition of av integrins. (A) qPCR of Col1A1 in eGFP+ cells sorted from mTmG;PDGFRβ mice cultured in the presence of CWHM 12 and CWHM 96 for 5 d. (B) qPCR of Col3A1 in eGFP+ cells sorted from mTmG;PDGFRβ mice cultured in the presence of CWHM12 and CWHM96 for 5 d.

Assessment of αv integrin heterodimer $\alpha_v\beta_8$ in skeletal muscle fibrosis

The αv integrin has five possible β subunit binding partners (β_1, β_3, β_5, β_6 and β_8), each of which has been reported to bind and/or activate latent TGFβ. We established that the expression of a number of the β subunits was significantly raised in response to CTX induced muscle injury (Figure 75, p209).

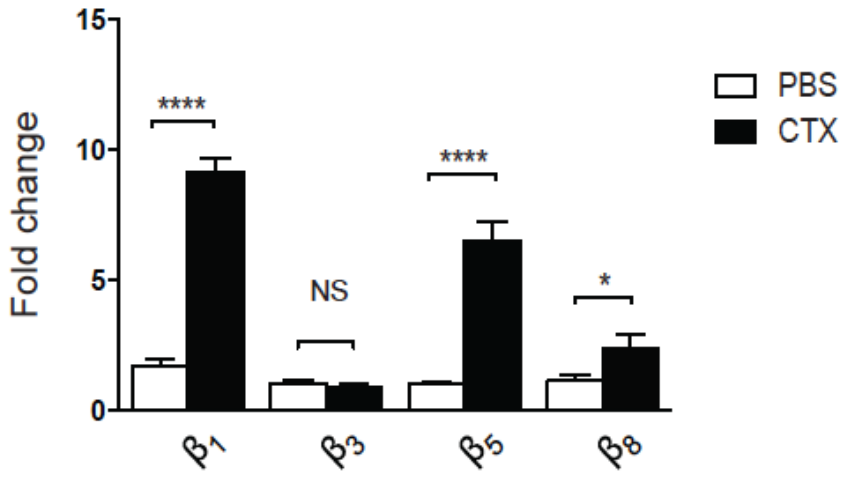

Figure 75 β subunit expression in freshly sorted eGFP+ cells from skeletal muscle at day 10following control (PBS) or CTX intramuscular injection.
(Data are expressed as mean ± SEM. *p<0.05, ****p<0.0001 (Student's t-test)).

To further assess a potential contribution of αv integrin heterodimers during skeletal muscle fibrosis, we evaluated the response to CTX injection in mice lacking β_8 integrins on PDGFRβ+ perivascular cells. Depletion of β_8 failed to protect mice from CTX induced fibrosis (Figure 76, p209), nor did it affect the degree of initial injury caused by CTX.

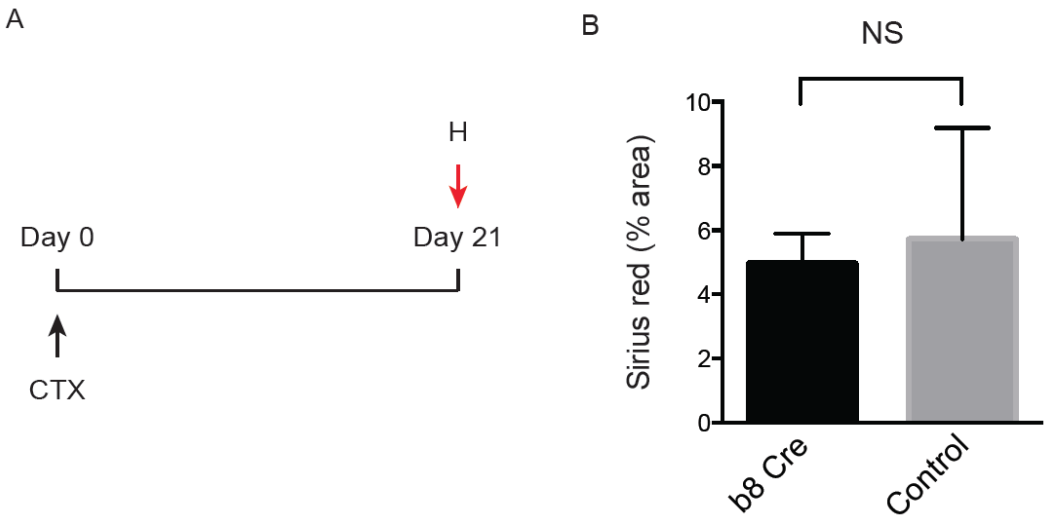

Figure 76 Deletion of β_8 subunit on PDGFRβ+ perivascular cells does not influence the degree of CTX induced muscle fibrosis.
Itgβ_8;PDGFRβ-Cre mouse muscle was harvested 21 days following CTX injection (A). There was no statistical difference in picrosirius red staining between muscles from β_8 null and control mice (Error bars are ± SEM, n = 8)

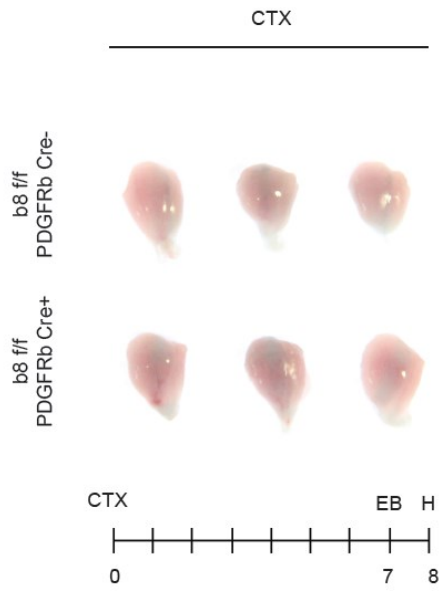

Figure 77 The degree of initial injury and efficacy of the initial regenerative response was not influenced by depletion of β_8 integrin subunit on PDGFRβ+ perivascular cells (n = 8, 3 representative muscles shown).

Blockade of αv integrins attenuates skeletal muscle fibrosis

Our data indicate that inhibition of αv integrins on PDGFRβ+ perivascular cells might represent a valuable therapeutic target. We therefore examined the potential of CWHM12 to prevent skeletal muscle fibrosis by inserting Alzet osmotic minipumps containing either CWHM12 or control R-enantiomer (CWHM96) into C57BL/6 mice, followed by IM CTX injection to the tibialis anterior muscle. These minipumps provide researchers with a method for controlled and continuous agent delivery *in vivo*, and can be used for systemic administration when implanted subcutaneously or intraperitoneally. Correct placement of the minipumps is critical to ensure uninterrupted delivery of inhibitor (Figure 78, p211). Treatment with CWHM12 (2.5mg/day/25mg mouse) significantly reduced skeletal muscle fibrosis, as determined by staining for collagen (picrosirius red staining) (Figure 79, p211).

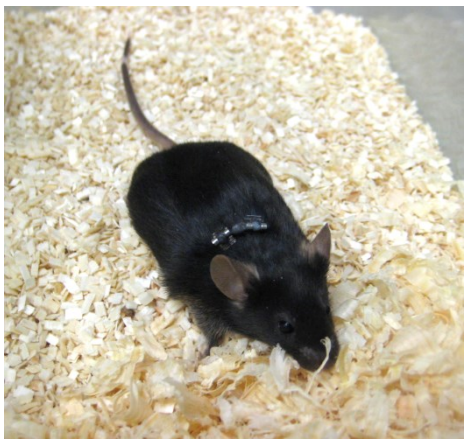

Figure 78 Correct positioning of the Alzet minipump
The usual site for subcutaneous implantation of osmotic pumps in mice is on the back, posterior to the shoulder blades and lateral to the midline. The subcutaneous pocket should be large enough to allow some free movement of the pump without allowing the pump to turn around or slip down the flank. The pump should not rest immediately beneath the incision, which could interfere with healing of the wound.

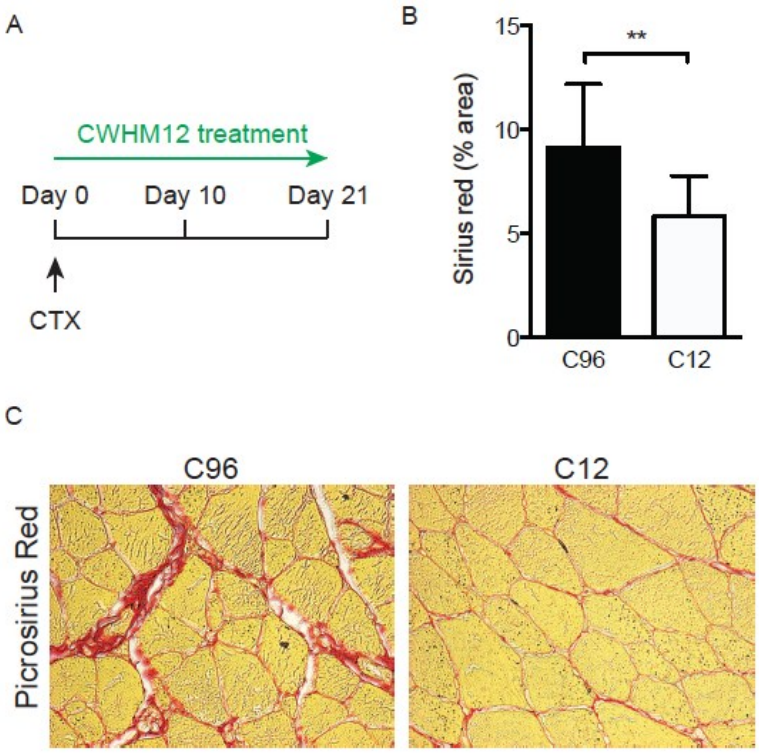

Figure 79 Blockade of αv integrins by the small molecule CWHM12 attenuates skeletal muscle fibrosis in a prophylactic model
(A) Dosing regime in the prophylactic skeletal muscle fibrosis model. Alzet osmotic minipumps containing CWHM12 or CWHM96 (control) were inserted, followed by intramuscular CTX injection. Tissues were harvested at day 21 following CTX injection. (B) Digital image analysis quantification of collagen (picrosirius red staining) in prophylactic model (n=11). (C) Picrosirius red staining of skeletal muscle tissue from control and CWHM 12 treated mice (prophylactic model) on day 21 following CTX injection. (images are x40).

We next asked whether CWHM12 could prevent further progression of established fibrosis. Alzet osmotic minipumps containing CWHM12 or CWHM96 were inserted subcutaneously 10 days following CTX injection. Mice then received 11 days of constant dosing prior to muscle harvest at d 21 following CTX injection. CWHM 12 significantly reduced skeletal muscle fibrosis even after the fibrotic disease had become established (Figure 80, p212)

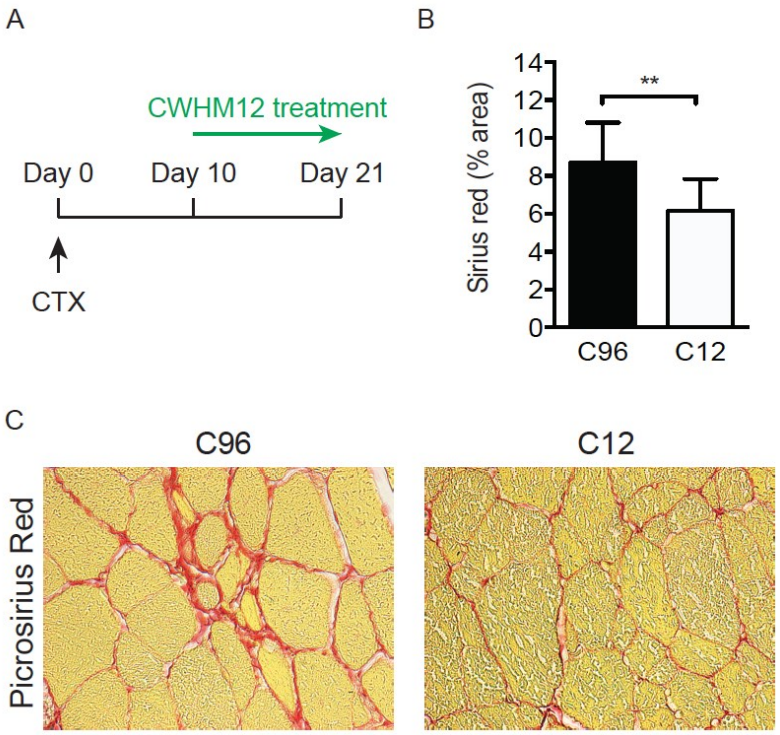

Figure 80 Blockade of αv integrins by the small molecule CWHM 12 attenuates skeletal muscle fibrosis in a therapeutic model
(A) Dosing regime in the therapeutic skeletal muscle fibrosis model. 10 days following intramuscular CTX injection, Alzet osmotic minipumps containing CWHM 12 or CWHM 96 (control) were inserted. Tissues were harvested at day 21 following CTX injection. (B) Digital image analysis quantification of collagen (picrosirius red staining) in the therapeutic model (n=10). (C) Picrosirius red staining of skeletal muscle tissue from control and CWHM 12 treated mice (therapeutic model) mTmG;PDGFRβ-Cre reporter mice. (images are x40). Data are mean ± SEM. *p<0.05, **p<0.01, ***p<0.001 (Student's t-test) n = 12 mice per group.

Chapter 2.6 Discussion

In this section we sought to establish the role of PDGFRβ+ perivascular cells in the development of skeletal muscle fibrosis. In order to achieve this we used transgenic mouse technology including Cre/Lox recombination, fluorescent reporters and gene knockdown. We were able to confirm that PDGFRβ-Cre targets PDGFRβ+ perivascular cells in skeletal muscle with high efficiency. We show that PDGFRβ-Cre targets a population of perivascular pre-MSC that proliferate and transition to a myofibroblast like phenotype in response to skeletal muscle injury. We have confirmed that the critical role for αv integrins in mediating myofibroblast activation and fibrogenesis within visceral organs also applies to skeletal muscle.

PDGFRβ-Cre labels perivascular cells with high efficiency

PDGFRβ-Cre has previously been used by our group to target pericytes that contribute to fibrosis in liver, lung and kidney[351]. We therefore used this system to target pro-fibrotic cells within skeletal muscle. We firstly sought to establish the phenotype of cells targeted using this constitutive system. Using the double reporter mouse mTmG we found that the PDGFRβ-Cre resulted in extremely efficient recombination in PDGFRβ+ cells with over 97% of PDGFRβ+ cells reporting for eGFP. We were also able to show that over 95% of GFP expressing cells stained positively for the antibody – confirming that eGFP was expressed in a minor number of cells that no longer expressed PDGFRβ.

PDGFRβ was only found in perivascular locations and was not expressed on endothelial cells. However, we found that PDGFRβ labeled a heterogeneous population of stromal cells residing in perivascular locations that could be subdivided based on their expression of PDGFRα and CD146 among others. The phenotype observed suggested

that PDGFRβ labels two populations of perivascular stem cells: namely PDGFRβ+PDGFRα+CD34+ adventitial cells and PDGFRβ+PDGFRα-CD34- pericytes. Both these populations fulfill the definition of MSC predecessors[33] and have been well characterized by our group and others[14 83].

eGFP+ myofibres in uninjured skeletal muscle of mTmG;PDGFRβ-Cre mice

Skeletal muscle fibres form by fusion of mesoderm progenitors called myoblasts. After birth, muscle fibres do not increase in number but continue to grow in size because of fusion of satellite cells, the postnatal myogenic cells responsible for muscle growth and regeneration. Numerous studies suggest that, on transplantation, cells from tissues other than muscle (for example bone marrow, brain, adipose tissue) can fuse with regenerating muscle fibres and also contribute to the satellite cell pool[211 391-393]. It was important to establish whether this contribution to skeletal muscle was restricted to the artificial conditions created by transplantation or whether it occurs in development and injury *in vivo*. Dellavalle *et al.*[121], demonstrated that pericytes, transgenically labelled with an inducible alkaline phosphatase CreERt2, but not endothelial cells, fuse with developing myofibres and enter the satellite cell compartment during unperturbed postnatal development. They reported that the percentage of myofibres originating from AP+ cells varied markedly between tissues with highest percentage seen in uninjured diaphragm (7.3 ± 1.2%) while only 0.6% ± 0.2% myofibres in TA originate from AP+ cells. They noted that the contribution of myofibres from pericytes was randomly distributed between fast and slow myofibres.

Dellavalle *et al.,* reported that the pericyte contribution to myogenesis increases

following acute injury or in chronically regenerating dystrophic muscle[121]. Following injury the percentage of myofibres originating from pericytes in tibialis anterior muscles had risen to 5%. In these experiments the tamoxifen was given at post-natal day (p) 1-3 and the authors note that if tamoxifen was given later (beyond p8) then the contribution of pericytes to myofibres drops dramatically. They were also able to show that the contribution of AP+ pericytes to myogenesis was minimal in adult muscle. When tamoxifen is given in mice aged 2-3 months minimal reporting was seen in myofibres. Furthermore, this minimal contribution in adulthood did not significantly increase after cardiotoxin-induced regeneration. (0.15 ± 0.1 in control TA and 0.93 ± 0.4 in CTX TA). In summary, this study demonstrated that AP+ cells could contribute to muscle fibres and the satellite cell pool but that this contribution occurs during the first month of postnatal growth becoming negligible in adult mice.

These findings are in keeping with the present study where we observed that around 2% of myofibres from mTmG;PDGFRβ-Cre mice in uninjured muscle expressed eGFP, indicating that they expressed PDGFRβ at some stage in their ontogeny. The contribution is marginally larger than those by *Dellavalle et al.*[121], (2.1% compared to 0.7%) which likely reflects contributions occurring prior to p1 in this constitutive Cre and differences in the PDGFRβ+ population compared to the NG2+ population.

It is also possible that the PDGFRβ+ cells do not contribute to myogenesis *in vivo* with transgenic artifact resulting in aberrant reporting of myofibres in our study. This can result from the random integration of Cre expression vectors and leak activity of cell type-specific Cre expression systems[394]. This may account for 'non-true reporting' of myofibres in our study. It is also possible that the PDGFRβ+ cell contribution to myogenesis is underestimated in the transgenic mouse model. We have seen that a

very small percentage of PDGFRβ+ cells do not express the eGFP reporter in mTmG;PDGFRβ+ mice. If these were precisely those involved in myogenesis then the true contribution of these cells to myogenesis would be underestimated.

Limitations of transgenic mouse systems

The rapid increase in powerful, sophisticated mouse genetic tools has greatly facilitated cellular fate-mapping and the understanding of gene function in multiple biological processes including fibrosis. The Cre/loxP system is widely used for this purpose[395]. A major problem in pericyte biology is the lack of specific markers[246], with pericytes recognized by their position in the vasculature more than by a precise phenotype[42 396]. As such investigations using transgenic technology must be carefully designed and interpreted accordingly.

Targeting populations that do not have a specific marker

The myofibroblast is widely considered to be the key cell type responsible for regulating fibrosis through the deposition of extracellular matrix[397]. Recent research has focused on defining the origin of myofibroblasts in different organs in order to accelerate the design of targeted anti-fibrotic therapies[398]. Preventing the transition from progenitor to myofibroblasts, or even reversing this process may facilitate the treatment of fibrosis in a broad spectrum of clinical settings[399]. Many cell types have been proposed as being a source for myofibroblasts including bone-marrow derived cells[400], fibrocytes[177 401 402], epithelial cells (via epithelial-mesenchymal transition (EMT))[175 176] and tissue resident cells[179]. The lack of a specific marker to target cells using recombination based technology is a major challenge to the field.

Perivascular cells, particularly pericytes, are emerging as the key protagonists in fibrosis across all organs[398]. To target these cells we elected to use PDGFRβ-Cre because it is known to label perivascular cells of mesenchymal origin important to fibrosis in liver, lung and kidney. However, alkaline phosphatase(AP)[121], NG2[382] and ADAM12[185] have also been used to target perivascular cells. Using an AP-Cre to target pericytes Dellavalle *et al.,* demonstrated that pericytes are a minor contributor to skeletal myofibres in normal development and following injury[121]. However, AP-Cre labels a proportion of endothelial cells. To overcome this, the authors performed parallel lineage tracing experiments with a well defined marker of endothelial cells - CD31 - to confirm that any contribution to the myofibre population did not emerge from endothelial cells. NG2-Cre has also been used to target pericyte populations in skeletal muscle[382] and other organs[42]. However, NG2 is thought to label only a subset of pericytes, limiting its value as a tool for "knockdown" experiments where high population coverage is generally required to ensure that experimental phenotypes are not masked. Furthermore, NG2 is found outside the vasculature on cell types other than pericytes such as glial progenitors[403].

ADAM12 is a membrane anchored metalloproteinase, expressed in several human diseases with a fibrotic component and in a restricted fashion during development[398]. Dulauroy *et al.,* demonstrated that ADAM12 labels a distinct subset of PDGFRα perivascular progenitors with a specific pro-fibrotic fate[185]. The authors fate mapped these cells with an inducible, tetracycline transactivator based system, involving the generation of triple transgenic mice that expressed tetracycline transactivator under the control of the ADAM12 locus, Cre under control of tetracycline transactivator and the conditional reporter ROSA26$^{floxSTOP\text{-}YFP}$. In these mice, yellow fluorescent protein

(YFP) labeling of ADAM12+ progeny was temporally controlled by doxycycline administration to prevent Cre expression, allowing separate fate-mapping of fetal and adult ADAM12+ cells following CTX induced skeletal muscle injury. Using these genetic strategies and parabiosis experiments in which transgenic mice were sutured to wildtype mice, the authors demonstrated that αSMA+, collagen producing myofibroblasts developing following muscle injury descended from ADAM12+ cells. Furthermore, ablation of ADAM12+ cells in skeletal muscle (using mice that also expressed the human diphtheria toxin receptor under control of the ADAM12 locus) markedly reduced the generation of pro-fibrotic cells and interstitial accumulation. To overcome dual labeling of ADAM12+ nerve cells the authors used a mouse that expressed Cre under the control of Wnt1 promoter, crossed to YFP, to confirm that Wnt1+ nerve and Schwann cells do not contribute to the pro-fibrotic stromal population following injury. By adopting several approaches (fluorescent reports, genetic ablation, parallel labeling) the authors were able to address many of the limitations of single promoter genetic systems and provide strong support to our observations that pericytes are a major contributor to the myofibroblast population that develops in muscle scarring.

In an attempt to identify specific markers for pericytes, ongoing studies in our laboratory are using RNAseq and Lyoplate (BD Biosciences) technology. This would allow us to target pericytes for fate tracing and knockdown technology while also enabling genetic ablation using subtype specific marker CreER/DTA mice, such as done by others[207 208], to clarify the response of subtypes in response to tissue injury.

Recombination efficiency / coverage

In addition to population specificity, a number of other factors influence the choice and

applicability of Cre-drivers. PDGFRβ-Cre has been shown to have high efficiency of recombination in multiple organs[351]. While broad coverage of recombination is not essential for lineage tracing studies it is critical in knockdown experiments where residual "non-recombined" cells may compensate for those lost to recombination and mask a true phenotype. In general, conditional Cres provide less efficient recombination and a lower coverage than constitutive Cre drivers.

PDGFRβ+ perivascular cells are a principal source of myofibroblasts in skeletal muscle

While our laboratory and others have shown that PDGFRβ+ perivascular cells contribute to fibrosis in visceral organs, we are the first to confirm this in skeletal muscle. In skeletal muscle, overgrowth of fibrous tissue originates from resident progenitors exposed to environmental modification associated with injury[221 364]. To date, the literature investigating pathogenesis of skeletal muscle fibrosis has identified PDGFRα, NG2 and ADAM12 as putative markers of myofibroblast precursors. PDGFRα has been widely reported to label mesenchymal cells that proliferate early upon muscle damage to promote tissue regeneration and show fibro-adipogenic bipotential *in vitro*[217 218]. Furthermore, chronic activation of PDGFRα leads to widespread organ fibrosis in mice[404]. Using transgenic reporters of NG2 and nestin, Birbrair *et al.*, demonstrated that a population of NG2+nestin–PDGFRβ+ perivascular cells contribute to skeletal muscle fibrosis following injury and these cells have been shown to be fibrogenic *in vitro*[382]. This contribution is likely to be underestimated due to the flaws in the lineage tracing system used (knock-in rather than inducible Cre).

Dulauroy *et al.,* demonstrated that ADAM12+ cells represent a distinct subset of PDGFRα+ perivascular progenitors with a specific profibrotic fate and function in mouse models of acute muscle injury[185]. Using fluorescent lineage tracing and genetic cell ablation they elegantly demonstrated that profibrotic progenitors originate from ADAM12+ perivascular cells. The progeny of fetal ADAM12+ cells includes a subpopulation of PDGFRβ+NG2+ perivascular cells.

While PDGFRα is the most widely recognised marker of pro-fibrotic perivascular progenitors in skeletal muscle, PDGFRβ is emerging as the key marker to identify pro-fibrotic cells within other organs including liver, lungs and kidney[181 351]. While there are likely to be subtle differences in the roles of cells within different organs, it is intuitive that the mechanisms responsible for a number of common processes are conserved. As such, we sought to explore the relationship between PDGFRα and PDGFRβ within our population. We found that there was significant overlap in these populations with over 65% of PDGFRα cells expressing eGFP (PDGFRβ-Cre) (Figure 62, p193). When considering our results, the results of previous studies into skeletal muscle, and published reports in other organs four possible explanations could marry the findings. Firstly the PDGFRβ+ subset represent the pro-fibrotic component of PDGFRα+ populations. Secondly, the PDGFRα+ subset are the pro-fibrotic component of PDGFRβ+ populations. Thirdly it is feasible that only cells expressing both PDGFRα and PDGFRβ are profibrotic. Finally it may be that all cells expressing PDGFRα or PDGFRβ contribute to the myofibroblast pool following injury. We are now investigating PDGFRα+PDGFRβ-, PDGFRα+PDGFRβ+, PDGFRα-PDGFRβ+ subpopulations to characterize their contribution to fibrosis. By exploring in greater depth the relationship of the PDGFRα+ and PDGFRβ+ cells it may be possible to identify a

targetable subset of pro-fibrotic perivascular cells on which to base novel anti-fibrotic therapies.

αv integrins regulate skeletal muscle fibrosis

A number of key physiological and pathological processes (e.g inflammation) are common in organs throughout the body and it is intuitive that the processes and mechanism of fibrosis would also be shared. Our laboratory was the first to show that the specific targeting of the αv subunit in fibrogenic myofibroblasts effectively reduces developing and established fibrosis in liver, kidney and lungs[351]. We used this system to delete the integrin αv subunit because of the suggested role of multiple αv integrins as central mediators of fibrosis in multiple organs[339]: TGFβ1 is secreted in a latent form and stored in the ECM and that release of the active cytokine depends on the binding of the transmembrane integrins $\alpha_v\beta_1$, $\alpha_v\beta_3$, $\alpha_v\beta_5$, $\alpha_v\beta_6$ and $\alpha_v\beta_8$ to an arginine-glycine–aspartic acid (RGD) consensus sequence in the latent TGFβ1 complex[405]. In this thesis we found that the depletion of myofibroblast αv integrins significantly inhibited fibrosis in skeletal muscle, identifying myofibroblast αv integrins as components of a core pathway of pathological fibrosis in this tissue.

TGFβ activation in skeletal muscle – αv integrins represent a major mechanism

TGFβ1 is a member of the TGFβ superfamily, a highly conserved group of cytokines, of which there are three mammalian isoforms (TGFβ1, -β2, and -β3). TGFβ1 is a pleiotropic cytokine that is ubiquitously expressed by all cells and tissues within the body. TGFβ1 is synthesized as a small latent complex consisting of active TGF-β1

noncovalently associated with the latency associated peptide (LAP), and this is in turn is secreted in association with the latent TGFβ–binding proteins as the large latent complex. Synthesis of latent TGFβ can be increased by inflammatory mediators such as TNF-α; however, it is sequestered as an inactive molecule, which is stored in the extracellular matrix and needs to be activated before it exerts a biological effect. Activation can occur *in vitro* through physical processes such as acidification, extreme temperature changes, and oxidation. In addition TGFβ can also be activated by a number of proteases, including plasmin, tryptase, thrombin, elastase, matrix metalloproteinase (MMP)-2, and MMP-9, and by interactions with thrombospondin or integrins. However, integrins remain the only class of TGFβ activators demonstrated to exert this effect *in vivo.*

Attempts to identify αv subunit binding partners critical to skeletal muscle fibrosis

As αv integrin is served by a number of β subunits, we sought to identify a β subunit partner responsible for TGFβ1 activation in skeletal muscle. Contrasting results have been reported in different organs. In mouse lungs, deletion or blocking of the epithelial integrin αvβ6 alone is sufficient to prevent latent TGFβ1 activation and development of bleomycin induced fibrosis without inducing the side effects of global TGFβ1 inhibition[343 406]. Yet $\alpha_v\beta_6$ depletion does not protect mice from liver fibrosis[351]. In non-epithelial tissues such as heart and muscle, mesenchymal cells are thought to come into play, expressing and upregulating all of the remaining αv integrins during myofibroblast differentiation in conditions of fibrosis.

Because we found β_8 subunit to be highly expressed in injured skeletal muscle (and as a suitable transgenic mouse was available in our laboratory), we asked whether β_8 was critical to skeletal muscle fibrosis. However, we were unable to effectively inhibit skeletal muscle fibrosis by individual depletion of the β_8 subunit partner of αv. Depletion of β_8 integrins also did not protect against liver fibrosis[351]. In fact, Henderson *et al.*, found that global deletion of some individual β integrin subunits that only pair with αv integrin (such as β_3 and β_5) did not protect against fibrosis in the liver[351]. This suggests that inhibition of multiple αv containing integrins may be required to effectively treat fibrosis or that the protection seen with αv depletion was due to loss of $\alpha_v\beta_1$ (which cannot be studied with the genetic tools currently available).

Mesenchymal cells may simply use the αv integrins which they express to activate latent TGFβ1. Rapid tissue repair by TGFβ1–differentiated myofibroblasts is fundamental for organism survival, and it is conceivable that different αv integrins are redundant in their function of latent TGFβ1 activation. Mesenchymal cells can pair αv with alternative β integrin subunits thus compensating for loss of any β integrin. Indeed, different αv integrins have been shown to activate latent TGFβ1 *in vitro* either by inducing a conformational change in latent TGFβ1 through cytoskeletal force transmission[345 407] or by supporting proteolytic activation[347]. It is conceivable that different αv integrins contribute to latent TGFβ1 activation in a setting dependent manner. For instance, αvβ6 integrin may be more important for the onset of lung fibrosis upon lung epithelial injury, whereas 'mesenchymal' αv integrins drive the progression and persistence of the disease, distant from the original insult[339].

So far the evidence suggests that only TGFβ1 and TGFβ3 are activated by αv integrins, not the TGFβ2 isoform. *In vitro* all five of the αv beta subunits i.e. $\alpha_v\beta_1$, $\alpha_v\beta_3$, $\alpha_v\beta_5$, $\alpha_v\beta_6$

and $\alpha_v\beta_8$ have been shown capable of activating TGFβ1 in *in vitro* cellular assays. However, *in vivo* data points toward a prominent role for β_1, β_6 and β_8, although it may be the case that all play a role to greater or lesser extents *in vivo*.

Culture conditions influence myofibroblast activation

We have shown that the PDGFRβ+ perivascular cells spontaneously transition to a myofibroblast phenotype *in vitro*. This transition occurred in both standard basal medium (DMEM10%FCS1%PS) and EGM2, although the expression of myofibroblast markers was significantly higher in DMEM10%FCS1%PS with αSMA expression rising by a mean 431.40 (SEM 19.01) compared with the mean fold change of 33.09 (SEM 0.95) in cells cultured in EGM2 (Figure 68, p200 and Figure 69, p201).

Macroscopic tissue stiffening is a feature of fibrotic disease, and it has been shown that the mechanical properties of underlying matrix are a principal determinant of pericyte activation to a myofibroblast phenotype.[408] In studies exploring liver pericyte (hepatic stellate cell) activation, the degree rather than speed of HSC activation correlated with substrate (polyacrylamide) stiffness, with cells cultured on supports of intermediate stiffness adopting intermediate phenotypes[409]. Changes in gene expression on increasingly stiff substrate parallel those observed with myofibroblastic differentiation on plastic. The rapid myofibroblastic activation of PDGFRβ+ perivascular cells on cell culture plastic is therefore not unexpected.

During normal wound healing, coagulation of extravasated blood initiates a complex cascade of signals that recruit inflammatory cells, stimulate fibroblasts and epithelial cell proliferation, direct cell migration, and induce angiogenesis to restore tissue

integrity[410]. Increasing serum concentrations have been shown to enhance the activation toward a myofibroblast phenotype[411], although there are contradicting reports[412]. Orlova *et al.,* showed that upon culture in DMEM10% FBS, stimulation with TGFβ and stimulation with PDGF-BB for 3 days pericytes upregulated the expression of myofibroblast markers αSMA, smooth muscle specific protein 22 (SM22) and caldesmon higher than those cells cultured in EGM2[413]. It is likely that the increase in serum concentration in DMEM10%FCS1%PS (10% FCS) over EGM2 (2% FCS) is responsible for the more dramatic rise in myofibroblast markers seen in our experiments.

Fibrosis/regeneration balance

A critical point raised in this thesis is the fibrosis/regeneration balance in the function of muscle pericytes. Although neglected for many years, pericytes have recently become an intensively studied cell population in skeletal muscle biology and pathophysiology. Pericytes are being shown to fulfil increasingly diverse roles[49]. Pericytes are stromal cells that support vasculature and can become MSC. They have been shown to play a critical role in angiogenesis[246], regulation of blood flow[246], as myogenic precursors[121] and progenitors of interstitial myofibroblasts[181 351].

We and others have shown that the pericyte population in skeletal muscle is heterogeneous in terms of marker expression[414 415]. Although their functional diversity is still unexplored, different pericyte subtypes may regulate each of the many demonstrated functions[416]. We have demonstrated that PDGFRβ + perivascular cells contribute to skeletal muscle regeneration by becoming myofibres, while also demonstrating their capacity to differentiate into myofibroblasts contributing to

fibrosis. While it is feasible that all pericytes are capable of fulfilling each and every one of these functions it appears more likely that pericyte subsets exist that are committed to fibrosis or the regenerative response.

Pericytes have been classically subdivided in two groups based on their ontogeny: during development, most of them derive from the mesoderm[417-420], while brain and thymus pericytes derive from the ectoderm[421-425]. However, with increasing evidence suggesting their phenotypic heterogeneity, attempts are being made to identify functionally distinct subsets. Using NG2DsRed nestinYFP knock-in reporters, Birbrair *et al.,* identified two subtypes of pericytes based on the expression of Nestin and NG2. In their classification Type 1 pericytes (NG2+nestin+) contributed to fibrosis in skeletal muscle while type 2 pericytes (NG2+nestin-) did not. However, this study provides limited insight as type 2 pericytes may have contributed to fibrosis by becoming NG2- myofibroblasts that would therefore no longer report DsRed[382]. In a further study utilising similar genetic systems, Birbrair *et al.,* showed that in skeletal muscle, only the subset of type 1 pericytes that is not involved in myogenesis produces collagen, thus contributing to fibrous tissue deposition in older mice[382].

In contrast to the dominant role of pericytes in skin, liver, and skeletal muscle fibrosis[185 426] their contribution to fibrous tissue formation in other organs remains controversial. Some kidney and lung studies show important participation[181 427]; others do not[180 428]. Variations in the results of reported studies may reflect the use of different mouse models, the small percentage of cells undergoing recombination in some studies, and pericyte markers expressed by other cells such as fibroblasts. Differing contributions of pericytes to fibrosis and regeneration between organs may also reflect differences in the proportions of functionally distinct pericyte subtypes. In future work

I aim to further clarify the differences in the roles of pericyte subtypes, so they can be used as increasingly specific cellular targets susceptible to pharmacological manipulation.

Strengths and limitations of the CTX model

To investigate the response to muscle injury and the basis of fibrosis we used cardiotoxin (CTX) to acutely injure the tibialis anterior (TA) muscles of mice. CTX administration induces local muscle necrosis, which is rapidly followed by recruitment of inflammatory cells, clearance of cellular debris and regeneration of injured muscle[218]. Information regarding the mechanistic basis for muscle injury and fibrosis has generally been obtained from studies using CTX, barium chloride (BaCl2) or notoxin. The CTX model is extremely simple and highly reproducible[216 380] and is emerging as the method of choice for producing injury in high impact publications investigating regeneration and fibrosis in skeletal muscle[14 215 216 360]. In particular the reproducibility of this model allows the detection of subtle phenotypes. However, whether the events that ensue following this extreme injury reflect the precise adaptions that occur in clinical injury has not been established[429].

Adult skeletal muscle possesses a remarkable regenerative ability and it has been argued by some that skeletal muscle regenerates almost completely without development of fibrotic scar tissue after CTX injury[430 431], and that this model reflects a reversible repair process rather than irreversible fibrosis[432]. However, we found that elevated ECM and disordered structure persist even at 60 days post CTX injection. In addition, fibrosis and disordered architecture is recognised following single acute muscle injury in human populations, such as sports injuries or surgical incisions[433 434].

In conditions of chronic injury, as occurs in muscular dystrophies, chronic inflammatory events result in the excessive accumulation of ECM components, which inhibit myogenic repair and lead to muscle being replaced by fibrotic/scar tissue[192]. In order to achieve a more dramatic phenotype I would like to repeat the experiments in dystrophic mice in future studies. The dramatic phenotype may then be amenable to functional testing and would confirm our findings in another setting of fibrosis.

Limitations of fibrosis quantification methods

The precise quantification of skeletal muscle fibrosis can be difficult. Typically, skeletal muscle assays quantify the cross-sectional area fraction of ECM by excluding muscle fibres using image-processing tools reporting the amount of ECM as 'area fraction'. Frequently, a number of arbitrary fields are selected from within a muscle section of each biological replicate. In order to minimise bias, we used a stereology microscope to select random fields within the injured area. Although the area of injury was carefully selected on the basis of centralisation of nuclei and myofibre size, this semi-quantitive method could theoretically introduce bias.

A further limitation of this approach is that if muscle fibres atrophy and ECM remain the same, ECM will occupy a greater fraction of the muscle cross section. This approach also gives no information about isoforms and cross-linking, which can also affect function. For normal muscle the ECM area fraction is typically below 5%, but this value can increase dramatically in diseased or injured states. In addition to the increased fractional area of ECM in fibrotic muscles, because the pathological response

often includes fibre degeneration and regeneration, muscle fibrosis is also accompanied by a large increase in muscle fibre size variation.

Skeletal muscle fibrosis can also be expressed in terms of the total amount of collagen present in the tissue, as measured by the content of hydroxyproline, a major component of collagen derived from hydroxylation of the amino acid proline by prolyloxidase. While this assay has been used for many years, expression of collagen mass relative to a known muscle protein is only rarely reported.

Functional assessment of muscle function

The primary function of skeletal muscle is to generate force. Muscle force is compromised in various forms of acquired and or inherited muscle diseases. An important goal of muscle therapies is to recover muscle strength. Methods for measuring murine muscle function include *ex-vivo* and *in-situ* analysis of the contractile profile of a single intact limb muscle, grip force and downhill treadmill exercise. *Ex-vivo* force measurement in a single muscle is extremely useful for analysis following discrete injury while grip force and treadmill assessment offer body wide evaluation of global muscle health.

In future studies I would like to incorporate functional assessment of muscle fibrosis, although this would be challenging using the CTX model used in this thesis. The degree of fibrosis seen following a single CTX injection is considerably lower than those seen with dystrophic muscle or chronic inflammation and the notoriously insensitive *in vivo* functional assessments may not pick up small yet significant differences seen on histological examination. Furthermore the tibialis anterior muscle

is difficult to functionally isolate with surrounding muscle groups compensating for reduced function even in severe fibrosis. This was illustrated by the mices' ability to walk without sign of injury only 48 h following CTX injection.

Conclusions – perivascular cells at the crossroads of tissue regeneration and pathology

The capacity for pericytes to play so many diverse roles in normal development and the response to injury highlights the complexity that underlies their regulation. Their roles in disease processes are increasingly appreciated, with pathological activation of the mesenchymal and fibroblastic phenotypes emerging as key themes in disease of skeletal muscle and other organs. Understanding how the expression of pericyte potentials is regulated within the perivascular niche will facilitate the development of therapeutic strategies to treat a wide range of skeletal muscle diseases including heterotopic ossification and fibrosis.

In addition to targeting the pathological behaviour of pericytes in disease, the regenerative capacities of pericytes holds great promise for regenerative medicine and tissue engineering. The work in this thesis has highlighted the diverse pathways involved in pericyte regulation, and the broad range of functions skeletal muscle pericytes display in both health and disease. The heterogeneity of pericyte populations is increasingly appreciated and the discovery of distinct "specialist" subsets of pericytes primarily responsible for each of the many biological roles described will facilitate the discovery of highly targeted therapies in the future.

References

1. Thomson JA, Itskovitz-Eldor J, Shapiro SS, Waknitz MA, Swiergiel JJ, Marshall VS, et al. Embryonic stem cell lines derived from human blastocysts. *Science* 1998;282(5391):1145-7.
2. Robinton DA, Daley GQ. The promise of induced pluripotent stem cells in research and therapy. *Nature* 2012;481(7381):295-305.
3. Friedenstein AJ, Chailakhjan RK, Lalykina KS. The development of fibroblast colonies in monolayer cultures of guinea-pig bone marrow and spleen cells. *Cell Tissue Kinet* 1970;3(4):393-403.
4. Friedenstein AJ, Chailakhyan RK, Latsinik NV, Panasyuk AF, Keiliss-Borok IV. Stromal cells responsible for transferring the microenvironment of the hemopoietic tissues. Cloning in vitro and retransplantation in vivo. *Transplantation* 1974;17(4):331-40.
5. Friedenstein AJ, Piatetzky S, II, Petrakova KV. Osteogenesis in transplants of bone marrow cells. *J Embryol Exp Morphol* 1966;16(3):381-90.
6. Owen M, Friedenstein AJ. Stromal stem cells: marrow-derived osteogenic precursors. *Ciba Found Symp* 1988;136:42-60.
7. Bianco P, Robey PG, Simmons PJ. Mesenchymal stem cells: revisiting history, concepts, and assays. *Cell Stem Cell* 2008;2(4):313-9.
8. Pittenger MF, Mackay AM, Beck SC, Jaiswal RK, Douglas R, Mosca JD, et al. Multilineage potential of adult human mesenchymal stem cells. *Science* 1999;284(5411):143-7.
9. Kolf CM, Cho E, Tuan RS. Mesenchymal stromal cells. Biology of adult mesenchymal stem cells: regulation of niche, self-renewal and differentiation. *Arthritis Res Ther* 2007;9(1):204.
10. Caplan AI. Adult mesenchymal stem cells for tissue engineering versus regenerative medicine. *J Cell Physiol* 2007;213(2):341-7.
11. Caplan AI. Mesenchymal stem cells. *J Orthop Res* 1991;9(5):641-50.
12. Zuk PA, Zhu M, Ashjian P, De Ugarte DA, Huang JI, Mizuno H, et al. Human adipose tissue is a source of multipotent stem cells. *Mol Biol Cell* 2002;13(12):4279-95.
13. Xu Y, Malladi P, Wagner DR, Longaker MT. Adipose-derived mesenchymal cells as a potential cell source for skeletal regeneration. *Curr Opin Mol Ther* 2005;7(4):300-5.
14. Crisan M, Yap S, Casteilla L, Chen CW, Corselli M, Park TS, et al. A perivascular origin for mesenchymal stem cells in multiple human organs. *Cell Stem Cell* 2008;3(3):301-13.
15. Asakura A, Komaki M, Rudnicki M. Muscle satellite cells are multipotential stem cells that exhibit myogenic, osteogenic, and adipogenic differentiation. *Differentiation* 2001;68(4-5):245-53.
16. Tsutsumi S, Shimazu A, Miyazaki K, Pan H, Koike C, Yoshida E, et al. Retention of multilineage differentiation potential of mesenchymal cells during proliferation in response to FGF. *Biochem Biophys Res Commun* 2001;288(2):413-9.
17. Kulterer B, Friedl G, Jandrositz A, Sanchez-Cabo F, Prokesch A, Paar C, et al. Gene expression profiling of human mesenchymal stem cells derived from bone marrow during expansion and osteoblast differentiation. *BMC Genomics* 2007;8:70.
18. Pochampally RR, Smith JR, Ylostalo J, Prockop DJ. Serum deprivation of human marrow stromal cells (hMSCs) selects for a subpopulation of early progenitor

cells with enhanced expression of OCT-4 and other embryonic genes. *Blood* 2004;103(5):1647-52.
19. Hishikawa K, Miura S, Marumo T, Yoshioka H, Mori Y, Takato T, et al. Gene expression profile of human mesenchymal stem cells during osteogenesis in three-dimensional thermoreversible gelation polymer. *Biochem Biophys Res Commun* 2004;317(4):1103-7.
20. Kratchmarova I, Blagoev B, Haack-Sorensen M, Kassem M, Mann M. Mechanism of divergent growth factor effects in mesenchymal stem cell differentiation. *Science* 2005;308(5727):1472-7.
21. Song L, Webb NE, Song Y, Tuan RS. Identification and functional analysis of candidate genes regulating mesenchymal stem cell self-renewal and multipotency. *Stem Cells* 2006;24(7):1707-18.
22. da Silva Meirelles L, Chagastelles PC, Nardi NB. Mesenchymal stem cells reside in virtually all post-natal organs and tissues. *J Cell Sci* 2006;119(Pt 11):2204-13.
23. Covas DT, Panepucci RA, Fontes AM, Silva WA, Jr., Orellana MD, Freitas MC, et al. Multipotent mesenchymal stromal cells obtained from diverse human tissues share functional properties and gene-expression profile with CD146+ perivascular cells and fibroblasts. *Experimental hematology* 2008;36(5):642-54.
24. De Bari C, Dell'Accio F, Tylzanowski P, Luyten FP. Multipotent mesenchymal stem cells from adult human synovial membrane. *Arthritis Rheum* 2001;44(8):1928-42.
25. Salingcarnboriboon R, Yoshitake H, Tsuji K, Obinata M, Amagasa T, Nifuji A, et al. Establishment of tendon-derived cell lines exhibiting pluripotent mesenchymal stem cell-like property. *Exp Cell Res* 2003;287(2):289-300.
26. Bi Y, Ehirchiou D, Kilts TM, Inkson CA, Embree MC, Sonoyama W, et al. Identification of tendon stem/progenitor cells and the role of the extracellular matrix in their niche. *Nat Med* 2007;13(10):1219-27.
27. Rogers I, Casper RF. Umbilical cord blood stem cells. *Best Pract Res Clin Obstet Gynaecol* 2004;18(6):893-908.
28. Shi S, Gronthos S. Perivascular niche of postnatal mesenchymal stem cells in human bone marrow and dental pulp. *J Bone Miner Res* 2003;18(4):696-704.
29. Seo BM, Miura M, Gronthos S, Bartold PM, Batouli S, Brahim J, et al. Investigation of multipotent postnatal stem cells from human periodontal ligament. *Lancet* 2004;364(9429):149-55.
30. Tsai MS, Lee JL, Chang YJ, Hwang SM. Isolation of human multipotent mesenchymal stem cells from second-trimester amniotic fluid using a novel two-stage culture protocol. *Hum Reprod* 2004;19(6):1450-6.
31. Toma JG, Akhavan M, Fernandes KJ, Barnabe-Heider F, Sadikot A, Kaplan DR, et al. Isolation of multipotent adult stem cells from the dermis of mammalian skin. *Nat Cell Biol* 2001;3(9):778-84.
32. Igura K, Zhang X, Takahashi K, Mitsuru A, Yamaguchi S, Takashi TA. Isolation and characterization of mesenchymal progenitor cells from chorionic villi of human placenta. *Cytotherapy* 2004;6(6):543-53.
33. Dominici M, Le Blanc K, Mueller I, Slaper-Cortenbach I, Marini F, Krause D, et al. Minimal criteria for defining multipotent mesenchymal stromal cells. The International Society for Cellular Therapy position statement. *Cytotherapy* 2006;8(4):315-7.
34. Peister A, Mellad JA, Larson BL, Hall BM, Gibson LF, Prockop DJ. Adult stem cells from bone marrow (MSCs) isolated from different strains of inbred mice vary in surface epitopes, rates of proliferation, and differentiation potential. *Blood* 2004;103(5):1662-8.

35. Dexter TM, Allen TD, Lajtha LG. Conditions controlling the proliferation of haemopoietic stem cells in vitro. *J Cell Physiol* 1977;91(3):335-44.
36. Simmons PJ, Torok-Storb B. Identification of stromal cell precursors in human bone marrow by a novel monoclonal antibody, STRO-1. *Blood* 1991;78(1):55-62.
37. Dennis JE, Carbillet JP, Caplan AI, Charbord P. The STRO-1+ marrow cell population is multipotential. *Cells Tissues Organs* 2002;170(2-3):73-82.
38. Devine SM, Bartholomew AM, Mahmud N, Nelson M, Patil S, Hardy W, et al. Mesenchymal stem cells are capable of homing to the bone marrow of non-human primates following systemic infusion. *Exp Hematol* 2001;29(2):244-55.
39. In 't Anker PS, Scherjon SA, Kleijburg-van der Keur C, Noort WA, Claas FH, Willemze R, et al. Amniotic fluid as a novel source of mesenchymal stem cells for therapeutic transplantation. *Blood* 2003;102(4):1548-9.
40. Bensidhoum M, Chapel A, Francois S, Demarquay C, Mazurier C, Fouillard L, et al. Homing of in vitro expanded Stro-1- or Stro-1+ human mesenchymal stem cells into the NOD/SCID mouse and their role in supporting human CD34 cell engraftment. *Blood* 2004;103(9):3313-9.
41. Farrington-Rock C, Crofts NJ, Doherty MJ, Ashton BA, Griffin-Jones C, Canfield AE. Chondrogenic and adipogenic potential of microvascular pericytes. *Circulation* 2004;110(15):2226-32.
42. Feng J, Mantesso A, De Bari C, Nishiyama A, Sharpe PT. Dual origin of mesenchymal stem cells contributing to organ growth and repair. *Proc Natl Acad Sci U S A* 2011;108(16):6503-8.
43. Sims DE. The pericyte--a review. *Tissue Cell* 1986;18(2):153-74.
44. Diaz-Flores L, Martin Herrera AI, Garcia Montelongo R, Gutierrez Garcia R. Role of pericytes and endothelial cells in tissue repair and related pathological processes. *Journal of cutaneous pathology* 1990;17(3):191-2.
45. Savvatis K, van Linthout S, Miteva K, Pappritz K, Westermann D, Schefold JC, et al. Mesenchymal stromal cells but not cardiac fibroblasts exert beneficial systemic immunomodulatory effects in experimental myocarditis. *PLoS ONE* 2012;7(7):e41047.
46. Jia Z, Jiao C, Zhao S, Li X, Ren X, Zhang L, et al. Immunomodulatory effects of mesenchymal stem cells in a rat corneal allograft rejection model. *Exp Eye Res* 2012;102:44-9.
47. Nauta AJ, Fibbe WE. Immunomodulatory properties of mesenchymal stromal cells. *Blood* 2007;110(10):3499-506.
48. Krampera M, Cosmi L, Angeli R, Pasini A, Liotta F, Andreini A, et al. Role for interferon-gamma in the immunomodulatory activity of human bone marrow mesenchymal stem cells. *Stem Cells* 2006;24(2):386-98.
49. Caplan AI, Correa D. The MSC: an injury drugstore. *Cell Stem Cell* 2011;9(1):11-5.
50. Aggarwal S, Pittenger MF. Human mesenchymal stem cells modulate allogeneic immune cell responses. *Blood* 2005;105(4):1815-22.
51. Dai W, Hale SL, Martin BJ, Kuang JQ, Dow JS, Wold LE, et al. Allogeneic mesenchymal stem cell transplantation in postinfarcted rat myocardium: short- and long-term effects. *Circulation* 2005;112(2):214-23.
52. Noiseux N, Gnecchi M, Lopez-Ilasaca M, Zhang L, Solomon SD, Deb A, et al. Mesenchymal stem cells overexpressing Akt dramatically repair infarcted myocardium and improve cardiac function despite infrequent cellular fusion or differentiation. *Mol Ther* 2006;14(6):840-50.
53. Kinnaird T, Stabile E, Burnett MS, Shou M, Lee CW, Barr S, et al. Local delivery of marrow-derived stromal cells augments collateral perfusion through paracrine mechanisms. *Circulation* 2004;109(12):1543-9.

54. Gnecchi M, He H, Liang OD, Melo LG, Morello F, Mu H, et al. Paracrine action accounts for marked protection of ischemic heart by Akt-modified mesenchymal stem cells. *Nat Med* 2005;11(4):367-8.
55. Caplan AI, Dennis JE. Mesenchymal stem cells as trophic mediators. *Journal of cellular biochemistry* 2006;98(5):1076-84.
56. Prockop DJ. Marrow stromal cells as stem cells for nonhematopoietic tissues. *Science* 1997;276(5309):71-4.
57. Baksh D, Song L, Tuan RS. Adult mesenchymal stem cells: characterization, differentiation, and application in cell and gene therapy. *J Cell Mol Med* 2004;8(3):301-16.
58. Schafer R, Dominici M, Muller I, Dazzi F, Bieback K, Godthardt K, et al. Progress in characterization, preparation and clinical applications of non-hematopoietic stem cells, 29-30 September 2006, Tubingen, Germany. *Cytotherapy* 2007;9(4):397-405.
59. Ratajczak MZ, Zuba-Surma EK, Wysoczynski M, Wan W, Ratajczak J, Wojakowski W, et al. Hunt for pluripotent stem cell -- regenerative medicine search for almighty cell. *J Autoimmun* 2008;30(3):151-62.
60. Jiang Y, Jahagirdar BN, Reinhardt RL, Schwartz RE, Keene CD, Ortiz-Gonzalez XR, et al. Pluripotency of mesenchymal stem cells derived from adult marrow. *Nature* 2002;418(6893):41-9.
61. D'Ippolito G, Diabira S, Howard GA, Menei P, Roos BA, Schiller PC. Marrow-isolated adult multilineage inducible (MIAMI) cells, a unique population of postnatal young and old human cells with extensive expansion and differentiation potential. *J Cell Sci* 2004;117(Pt 14):2971-81.
62. Beltrami AP, Cesselli D, Bergamin N, Marcon P, Rigo S, Puppato E, et al. Multipotent cells can be generated in vitro from several adult human organs (heart, liver, and bone marrow). *Blood* 2007;110(9):3438-46.
63. Bellantuono I, Aldahmash A, Kassem M. Aging of marrow stromal (skeletal) stem cells and their contribution to age-related bone loss. *Biochim Biophys Acta* 2009;1792(4):364-70.
64. Devine SM, Cobbs C, Jennings M, Bartholomew A, Hoffman R. Mesenchymal stem cells distribute to a wide range of tissues following systemic infusion into nonhuman primates. *Blood* 2003;101(8):2999-3001.
65. Mohanty ST, Bellantuono I. Intra-femoral injection of human mesenchymal stem cells. *Methods Mol Biol* 2013;976:131-41.
66. Mohanty ST, Cairney CJ, Chantry AD, Madan S, Fernandes JA, Howe SJ, et al. A small molecule modulator of prion protein increases human mesenchymal stem cell lifespan, ex vivo expansion, and engraftment to bone marrow in NOD/SCID mice. *Stem Cells* 2012;30(6):1134-43.
67. Ratajczak MZ, Zuba-Surma EK, Machalinski B, Kucia M. Bone-marrow-derived stem cells--our key to longevity? *J Appl Genet* 2007;48(4):307-19.
68. Rojewski MT, Weber BM, Schrezenmeier H. Phenotypic Characterization of Mesenchymal Stem Cells from Various Tissues. *Transfus Med Hemother* 2008;35(3):168-84.
69. Lindner U, Kramer J, Behrends J, Driller B, Wendler NO, Boehrnsen F, et al. Improved proliferation and differentiation capacity of human mesenchymal stromal cells cultured with basement-membrane extracellular matrix proteins. *Cytotherapy* 2010;12(8):992-1005.
70. Jones EA, Kinsey SE, English A, Jones RA, Straszynski L, Meredith DM, et al. Isolation and characterization of bone marrow multipotential mesenchymal progenitor cells. *Arthritis Rheum* 2002;46(12):3349-60.

71. Levi B, Wan DC, Glotzbach JP, Hyun J, Januszyk M, Montoro D, et al. CD105 Protein Depletion Enhances Human Adipose-derived Stromal Cell Osteogenesis through Reduction of Transforming Growth Factor beta1 (TGF-beta1) Signaling. *J Biol Chem* 2011;286(45):39497-509.
72. Quirici N, Soligo D, Bossolasco P, Servida F, Lumini C, Deliliers GL. Isolation of bone marrow mesenchymal stem cells by anti-nerve growth factor receptor antibodies. *Exp Hematol* 2002;30(7):783-91.
73. Meyerrose TE, De Ugarte DA, Hofling AA, Herrbrich PE, Cordonnier TD, Shultz LD, et al. In vivo distribution of human adipose-derived mesenchymal stem cells in novel xenotransplantation models. *Stem Cells* 2007;25(1):220-7.
74. Daquinag AC, Zhang Y, Amaya-Manzanares F, Simmons PJ, Kolonin MG. An isoform of decorin is a resistin receptor on the surface of adipose progenitor cells. *Cell Stem Cell* 2011;9(1):74-86.
75. Mariotti E, Mirabelli P, Abate G, Schiattarella M, Martinelli P, Fortunato G, et al. Comparative characteristics of mesenchymal stem cells from human bone marrow and placenta: CD10, CD49d, and CD56 make a difference. *Stem Cells Dev* 2008;17(6):1039-41.
76. Gronthos S, Franklin DM, Leddy HA, Robey PG, Storms RW, Gimble JM. Surface protein characterization of human adipose tissue-derived stromal cells. *J Cell Physiol* 2001;189(1):54-63.
77. Niehage C, Steenblock C, Pursche T, Bornhauser M, Corbeil D, Hoflack B. The cell surface proteome of human mesenchymal stromal cells. *PLoS One* 2011;6(5):e20399.
78. Gimble JM, Katz AJ, Bunnell BA. Adipose-derived stem cells for regenerative medicine. *Circ Res* 2007;100(9):1249-60.
79. Brooke G, Tong H, Levesque JP, Atkinson K. Molecular trafficking mechanisms of multipotent mesenchymal stem cells derived from human bone marrow and placenta. *Stem Cells Dev* 2008;17(5):929-40.
80. Dar A, Domev H, Ben-Yosef O, Tzukerman M, Zeevi-Levin N, Novak A, et al. Multipotent vasculogenic pericytes from human pluripotent stem cells promote recovery of murine ischemic limb. *Circulation* 2012;125(1):87-99.
81. Tallone T, Realini C, Bohmler A, Kornfeld C, Vassalli G, Moccetti T, et al. Adult human adipose tissue contains several types of multipotent cells. *J Cardiovasc Transl Res* 2011;4(2):200-10.
82. Zimmerlin L, Donnenberg VS, Rubin JP, Donnenberg AD. Mesenchymal markers on human adipose stem/progenitor cells. *Cytometry A* 2013;83(1):134-40.
83. Corselli M, Chen CW, Sun B, Yap S, Rubin JP, Peault B. The tunica adventitia of human arteries and veins as a source of mesenchymal stem cells. *Stem Cells Dev* 2012;21(8):1299-308.
84. Kern S, Eichler H, Stoeve J, Kluter H, Bieback K. Comparative analysis of mesenchymal stem cells from bone marrow, umbilical cord blood, or adipose tissue. *Stem Cells* 2006;24(5):1294-301.
85. Corselli M, Chen CW, Crisan M, Lazzari L, Peault B. Perivascular ancestors of adult multipotent stem cells. *Arterioscler Thromb Vasc Biol* 2010;30(6):1104-9.
86. Zimmerlin L, Donnenberg VS, Pfeifer ME, Meyer EM, Peault B, Rubin JP, et al. Stromal vascular progenitors in adult human adipose tissue. *Cytometry A* 2010;77(1):22-30.
87. Psaltis PJ, Harbuzariu A, Delacroix S, Holroyd EW, Simari RD. Resident vascular progenitor cells--diverse origins, phenotype, and function. *J Cardiovasc Transl Res* 2011;4(2):161-76.

88. Zannettino AC, Paton S, Arthur A, Khor F, Itescu S, Gimble JM, et al. Multipotential human adipose-derived stromal stem cells exhibit a perivascular phenotype in vitro and in vivo. *J Cell Physiol* 2008;214(2):413-21.
89. Buhring HJ, Battula VL, Treml S, Schewe B, Kanz L, Vogel W. Novel markers for the prospective isolation of human MSC. *Ann N Y Acad Sci* 2007;1106:262-71.
90. Katz AJ, Tholpady A, Tholpady SS, Shang H, Ogle RC. Cell surface and transcriptional characterization of human adipose-derived adherent stromal (hADAS) cells. *Stem Cells* 2005;23(3):412-23.
91. Mitchell JB, McIntosh K, Zvonic S, Garrett S, Floyd ZE, Kloster A, et al. Immunophenotype of human adipose-derived cells: temporal changes in stromal-associated and stem cell-associated markers. *Stem Cells* 2006;24(2):376-85.
92. Kilroy GE, Foster SJ, Wu X, Ruiz J, Sherwood S, Heifetz A, et al. Cytokine profile of human adipose-derived stem cells: expression of angiogenic, hematopoietic, and pro-inflammatory factors. *J Cell Physiol* 2007;212(3):702-9.
93. De Ugarte DA, Alfonso Z, Zuk PA, Elbarbary A, Zhu M, Ashjian P, et al. Differential expression of stem cell mobilization-associated molecules on multi-lineage cells from adipose tissue and bone marrow. *Immunol Lett* 2003;89(2-3):267-70.
94. Vogel W, Grunebach F, Messam CA, Kanz L, Brugger W, Buhring HJ. Heterogeneity among human bone marrow-derived mesenchymal stem cells and neural progenitor cells. *Haematologica* 2003;88(2):126-33.
95. Mihu CM, Mihu D, Costin N, Rus Ciuca D, Susman S, Ciortea R. Isolation and characterization of stem cells from the placenta and the umbilical cord. *Romanian journal of morphology and embryology = Revue roumaine de morphologie et embryologie* 2008;49(4):441-6.
96. Bottai D, Cigognini D, Nicora E, Moro M, Grimoldi MG, Adami R, et al. Third trimester amniotic fluid cells with the capacity to develop neural phenotypes and with heterogeneity among sub-populations. *Restorative neurology and neuroscience* 2012;30(1):55-68.
97. Kuci S, Kuci Z, Kreyenberg H, Deak E, Putsch K, Huenecke S, et al. CD271 antigen defines a subset of multipotent stromal cells with immunosuppressive and lymphohematopoietic engraftment-promoting properties. *Haematologica* 2010;95(4):651-9.
98. Battula VL, Treml S, Bareiss PM, Gieseke F, Roelofs H, de Zwart P, et al. Isolation of functionally distinct mesenchymal stem cell subsets using antibodies against CD56, CD271, and mesenchymal stem cell antigen-1. *Haematologica* 2009;94(2):173-84.
99. Nichols JE, Niles JA, Dewitt D, Prough D, Parsley M, Vega S, et al. Neurogenic and neuro-protective potential of a novel subpopulation of peripheral blood-derived CD133+ ABCG2+CXCR4+ mesenchymal stem cells: development of autologous cell based therapeutics for traumatic brain injury. *Stem cell research & therapy* 2013;4(1):3.
100. Russell KC, Phinney DG, Lacey MR, Barrilleaux BL, Meyertholen KE, O'Connor KC. In vitro high-capacity assay to quantify the clonal heterogeneity in trilineage potential of mesenchymal stem cells reveals a complex hierarchy of lineage commitment. *Stem Cells* 2010;28(4):788-98.
101. Watt FM, Hogan BL. Out of Eden: stem cells and their niches. *Science* 2000;287(5457):1427-30.
102. Kunisaki Y, Frenette PS. The secrets of the bone marrow niche: Enigmatic niche brings challenge for HSC expansion. *Nat Med* 2012;18(6):864-5.
103. Braun KM, Niemann C, Jensen UB, Sundberg JP, Silva-Vargas V, Watt FM. Manipulation of stem cell proliferation and lineage commitment: visualisation

of label-retaining cells in wholemounts of mouse epidermis. *Development* 2003;130(21):5241-55.
104. Gould E, Reeves AJ, Graziano MS, Gross CG. Neurogenesis in the neocortex of adult primates. *Science* 1999;286(5439):548-52.
105. da Silva Meirelles L, Caplan AI, Nardi NB. In search of the in vivo identity of mesenchymal stem cells. *Stem Cells* 2008;26(9):2287-99.
106. Rochefort GY, Delorme B, Lopez A, Herault O, Bonnet P, Charbord P, et al. Multipotential mesenchymal stem cells are mobilized into peripheral blood by hypoxia. *Stem Cells* 2006;24(10):2202-8.
107. Lazarus HM, Haynesworth SE, Gerson SL, Caplan AI. Human bone marrow-derived mesenchymal (stromal) progenitor cells (MPCs) cannot be recovered from peripheral blood progenitor cell collections. *J Hematother* 1997;6(5):447-55.
108. Wexler SA, Donaldson C, Denning-Kendall P, Rice C, Bradley B, Hows JM. Adult bone marrow is a rich source of human mesenchymal 'stem' cells but umbilical cord and mobilized adult blood are not. *Br J Haematol* 2003;121(2):368-74.
109. Bianco P, Riminucci M, Gronthos S, Robey PG. Bone marrow stromal stem cells: nature, biology, and potential applications. *Stem Cells* 2001;19(3):180-92.
110. Crisan M. A perivascular origin for mesenchymal stem cells in multiple human organs. *Cell Stem Cell* 2008.
111. James AW, Zara JN, Corselli M, Chiang M, Yuan W, Nguyen V, et al. Use of human perivascular stem cells for bone regeneration. *J Vis Exp* 2012(63):e2952.
112. James AW, Zara JN, Corselli M, Askarinam A, Zhou AM, Hourfar A, et al. An abundant perivascular source of stem cells for bone tissue engineering. *Stem cells translational medicine* 2012;1(9):673-84.
113. Zimmerlin L, Donnenberg VS, Rubin JP, Donnenberg AD. Mesenchymal markers on human adipose stem/progenitor cells. *Cytometry. Part A : the journal of the International Society for Analytical Cytology* 2012.
114. Crisan M, Chen CW, Corselli M, Andriolo G, Lazzari L, Peault B. Perivascular multipotent progenitor cells in human organs. *Ann N Y Acad Sci* 2009;1176:118-23.
115. Park TS, Gavina M, Chen CW, Sun B, Teng PN, Huard J, et al. Placental perivascular cells for human muscle regeneration. *Stem Cells Dev* 2011;20(3):451-63.
116. Tu Z, Li Y, Smith DS, Sheibani N, Huang S, Kern T, et al. Retinal pericytes inhibit activated T cell proliferation. *Investigative ophthalmology & visual science* 2011;52(12):9005-10.
117. Maier CL, Pober JS. Human placental pericytes poorly stimulate and actively regulate allogeneic CD4 T cell responses. *Arteriosclerosis, thrombosis, and vascular biology* 2011;31(1):183-9.
118. Tottey S, Corselli M, Jeffries EM, Londono R, Peault B, Badylak SF. Extracellular matrix degradation products and low-oxygen conditions enhance the regenerative potential of perivascular stem cells. *Tissue Eng Part A* 2011;17(1-2):37-44.
119. Beck B, Driessens G, Goossens S, Youssef KK, Kuchnio A, Caauwe A, et al. A vascular niche and a VEGF-Nrp1 loop regulate the initiation and stemness of skin tumours. *Nature* 2011;478(7369):399-403.
120. Dellavalle A, Sampaolesi M, Tonlorenzi R, Tagliafico E, Sacchetti B, Perani L, et al. Pericytes of human skeletal muscle are myogenic precursors distinct from satellite cells. *Nat Cell Biol* 2007;9(3):255-67.
121. Dellavalle A, Maroli G, Covarello D, Azzoni E, Innocenzi A, Perani L, et al. Pericytes resident in postnatal skeletal muscle differentiate into muscle fibres and generate satellite cells. *Nat Commun* 2011;2:499.

122. Hoshino A, Chiba H, Nagai K, Ishii G, Ochiai A. Human vascular adventitial fibroblasts contain mesenchymal stem/progenitor cells. *Biochem Biophys Res Commun* 2008;368(2):305-10.
123. Sartore S, Chiavegato A, Faggin E, Franch R, Puato M, Ausoni S, et al. Contribution of adventitial fibroblasts to neointima formation and vascular remodeling: from innocent bystander to active participant. *Circ Res* 2001;89(12):1111-21.
124. Siow RC, Mallawaarachchi CM, Weissberg PL. Migration of adventitial myofibroblasts following vascular balloon injury: insights from in vivo gene transfer to rat carotid arteries. *Cardiovasc Res* 2003;59(1):212-21.
125. Hu Y, Zhang Z, Torsney E, Afzal AR, Davison F, Metzler B, et al. Abundant progenitor cells in the adventitia contribute to atherosclerosis of vein grafts in ApoE-deficient mice. *J Clin Invest* 2004;113(9):1258-65.
126. Haurani MJ, Pagano PJ. Adventitial fibroblast reactive oxygen species as autacrine and paracrine mediators of remodeling: bellwether for vascular disease? *Cardiovasc Res* 2007;75(4):679-89.
127. Herrmann J, Samee S, Chade A, Rodriguez Porcel M, Lerman LO, Lerman A. Differential effect of experimental hypertension and hypercholesterolemia on adventitial remodeling. *Arterioscler Thromb Vasc Biol* 2005;25(2):447-53.
128. Stenmark KR, Davie N, Frid M, Gerasimovskaya E, Das M. Role of the adventitia in pulmonary vascular remodeling. *Physiology (Bethesda)* 2006;21:134-45.
129. Caplan AI. All MSCs are pericytes? *Cell Stem Cell* 2008;3(3):229-30.
130. Corselli M, Chen CW, Sun B, Yap S, Rubin JP, B PA. The Tunica Adventitia of Human Arteries and Veins as a Source of Mesenchymal Stem Cells. *Stem Cells Dev* 2011.
131. Chen CW, Montelatici E, Crisan M, Corselli M, Huard J, Lazzari L, et al. Perivascular multi-lineage progenitor cells in human organs: regenerative units, cytokine sources or both? *Cytokine Growth Factor Rev* 2009;20(5-6):429-34.
132. Paredes B, Santana A, Arribas MI, Vicente-Salar N, de Aza PN, Roche E, et al. Phenotypic differences during the osteogenic differentiation of single cell-derived clones isolated from human lipoaspirates. *Journal of tissue engineering and regenerative medicine* 2010.
133. Muller AM, Mehrkens A, Schafer DJ, Jaquiery C, Guven S, Lehmicke M, et al. Towards an intraoperative engineering of osteogenic and vasculogenic grafts from the stromal vascular fraction of human adipose tissue. *Eur Cell Mater* 2010;19:127-35.
134. Cheung WK, Working DM, Galuppo LD, Leach JK. Osteogenic comparison of expanded and uncultured adipose stromal cells. *Cytotherapy* 2010;12(4):554-62.
135. Rajashekhar G, Traktuev DO, Roell WC, Johnstone BH, Merfeld-Clauss S, Van Natta B, et al. IFATS collection: Adipose stromal cell differentiation is reduced by endothelial cell contact and paracrine communication: role of canonical Wnt signaling. *Stem Cells* 2008;26(10):2674-81.
136. Meury T, Verrier S, Alini M. Human endothelial cells inhibit BMSC differentiation into mature osteoblasts in vitro by interfering with osterix expression. *J Cell Biochem* 2006;98(4):992-1006.
137. Dahl JA, Duggal S, Coulston N, Millar D, Melki J, Shahdadfar A, et al. Genetic and epigenetic instability of human bone marrow mesenchymal stem cells expanded in autologous serum or fetal bovine serum. *Int J Dev Biol* 2008;52(8):1033-42.
138. Rosland GV, Svendsen A, Torsvik A, Sobala E, McCormack E, Immervoll H, et al. Long-term cultures of bone marrow-derived human mesenchymal stem cells frequently undergo spontaneous malignant transformation. *Cancer Res* 2009;69(13):5331-9.

139. Ren Z, Wang J, Zhu W, Guan Y, Zou C, Chen Z, et al. Spontaneous transformation of adult mesenchymal stem cells from cynomolgus macaques in vitro. *Exp Cell Res* 2011;317(20):2950-7.
140. Torsvik A, Rosland GV, Svendsen A, Molven A, Immervoll H, McCormack E, et al. Spontaneous malignant transformation of human mesenchymal stem cells reflects cross-contamination: putting the research field on track - letter. *Cancer Res* 2010;70(15):6393-6.
141. Muraglia A, Cancedda R, Quarto R. Clonal mesenchymal progenitors from human bone marrow differentiate in vitro according to a hierarchical model. *Journal of cell science* 2000;113 (Pt 7):1161-6.
142. Baxter MA, Wynn RF, Jowitt SN, Wraith JE, Fairbairn LJ, Bellantuono I. Study of telomere length reveals rapid aging of human marrow stromal cells following in vitro expansion. *Stem Cells* 2004;22(5):675-82.
143. Meliga E, Strem BM, Duckers HJ, Serruys PW. Adipose-derived cells. *Cell Transplant* 2007;16(9):963-70.
144. Tarnok A, Ulrich H, Bocsi J. Phenotypes of stem cells from diverse origin. *Cytometry A* 2010;77(1):6-10.
145. Schaffler A, Buchler C. Concise review: adipose tissue-derived stromal cells--basic and clinical implications for novel cell-based therapies. *Stem Cells* 2007;25(4):818-27.
146. James AW, Zara JN, Zhang X, Askarinam A, Goyal R, Chiang M, et al. Perivascular stem cells: a prospectively purified mesenchymal stem cell population for bone tissue engineering. *Stem Cells Transl Med* 2012;1(6):510-9.
147. Djouad F, Fritz V, Apparailly F, Louis-Plence P, Bony C, Sany J, et al. Reversal of the immunosuppressive properties of mesenchymal stem cells by tumor necrosis factor alpha in collagen-induced arthritis. *Arthritis Rheum* 2005;52(5):1595-603.
148. Bruder SP, Fink DJ, Caplan AI. Mesenchymal stem cells in bone development, bone repair, and skeletal regeneration therapy. *J Cell Biochem* 1994;56(3):283-94.
149. Cao L, Liu G, Gan Y, Fan Q, Yang F, Zhang X, et al. The use of autologous enriched bone marrow MSCs to enhance osteoporotic bone defect repair in long-term estrogen deficient goats. *Biomaterials* 2012;33(20):5076-84.
150. Guillot PV, De Bari C, Dell'Accio F, Kurata H, Polak J, Fisk NM. Comparative osteogenic transcription profiling of various fetal and adult mesenchymal stem cell sources. *Differentiation; research in biological diversity* 2008;76(9):946-57.
151. Murphy JM, Fink DJ, Hunziker EB, Barry FP. Stem cell therapy in a caprine model of osteoarthritis. *Arthritis and rheumatism* 2003;48(12):3464-74.
152. Hillel AT, Taube JM, Cornish TC, Sharma B, Halushka M, McCarthy EF, et al. Characterization of human mesenchymal stem cell-engineered cartilage: analysis of its ultrastructure, cell density and chondrocyte phenotype compared to native adult and fetal cartilage. *Cells Tissues Organs* 2010;191(1):12-20.
153. Erickson IE, Huang AH, Chung C, Li RT, Burdick JA, Mauck RL. Differential maturation and structure-function relationships in mesenchymal stem cell- and chondrocyte-seeded hydrogels. *Tissue Eng Part A* 2009;15(5):1041-52.
154. Noth U, Steinert AF, Tuan RS. Technology insight: adult mesenchymal stem cells for osteoarthritis therapy. *Nat Clin Pract Rheumatol* 2008;4(7):371-80.
155. Reichert JC, Cipitria A, Epari DR, Saifzadeh S, Krishnakanth P, Berner A, et al. A tissue engineering solution for segmental defect regeneration in load-bearing long bones. *Sci Transl Med* 2012;4(141):141ra93.
156. Zhao Y, Li T, Wei X, Bianchi G, Hu J, Sanchez PG, et al. Mesenchymal stem cell transplantation improves regional cardiac remodeling following ovine infarction. *Stem cells translational medicine* 2012;1(9):685-95.

157. Wang N, Ren GD, Zhou Z, Xu Y, Qin T, Yu RF, et al. Cooperation of myocardin and Smad2 in inducing differentiation of mesenchymal stem cells into smooth muscle cells. *IUBMB life* 2012;64(4):331-9.
158. Uysal AC, Mizuno H. Tendon regeneration and repair with adipose derived stem cells. *Curr Stem Cell Res Ther* 2010;5(2):161-7.
159. Leroux L, Descamps B, Tojais NF, Seguy B, Oses P, Moreau C, et al. Hypoxia preconditioned mesenchymal stem cells improve vascular and skeletal muscle fiber regeneration after ischemia through a Wnt4-dependent pathway. *Mol Ther* 2010;18(8):1545-52.
160. Chen J, Li Y, Katakowski M, Chen X, Wang L, Lu D, et al. Intravenous bone marrow stromal cell therapy reduces apoptosis and promotes endogenous cell proliferation after stroke in female rat. *Journal of neuroscience research* 2003;73(6):778-86.
161. Rosova I, Dao M, Capoccia B, Link D, Nolta JA. Hypoxic preconditioning results in increased motility and improved therapeutic potential of human mesenchymal stem cells. *Stem cells* 2008;26(8):2173-82.
162. Gupta PK, Chullikana A, Parakh R, Desai S, Das A, Gottipamula S, et al. A double blind randomized placebo controlled phase I/II study assessing the safety and efficacy of allogeneic bone marrow derived mesenchymal stem cell in critical limb ischemia. *J Transl Med* 2013;11:143.
163. Serbeniuk Ts V, Sychev VS, Lelekova TV. [Bilevel organization of the spinal center of the frog lymph heart]. *Nauchnye doklady vysshei shkoly. Biologicheskie nauki* 1976(7):82-6.
164. Laflamme MA, Murry CE. Regenerating the heart. *Nature biotechnology* 2005;23(7):845-56.
165. Burst V, Putsch F, Kubacki T, Volker LA, Bartram MP, Muller RU, et al. Survival and distribution of injected haematopoietic stem cells in acute kidney injury. *Nephrology, dialysis, transplantation : official publication of the European Dialysis and Transplant Association - European Renal Association* 2012.
166. Wise AF, Ricardo SD. Mesenchymal stem cells in kidney inflammation and repair. *Nephrology* 2012;17(1):1-10.
167. Alfarano C, Roubeix C, Chaaya R, Ceccaldi C, Calise D, Mias C, et al. Intraparenchymal injection of bone marrow mesenchymal stem cells reduces kidney fibrosis after ischemia-reperfusion in cyclosporine-immunosuppressed rats. *Cell Transplant* 2012;21(9):2009-19.
168. Dai LJ, Li HY, Guan LX, Ritchie G, Zhou JX. The therapeutic potential of bone marrow-derived mesenchymal stem cells on hepatic cirrhosis. *Stem Cell Res* 2009;2(1):16-25.
169. Ishikawa T, Banas A, Hagiwara K, Iwaguro H, Ochiya T. Stem cells for hepatic regeneration: the role of adipose tissue derived mesenchymal stem cells. *Curr Stem Cell Res Ther*;5(2):182-9.
170. Aquino JB, Bolontrade MF, Garcia MG, Podhajcer OL, Mazzolini G. Mesenchymal stem cells as therapeutic tools and gene carriers in liver fibrosis and hepatocellular carcinoma. *Gene Ther*;17(6):692-708.
171. Xia Z, Zhang C, Zeng Y, Wang T, Ai G. Transplantation of BMSCs expressing hVEGF(165) /hBD3 promotes wound healing in rats with combined radiation-wound injury. *International wound journal* 2012.
172. Kim SO, Na HS, Kwon D, Joo SY, Kim HS, Ahn Y. Bone-marrow-derived mesenchymal stem cell transplantation enhances closing pressure and leak point pressure in a female urinary incontinence rat model. *Urol Int* 2011;86(1):110-6.

173. Wynn TA, Ramalingam TR. Mechanisms of fibrosis: therapeutic translation for fibrotic disease. *Nat Med* 2012;18(7):1028-40.
174. Hinz B, Phan SH, Thannickal VJ, Prunotto M, Desmouliere A, Varga J, et al. Recent developments in myofibroblast biology: paradigms for connective tissue remodeling. *Am J Pathol* 2012;180(4):1340-55.
175. Kim KK, Kugler MC, Wolters PJ, Robillard L, Galvez MG, Brumwell AN, et al. Alveolar epithelial cell mesenchymal transition develops in vivo during pulmonary fibrosis and is regulated by the extracellular matrix. *Proc Natl Acad Sci U S A* 2006;103(35):13180-5.
176. Iwano M, Plieth D, Danoff TM, Xue C, Okada H, Neilson EG. Evidence that fibroblasts derive from epithelium during tissue fibrosis. *J Clin Invest* 2002;110(3):341-50.
177. Fathke C, Wilson L, Hutter J, Kapoor V, Smith A, Hocking A, et al. Contribution of bone marrow-derived cells to skin: collagen deposition and wound repair. *Stem Cells* 2004;22(5):812-22.
178. Hashimoto N, Jin H, Liu T, Chensue SW, Phan SH. Bone marrow-derived progenitor cells in pulmonary fibrosis. *J Clin Invest* 2004;113(2):243-52.
179. Koesters R, Kaissling B, Lehir M, Picard N, Theilig F, Gebhardt R, et al. Tubular overexpression of transforming growth factor-beta1 induces autophagy and fibrosis but not mesenchymal transition of renal epithelial cells. *Am J Pathol* 2010;177(2):632-43.
180. Rock JR, Barkauskas CE, Cronce MJ, Xue Y, Harris JR, Liang J, et al. Multiple stromal populations contribute to pulmonary fibrosis without evidence for epithelial to mesenchymal transition. *Proc Natl Acad Sci U S A* 2011;108(52):E1475-83.
181. Humphreys BD, Lin SL, Kobayashi A, Hudson TE, Nowlin BT, Bonventre JV, et al. Fate tracing reveals the pericyte and not epithelial origin of myofibroblasts in kidney fibrosis. *Am J Pathol* 2010;176(1):85-97.
182. Goritz C, Dias DO, Tomilin N, Barbacid M, Shupliakov O, Frisen J. A pericyte origin of spinal cord scar tissue. *Science* 2011;333(6039):238-42.
183. Kisseleva T, Cong M, Paik Y, Scholten D, Jiang C, Benner C, et al. Myofibroblasts revert to an inactive phenotype during regression of liver fibrosis. *Proc Natl Acad Sci U S A* 2012;109(24):9448-53.
184. Diaz-Manera J, Gallardo E, de Luna N, Navas M, Soria L, Garibaldi M, et al. The increase of pericyte population in human neuromuscular disorders supports their role in muscle regeneration in vivo. *J Pathol* 2012.
185. Dulauroy S, Di Carlo SE, Langa F, Eberl G, Peduto L. Lineage tracing and genetic ablation of ADAM12(+) perivascular cells identify a major source of profibrotic cells during acute tissue injury. *Nat Med* 2012;18(8):1262-70.
186. Murray CJ, Vos T, Lozano R, Naghavi M, Flaxman AD, Michaud C, et al. Disability-adjusted life years (DALYs) for 291 diseases and injuries in 21 regions, 1990-2010: a systematic analysis for the Global Burden of Disease Study 2010. *Lancet* 2012;380(9859):2197-223.
187. Tippets DM, Zaryanov AV, Vincent Burke W, Patel PD, Suarez JC, Ely EE, et al. Incidence of Heterotopic Ossification in Direct Anterior Total Hip Arthroplasty: A Retrospective Radiographic Review. *J Arthroplasty* 2014.
188. Ramirez DM, Ramirez MR, Reginato AM, Medici D. Molecular and cellular mechanisms of heterotopic ossification. *Histol Histopathol* 2014.
189. Kan L, Peng CY, McGuire TL, Kessler JA. Glast-expressing progenitor cells contribute to heterotopic ossification. *Bone* 2013;53(1):194-203.
190. Emery AE. The muscular dystrophies. *Lancet* 2002;359(9307):687-95.
191. Angelini C. The role of corticosteroids in muscular dystrophy: a critical appraisal. *Muscle Nerve* 2007;36(4):424-35.

192. Mann CJ, Perdiguero E, Kharraz Y, Aguilar S, Pessina P, Serrano AL, et al. Aberrant repair and fibrosis development in skeletal muscle. *Skelet Muscle* 2011;1(1):21.
193. Croisier JL, Forthomme B, Namurois MH, Vanderthommen M, Crielaard JM. Hamstring muscle strain recurrence and strength performance disorders. *Am J Sports Med* 2002;30(2):199-203.
194. Garrett WE, Jr. Muscle strain injuries. *Am J Sports Med* 1996;24(6 Suppl):S2-8.
195. Verrall GM, Slavotinek JP, Barnes PG, Fon GT, Spriggins AJ. Clinical risk factors for hamstring muscle strain injury: a prospective study with correlation of injury by magnetic resonance imaging. *Br J Sports Med* 2001;35(6):435-9; discussion 40.
196. Schiaffino S, Reggiani C. Fiber types in mammalian skeletal muscles. *Physiol Rev* 2011;91(4):1447-531.
197. Judson RN, Zhang RH, Rossi FM. Tissue-resident mesenchymal stem/progenitor cells in skeletal muscle: collaborators or saboteurs? *FEBS J* 2013;280(17):4100-8.
198. Yin H, Pasut A, Soleimani VD, Bentzinger CF, Antoun G, Thorn S, et al. MicroRNA-133 controls brown adipose determination in skeletal muscle satellite cells by targeting Prdm16. *Cell Metab* 2013;17(2):210-24.
199. Mauro A. Satellite cell of skeletal muscle fibers. *J Biophys Biochem Cytol* 1961;9:493-5.
200. Seale P, Sabourin LA, Girgis-Gabardo A, Mansouri A, Gruss P, Rudnicki MA. Pax7 is required for the specification of myogenic satellite cells. *Cell* 2000;102(6):777-86.
201. Kuang S, Kuroda K, Le Grand F, Rudnicki MA. Asymmetric self-renewal and commitment of satellite stem cells in muscle. *Cell* 2007;129(5):999-1010.
202. Rocheteau P, Gayraud-Morel B, Siegl-Cachedenier I, Blasco MA, Tajbakhsh S. A subpopulation of adult skeletal muscle stem cells retains all template DNA strands after cell division. *Cell* 2012;148(1-2):112-25.
203. Sacco A, Doyonnas R, Kraft P, Vitorovic S, Blau HM. Self-renewal and expansion of single transplanted muscle stem cells. *Nature* 2008;456(7221):502-6.
204. Collins CA, Olsen I, Zammit PS, Heslop L, Petrie A, Partridge TA, et al. Stem cell function, self-renewal, and behavioral heterogeneity of cells from the adult muscle satellite cell niche. *Cell* 2005;122(2):289-301.
205. Montarras D, Morgan J, Collins C, Relaix F, Zaffran S, Cumano A, et al. Direct isolation of satellite cells for skeletal muscle regeneration. *Science* 2005;309(5743):2064-7.
206. Cerletti M, Jurga S, Witczak CA, Hirshman MF, Shadrach JL, Goodyear LJ, et al. Highly efficient, functional engraftment of skeletal muscle stem cells in dystrophic muscles. *Cell* 2008;134(1):37-47.
207. Sambasivan R, Yao R, Kissenpfennig A, Van Wittenberghe L, Paldi A, Gayraud-Morel B, et al. Pax7-expressing satellite cells are indispensable for adult skeletal muscle regeneration. *Development* 2011;138(17):3647-56.
208. Lepper C, Partridge TA, Fan CM. An absolute requirement for Pax7-positive satellite cells in acute injury-induced skeletal muscle regeneration. *Development* 2011;138(17):3639-46.
209. Murphy MM, Lawson JA, Mathew SJ, Hutcheson DA, Kardon G. Satellite cells, connective tissue fibroblasts and their interactions are crucial for muscle regeneration. *Development* 2011;138(17):3625-37.
210. Tamaki T, Akatsuka A, Ando K, Nakamura Y, Matsuzawa H, Hotta T, et al. Identification of myogenic-endothelial progenitor cells in the interstitial spaces of skeletal muscle. *J Cell Biol* 2002;157(4):571-7.

211. Asakura A, Seale P, Girgis-Gabardo A, Rudnicki MA. Myogenic specification of side population cells in skeletal muscle. *J Cell Biol* 2002;159(1):123-34.
212. Gussoni E, Soneoka Y, Strickland CD, Buzney EA, Khan MK, Flint AF, et al. Dystrophin expression in the mdx mouse restored by stem cell transplantation. *Nature* 1999;401(6751):390-4.
213. Uezumi A, Ojima K, Fukada S, Ikemoto M, Masuda S, Miyagoe-Suzuki Y, et al. Functional heterogeneity of side population cells in skeletal muscle. *Biochem Biophys Res Commun* 2006;341(3):864-73.
214. Mitchell KJ, Pannerec A, Cadot B, Parlakian A, Besson V, Gomes ER, et al. Identification and characterization of a non-satellite cell muscle resident progenitor during postnatal development. *Nat Cell Biol* 2010;12(3):257-66.
215. Zheng B, Cao B, Crisan M, Sun B, Li G, Logar A, et al. Prospective identification of myogenic endothelial cells in human skeletal muscle. *Nat Biotechnol* 2007;25(9):1025-34.
216. Heredia JE, Mukundan L, Chen FM, Mueller AA, Deo RC, Locksley RM, et al. Type 2 innate signals stimulate fibro/adipogenic progenitors to facilitate muscle regeneration. *Cell* 2013;153(2):376-88.
217. Joe AW, Yi L, Natarajan A, Le Grand F, So L, Wang J, et al. Muscle injury activates resident fibro/adipogenic progenitors that facilitate myogenesis. *Nat Cell Biol* 2010;12(2):153-63.
218. Uezumi A, Fukada S, Yamamoto N, Takeda S, Tsuchida K. Mesenchymal progenitors distinct from satellite cells contribute to ectopic fat cell formation in skeletal muscle. *Nat Cell Biol* 2010;12(2):143-52.
219. Uezumi A, Ito T, Morikawa D, Shimizu N, Yoneda T, Segawa M, et al. Fibrosis and adipogenesis originate from a common mesenchymal progenitor in skeletal muscle. *J Cell Sci* 2011;124(Pt 21):3654-64.
220. Wosczyna MN, Biswas AA, Cogswell CA, Goldhamer DJ. Multipotent progenitors resident in the skeletal muscle interstitium exhibit robust BMP-dependent osteogenic activity and mediate heterotopic ossification. *J Bone Miner Res* 2012;27(5):1004-17.
221. Brack AS, Conboy MJ, Roy S, Lee M, Kuo CJ, Keller C, et al. Increased Wnt signaling during aging alters muscle stem cell fate and increases fibrosis. *Science* 2007;317(5839):807-10.
222. Calhabeu F, Hayashi S, Morgan JE, Relaix F, Zammit PS. Alveolar rhabdomyosarcoma-associated proteins PAX3/FOXO1A and PAX7/FOXO1A suppress the transcriptional activity of MyoD-target genes in muscle stem cells. *Oncogene* 2013;32(5):651-62.
223. Gnocchi VF, White RB, Ono Y, Ellis JA, Zammit PS. Further characterisation of the molecular signature of quiescent and activated mouse muscle satellite cells. *PLoS One* 2009;4(4):e5205.
224. Mathew SJ, Hansen JM, Merrell AJ, Murphy MM, Lawson JA, Hutcheson DA, et al. Connective tissue fibroblasts and Tcf4 regulate myogenesis. *Development* 2011;138(2):371-84.
225. Scadden DT. The stem-cell niche as an entity of action. *Nature* 2006;441(7097):1075-9.
226. Wurmser AE, Palmer TD, Gage FH. Neuroscience. Cellular interactions in the stem cell niche. *Science* 2004;304(5675):1253-5.
227. Schofield R. The relationship between the spleen colony-forming cell and the haemopoietic stem cell. *Blood Cells* 1978;4(1-2):7-25.
228. Korbling M, Estrov Z. Adult stem cells for tissue repair - a new therapeutic concept? *N Engl J Med* 2003;349(6):570-82.

229. Calvi LM, Adams GB, Weibrecht KW, Weber JM, Olson DP, Knight MC, et al. Osteoblastic cells regulate the haematopoietic stem cell niche. *Nature* 2003;425(6960):841-6.
230. Palmer TD, Willhoite AR, Gage FH. Vascular niche for adult hippocampal neurogenesis. *J Comp Neurol* 2000;425(4):479-94.
231. Ohlstein B, Spradling A. The adult Drosophila posterior midgut is maintained by pluripotent stem cells. *Nature* 2006;439(7075):470-4.
232. Marthiens V, Kazanis I, Moss L, Long K, Ffrench-Constant C. Adhesion molecules in the stem cell niche--more than just staying in shape? *J Cell Sci* 2010;123(Pt 10):1613-22.
233. Jensen UB, Lowell S, Watt FM. The spatial relationship between stem cells and their progeny in the basal layer of human epidermis: a new view based on whole-mount labelling and lineage analysis. *Development* 1999;126(11):2409-18.
234. Garcion E, Halilagic A, Faissner A, ffrench-Constant C. Generation of an environmental niche for neural stem cell development by the extracellular matrix molecule tenascin C. *Development* 2004;131(14):3423-32.
235. Katayama Y, Battista M, Kao WM, Hidalgo A, Peired AJ, Thomas SA, et al. Signals from the sympathetic nervous system regulate hematopoietic stem cell egress from bone marrow. *Cell* 2006;124(2):407-21.
236. Ehninger A, Trumpp A. The bone marrow stem cell niche grows up: mesenchymal stem cells and macrophages move in. *J Exp Med* 2011;208(3):421-8.
237. Tavazoie M, Van der Veken L, Silva-Vargas V, Louissaint M, Colonna L, Zaidi B, et al. A specialized vascular niche for adult neural stem cells. *Cell Stem Cell* 2008;3(3):279-88.
238. Ergun S, Tilki D, Klein D. Vascular wall as a reservoir for different types of stem and progenitor cells. *Antioxid Redox Signal* 2011;15(4):981-95.
239. Kirton JP, Wilkinson FL, Canfield AE, Alexander MY. Dexamethasone downregulates calcification-inhibitor molecules and accelerates osteogenic differentiation of vascular pericytes: implications for vascular calcification. *Circ Res* 2006;98(10):1264-72.
240. Mathews S, Bhonde R, Gupta PK, Totey S. Extracellular matrix protein mediated regulation of the osteoblast differentiation of bone marrow derived human mesenchymal stem cells. *Differentiation* 2012;84(2):185-92.
241. Stratman AN, Schwindt AE, Malotte KM, Davis GE. Endothelial-derived PDGF-BB and HB-EGF coordinately regulate pericyte recruitment during vasculogenic tube assembly and stabilization. *Blood* 2010;116(22):4720-30.
242. Stratman AN, Malotte KM, Mahan RD, Davis MJ, Davis GE. Pericyte recruitment during vasculogenic tube assembly stimulates endothelial basement membrane matrix formation. *Blood* 2009;114(24):5091-101.
243. Gerhardt H, Betsholtz C. Endothelial-pericyte interactions in angiogenesis. *Cell Tissue Res* 2003;314(1):15-23.
244. Diaz-Flores L, Gutierrez R, Madrid JF, Varela H, Valladares F, Acosta E, et al. Pericytes. Morphofunction, interactions and pathology in a quiescent and activated mesenchymal cell niche. *Histol Histopathol* 2009;24(7):909-69.
245. Gaengel K, Genove G, Armulik A, Betsholtz C. Endothelial-mural cell signaling in vascular development and angiogenesis. *Arterioscler Thromb Vasc Biol* 2009;29(5):630-8.
246. Armulik A, Genove G, Betsholtz C. Pericytes: developmental, physiological, and pathological perspectives, problems, and promises. *Dev Cell* 2011;21(2):193-215.

247. Ozerdem U, Stallcup WB. Early contribution of pericytes to angiogenic sprouting and tube formation. *Angiogenesis* 2003;6(3):241-9.
248. Ozerdem U, Grako KA, Dahlin-Huppe K, Monosov E, Stallcup WB. NG2 proteoglycan is expressed exclusively by mural cells during vascular morphogenesis. *Dev Dyn* 2001;222(2):218-27.
249. Reynolds LP, Grazul-Bilska AT, Redmer DA. Angiogenesis in the corpus luteum. *Endocrine* 2000;12(1):1-9.
250. Enge M, Bjarnegard M, Gerhardt H, Gustafsson E, Kalen M, Asker N, et al. Endothelium-specific platelet-derived growth factor-B ablation mimics diabetic retinopathy. *EMBO J* 2002;21(16):4307-16.
251. Hellstrom M, Kalen M, Lindahl P, Abramsson A, Betsholtz C. Role of PDGF-B and PDGFR-beta in recruitment of vascular smooth muscle cells and pericytes during embryonic blood vessel formation in the mouse. *Development* 1999;126(14):3047-55.
252. Hirschi KK, Rohovsky SA, Beck LH, Smith SR, D'Amore PA. Endothelial cells modulate the proliferation of mural cell precursors via platelet-derived growth factor-BB and heterotypic cell contact. *Circ Res* 1999;84(3):298-305.
253. Lindahl P, Johansson BR, Leveen P, Betsholtz C. Pericyte loss and microaneurysm formation in PDGF-B-deficient mice. *Science* 1997;277(5323):242-5.
254. Saleh FA, Whyte M, Genever PG. Effects of endothelial cells on human mesenchymal stem cell activity in a three-dimensional in vitro model. *Eur Cell Mater* 2011;22:242-57; discussion 57.
255. Saleh FA, Whyte M, Ashton P, Genever PG. Regulation of mesenchymal stem cell activity by endothelial cells. *Stem Cells Dev* 2011;20(3):391-403.
256. Xue Y, Xing Z, Hellem S, Arvidson K, Mustafa K. Endothelial cells influence the osteogenic potential of bone marrow stromal cells. *Biomed Eng Online* 2009;8:34.
257. Kaigler D, Krebsbach PH, West ER, Horger K, Huang YC, Mooney DJ. Endothelial cell modulation of bone marrow stromal cell osteogenic potential. *FASEB J* 2005;19(6):665-7.
258. Li H, Daculsi R, Grellier M, Bareille R, Bourget C, Amedee J. Role of neural-cadherin in early osteoblastic differentiation of human bone marrow stromal cells cocultured with human umbilical vein endothelial cells. *Am J Physiol Cell Physiol* 2010;299(2):C422-30.
259. Grellier M, Bordenave L, Amedee J. Cell-to-cell communication between osteogenic and endothelial lineages: implications for tissue engineering. *Trends Biotechnol* 2009;27(10):562-71.
260. Villars F, Guillotin B, Amedee T, Dutoya S, Bordenave L, Bareille R, et al. Effect of HUVEC on human osteoprogenitor cell differentiation needs heterotypic gap junction communication. *Am J Physiol Cell Physiol* 2002;282(4):C775-85.
261. Villars F, Bordenave L, Bareille R, Amedee J. Effect of human endothelial cells on human bone marrow stromal cell phenotype: role of VEGF? *J Cell Biochem* 2000;79(4):672-85.
262. Guillotin B, Bourget C, Remy-Zolgadri M, Bareille R, Fernandez P, Conrad V, et al. Human primary endothelial cells stimulate human osteoprogenitor cell differentiation. *Cell Physiol Biochem* 2004;14(4-6):325-32.
263. Takada I, Kouzmenko AP, Kato S. PPAR-gamma Signaling Crosstalk in Mesenchymal Stem Cells. *PPAR Res* 2010;2010.
264. Muruganandan S, Roman AA, Sinal CJ. Adipocyte differentiation of bone marrow-derived mesenchymal stem cells: cross talk with the osteoblastogenic program. *Cell Mol Life Sci* 2009;66(2):236-53.

265. Fontaine C, Cousin W, Plaisant M, Dani C, Peraldi P. Hedgehog signaling alters adipocyte maturation of human mesenchymal stem cells. *Stem Cells* 2008;26(4):1037-46.
266. Camplejohn KL, Allard SA. Limitations of safranin 'O' staining in proteoglycan-depleted cartilage demonstrated with monoclonal antibodies. *Histochemistry* 1988;89(2):185-8.
267. Tomkinson A, Reeve J, Shaw RW, Noble BS. The death of osteocytes via apoptosis accompanies estrogen withdrawal in human bone. *J Clin Endocrinol Metab* 1997;82(9):3128-35.
268. Farquharson C, Whitehead C, Rennie S, Thorp B, Loveridge N. Cell proliferation and enzyme activities associated with the development of avian tibial dyschondroplasia: an in situ biochemical study. *Bone* 1992;13(1):59-67.
269. De Witt Hamer PC, Jonker A, Leenstra S, Ruijter JM, Van Noorden CJ. Quantification of viability in organotypic multicellular spheroids of human malignant glioma using lactate dehydrogenase activity: a rapid and reliable automated assay. *J Histochem Cytochem* 2005;53(1):23-34.
270. Corselli M, Crisan M, Murray IR, West CC, Scholes J, Codrea F, et al. Identification of perivascular mesenchymal stromal/stem cells by flow cytometry. *Cytometry A* 2013;83(8):714-20.
271. van Beijnum JR, Rousch M, Castermans K, van der Linden E, Griffioen AW. Isolation of endothelial cells from fresh tissues. *Nat Protoc* 2008;3(6):1085-91.
272. Kumar TP, Vasudevan A. Isolation and culture of endothelial cells from the embryonic forebrain. *J Vis Exp* 2014(83):e51021.
273. Scott PA, Bicknell R. The isolation and culture of microvascular endothelium. *J Cell Sci* 1993;105 (Pt 2):269-73.
274. James AW, Zara JN, Corselli M, Askarinam A, Zhou AM, Hourfar A, et al. An abundant perivascular source of stem cells for bone tissue engineering. *Stem Cells Transl Med* 2012;1(9):673-84.
275. Californian Institute of Regenerative Medicine. Early Translational Award: Harnessing native fat-residing stem cells for bone regeneration, 2012.
276. Jackson WM, Aragon AB, Bulken-Hoover JD, Nesti LJ, Tuan RS. Putative heterotopic ossification progenitor cells derived from traumatized muscle. *J Orthop Res* 2009;27(12):1645-51.
277. Crisan M, Huard J, Zheng B, Sun B, Yap S, Logar A, et al. Purification and culture of human blood vessel-associated progenitor cells. *Curr Protoc Stem Cell Biol* 2008;Chapter 2:Unit 2B 2 1-2B 2 13.
278. Zhou L, Sohet F, Daneman R. Purification and culture of central nervous system pericytes. *Cold Spring Harb Protoc* 2014;2014(6):pdb top070888.
279. Ramsey WS, Hertl W, Nowlan ED, Binkowski NJ. Surface treatments and cell attachment. *In Vitro* 1984;20(10):802-8.
280. Neuhuber B, Swanger SA, Howard L, Mackay A, Fischer I. Effects of plating density and culture time on bone marrow stromal cell characteristics. *Exp Hematol* 2008;36(9):1176-85.
281. Lee MW, Kim DS, Yoo KH, Kim HR, Jang IK, Lee JH, et al. Human bone marrow-derived mesenchymal stem cell gene expression patterns vary with culture conditions. *Blood Res* 2013;48(2):107-14.
282. Pasut A, Oleynik P, Rudnicki MA. Isolation of muscle stem cells by fluorescence activated cell sorting cytometry. *Methods Mol Biol* 2012;798:53-64.
283. Chen WC, Park TS, Murray IR, Zimmerlin L, Lazzari L, Huard J, et al. Cellular kinetics of perivascular MSC precursors. *Stem Cells Int* 2013;2013:983059.
284. Nanaev AK, Rukosuev VS, Shirinsky VP, Milovanov AP, Domogatsky SP, Duance VC, et al. Confocal and conventional immunofluorescent and immunogold electron

microscopic localization of collagen types III and IV in human placenta. *Placenta* 1991;12(6):573-95.
285. Armulik A, Abramsson A, Betsholtz C. Endothelial/pericyte interactions. *Circ Res* 2005;97(6):512-23.
286. Yamagishi S, Hsu CC, Kobayashi K, Yamamoto H. Endothelin 1 mediates endothelial cell-dependent proliferation of vascular pericytes. *Biochem Biophys Res Commun* 1993;191(3):840-6.
287. Zhang X, Peault B, Chen W, Li W, Corselli M, James AW, et al. The Nell-1 growth factor stimulates bone formation by purified human perivascular cells. *Tissue Eng Part A* 2011;17(19-20):2497-509.
288. Simonsen JL, Rosada C, Serakinci N, Justesen J, Stenderup K, Rattan SI, et al. Telomerase expression extends the proliferative life-span and maintains the osteogenic potential of human bone marrow stromal cells. *Nat Biotechnol* 2002;20(6):592-6.
289. Dayoub H, Dumont RJ, Li JZ, Dumont AS, Hankins GR, Kallmes DF, et al. Human mesenchymal stem cells transduced with recombinant bone morphogenetic protein-9 adenovirus promote osteogenesis in rodents. *Tissue Eng* 2003;9(2):347-56.
290. Nakahara H, Misawa H, Hayashi T, Kondo E, Yuasa T, Kubota Y, et al. Bone repair by transplantation of hTERT-immortalized human mesenchymal stem cells in mice. *Transplantation* 2009;88(3):346-53.
291. Sekiya I, Vuoristo JT, Larson BL, Prockop DJ. In vitro cartilage formation by human adult stem cells from bone marrow stroma defines the sequence of cellular and molecular events during chondrogenesis. *Proc Natl Acad Sci U S A* 2002;99(7):4397-402.
292. Hiraoka K, Grogan S, Olee T, Lotz M. Mesenchymal progenitor cells in adult human articular cartilage. *Biorheology* 2006;43(3-4):447-54.
293. Koay EJ, Athanasiou KA. Hypoxic chondrogenic differentiation of human embryonic stem cells enhances cartilage protein synthesis and biomechanical functionality. *Osteoarthritis Cartilage* 2008;16(12):1450-6.
294. Takada I, Kouzmenko AP, Kato S. Wnt and PPARgamma signaling in osteoblastogenesis and adipogenesis. *Nat Rev Rheumatol* 2009;5(8):442-7.
295. Goodwin AM, Sullivan KM, D'Amore PA. Cultured endothelial cells display endogenous activation of the canonical Wnt signaling pathway and express multiple ligands, receptors, and secreted modulators of Wnt signaling. *Dev Dyn* 2006;235(11):3110-20.
296. Cadigan KM, Nusse R. Wnt signaling: a common theme in animal development. *Genes Dev* 1997;11(24):3286-305.
297. Chien AJ, Conrad WH, Moon RT. A Wnt survival guide: from flies to human disease. *J Invest Dermatol* 2009;129(7):1614-27.
298. Ling L, Nurcombe V, Cool SM. Wnt signaling controls the fate of mesenchymal stem cells. *Gene* 2009;433(1-2):1-7.
299. Reya T, Clevers H. Wnt signalling in stem cells and cancer. *Nature* 2005;434(7035):843-50.
300. Wodarz A, Nusse R. Mechanisms of Wnt signaling in development. *Annu Rev Cell Dev Biol* 1998;14:59-88.
301. Huelsken J, Birchmeier W. New aspects of Wnt signaling pathways in higher vertebrates. *Curr Opin Genet Dev* 2001;11(5):547-53.
302. Huelsken J, Behrens J. The Wnt signalling pathway. *J Cell Sci* 2002;115(Pt 21):3977-8.
303. Miller JR. The Wnts. *Genome Biol* 2002;3(1):REVIEWS3001.

304. Mao B, Wu W, Davidson G, Marhold J, Li M, Mechler BM, et al. Kremen proteins are Dickkopf receptors that regulate Wnt/beta-catenin signalling. *Nature* 2002;417(6889):664-7.
305. Li X, Zhang Y, Kang H, Liu W, Liu P, Zhang J, et al. Sclerostin binds to LRP5/6 and antagonizes canonical Wnt signaling. *J Biol Chem* 2005;280(20):19883-7.
306. Semenov MV, Tamai K, Brott BK, Kuhl M, Sokol S, He X. Head inducer Dickkopf-1 is a ligand for Wnt coreceptor LRP6. *Curr Biol* 2001;11(12):951-61.
307. Etheridge SL, Spencer GJ, Heath DJ, Genever PG. Expression profiling and functional analysis of wnt signaling mechanisms in mesenchymal stem cells. *Stem Cells* 2004;22(5):849-60.
308. Papkoff J, Schryver B. Secreted int-1 protein is associated with the cell surface. *Mol Cell Biol* 1990;10(6):2723-30.
309. Westendorf JJ, Kahler RA, Schroeder TM. Wnt signaling in osteoblasts and bone diseases. *Gene* 2004;341:19-39.
310. Krishnan V, Bryant HU, Macdougald OA. Regulation of bone mass by Wnt signaling. *J Clin Invest* 2006;116(5):1202-9.
311. Johnson ML, Rajamannan N. Diseases of Wnt signaling. *Rev Endocr Metab Disord* 2006;7(1-2):41-9.
312. Boland GM, Perkins G, Hall DJ, Tuan RS. Wnt 3a promotes proliferation and suppresses osteogenic differentiation of adult human mesenchymal stem cells. *J Cell Biochem* 2004;93(6):1210-30.
313. Ross SE, Hemati N, Longo KA, Bennett CN, Lucas PC, Erickson RL, et al. Inhibition of adipogenesis by Wnt signaling. *Science* 2000;289(5481):950-3.
314. Cawthorn WP, Bree AJ, Yao Y, Du B, Hemati N, Martinez-Santibanez G, et al. Wnt6, Wnt10a and Wnt10b inhibit adipogenesis and stimulate osteoblastogenesis through a beta-catenin-dependent mechanism. *Bone* 2012;50(2):477-89.
315. Kirton JP, Crofts NJ, George SJ, Brennan K, Canfield AE. Wnt/beta-catenin signaling stimulates chondrogenic and inhibits adipogenic differentiation of pericytes: potential relevance to vascular disease? *Circ Res* 2007;101(6):581-9.
316. Couffinhal T, Dufourcq P, Duplaa C. Beta-catenin nuclear activation: common pathway between Wnt and growth factor signaling in vascular smooth muscle cell proliferation? *Circ Res* 2006;99(12):1287-9.
317. Lacorre DA, Baekkevold ES, Garrido I, Brandtzaeg P, Haraldsen G, Amalric F, et al. Plasticity of endothelial cells: rapid dedifferentiation of freshly isolated high endothelial venule endothelial cells outside the lymphoid tissue microenvironment. *Blood* 2004;103(11):4164-72.
318. Gargett CE, Bucak K, Rogers PA. Isolation, characterization and long-term culture of human myometrial microvascular endothelial cells. *Hum Reprod* 2000;15(2):293-301.
319. Lozito TP, Taboas JM, Kuo CK, Tuan RS. Mesenchymal stem cell modification of endothelial matrix regulates their vascular differentiation. *J Cell Biochem* 2009;107(4):706-13.
320. Gregory CA, Gunn WG, Peister A, Prockop DJ. An Alizarin red-based assay of mineralization by adherent cells in culture: comparison with cetylpyridinium chloride extraction. *Anal Biochem* 2004;329(1):77-84.
321. Doherty M, Boot-Handford RP, Grant ME, Canfield AE. Identification of genes expressed during the osteogenic differentiation of vascular pericytes in vitro. *Biochem Soc Trans* 1998;26(1):S4.
322. Doherty MJ, Canfield AE. Gene expression during vascular pericyte differentiation. *Crit Rev Eukaryot Gene Expr* 1999;9(1):1-17.
323. Vandesompele J, De Preter K, Pattyn F, Poppe B, Van Roy N, De Paepe A, et al. Accurate normalization of real-time quantitative RT-PCR data by geometric

averaging of multiple internal control genes. *Genome Biol* 2002;3(7):RESEARCH0034.
324. Bustin SA, Benes V, Garson JA, Hellemans J, Huggett J, Kubista M, et al. The MIQE guidelines: minimum information for publication of quantitative real-time PCR experiments. *Clin Chem* 2009;55(4):611-22.
325. Liu Y, Teoh SH, Chong MS, Lee ES, Mattar CN, Randhawa NK, et al. Vasculogenic and Osteogenesis-Enhancing Potential of Human Umbilical Cord Blood Endothelial Colony-Forming Cells. *Stem Cells* 2012.
326. Clarkin CE, Emery RJ, Pitsillides AA, Wheeler-Jones CP. Evaluation of VEGF-mediated signaling in primary human cells reveals a paracrine action for VEGF in osteoblast-mediated crosstalk to endothelial cells. *J Cell Physiol* 2008;214(2):537-44.
327. Potenta S, Zeisberg E, Kalluri R. The role of endothelial-to-mesenchymal transition in cancer progression. *Br J Cancer* 2008;99(9):1375-9.
328. Medici D, Shore EM, Lounev VY, Kaplan FS, Kalluri R, Olsen BR. Conversion of vascular endothelial cells into multipotent stem-like cells. *Nat Med* 2010;16(12):1400-6.
329. Lounev VY, Ramachandran R, Wosczyna MN, Yamamoto M, Maidment AD, Shore EM, et al. Identification of progenitor cells that contribute to heterotopic skeletogenesis. *J Bone Joint Surg Am* 2009;91(3):652-63.
330. Medici D, Olsen BR. The role of endothelial-mesenchymal transition in heterotopic ossification. *J Bone Miner Res* 2012;27(8):1619-22.
331. Gimble JM, Zvonic S, Floyd ZE, Kassem M, Nuttall ME. Playing with bone and fat. *J Cell Biochem* 2006;98(2):251-66.
332. Kha HT, Basseri B, Shouhed D, Richardson J, Tetradis S, Hahn TJ, et al. Oxysterols regulate differentiation of mesenchymal stem cells: pro-bone and anti-fat. *J Bone Miner Res* 2004;19(5):830-40.
333. Gimble JM, Morgan C, Kelly K, Wu X, Dandapani V, Wang CS, et al. Bone morphogenetic proteins inhibit adipocyte differentiation by bone marrow stromal cells. *J Cell Biochem* 1995;58(3):393-402.
334. Dorheim MA, Sullivan M, Dandapani V, Wu X, Hudson J, Segarini PR, et al. Osteoblastic gene expression during adipogenesis in hematopoietic supporting murine bone marrow stromal cells. *J Cell Physiol* 1993;154(2):317-28.
335. Duque G. Bone and fat connection in aging bone. *Curr Opin Rheumatol* 2008;20(4):429-34.
336. Georgiou KR, Scherer MA, Fan CM, Cool JC, King TJ, Foster BK, et al. Methotrexate chemotherapy reduces osteogenesis but increases adipogenic potential in the bone marrow. *J Cell Physiol* 2012;227(3):909-18.
337. Cristancho AG, Lazar MA. Forming functional fat: a growing understanding of adipocyte differentiation. *Nat Rev Mol Cell Biol* 2011;12(11):722-34.
338. Kang S, Bennett CN, Gerin I, Rapp LA, Hankenson KD, Macdougald OA. Wnt signaling stimulates osteoblastogenesis of mesenchymal precursors by suppressing CCAAT/enhancer-binding protein alpha and peroxisome proliferator-activated receptor gamma. *J Biol Chem* 2007;282(19):14515-24.
339. Hinz B. It has to be the alphav: myofibroblast integrins activate latent TGF-beta1. *Nat Med* 2013;19(12):1567-8.
340. Pohlers D, Brenmoehl J, Loffler I, Muller CK, Leipner C, Schultze-Mosgau S, et al. TGF-beta and fibrosis in different organs - molecular pathway imprints. *Biochim Biophys Acta* 2009;1792(8):746-56.
341. Biernacka A, Dobaczewski M, Frangogiannis NG. TGF-beta signaling in fibrosis. *Growth Factors* 2011;29(5):196-202.

342. Roberts AB, Sporn MB. Differential expression of the TGF-beta isoforms in embryogenesis suggests specific roles in developing and adult tissues. *Mol Reprod Dev* 1992;32(2):91-8.
343. Munger JS, Huang X, Kawakatsu H, Griffiths MJ, Dalton SL, Wu J, et al. The integrin alpha v beta 6 binds and activates latent TGF beta 1: a mechanism for regulating pulmonary inflammation and fibrosis. *Cell* 1999;96(3):319-28.
344. Annes JP, Munger JS, Rifkin DB. Making sense of latent TGFbeta activation. *J Cell Sci* 2003;116(Pt 2):217-24.
345. Shi M, Zhu J, Wang R, Chen X, Mi L, Walz T, et al. Latent TGF-beta structure and activation. *Nature* 2011;474(7351):343-9.
346. Wipff PJ, Rifkin DB, Meister JJ, Hinz B. Myofibroblast contraction activates latent TGF-beta1 from the extracellular matrix. *J Cell Biol* 2007;179(6):1311-23.
347. Mu D, Cambier S, Fjellbirkeland L, Baron JL, Munger JS, Kawakatsu H, et al. The integrin alpha(v)beta8 mediates epithelial homeostasis through MT1-MMP-dependent activation of TGF-beta1. *J Cell Biol* 2002;157(3):493-507.
348. Munger JS, Harpel JG, Giancotti FG, Rifkin DB. Interactions between growth factors and integrins: latent forms of transforming growth factor-beta are ligands for the integrin alphavbeta1. *Mol Biol Cell* 1998;9(9):2627-38.
349. Asano Y, Ihn H, Yamane K, Jinnin M, Mimura Y, Tamaki K. Increased expression of integrin alpha(v)beta3 contributes to the establishment of autocrine TGF-beta signaling in scleroderma fibroblasts. *J Immunol* 2005;175(11):7708-18.
350. Asano Y, Ihn H, Yamane K, Jinnin M, Tamaki K. Increased expression of integrin alphavbeta5 induces the myofibroblastic differentiation of dermal fibroblasts. *Am J Pathol* 2006;168(2):499-510.
351. Henderson NC, Arnold TD, Katamura Y, Giacomini MM, Rodriguez JD, McCarty JH, et al. Targeting of alphav integrin identifies a core molecular pathway that regulates fibrosis in several organs. *Nat Med* 2013;19(12):1617-24.
352. Muzumdar MD, Tasic B, Miyamichi K, Li L, Luo L. A global double-fluorescent Cre reporter mouse. *Genesis* 2007;45(9):593-605.
353. Foo SS, Turner CJ, Adams S, Compagni A, Aubyn D, Kogata N, et al. Ephrin-B2 controls cell motility and adhesion during blood-vessel-wall assembly. *Cell* 2006;124(1):161-73.
354. Lacy-Hulbert A, Smith AM, Tissire H, Barry M, Crowley D, Bronson RT, et al. Ulcerative colitis and autoimmunity induced by loss of myeloid alphav integrins. *Proc Natl Acad Sci U S A* 2007;104(40):15823-8.
355. Proctor JM, Zang K, Wang D, Wang R, Reichardt LF. Vascular development of the brain requires beta8 integrin expression in the neuroepithelium. *J Neurosci* 2005;25(43):9940-8.
356. Horton WA. Skeletal development: insights from targeting the mouse genome. *Lancet* 2003;362(9383):560-9.
357. Rosen CJ, Beamer WG, Donahue LR. Defining the genetics of osteoporosis: using the mouse to understand man. *Osteoporos Int* 2001;12(10):803-10.
358. Davidson MK, Lindsey JR, Davis JK. Requirements and selection of an animal model. *Isr J Med Sci* 1987;23(6):551-5.
359. Shimshek DR, Kim J, Hubner MR, Spergel DJ, Buchholz F, Casanova E, et al. Codon-improved Cre recombinase (iCre) expression in the mouse. *Genesis* 2002;32(1):19-26.
360. Nagy A. Cre recombinase: the universal reagent for genome tailoring. *Genesis* 2000;26(2):99-109.
361. Heffner CS, Herbert Pratt C, Babiuk RP, Sharma Y, Rockwood SF, Donahue LR, et al. Supporting conditional mouse mutagenesis with a comprehensive cre characterization resource. *Nat Commun* 2012;3:1218.

362. Genetic manipulation of animals. In: Strachan T RA, editor. *Human Molecular Genetics*. 2nd ed. New York: Wiley-Liss, 1999.
363. Lakhe-Reddy S, Li V, Arnold TD, Khan S, Schelling JR. Mesangial cell alphavbeta8-integrin regulates glomerular capillary integrity and repair. *Am J Physiol Renal Physiol* 2014;306(12):F1400-9.
364. Li Y, Foster W, Deasy BM, Chan Y, Prisk V, Tang Y, et al. Transforming growth factor-beta1 induces the differentiation of myogenic cells into fibrotic cells in injured skeletal muscle: a key event in muscle fibrogenesis. *Am J Pathol* 2004;164(3):1007-19.
365. Chan YS, Li Y, Foster W, Horaguchi T, Somogyi G, Fu FH, et al. Antifibrotic effects of suramin in injured skeletal muscle after laceration. *J Appl Physiol (1985)* 2003;95(2):771-80.
366. Desguerre I, Arnold L, Vignaud A, Cuvellier S, Yacoub-Youssef H, Gherardi RK, et al. A new model of experimental fibrosis in hindlimb skeletal muscle of adult mdx mouse mimicking muscular dystrophy. *Muscle Nerve* 2012;45(6):803-14.
367. Takahashi M, Ward SR, Friden J, Lieber RL. Muscle excursion does not correlate with increased serial sarcomere number after muscle adaptation to stretched tendon transfer. *J Orthop Res* 2012;30(11):1774-80.
368. Jarvinen TA, Jozsa L, Kannus P, Jarvinen TL, Jarvinen M. Organization and distribution of intramuscular connective tissue in normal and immobilized skeletal muscles. An immunohistochemical, polarization and scanning electron microscopic study. *J Muscle Res Cell Motil* 2002;23(3):245-54.
369. Heinemeier KM, Olesen JL, Haddad F, Schjerling P, Baldwin KM, Kjaer M. Effect of unloading followed by reloading on expression of collagen and related growth factors in rat tendon and muscle. *J Appl Physiol (1985)* 2009;106(1):178-86.
370. Barton ER, Gimbel JA, Williams GR, Soslowsky LJ. Rat supraspinatus muscle atrophy after tendon detachment. *J Orthop Res* 2005;23(2):259-65.
371. Meyer DC, Gerber C, Von Rechenberg B, Wirth SH, Farshad M. Amplitude and strength of muscle contraction are reduced in experimental tears of the rotator cuff. *Am J Sports Med* 2011;39(7):1456-61.
372. Safran O, Derwin KA, Powell K, Iannotti JP. Changes in rotator cuff muscle volume, fat content, and passive mechanics after chronic detachment in a canine model. *J Bone Joint Surg Am* 2005;87(12):2662-70.
373. Samagh SP, Kramer EJ, Melkus G, Laron D, Bodendorfer BM, Natsuhara K, et al. MRI quantification of fatty infiltration and muscle atrophy in a mouse model of rotator cuff tears. *J Orthop Res* 2013;31(3):421-6.
374. Thacker BE, Tomiya A, Hulst JB, Suzuki KP, Bremner SN, Gastwirt RF, et al. Passive mechanical properties and related proteins change with botulinum neurotoxin A injection of normal skeletal muscle. *J Orthop Res* 2012;30(3):497-502.
375. Kafadar KA, Yi L, Ahmad Y, So L, Rossi F, Pavlath GK. Sca-1 expression is required for efficient remodeling of the extracellular matrix during skeletal muscle regeneration. *Dev Biol* 2009;326(1):47-59.
376. Hori YS, Kuno A, Hosoda R, Tanno M, Miura T, Shimamoto K, et al. Resveratrol ameliorates muscular pathology in the dystrophic mdx mouse, a model for Duchenne muscular dystrophy. *J Pharmacol Exp Ther* 2011;338(3):784-94.
377. Alnaqeeb MA, Al Zaid NS, Goldspink G. Connective tissue changes and physical properties of developing and ageing skeletal muscle. *J Anat* 1984;139 (Pt 4):677-89.
378. Hamer PW, McGeachie JM, Davies MJ, Grounds MD. Evans Blue Dye as an in vivo marker of myofibre damage: optimising parameters for detecting initial myofibre membrane permeability. *J Anat* 2002;200(Pt 1):69-79.

379. Arsic N, Zacchigna S, Zentilin L, Ramirez-Correa G, Pattarini L, Salvi A, et al. Vascular endothelial growth factor stimulates skeletal muscle regeneration in vivo. *Mol Ther* 2004;10(5):844-54.
380. Lei H, Leong D, Smith LR, Barton ER. Matrix-metalloproteinase 13 (MMP-13) is a new contributor to skeletal muscle regeneration and critical for myoblast migration. *Am J Physiol Cell Physiol* 2013.
381. Moyer AL, Wagner KR. Regeneration versus fibrosis in skeletal muscle. *Curr Opin Rheumatol* 2011;23(6):568-73.
382. Birbrair A, Zhang T, Wang ZM, Messi ML, Mintz A, Delbono O. Type-1 pericytes participate in fibrous tissue deposition in aged skeletal muscle. *Am J Physiol Cell Physiol* 2013;305(11):C1098-113.
383. Horwitz EM, Le Blanc K, Dominici M, Mueller I, Slaper-Cortenbach I, Marini FC, et al. Clarification of the nomenclature for MSC: The International Society for Cellular Therapy position statement. *Cytotherapy* 2005;7(5):393-5.
384. Murray IR, West CC, Hardy WR, James AW, Park TS, Nguyen A, et al. Natural history of mesenchymal stem cells, from vessel walls to culture vessels. *Cell Mol Life Sci* 2013.
385. Askarinam A, James AW, Zara JN, Goyal R, Corselli M, Pan A, et al. Human Perivascular Stem Cells Show Enhanced Osteogenesis and Vasculogenesis with NELL-1 Protein. *Tissue Eng Part A* 2013.
386. Akhurst RJ, Hata A. Targeting the TGFbeta signalling pathway in disease. *Nat Rev Drug Discov* 2012;11(10):790-811.
387. Gleizes PE, Munger JS, Nunes I, Harpel JG, Mazzieri R, Noguera I, et al. TGF-beta latency: biological significance and mechanisms of activation. *Stem Cells* 1997;15(3):190-7.
388. Munger JS, Harpel JG, Gleizes PE, Mazzieri R, Nunes I, Rifkin DB. Latent transforming growth factor-beta: structural features and mechanisms of activation. *Kidney Int* 1997;51(5):1376-82.
389. Wang B, Dolinski BM, Kikuchi N, Leone DR, Peters MG, Weinreb PH, et al. Role of alphavbeta6 integrin in acute biliary fibrosis. *Hepatology* 2007;46(5):1404-12.
390. Ma LJ, Yang H, Gaspert A, Carlesso G, Barty MM, Davidson JM, et al. Transforming growth factor-beta-dependent and -independent pathways of induction of tubulointerstitial fibrosis in beta6(-/-) mice. *Am J Pathol* 2003;163(4):1261-73.
391. LaBarge MA, Blau HM. Biological progression from adult bone marrow to mononucleate muscle stem cell to multinucleate muscle fiber in response to injury. *Cell* 2002;111(4):589-601.
392. Peault B, Rudnicki M, Torrente Y, Cossu G, Tremblay JP, Partridge T, et al. Stem and progenitor cells in skeletal muscle development, maintenance, and therapy. *Mol Ther* 2007;15(5):867-77.
393. Tedesco FS, Dellavalle A, Diaz-Manera J, Messina G, Cossu G. Repairing skeletal muscle: regenerative potential of skeletal muscle stem cells. *J Clin Invest* 2010;120(1):11-9.
394. Rawlins EL, Perl AK. The a"MAZE"ing world of lung-specific transgenic mice. *Am J Respir Cell Mol Biol* 2012;46(3):269-82.
395. Branda CS, Dymecki SM. Talking about a revolution: The impact of site-specific recombinases on genetic analyses in mice. *Dev Cell* 2004;6(1):7-28.
396. Sa-Pereira I, Brites D, Brito MA. Neurovascular unit: a focus on pericytes. *Mol Neurobiol* 2012;45(2):327-47.
397. Hinz B, Gabbiani G. Fibrosis: recent advances in myofibroblast biology and new therapeutic perspectives. *F1000 Biol Rep* 2010;2:78.
398. Greenhalgh SN, Iredale JP, Henderson NC. Origins of fibrosis: pericytes take centre stage. *F1000Prime Rep* 2013;5:37.

399. Friedman SL, Sheppard D, Duffield JS, Violette S. Therapy for fibrotic diseases: nearing the starting line. *Sci Transl Med* 2013;5(167):167sr1.
400. Picard N, Baum O, Vogetseder A, Kaissling B, Le Hir M. Origin of renal myofibroblasts in the model of unilateral ureter obstruction in the rat. *Histochem Cell Biol* 2008;130(1):141-55.
401. Poulsom R, Forbes SJ, Hodivala-Dilke K, Ryan E, Wyles S, Navaratnarasah S, et al. Bone marrow contributes to renal parenchymal turnover and regeneration. *J Pathol* 2001;195(2):229-35.
402. Forbes SJ, Russo FP, Rey V, Burra P, Rugge M, Wright NA, et al. A significant proportion of myofibroblasts are of bone marrow origin in human liver fibrosis. *Gastroenterology* 2004;126(4):955-63.
403. Esner M, Meilhac SM, Relaix F, Nicolas JF, Cossu G, Buckingham ME. Smooth muscle of the dorsal aorta shares a common clonal origin with skeletal muscle of the myotome. *Development* 2006;133(4):737-49.
404. Olson LE, Soriano P. Increased PDGFRalpha activation disrupts connective tissue development and drives systemic fibrosis. *Dev Cell* 2009;16(2):303-13.
405. Robertson IB, Rifkin DB. Unchaining the beast; insights from structural and evolutionary studies on TGFbeta secretion, sequestration, and activation. *Cytokine Growth Factor Rev* 2013;24(4):355-72.
406. Horan GS, Wood S, Ona V, Li DJ, Lukashev ME, Weinreb PH, et al. Partial inhibition of integrin alpha(v)beta6 prevents pulmonary fibrosis without exacerbating inflammation. *Am J Respir Crit Care Med* 2008;177(1):56-65.
407. Buscemi L, Ramonet D, Klingberg F, Formey A, Smith-Clerc J, Meister JJ, et al. The single-molecule mechanics of the latent TGF-beta1 complex. *Curr Biol* 2011;21(24):2046-54.
408. Arora PD, Narani N, McCulloch CA. The compliance of collagen gels regulates transforming growth factor-beta induction of alpha-smooth muscle actin in fibroblasts. *Am J Pathol* 1999;154(3):871-82.
409. Olsen AL, Bloomer SA, Chan EP, Gaca MD, Georges PC, Sackey B, et al. Hepatic stellate cells require a stiff environment for myofibroblastic differentiation. *Am J Physiol Gastrointest Liver Physiol* 2011;301(1):G110-8.
410. Chang HY, Sneddon JB, Alizadeh AA, Sood R, West RB, Montgomery K, et al. Gene expression signature of fibroblast serum response predicts human cancer progression: similarities between tumors and wounds. *PLoS Biol* 2004;2(2):E7.
411. Franke J, Abs V, Zizzadoro C, Abraham G. Comparative study of the effects of fetal bovine serum versus horse serum on growth and differentiation of primary equine bronchial fibroblasts. *BMC Vet Res* 2014;10(1):119.
412. Galie PA, Westfall MV, Stegemann JP. Reduced serum content and increased matrix stiffness promote the cardiac myofibroblast transition in 3D collagen matrices. *Cardiovasc Pathol* 2011;20(6):325-33.
413. Orlova VV, van den Hil FE, Petrus-Reurer S, Drabsch Y, Ten Dijke P, Mummery CL. Generation, expansion and functional analysis of endothelial cells and pericytes derived from human pluripotent stem cells. *Nat Protoc* 2014;9(6):1514-31.
414. Birbrair A, Zhang T, Wang ZM, Messi ML, Enikolopov GN, Mintz A, et al. Skeletal muscle pericyte subtypes differ in their differentiation potential. *Stem Cell Res* 2013;10(1):67-84.
415. Sims D, Horne MM, Creighan M, Donald A. Heterogeneity of pericyte populations in equine skeletal muscle and dermal microvessels: a quantitative study. *Anat Histol Embryol* 1994;23(3):232-8.
416. Nehls V, Drenckhahn D. Heterogeneity of microvascular pericytes for smooth muscle type alpha-actin. *J Cell Biol* 1991;113(1):147-54.

417. Wilm B, Ipenberg A, Hastie ND, Burch JB, Bader DM. The serosal mesothelium is a major source of smooth muscle cells of the gut vasculature. *Development* 2005;132(23):5317-28.
418. Que J, Wilm B, Hasegawa H, Wang F, Bader D, Hogan BL. Mesothelium contributes to vascular smooth muscle and mesenchyme during lung development. *Proc Natl Acad Sci U S A* 2008;105(43):16626-30.
419. Asahina K, Zhou B, Pu WT, Tsukamoto H. Septum transversum-derived mesothelium gives rise to hepatic stellate cells and perivascular mesenchymal cells in developing mouse liver. *Hepatology* 2011;53(3):983-95.
420. Zhou B, Ma Q, Rajagopal S, Wu SM, Domian I, Rivera-Feliciano J, et al. Epicardial progenitors contribute to the cardiomyocyte lineage in the developing heart. *Nature* 2008;454(7200):109-13.
421. Bergwerff M, Verberne ME, DeRuiter MC, Poelmann RE, Gittenberger-de Groot AC. Neural crest cell contribution to the developing circulatory system: implications for vascular morphology? *Circ Res* 1998;82(2):221-31.
422. Etchevers HC, Vincent C, Le Douarin NM, Couly GF. The cephalic neural crest provides pericytes and smooth muscle cells to all blood vessels of the face and forebrain. *Development* 2001;128(7):1059-68.
423. Korn J, Christ B, Kurz H. Neuroectodermal origin of brain pericytes and vascular smooth muscle cells. *J Comp Neurol* 2002;442(1):78-88.
424. Heglind M, Cederberg A, Aquino J, Lucas G, Ernfors P, Enerback S. Lack of the central nervous system- and neural crest-expressed forkhead gene Foxs1 affects motor function and body weight. *Mol Cell Biol* 2005;25(13):5616-25.
425. Muller SM, Stolt CC, Terszowski G, Blum C, Amagai T, Kessaris N, et al. Neural crest origin of perivascular mesenchyme in the adult thymus. *J Immunol* 2008;180(8):5344-51.
426. Mederacke I, Hsu CC, Troeger JS, Huebener P, Mu X, Dapito DH, et al. Fate tracing reveals hepatic stellate cells as dominant contributors to liver fibrosis independent of its aetiology. *Nat Commun* 2013;4:2823.
427. Hung C, Linn G, Chow YH, Kobayashi A, Mittelsteadt K, Altemeier WA, et al. Role of lung pericytes and resident fibroblasts in the pathogenesis of pulmonary fibrosis. *Am J Respir Crit Care Med* 2013;188(7):820-30.
428. LeBleu VS, Taduri G, O'Connell J, Teng Y, Cooke VG, Woda C, et al. Origin and function of myofibroblasts in kidney fibrosis. *Nat Med* 2013;19(8):1047-53.
429. Boppart MD, De Lisio M, Zou K, Huntsman HD. Defining a role for non-satellite stem cells in the regulation of muscle repair following exercise. *Front Physiol* 2013;4:310.
430. Hawke TJ, Garry DJ. Myogenic satellite cells: physiology to molecular biology. *J Appl Physiol (1985)* 2001;91(2):534-51.
431. Harris JB. Myotoxic phospholipases A2 and the regeneration of skeletal muscles. *Toxicon* 2003;42(8):933-45.
432. Uezumi A, Ikemoto-Uezumi M, Tsuchida K. Roles of nonmyogenic mesenchymal progenitors in pathogenesis and regeneration of skeletal muscle. *Front Physiol* 2014;5:68.
433. Usas A, Usaite D, Gao X, Huard J, Clymer JW, Malaviya P. Use of an ultrasonic blade facilitates muscle repair after incision injury. *J Surg Res* 2011;167(2):e177-84.
434. Prisk V, Huard J. Muscle injuries and repair: the role of prostaglandins and inflammation. *Histol Histopathol* 2003;18(4):1243-56.

Appendix 1 – Manuscripts in preparation

I am preparing to submit a number of original research articles based on data included in this thesis.

1. **Murray IR,** Gonzalez ZG, West CC, Hardy WR, Corselli M, Miranda-Carboni G, Péault B. Endothelial cells accelerate the osteogenic differentiation of pericytes.

2. **Murray IR,** Hardy WR, West CC, Corselli M, Soo C, Péault B. A perivascular source of purified autologous mesenchymal stem cells for tissue engineering.

3. **Murray IR,** Gonzalez ZG, Baily J, West CC, Smith J, Greenhalgh S, Thomson A, Conroy C, Iredale J, Péault B, Henderson N. αv integrin depletion in PDGFRβ perivascular cells regulates skeletal muscle fibrosis.

Appendix 2 – Review article publications

As part of my PhD studies I have written and contributed to a number of review articles based on the themes of this thesis. These articles, listed below, are included in the subsequent pages.

1. **Murray IR**, West CC, Hardy WR, James AW, Park TS, Lazzari L, Soo C, Péault B. Natural History of Mesenchymal Stem Cells, from Vessel Walls to Culture Vessels. Cellular and Molecular Life Sciences 2014;71(8):1353-74

2. **Murray IR,** Corselli M, Petrigliano F, Soo C, Péault B. Recent insights into mesenchymal stem cell identity: implications for orthopaedic applications. *Bone and Joint Journal* 2014;96-B(3):291-8.

3. West CC, **Murray IR,** González ZN, Hindle P, Hay DC, Stewart KJ, Péault B. Ethical, legal and practical issues of establishing an adipose stem cell bank for research. J Plast Reconstr Aesthet Surg. 2014 Jun;67(6):745-751.

4. Chen WC, Park TS, **Murray IR,** Zimmerlin L, Lazzari L, Huard J, Péault B. Cellular kinetics of perivascular MSC precursors. Stem Cells International. EPub Aug 19 2013 Doi:10.1155/2013/983059.

5. Corselli M, Crisan M, **Murray IR,** West CC, Scholes J, Codrea F, Khan N, Péault B. Identification and purification of perivascular progenitors of mesenchymal stromal cells by flow cytometry. Cytometry Part A, 2013;83(8):714-20.